

UNIVERSITA' DEGLI STUDI DELL'INSUBRIA



DOTTORATO DI RICERCA IN BIOTECNOLOGIE, SCIENZE
DELLA VITA E TECNOLOGIE CHIRURGICHE
XXXII CICLO

***Regulation mechanisms of human D-amino acid
oxidase***

***Meccanismi di regolazione della D-amminoacido
ossidasi umana***

Docente guida: Prof. Silvia Sacchi
Tutor: Prof. Loredano Pollegioni

Tesi di dottorato di:
Giulia Murtas
712548

Dip. Biotecnologie e Scienze della Vita - Università degli Studi dell'Insubria
Anno accademico 2018/2019

Contents

List of abbreviations.....	1
Abstract.....	2
1. Introduction.....	4
1.1 Physiological and pathological role of DAAO.....	8
1.2 Cellular function and localization of hDAAO.....	14
1.3 Structural properties of hDAAO.....	15
1.3.1 FAD binding.....	19
1.3.2 Kinetic mechanism and substrate preference.....	20
1.4 Modulation of hDAAO activity.....	21
1.4.1 By protein interaction.....	21
1.4.2 By hDAAO inhibitors.....	23
1.4.3 By point substitutions.....	26
1.4.4 By post-translational modifications.....	28
1.4.5 By protein mistargeting.....	30
2. Aim.....	32
3. Results.....	35
3.1 Biochemical properties of human D-amino acid oxidase.....	36
3.2 Human D-amino acid oxidase: the inactive G183R variant.....	47
3.3 Substitution of arginine 120 in human D-amino acid oxidase favors FAD-binding and nuclear mistargeting.....	56
3.4 Antimicrobial D-amino acid oxidase-derived peptides specify gut Microbiota.....	66
4. Discussion.....	110
References.....	122
Other publications.....	138

List of abbreviations

3MST: 3-mercaptopyruvate sulfurtransferase

AD: alzheimer's disease

ALS: amyotrophic lateral sclerosis

CAMPs: cationic antimicrobial peptides

CBIO: 5-chloro-benzo[d]isoxazol-3-ol

CNS: central nervous system

DAAO: D-amino acid oxidase

D-AAs: D-amino acids

D-Ala: D-alanine

D-Cys: D-cysteine

D-Ser: D-serine

DOPA: 3,4-dihydroxyphenylalanine

FAD: flavin adenine dinucleotide

H₂O₂: hydrogen peroxide

hDAAO: human D-amino acid oxidase

IC₅₀: half maximal inhibitory concentration

***k_{cat}*:** turnover number

K_d: dissociation constant

K_i: inhibitory constant

K_m: Michaelis constant

NMDAr: N-methyl-D-aspartate receptor

NLS: nuclear localization sequence

NTS: nuclear translocation signal

pkDAAO: porcine kidney D-amino acid oxidase

PTMs: post-translational modifications

PTS1: peroxisomal targeting signal 1

rDAAO: rat D-amino acid oxidase

RgDAAO: *Rhodotorula gracilis* D-amino acid oxidase

T_m: melting temperature

TvDAAO: *Trigonopsis variabilis* D-amino acid oxidase

Abstract

The human peroxisomal FAD-dependent enzyme D-amino acid oxidase (hDAAO, EC 1.4.3.3) plays a key role in important physiological processes by catalyzing the stereospecific degradation of several D-amino acids (D-AAs). A number of studies demonstrated that a dysregulation in processes regulating D-AAs concentration is related to the mechanism(s) predisposing to several pathologies (i.e. renal damage, schizophrenia, Alzheimer's disease, amyotrophic lateral sclerosis). The important role played by hDAAO in modulating D-AAs levels increased the interest for this flavoenzyme: while structural and biochemical properties have been extensively investigated, the modulation of its functionality by FAD and ligand binding remain elusive. Recently, it has been suggested that the flavoenzyme could be mistargeted (to cytosol and nuclei) following treatment with propiverine. A putative nuclear translocation signal (NTS) in the primary sequence of rDAAO has been identified (117-TPS-119, corresponding to the 118-TPR-120 sequence in hDAAO). Mistargeting also alters DAAO degradation as the nuclear form of the flavoenzyme is pushed to proteasomal degradation. Moreover, it has been reported that a processed form of the mouse DAAO is secreted in the intestinal lumen after the cleavage of a signal peptide near the N-terminus. Thus, the DAAO has been proposed to control the homeostasis of gut microbiota by the production of hydrogen peroxide generated by its activity on intestinal D-amino acids, originating from food or microbial cell wall.

Here, we deepened the investigation on some of the key biochemical properties of the recombinant enzyme. These studies demonstrate that hDAAO activity is finely tuned through ligand/flavin binding.

Moreover, we focused on mistargeting by studying a DAAO variant lacking the N-terminal signal peptide (thus shedding light on the mechanism of microbiota selection in the gut) and two variants at position 120 residue belonging to a nuclear translocation signal. The targeting seems a way to modulate hDAAO functionality.

Modulation of cellular targeting allows hDAAO to fulfil different physiological functions, such as the control of the levels of the neuromodulator D-Ser in

the CNS and of other D-AAs in different tissues or the selection of microbiota in the gut.

A full elucidation of the regulation mechanisms of this human flavoenzyme, especially related to its role in different tissues, will allow to clarify important physiological processes and to develop novel targeted therapies to relevant human diseases.

1. Introduction

D-amino acid oxidase (DAAO, E.C. 1.4.3.3) has been discovered in 1935 in pig kidney by H. Krebs, who reported that this tissue contains the system to deaminate, by oxidation, not only the “natural” L-amino acids, but also those “non-natural” belonging to the D-series (Krebs, 1935). DAAO catalyzes the specific oxidative deamination of hydrophobic, neutral, polar and basic D-amino acids to the corresponding imino acids, which in aqueous solutions non-enzymatically hydrolyze to the corresponding α -ketoacids and ammonia, in concomitance with the reduction of FAD. The cofactor then reoxidizes on molecular oxygen, yielding hydrogen peroxide (Figure 1) (Massey et al., 1961; Pilone et al., 1989; Pilone, 2000; Pollegioni et al., 2007; Molla, 2017).

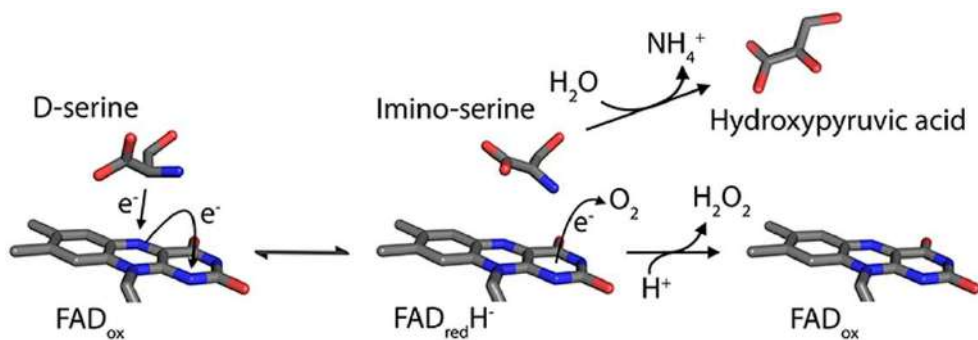


Figure 1. Schematic reaction of D-amino acid oxidase (Sacchi et al., 2018).

During the years, DAAO has been extensively investigated and soon became the prototype of FAD-containing oxidases (Curti et al., 1992). All the chemical aspects of the flavoenzyme reactivity and its biochemical properties were described in detail between 1950 and 1980 using the proteins purified from pig kidney (pkDAAO), *Rhodotorula gracilis* (RgDAAO) and *Trigonopsis variabilis* (TvDAAO) which 3D structures were solved in 1996 and 2000 (Mattevi et al., 1996; Mizutani et al., 1996; Umhau et al., 2000). Less was known at that time about the human enzyme although in humans the DAAO activity was detected in the central nervous system (CNS) for the first time in 1966 (Neims et al., 1966) and the DAAO gene was cloned in the 1980s (Momoi et al., 1988), the recombinant protein was purified and partially characterized in 2000 (0.3-0.5 mg protein/L culture medium) (Raibekas et al.,

2000). Significant improvement in the purification procedure (4 mg/L) together with a more detailed characterization was obtained in 2006 (Molla et al., 2006) and the 3D structure of hDAAO was published in the same year (Kawazoe et al., 2006). The physiological role of human DAAO (hDAAO) remained elusive until 1992, when substantial amounts of free D-amino acids were detected in the brain and other tissues by novel sensitive analytical methods (Hashimoto et al., 1992; Hashimoto et al., 1993; Nagata et al., 1992a; Nagata et al., 1992b). Subsequently several studies were conducted with the aim to identify specific physiological roles for D-amino acids and the role of DAAO in their metabolic control (Wang et al., 2000; Wolosker et al., 2002; Fuchs et al., 2005). The elucidation of the physiological functions of DAAO was also due to the use of the mutant ddY/DAAO^{-/-} mice strain expressing the inactive G181R variant (Konno & Yasumura, 1983): large amounts of D-amino acids were present in the urines and tissues of these animals. In particular, D-serine (D-Ser) levels were increased (10-fold) in brain regions where DAAO is expressed (Konno & Yasumura, 1983). Interestingly, also the occupancy of the N-methyl-D-aspartate receptors (NMDAr) glycine modulatory site and the NMDAr activity appeared to be enhanced, thus suggesting a putative regulative role for DAAO on the degradation of this D-AA and consequently on NMDAr mediated neurotransmission (Konno & Yasumura, 1983). Subsequently, the endogenous distribution of this D-amino acid in the brain appeared to be strictly related with the NMDAr one (Hashimoto et al. 1993; Schell et al., 1995). This observation provided the evidence that it might act as a neuromodulator of glutamatergic neurotransmission (Figure 2) (Mothet et al., 2000). NMDAr are the most important synaptic receptors in the CNS: distributed throughout the brain, they play a major role in glutamatergic synaptic transmission (Wenthold et al., 2003).

The NMDAr are known as “coincidence detectors” because of their requirement for more than one agonist to operate: the receptor channel is blocked by Mg²⁺, depolarization removes this block and enables ion flux when the receptor binds both glutamate (on NR2 subunit) and a co-agonist (on NR1

subunit) (Kemp & McKernan, 2002; Prybylowski & Wenthold, 2004; Inanobe et al., 2005). The regulation of NMDAr transmission by a second agonist may be considered a mechanism to protect against the effects of overstimulation of the NMDAr (excitotoxicity) (Johnson & Ascher, 1987; McBain et al., 1989; Wenthold et al., 2003; Fuchs et al., 2011). Co-agonist binding increases the receptor's affinity for glutamate, decreases its desensitization and promotes NMDAr turnover by internalization.

In the brain, D-Ser is synthesized in neurons from the L-enantiomer precursor by the PLP-dependent enzyme Serine Racemase (SR, E.C. 5.1.1.18) (Wolosker et al., 1999) and is degraded either by SR itself (through an $\alpha\beta$ -elimination reaction) and DAAO (Foltyn et al., 2005; Pollegioni & Sacchi, 2010) .

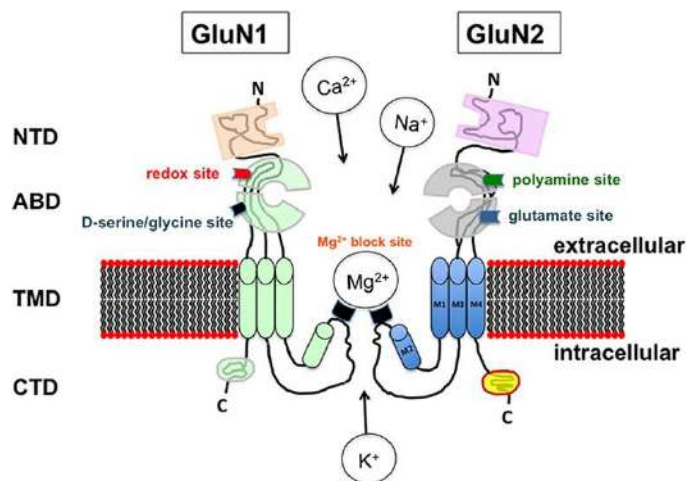


Figure 2. Schematic representation of the NMDAr. Glutamate and D-Ser bind to the GluN1 and GluN2 subunit, respectively, of the agonist-binding domain (ABD) on the extracellular segment, which also includes the N-terminal domain (NTD), the redox and polyamine regulatory sites. The transmembrane domain (TMD) contains the ion channel and the site for the magnesium blockade. The C-terminal domain (CTD) is located on the intracellular side of the membrane (Billard, 2018).

According to the so call “serine shuttle” model (Figure 3), once D-Ser is released by neurons, it is taken up by the surrounding astrocytes for storage and subsequent activity-dependent release (Wolosker, 2011; Wolosker & Radzishevsky, 2013). Considering the poor expression of SR in astrocytes, in these cells DAAO is the main enzyme responsible for the degradation of D-

Ser. Thus the flavoenzyme can indirectly control the concentrations of D-Ser at the synapses and consequently regulate the activation of NMDAr by modulating the availability of the neuromodulator at the coagonist binding-site (Wolosker, 2011).

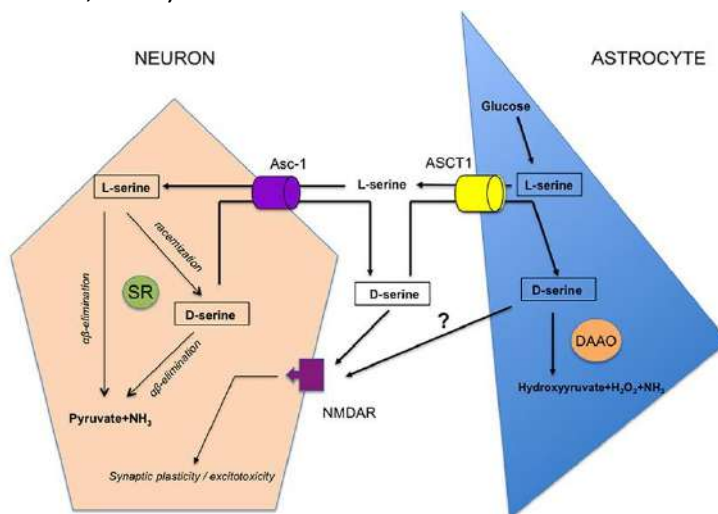


Figure 3. The serine shuttle model. L-serine is synthesized from glucose in the astrocytes and released through the ASCT1 transporter. It is then taken-up by neurons through the Asc-1 transporter where it is converted to D-Ser by SR. D-Ser is released in the extracellular space through Asc-1 and taken-up through ASCT1 by astrocytes where it is degraded by DAAO (Wolosker, 2011). Figure from (Billard, 2018).

1.1 Physiological and pathological role of DAAO

Putative *DAAO* genes have been identified in all kingdoms; the main exception is represented by plants. The residues of the active-site and those interacting with the cofactor are highly conserved across species. DAAO plays several roles in different organisms. In microorganisms, it plays a key role in the catabolism of D-AAAs: they may represent a carbon, nitrogen and energy source. In invertebrates and lower vertebrates it has diverse and specific functions, such as the biosynthesis of eye pigment in *D. melanogaster*, the regression of the tail in amphibians, and the intestinal adsorption of D-AAAs in birds (Pollegioni et al., 2007). In humans, *DAAO* gene is encoded in a single copy in the genome on chromosome 12 (region 12q23-24) (Konno, 2001) and

it is constituted by 11 exons and 10 introns and covers 20 kb (Figure 4) (Fukui & Miyake, 1992).

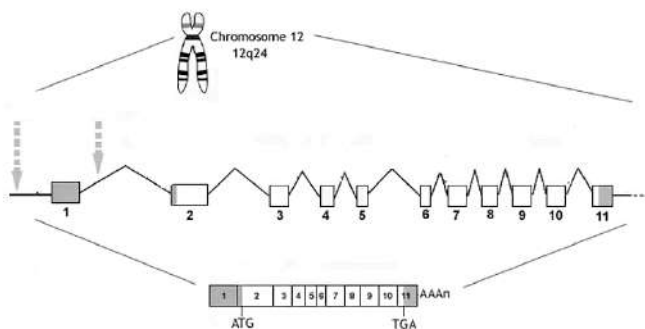


Figure 4. The *DAAO* gene and transcript. The *DAAO* gene is located on 12q24 region. It includes 11 exons (numbered). The 5' untranslated region (shaded gray) is on exon 1 and part of exon 2, exons 2-11 encode the open-reading frame, and the 3' untranslated region (shaded gray) is located on exon 11. The long grey dashed arrow indicates the transcriptional start site (exon 1) and the GC box, cAMP-responsive element, and sterol-dependent repressor sequences. The short grey dashed arrow indicates the additional regulatory sequences, three TATA boxes and a transcription-enhancing CAAT box. Figure modified from (Verrall et al., 2010).

The overall AA sequence is well conserved among the mammalian DAAOs (Pollegioni et al., 2007). The protein is highly expressed in liver, kidney, and brain (Figure 5). In liver and kidney DAAO is responsible for the detoxification and degradation of D-amino acids originating from the cell wall of intestinal bacteria, from diet and endogenous racemization. Interestingly, the urine of *ddY/DAAO^{-/-}* mice was reported to contain abnormally high amounts of D-AAs, thus confirming this hypothesis (Koibuchi et al., 1995; Sasabe et al., 2014). In kidney the enzyme is expressed in proximal tubule cells and is associated with renal damage due to the nephrotoxicity caused by the production of H₂O₂ during the elimination of D-Ser and D-proparglyglycine mediated by DAAO (Konno et al., 2000; Maekawa et al., 2005). Accordingly, renal ROS levels are strongly affected by DAAO activity: the injection of high doses of D-Ser in rats causes massive and generalized aminoaciduria, glucosuria, and proteinuria, due to the oxidative stress generated in tubule cells (Krug et al., 2007).

Notably, it has been recently proposed that in kidney and brain DAAO could take part in a new pathway (DAAO/3-MST) linked to hydrogen sulfide (H₂S) production (Shibuya et al., 2013): DAAO degrades D-cysteine (D-Cys) yielding 3-mercaptopyruvate, which is converted to H₂S by the mitochondrial 3-mercaptopyruvate sulfurtransferase (3MST). It is known that H₂S could affect the release of renin regulating kidney excretory function and blood pressure (Shibuya & Kimura, 2013). Interestingly, in the brain H₂S act as an endogenous gaseous transmitter which is able to modulate synaptic signaling by activating NMDAr in neurons, as well as astrocytes that surround the synapse (Abe & Kimura, 1996; Nagai et al., 2004).

The DAAO expression has been also reported on the surface of human neutrophilic leucocytes, where the enzyme, together with the myeloperoxidase, may generate H₂O₂ upon the oxidation of D-Ala derived from bacterial peptidoglycan, thus playing a protective role against infections (Robinson et al., 1978). These findings were supported by the observation that, compared to the wild-type mice, the *ddY/DAAO*^{-/-} are more susceptible to *S. aureus* infection (Nakamura et al., 2012).

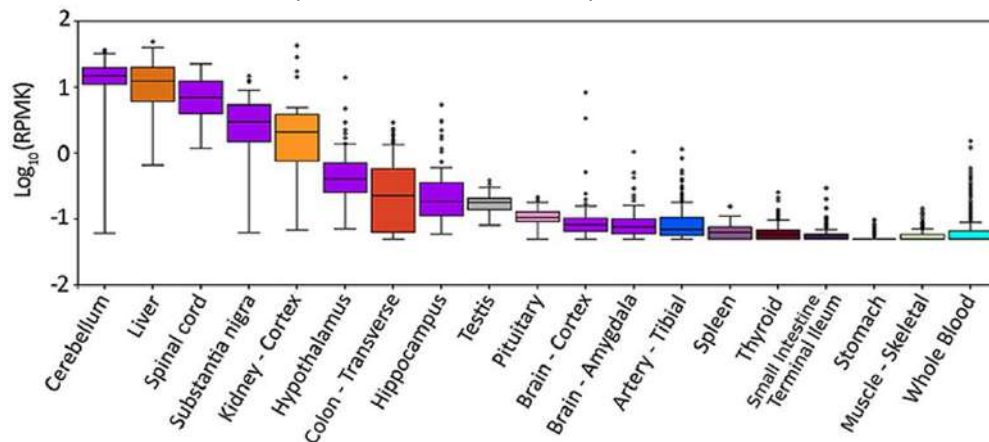


Figure 5. Schematic representation of expression pattern of *DAAO* gene in different human tissues. Values are shown as logarithm of RPKM value (reads per kilobase of transcript per million mapped reads). The data presented in this plot were obtained from the Genotype-Tissue Expression (GTEx) Project Portal (<https://www.gtexportal.org/home/gene/DAO>) (Molla, 2017).

Recently, it has been proposed that in mice hDAAO could be secreted into the lumen by intestinal epithelial cells, where the enzyme could control the composition of gut microbiota (Sasabe et al., 2016): both DAAO protein and activity were detected in the villus epithelium of the proximal and middle small intestine of mice and humans. A processed form of the murine protein appeared to be secreted by goblet cells, likely due to the presence of a signal peptide and a predicted cleavage site near the N-terminus (Sasabe et al., 2016). Host DAAO has been proposed to be induced and released as a response to certain intestinal microbiota to react to microbial metabolites. Indeed, several free D-AAs (known as DAAO substrates) are released in the colonic lumen by commensal microbiota activity (Matsumoto et al., 2018). The H_2O_2 produced by DAAO reaction could thus exert a dual role: in host defense limiting colonization of pathogenic bacteria, and in controlling microbiota composition since certain bacteria receive benefits from D-AAs for their growth (Sasabe et al., 2016).

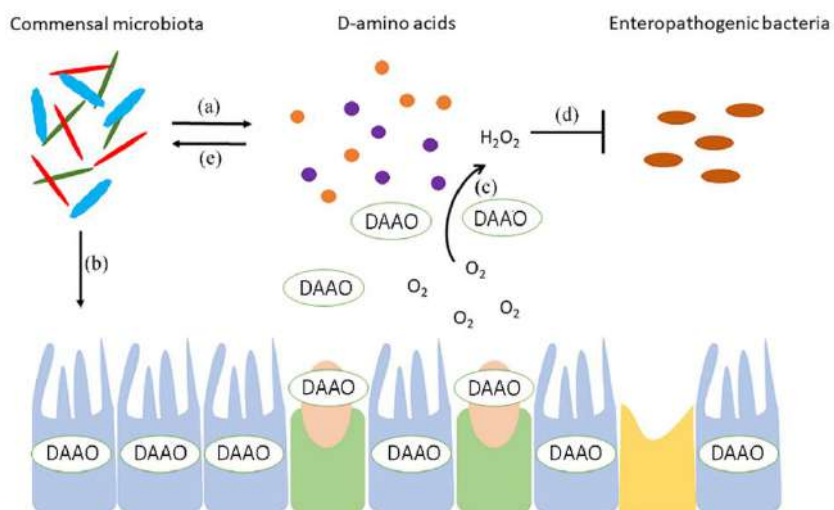


Figure 6. A model of intestinal epithelial homeostasis established by the interplay of D-AAs and DAAO, proposed by (Sasabe et al., 2016). Commensal microbiota produce free D-AAs (a). The microbiota induces production of DAAO by the intestinal epithelium (b) which is secreted into the lumen by goblet cells and oxidizes mucosal D-AAs (c). Hydrogen peroxide produced by DAAO reaction protects the proximal intestinal mucosa from enteropathogens (d) and modulates the composition of gut microbiota (e).

In the CNS DAAO degrades D-Ser, and hDAAO expression is complementary to the observed levels of the coagonist: the enzyme is detected in the cerebellum and brainstem (where D-Der levels are low) while its expression is lower in the forebrain (where D-Ser concentration is higher) (Horiike et al., 1994; Verrall et al., 2007; Madeira et al., 2008). Recently, hDAAO activity has been confirmed in the forebrain. It has also been identified in the corticospinal tract of the white matter and in the motor pathway of the gray matter at astrocytic level, where the enzyme activity could prevent excitotoxicity due to an overactivation of the NMDAR-mediated transmission (Sacchi et al., 2011; Sasabe et al., 2014). Furthermore, the flavoenzyme activity was detected in dopaminergic neurons of the nigrostriatal system (Sasabe et al., 2014). Here, hDAAO efficiently metabolizes D-DOPA, which is converted to dihydroxyphenylpyruvic acid and then transaminated to L-DOPA, thus affecting the metabolism of dopamine, norepinephrine and epinephrine.

From a pathological point of view, an anomalous activity of the enzyme might produce remarkable alterations in D-Ser concentration in the brain, and consequently in NMDAR functioning. Notably, such a dysfunction has been proposed as one of the mechanisms that concur to the settle of various pathologies such as amyotrophic lateral sclerosis, Alzheimer's disease, schizophrenia, etc. (Verrall et al., 2007; Billard, 2008; Madeira et al., 2008; Wolosker et al., 2008; Verrall et al., 2010).

Recently, DNA variants located on *DAAO* gene have been associated to the outcome of familial amyotrophic lateral sclerosis (fALS) (an adult-onset neurodegenerative disease caused by the loss of motor neurons): the R199W substitution in hDAAO has been correlated to the onset of the pathology (Mitchell et al., 2010; Cirulli et al., 2015). This substitution abolishes DAAO activity due to protein instability and lower kinetic efficiency on D-Ser (Cappelletti et al., 2015a), promotes the formation of protein aggregates, activates the autophagy system and increases apoptosis in motor neuron cell lines or primary motor neuron cultures (Figure 7) (Paul & De Bellerocche, 2012; Paul et al., 2014). The neurotoxic effect depends from D-Ser: co-

culturing motor neurons with glial cells expressing R199W hDAAO variant was sufficient to induce apoptosis in motor neurons, an effect not observed in the presence of an NMDAR antagonist specific for D-Ser binding-site (Paul et al., 2014). Studies on the recombinant R199W hDAAO variant suggest that the pathological effect of this substitution could be related to D-Ser accumulation due to the loss of function of the catabolic enzyme (Cappelletti et al., 2015a), yielding *in vivo* to an increase in synaptic concentration of the neuromodulator and, as a result, to the overactivation of NMDAR-mediated transmission and the consequent excitotoxicity (Figure 7). Furthermore, the transgenic mouse lines expressing R199W DAAO variant exhibit the same features of the others ALS mice models (SOD1^{G93A} mice) (Kondori et al., 2017). Moreover, both in these mice and in the SOD1^{G93A} models, D-Ser accumulated in the spinal cord and DAAO activity resulted suppressed in the reticulospinal tract (Sasabe et al., 2012).

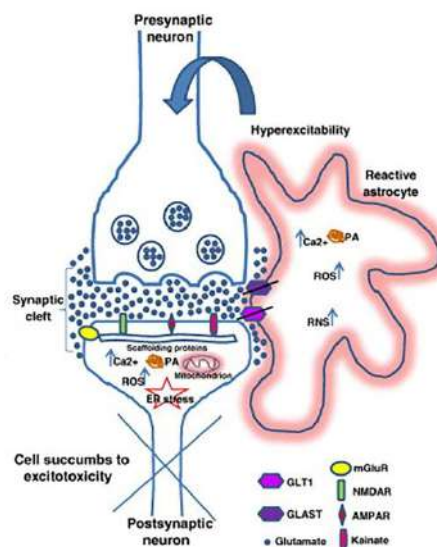


Figure 7. Glutamatergic transmission in ALS. The presynaptic hyperexcitability generates excessive glutamate release from the presynaptic neuron. Moreover, the reduced expression of the glial transporter GLAST/GLT1 causes an increase in the extracellular levels of glutamate, producing an hyperactivation of NMDAR, with a consequent cellular excitotoxicity. Moreover, both neurons and astrocytes accumulate protein aggregates, increased Ca²⁺ and ROS/RNS concentrations. An abnormally high concentration of D-Ser at the synapse would be crucial for these processes to occur. Figure modified from (Spalloni et al., 2013).

Neurodegeneration mediated by NMDAr and D-Ser concentration alterations were also proposed to contribute to Alzheimer's disease (AD) and aging progression and alterations in D-Ser levels were observed in AD patient (Billard, 2008; Madeira et al., 2015). A defective activation of NMDAr, due to decreased level of D-Ser, was shown to occur in aged tissues: the hypoactivation of these receptors might result in a loss of plasticity and cognitive deficits in the aging brain (Ikonomidou et al., 1999). Indeed, increased levels of DAAO have been reported in the serum of patients with mild cognitive impairment or with severe AD. Nevertheless, the role of NMDAr in AD pathogenesis is more complex: excitotoxicity, due to the overstimulation of NMDAr, has been also correlated to the onset of AD (Tannenbergh et al., 2004). Increased D-Ser levels were reported in AD patients (Madeira et al., 2008).

A hypofunction of NMDAr mediated transmission is thought to be possibly involved in schizophrenia, due to a decrease in synaptic D-Ser levels. Interestingly, increased enzymatic activity and gene or protein expression of hDAAO were reported in cerebral cortex, cerebellum, medulla oblongata and choroid plexus of schizophrenic patients (Coyle et al., 2003; Coyle, 2006; Kapoor et al., 2006; Verrall et al., 2007; Burnet et al., 2008; Madeira et al., 2008; Ono et al., 2009; Verrall et al., 2010). Alongside, clinical trials demonstrated the beneficial effects of D-Ser as add-on pharmacotherapy (Heresco-Levy et al., 2005). Moreover, in 2002 the *G72* gene encoding a small protein (pLG72), which is the main interactor of DAAO, was linked to schizophrenia as the *DAAO* gene itself (Chumakov et al., 2002; Sacchi et al., 2016).

1.2 Cellular function and localization of hDAAO

Concerning the subcellular localization of hDAAO, the flavoenzyme contains the PTS1 signal at C-terminus: the peptide Ser-His-Leu which directs its targeting to the peroxisomes (Horiike et al., 1994; Moreno et al., 1999). An intriguing issue concerns the way in which the peroxisomal hDAAO can access D-Ser cytosolic storage: D-Ser could enter to the peroxisomes through a not yet assessed membrane transport mechanism; alternatively, an active

form of DAAO might exist in the cytosol, directly affecting D-Ser cellular concentration. As a matter of fact, an active form of DAAO has been identified in cytosol both in glial cells and neurons (Sacchi et al., 2008; Popiolek et al., 2011; Sacchi et al., 2011). In U87 human glioblastoma cells, the flavoenzyme shows a different distribution dependent on time after transfection: at 24 h, a fraction of active and folded enzyme is largely diffused in the cytosol, where it might interact with different proteins; at 48 h and 72 h after transfection, the signal of the flavoenzyme largely overlapped that of peroxisomes (Sacchi et al., 2011).

Recently, it has been suggested that the flavoenzyme could be mistargeted (to cytosol and nuclei) or secreted: rat DAAO is present both in cytosol and nuclei of proximal tubule epithelial cells after the treatment with the drug propiverine (Luks et al., 2017). A putative nuclear translocation signal (NTS) in the primary sequence of hDAAO that could facilitate nuclear import via importin 7 after the phosphorylation of an TPx sequence has been identified (Chuderland et al., 2008). Moreover, it has been proposed that hDAAO could be secreted into the lumen by intestinal epithelial cells in mice (see above) (Sasabe et al., 2016).

hDAAO subcellular localization has been shown to influence its degradation pathway. hDAAO is a stable protein with a long half-life ($t_{1/2} \sim 60$ h). In U87 cells, the peroxisomal hDAAO is degraded by the lysosomal/endosomal pathway while cytosolic hDAAO is targeted to the proteasome system after ubiquitination (Cappelletti et al., 2014).

1.3 Structural properties of hDAAO

The evidence of the important physiological role played by hDAAO in the metabolism of D-Ser has resulted in an increased interest for this flavoenzyme: during the past few years, the structure and the biochemical properties of hDAAO have been extensively investigated using the recombinant enzyme produced in *E. coli* (Raibekas et al., 2000; Molla et al., 2006a; Romano et al., 2009) and the crystallographic structure has been resolved (Kawazoe et al., 2006, 2007).

From a structural point of view, the human enzyme (347 AA, 40.3 kDa) contains 11 α -helix and 14 β -strands that fold into two interconnected regions: an interface domain, in which a large twisted antiparallel β -sheet forms the active-site roof and part of the oligomerization interface, and a FAD binding site possessing the Rossman fold motif. The loop following the α -helix 2 (58-61), the active site loop (216-228) and the loop between β -strands 13 and 14 (296-303) represents the regions of the protein with the highest conformational diversity. hDAAO shows an active site with a cavity of 220 \AA^3 .

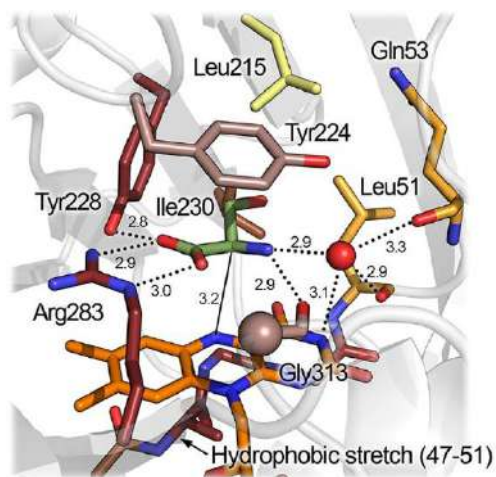


Figure 8. Detail of the active site. The substrate D-Ser was modeled based on the structure of the enzyme in complex with imino-serine (Molla, 2018).

The substrate is located above the *re*-side of the cofactor and interacts with several residues of the active site (Arg283 and Tyr 228 with the α -COOH group, and Gly313 and C(4)=O of the cofactor with the α -NH₂ group) (Figure 8). Moreover, an additional ligand-binding site located at the monomer-monomer interface has been recently identified by computational and labeling studies (Kohiki et al., 2017) (Figure 9A-9B).

The upper part of the active site, where is located the side chain of the substrate is constituted by bulky and hydrophobic residues (Leu51, Gln53, Leu215 and Ile230) (Kawazoe et al., 2006). The less-conserved active-site residue is Leu51, which is the key position determining the substrate specificity. The roof of the active site is formed by the side chain of Tyr224,

that is part of a loop (216-228) that could switch during catalysis from an open to a close conformation, reducing the turnover, increasing the hydrophobicity of the active site and allowing hDAAO to bind larger substrates (Molla et al., 2006; Kawazoe et al., 2007).

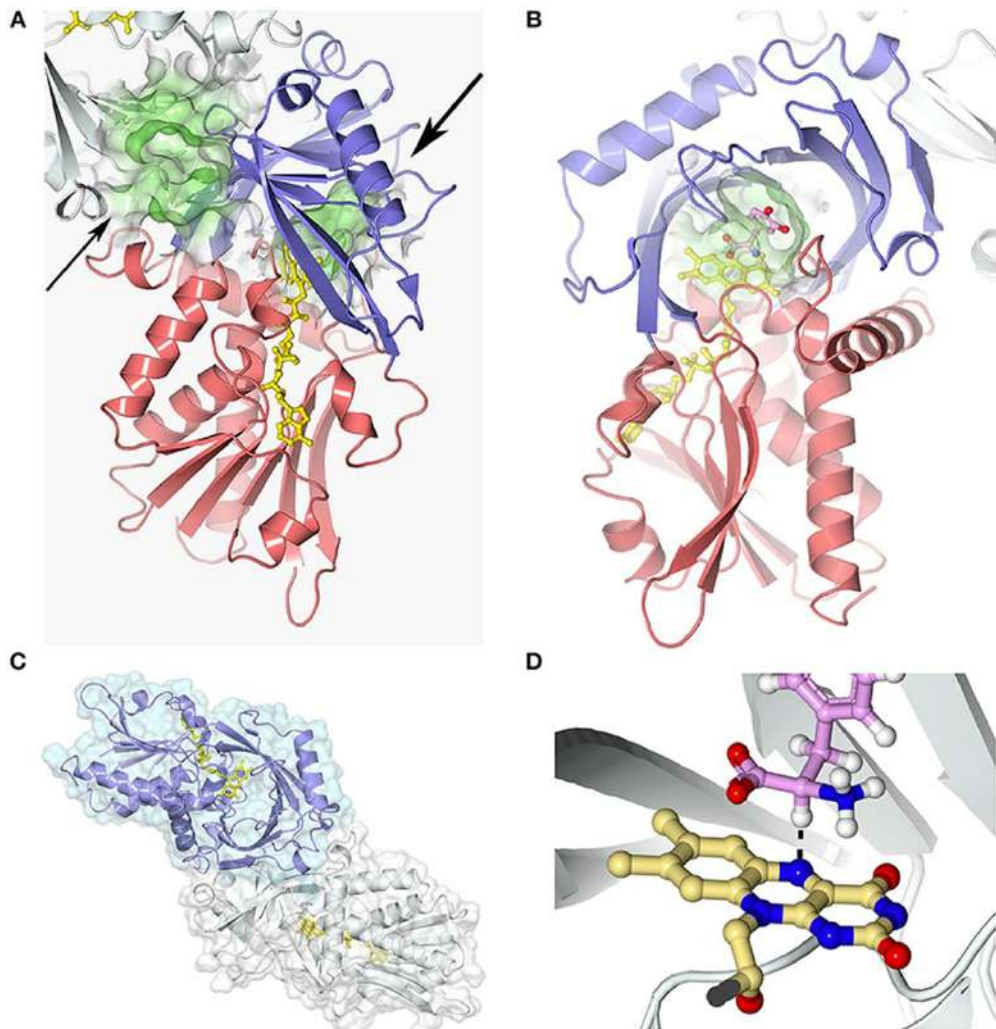


Figure 9. 3D structure of hDAAO (PDB 2e49). **A.** A monomer of hDAAO is constituted by two domains: the substrate (blue) and the FAD binding domain (red). The large arrow indicates the entrance of the active-site while the thin one indicates the additional-binding site proposed by (Kohiki et al., 2017). **B.** hDAAO active-site architecture. **C.** Oligomerization mode of hDAAO. **D.** Schematic representation of the substrate dehydrogenation during the reaction catalyzed by hDAAO. Figure prepared with 3dproteinimaging.com (Pollegioni et al., 2018).

hDAAO belongs to the FAD-containing flavooxidases family, of which exhibits the well-known properties: it stabilizes the anionic semiquinone, it is able to covalently bind sulfite, in anaerobic condition it is fully reduced after adding the substrate, and the FADH₂ is highly reactive with oxygen (Pollegioni et al., 2007). However, hDAAO shows some peculiar features that distinguish it from other DAAOs.

Mammalian DAAOs are different in their oligomerization state: for the porcine enzyme (pkDAAO) it is dependent on the concentration in solution (in the crystal, the enzyme is a homodimer containing a molecule of noncovalently bound cofactor per subunit, whereas in solution it exists as a mixture of monomers, dimers, and even higher molecular aggregates in equilibrium, depending mainly upon the protein concentration and the presence of ligands; the apoprotein is monomeric); rat DAAO is always monomeric; hDAAO is a stable head-to-head homodimer (Figure 9C) (80 kDa) in both the holo- and the apoprotein form (Mattevi et al., 1996; Molla et al., 2006b; Pollegioni et al., 2007; Frattini et al., 2011). The rationale of this characteristic is in a different charge distribution at the dimer interface in hDAAO compared to pkDAAO (negatively and positively charged, respectively) (Figure 10) due to a higher substitution frequency of the residues of the interface region compared to the overall protein (33% vs 15%) (Kawazoe et al., 2006). Interestingly, the monomeric ratDAAO shows the substitution of three residues at the protein interface (His78, Arg120 and Gln234 in human enzyme are replaced by Cys77, Ser119 and Lys233 in ratDAAO) that fully abolished the protein ability to dimerize

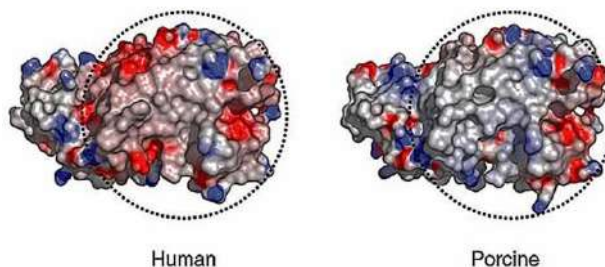


Figure 10. The monomer-monomer interface of hDAAO is negatively charged while that of pkDAAO is positively charged. The surface is colored from blue (positive) to red (negative). Figure modified from (Kawazoe et al., 2006).

In particular, Arg120 in the human enzyme highly stabilizes the monomer-monomer interface (Frattini et al., 2011). Arg120 belongs to α -helix 6. It is involved in electrostatic interactions with the carboxylic group of D73 (α -helix 3) and hydrogen-bonded to the backbone C=O groups of D109 (α -helix 5), T110 and V111 (loop between α -helix 5 and β -strand 4) located at the interface of the opposite monomer.

1.3.1 FAD binding

The cofactor, bound in a non-covalent way, is located at the interface of the two domains, buried in the protein core in an elongated conformation, with the *re*-face in the inner part of the active site (Kawazoe et al., 2006; Molla, 2017). While the conformation of the residues located at the *re*-face of the flavin ring is highly conserved, at the *si*-face the conformation of the hydrophobic stretch (47-VAAGL-51) differs between the human and porcine enzymes, causing the loss of the H-bond established between Ala49 and N(5) of the cofactor and decreasing the strength of the interaction and the rate of flavin reduction (see below) (Figure 11) (Kawazoe et al., 2006).

The binding of the flavin cofactor to the human enzyme is the weakest among known DAAOs ($K_d = 8.0 \mu\text{M}$), but the presence of a ligand in the active site stabilizes the flavin interaction ($K_d = 0.3 \mu\text{M}$) (Molla et al., 2006; Caldinelli et al., 2010). Because of the low interaction with FAD and the *in vivo* concentration of the cofactor (2 - 5 μM), the hDAAO is present in solution as an equilibrium of holo- and apoprotein forms, with the latter one predominant in absence of an active-site ligand (Caldinelli et al., 2010).

The holoenzyme reconstitution follows a sequential process: in the first step, the apoprotein quickly recovers the activity due to the binding with the cofactor; in the second step, slower than the first one, a conformational change led to the generation of the final conformation.

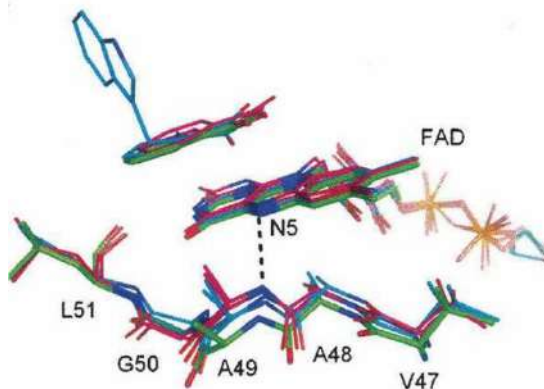


Figure 11. Conformational variability of the hydrophobic stretch (VAAGL, residues 47–51) at the *si*-face of the flavin ring of human (carbons in green) and porcine (carbons in magenta) DAAO. Figure modified from (Kawazoe et al., 2006).

1.3.2 Kinetic mechanism and substrate preference

The oxidative deamination catalyzed by hDAAO follows a sequential kinetic mechanism, in which the substrate dehydrogenation proceeds by directly transferring of an hydride, i.e. the α -hydrogen from the α -carbon of the substrate, to the flavin N(5) (Figure 9D). The first reductive-half reaction (the conversion of the D-amino acid into the planar imino acid together with the flavin reduction) is very fast ($117 \pm 6 \text{ s}^{-1}$ on D-Ser), more than the turnover ($6.3 \pm 1.4 \text{ s}^{-1}$). The rate limiting step in DAAO catalysis is the product release, since the conformational change of the active site loop (217-227) acting as a lid and allowing the product/substrate exchange is relatively slow (Molla et al., 2006). The rate of the release of the imino acid product from the reduced enzyme is very slow ($< 1 \text{ s}^{-1}$); therefore, the reoxidation step does not start from the free enzyme but from the reduced enzyme-imino acid complex with a second-order reaction corresponding to $1.25 \times 10^5 \text{ M}^{-1} \text{ s}^{-1}$ (Molla et al., 2006; Molla, 2017).

The human enzyme shows a broad substrate preference due to the plasticity of the active site lid: the favorite substrates are bulky hydrophobic D-amino acids (D-DOPA, D-Phe, D-Tyr, D-Trp), followed by the small uncharged ones (D-Ala, D-Pro, D-Ser). The D-DOPA can be converted into the L-enantiomer (then used to synthesize dopamine) by the reactions of DAAO and a

transaminase. As shown by (Kawazoe et al., 2007), the apparent maximal activity, as well as the catalytic efficiency, is the greatest among tested D-amino acids (Table 1) but the oxidation of this compound is hampered by the observed substrate inhibition effect (K_i 0.5 mM). Very small or acidic amino acids are not or are poorly degraded by the flavoenzyme (Table 1) (Molla et al., 2006; Kawazoe et al., 2007).

Table 1. Substrate preference of hDAAO. The apparent kinetic properties determined on several D-amino acids.

	k_{cat} (s^{-1})	K_m (mM)	k_{cat}/K_m ($s^{-1} mM$)
D-DOPA³	21.7	1.5 (K_i 0.5)	14.5
D-Tyr³	14.8	1.1	13.4
D-Ser	3.0 ¹	7.5 ¹	0.4 ¹
	4.0 ³	3.9 ³	1.0 ³
D-Phe³	15.5	1.2	12.9
D-Pro¹	10.2	8.5	1.2
D-Ala¹	5.2	1.3	4.0
D-Asp¹	6.7	2000	<0.01
Gly¹	0.9	180	<0.01

¹(Molla et al., 2006); ²(Caldinelli et al., 2010); ³(Kawazoe et al., 2007)

1.4 Modulation of hDAAO activity

The substrate promiscuity of hDAAO supports the hypothesis that this flavoenzyme might play different roles in different cells and tissues. The flavoenzyme activity must be finely tuned to fulfill what is thought to be its most important function in the brain.

1.4.1 By protein interaction

The functionality of the human enzyme is modulated *in vivo* by other proteins. hDAAO interacts with the Pex5p receptor, which is involved in peroxisomal protein import and in the assembly of functional peroxisomes, through the C-terminal PTS1 peroxisomal-targeting signal (Ghosh & Berg, 2010).

The second hDAAO partner is pLG72, a primate-specific protein (153 residues, 18.1 kDa) encoded by the *G72* gene, which has been associated by genome-wide association and meta-studies with schizophrenia and other psychiatric disorders (Chumakov et al., 2002; Sacchi et al., 2016; Pollegioni et al., 2018). The interaction between the two human proteins was confirmed *in vitro* using the recombinant enzymes: gel-permeation chromatography and surface-plasmon experiments demonstrated that hDAAO interacts with pLG72, yielding the formation of a 200 kDa complex. The interaction does not modify the kinetic parameters of hDAAO or its binding to the cofactor, but alters its tertiary structure, causing a time-dependent loss of activity (Sacchi et al., 2008; Caldinelli et al., 2010). Recently, low-resolution technique experiments (limited proteolysis coupled to mass spectroscopy and cross-linking analysis) allowed the identification of the structural determinants of the proteins involved in forming the interface surface in hDAAO-pLG72 complex: it has been suggested that the N-terminal region could play an important role in the formation of the complex (Birolo et al., 2016; Sacchi et al., 2017).

The role of pLG72 interaction was investigated at cellular level using U87 cells expressing hDAAO and pLG72: D-Ser levels decreased in U87 overexpressing hDAAO while the co-expression of pLG72 restored D-Ser concentration, confirming that pLG72 acts as a negative effector of the human enzyme (Sacchi et al., 2008). On the other hand, pLG72 overexpression in U251 cells failed to influence the activity of endogenous hDAAO: in this work hDAAO activity was assayed on D-proline as substrate, which is also oxidized by D-aspartate oxidase (Kvajo et al., 2008). Moreover, pLG72 was found to increase hDAAO activity in kidney-like HEK293 cells, while in neuron-like SH-SY5Y and in astrocyte-like 1321N1 cells there were no significant differences in the flavoenzyme activity, suggesting an intriguing cell-specific hDAAO-pLG72 interaction (Jagannath et al., 2017). *In vivo*, hDAAO is present in peroxisomes and cytosol while pLG72 is localized at mitochondrial level: confocal microscopy and FRET analysis showed that after the synthesis, hDAAO could interact with pLG72 exposed on the cytosolic side of the outer

mitochondrial membrane before the targeting to peroxisomes (Figure 12) (Sacchi et al., 2011).

The degradation pathway of hDAAO and pLG72 was investigated in U87 cells expressing the two proteins: the interaction between these proteins increases the D-Ser level and decreases the half-life of the human flavoenzyme ($t_{1/2} \sim 6$ h). Moreover, pLG72 has been proposed to target the cytosolic form of hDAAO to the ubiquitin-proteasome system for degradation (Sacchi et al., 2008, 2011; Cappelletti et al., 2014). This could represent a regulation process of D-Ser levels in the hindbrain, where DAAO is mainly glial: the interaction between hDAAO and pLG72 induces enzyme inactivation and speeds up its degradation, preserving cytosolic D-Ser and protecting cells from oxidative stress by hydrogen peroxide generated by the flavoenzyme reaction in the cytosol.

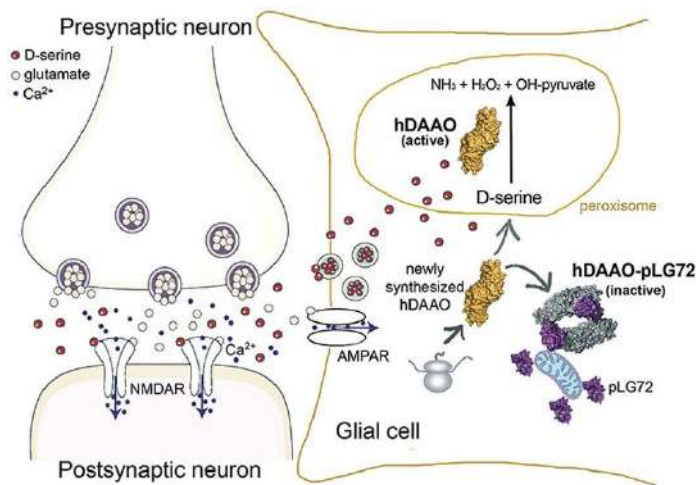


Figure 12. Proposed role of pLG72 on D-Ser metabolism based on its binding to hDAAO (Pollegioni et al., 2018).

Following co-immunoprecipitation experiments in rat cerebellar extracts, the proteins bassoon and piccolo, two cytoskeletal matrix components localized at the presynaptic active zone, have been proposed as DAAO interacting proteins (Popiolek et al., 2011). DAAO was shown to be present in the presynaptic “bouton”, where it can metabolize D-Ser, finely tuning its concentration within the synapse and eventually influencing NMDAR

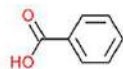
activation. Intriguingly, a molar excess of bassoon (a condition most likely present in the presynaptic active zone) was found to strongly inhibit the activity of the extraperoxisomal form of hDAAO (Popiolek et al., 2011). Indeed, the detection of the enzyme activity in the forebrain, where it is mostly expressed in neurons, has been always difficult, probably due to the inhibitory effect of bassoon (Verrall et al., 2007).

1.4.2 By hDAAO inhibitors

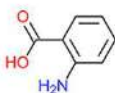
Alterations of D-Ser levels due to an abnormal change in hDAAO activity have been correlated to several disorders, thus the identification of hDAAO inhibitors that could be used as drugs has generated growing interest. hDAAO inhibitors can be classified as substrate competitive inhibitors or as those that do not compete with the substrate (only ADP and CPZ) (Figure 13) (Terry-Lorenzo et al., 2014; Molla et al., 2017). During the past years, more than 500 substrate competitive inhibitors have been identified (Gilson et al., 2016). Analogously to the substrate, these compounds contain a planar portion that interact with the core of the active-site; and a second region which is placed in the substrate side chain binding pocket. hDAAO inhibitors can be divided into several classes (Molla et al., 2017):

- Classical inhibitors, i.e benzoate, anthranilate and improved derivatives, formed by a carboxylic group, that interacts with Arg283, and a single aromatic ring, that interacts with Tyr224 (Katane et al., 2013; Sacchi et al., 2013). The prototype of this class is the compound 5-methylpyrazole-3-carboxylic acid. This compound is able to cross the blood-brain barrier in rats, increasing D-Ser levels in certain areas of the brain and reversing the effect of the dissociative anesthetic PCP (Adage et al., 2008).
- Second-generation inhibitors, i.e. compounds formed by two substituted, heterocyclically fused rings, that bind the residues of the active site with additional van der Waals and H-bond interactions (i.e. 3-hydroxyquinolin-2(1H)-one and CBIO) (Ferraris et al., 2008; Katane et al., 2013). The main limit of this compound is the low ability to pass the blood-brain barriers (Ferraris et al., 2008).

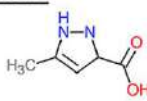
Substrate-competitive hDAAO inhibitors:



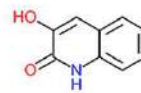
Benzoate



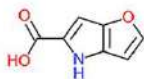
o-Aminobenzoate
(anthranilic acid)



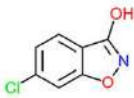
5-Methyl-pyrazole-
3-carboxylate



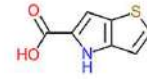
3-Hydroxyquinolin-
2(1H)-one



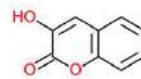
4H-Furo[3,2-b]pyrrole-
5-carboxylic acid



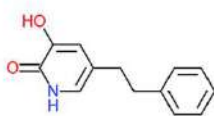
6-Chloro-benzo[d]
isoxazole-3-ol
(CBIO)



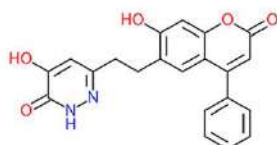
4H-Thieno[3,2-b]pyrrole-
5-carboxylic acid



3-Hydroxy-2H-
chromen-2-one

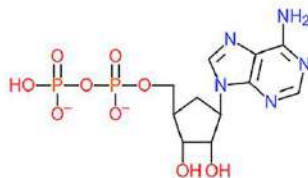


3-Hydroxy-5-(2-phenylethyl)
pyridin-2(1H)-one

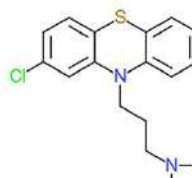


4-Hydroxy-6-[2-(7-hydroxy-2-oxo-
4-phenyl-2H-chromen-6-yl)
ethyl]pyridazin-3(2H)-one

FAD-competitive hDAAO inhibitors:

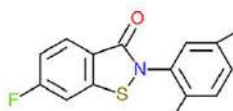


Adenosine diphosphate
(ADP)



Chlorpromazine
(CPZ)

Substrate- and FAD-competitive inhibitor:



2-(2,5-dimethylphenyl)-6-fluorobenzo[d]
isothiazol-3(2H)-on

Figure 13. Structural formula of hDAAO inhibitors classified based on their mechanism of enzyme inhibition (Pollegioni et al., 2018b).

- Third-generation inhibitors, i.e. bulky and flexible compounds that could interact with the subpocket generated by the conformational change of Tyr224 (Kawazoe et al., 2007; Raje et al., 2013; Terry-Lorenzo et al., 2014).
- Novel-generation inhibitors, that interact with the hDAAO-pLG72 complex. A high-throughput screening identified compounds which inhibitory effect was more potent in the presence of pLG72 (class A compounds) and molecules which were 5- to 10-fold less potent in the same condition (class C compounds). All these compounds contain the ebsulfur substructure (2-phenyl-2,3-dihydro-1,2-benzothiazol-3-one) which can interact with the cysteines of hDAAO forming S-S thiol bonds, when the protein is partially unfolded due to the presence of pLG72 (Terry-Lorenzo et al., 2015).

1.4.3 By point substitutions

hDAAO variants corresponding to known single nucleotide polymorphisms (SNPs) or sequence conflicts could be divided into two classes based on their activity: i) hypoactive and ii) hyperactive (Figure 14) (Sacchi et al., 2018). In general, U87 cells overexpressing these hDAAO variants showed a significant alteration in D-Ser cellular levels, suggesting an implication in the susceptibility to neurodegenerative or psychiatric disorders (Caldinelli et al., 2013; Cappelletti et al., 2015).

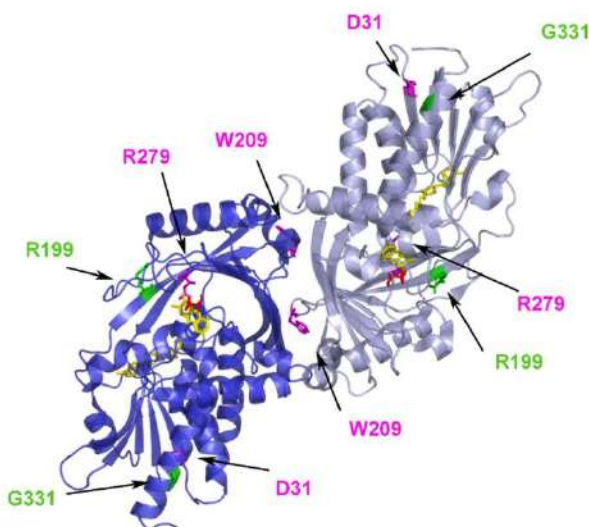


Figure 14. 3D-Structure of hDAAO (PDB 2e49). The residues mutated are shown as sticks in green (hypoactive) and in magenta (hyperactive). FAD is depicted in yellow, the product imino-serine in red. Figure prepared with PyMol.

The inactivating substitutions R199W (the variant associated with the onset of fALS) and R199Q hDAAO variants show a significant modification in protein conformation: altered tertiary conformation of the holoenzyme form, a tetrameric oligomeric state at a concentration > 1 mg/mL and a significant increase in melting temperature related to protein conformation have been reported. The paper from (Cappelletti et al., 2015) provided the rationale for the effect of Arg199 substitution: it significantly affected the ability to bind the flavin cofactor and the substrate, yielding a significant decrease in enzymatic activity (Figure 15); indeed, at 1 mM D-Ser (a concentration similar to that observed in physiological conditions in brain) the activity of R199 variants was negligible (Cappelletti et al., 2015). Arg199 is located on the protein surface, near the isoalloxazine ring of the cofactor, at the center of a network of secondary structure elements belonging to the interface domain (α -helix α 10 and β -strands β 8 and β 12). Moreover, Arg199 interacts with Arg283 and Thr280, important for ligand binding (Cappelletti et al., 2015).

The substitution of glycine located at position 331 with a valine (G331V) causes a change in the C-terminal α -helix and produces an hydrophobic surface, altering the solubility of the enzyme and promoting protein aggregation. Accordingly, human U87 cells expressing this hDAAO variant show a significant decrease in cell viability: at cellular level, this variant is mistargeted forming cytosolic protein aggregates, which largely colocalize with ubiquitin, and resulted in increased protein apoptosis (Caldinelli et al., 2013).

The D31H, W209R and R279A hDAAO hyper-active variants showed, on the other hand, the opposite effect: the introduced substitutions resulted in a significant improved catalytic efficiency (Figure 15) and FAD affinity.

Among these variants, hDAAO W209R, due to the higher affinity for the cofactor binding and the increased amount of the holoenzyme in solution, shows a 2-fold increase in the turnover number compared to the wild-type

enzyme (Figure 15), in particular with D-Ser and FAD concentrations resembling physiological conditions (0.3 mM of D-Ser and 5 μ M of FAD), suggesting a faster rate of imino acid dissociation from the reoxidized enzyme form (Cappelletti et al., 2015). Accordingly, the ability of W209R hDAAO to degrade D-Ser is improved in U87 cells transiently expressing this variant. Moreover, the excessive production of hydrogen peroxide may affect cell viability after stable transfection (Cappelletti et al., 2015). Trp209 is located at the monomer-monomer interface but it is not involved in relevant hydrophobic interactions with the residues belonging the other monomer. The substitution of Trp with an Arg adds an additional electrostatic interaction with Glu85, stabilizing the dimeric structure of DAAO (Cappelletti et al., 2015).

Thermal stability, dimeric oligomerization, binding affinity for the inhibitors and the ability to interact with pLG72 were not altered in D31H and R279A hDAAO variants, while their kinetic efficiency and the affinity for the substrate and the cofactor were increased compared to the wild-type enzyme. While the substitution of Asp31 may affect protein conformation through a general, long-range interactions, the R279A substitution affects the FAD binding affinity through the loss of the H-bond with Pro41, thus altering the conformation of SAP hDAAO region (Caldinelli et al., 2013).

1.4.4 By post-translation modifications

A large number of proteins are subjected to post-translational modifications (PTMs), thus increasing the actual complexity of the proteome. PTMs consist in a modification of the residues of the primary structure and create a much larger array of possible protein species (Walsh et al., 2005). In specific physiological conditions, PTMs play an important role in regulating many biological functions (Walsh et al., 2006), such as protein localization in the cell (Fairbank et al., 2012), protein stability (Maeda et al., 2010) and modulation of enzymatic activity (Audagnotto & Dal Peraro, 2017; Hunter et al., 2009).

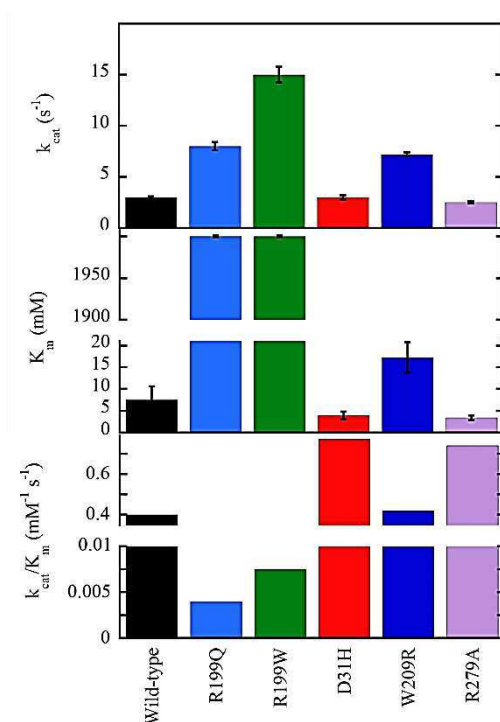


Figure 15. Apparent kinetic parameters of wild-type and hDAAO variants, determined at air saturation (0.25 mM oxygen), 25 °C, and pH 8.5 (Pollegioni et al., 2018b).

A strict regulation of hDAAO activity by post-translational modifications is expected. In particular, at cellular level hDAAO has been proposed to be regulated by nitrosylation: in membrane fractions of glioblastoma cells the activity of DAAO in U87 cells was enhanced by NO in a dose-dependent manner (Shoji et al., 2006). Moreover, also SR appeared to be activated by denitrosylation elicited by D-Ser and to be inhibited by NO (Shoji et al., 2006b). The authors proposed that in astrocytes NO may accelerate D-Ser elimination not only by inhibiting SR but also by enhancing DAAO activity, thus acting as mediator of D-Ser metabolism. Following D-Ser supply from astrocytes to neurons, NO synthesis in neurons may be temporary enhanced. In astrocytes switch-off of D-Ser synthesis may mainly be achieved by neuron-derived NO, which exert the aforementioned dual function (Figure 16) (Shoji et al., 2006a).

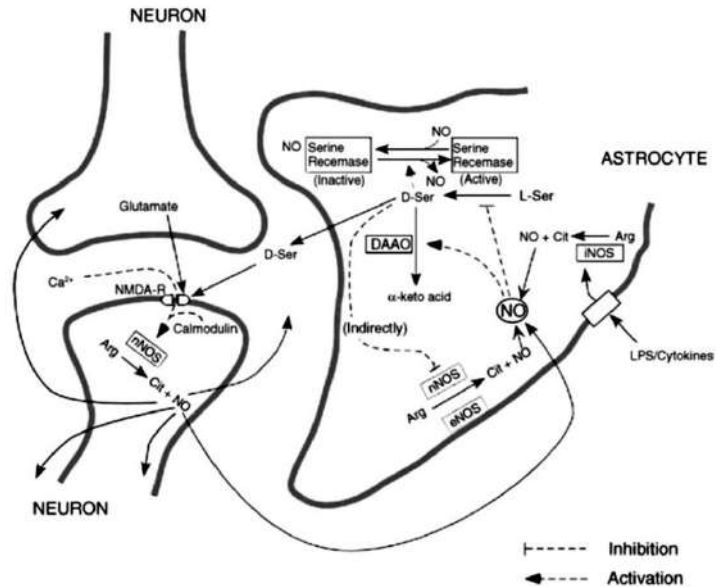


Figure 16. Regulatory loop between D-Ser and NO metabolism. In astrocytes, NO, produced by n/eNOS under normal conditions or by iNOS under inflammatory conditions, inhibit SR activity and enhance hDAAO activity. On the other hand, D-Ser enhances SR and decreases nNOS activity (Shoji et al., 2006a).

1.4.5 By protein mistargeting

hDAAO is a peroxisomal enzyme: it is synthesized in the cytosol and then targeted to peroxisomes. The C-terminal PTS1 sequence is recognized by a specific receptor, Pex5p, which is involved in protein import to peroxisomes, where specific transmembrane transporters mediate the entrance to the matrix (Meinecke et al., 2010; Montilla-Martinez et al., 2015).

Recently, it has been suggested that hDAAO could be mistargeted (to cytosol and nuclei) or secreted: rat DAAO has been identified both in cytosol and nuclei of proximal tubule epithelial cells following treatment with the drug propiverine, an anticholinergic drug used for the treatment of overactive bladder syndrome (Luks et al., 2017). The conventional nuclear import is due to the presence of a nuclear localization sequence (NLS), which is recognized by specific importin which facilitate the passage of proteins through the NPC nuclear complex (Tran & Wentz, 2006). However, other molecular mechanisms permits the entrance of protein to the nucleus. In particular, it

has been identified a putative nuclear translocation signal (NTS), constituted by three residues (SPS) that could facilitate nuclear import via importin 7 after the phosphorylation of the signal sequence (Chuderland et al., 2008). Recently, it has been identified a putative NTS signal in the primary sequence of hDAAO: the T₁₁₈-P₁₁₉-R₁₂₀ sequence (Luks et al., 2017).

Indeed, it has been also proposed that hDAAO could be secreted into the lumen by intestinal epithelial cells in mice (Sasabe et al., 2016). Protein secretion is a multistep process (Pigino et al., 2012): after the synthesis, proteins translocate into the ER lumen, where they are glycosylated and molecular chaperones aid protein folding. The vesicles containing the properly folded proteins then access to the Golgi apparatus, where proteins are further modified. Successively, the proteins in the secretory vesicles are exocytated through a structure called the porosome (Anderson, 2006). Proteins that are designated to the secretory pathway contain a signal peptide, i.e. a short sequence (usually 16-30 amino acids long) present at the N-terminus of newly synthesized proteins (Kapp et al., 2013). There are many proteins which do not use the classical ER-Golgi pathway but follow various nonclassical mechanisms. Unconventional protein secretion is largely triggered by several conditions, ie. cellular stress and inflammation. Unconventional protein secretion includes mechanisms without a signal peptide or a transmembrane domain that help translocation across the plasma membrane (Rabouille, 2017).

In the small intestine, DAAO has been proposed to be secreted in the lumen of human and mice by goblet cells of the villus epithelium, suggesting a role for the flavoenzyme in controlling gut microbiota (Sasabe et al., 2016).

2. Aim

D-amino acid oxidase is a peroxisomal FAD-dependent enzyme that preferentially catalyzes the degradation of small, uncharged D-amino acids (Pollegioni et al., 2007). Alterations in DAAO functionality might be highly relevant in pathological conditions related to the dysregulation of the glutamatergic system. During the past few years hDAAO structural/functional relationships have been investigated using the recombinant protein produced in *E. coli* (Molla et al., 2006; Pollegioni et al., 2007; Sacchi et al., 2012), nevertheless the modulation mechanisms of the enzyme activity remain elusive.

It has been suggested that the flavoenzyme could be mistargeted (to cytosol and nucleus) or secreted. Recent reports on rats demonstrated that DAAO is present both in cytosol and nuclei of proximal tubule epithelial cells following treatment with the drug propiverine (Luks et al., 2017). A putative nuclear translocation signal (NTS) in the primary sequence of hDAAO that could facilitate nuclear import via importin 7 after the phosphorylation of an TPx sequence has been identified (Chuderland et al., 2008). Moreover, it has been proposed that the flavoenzyme could be secreted into the lumen by intestinal epithelial cells in mice. DAAO has been proposed to play a role in controlling the homeostasis of gut microbiota: DAAO protein and activity were detected in the proximal and middle small intestine of mice and humans, associated to the villus epithelium. A processed form of the mouse protein appeared to be secreted in the lumen by goblet cells, likely due to the presence of a signal peptide and a predicted cleavage site near the N-terminus (Sasabe et al., 2016). DAAO was proposed to select the gut microbiota facilitating the elimination of pathologic microbial strains.

Because of the important physiological and pathological role of hDAAO in several tissues, this PhD project was aimed to deepen the investigation on some of the key biochemical properties of the recombinant enzyme, such as its stability (to pH and temperature), the kinetic properties on alternative substrates, the effect of various physiological ligands and of the binding of the flavin cofactor. Subsequently, we studied the effect of single positions in the functionality of the enzyme, focusing on G183R and R120E and R120L

hDAAO variants. The first one is the human counterpart of the natural single-base mutation (yielding the G181R substitution) that in ddY mice inactivates the enzyme and that was used to perform behavioral tests to clarify the role of DAAO in the mechanisms related to NMDA_R transmission. The investigation on the two variants at position 120 (of the TPx sequence) aimed to clarify the role of this residues on the ligand and FAD binding process to the flavoenzyme and of the nuclear translocation due to the presence of the NTS sequence.

Concerning the mistargeting of the flavoenzyme, we started the investigation of the role of the DAAO in gut by studying a variant lacking the N-terminal signal peptide and by employing bioinformatics, biochemical, microbial, cellular and tissue analyses: we suggest that secreted DAAO could not fold and maintain the enzymatic activity following the elimination of the N-terminal sequence and that its ability to select the intestinal microbiota is due to the generation of specific antibacterial peptides by proteolytic digestion of the flavoenzyme.

3. Results



Biochemical Properties of Human D-Amino Acid Oxidase

Giulia Murtas¹, Silvia Sacchi^{1,2}, Mattia Valentino^{2,3} and Loredano Pollegioni^{1,2*}

¹ Dipartimento di Biotecnologie e Scienze della Vita, Università degli Studi dell'Insubria, Varese, Italy, ² The Protein Factory, Politecnico di Milano and Università degli Studi dell'Insubria, Milan, Italy, ³ Sezione Adolfo Quilico, Istituto di Chimica del Riconoscimento Molecolare, CNR, Milan, Italy

OPEN ACCESS

Edited by:

Andrea Mozzarelli,
Università degli Studi di Parma, Italy

Reviewed by:

Mariarita Bertoldi,
University of Verona, Italy
Willem J. H. Van Berkel,
Wageningen University and Research,
Netherlands

Robert Stephen Phillips,
University of Georgia, United States

*Correspondence:

Loredano Pollegioni
loredano.pollegioni@uninsubria.it

Specialty section:

This article was submitted to
Structural Biology,
a section of the journal
Frontiers in Molecular Biosciences

Received: 19 September 2017

Accepted: 05 December 2017

Published: 15 December 2017

Citation:

Murtas G, Sacchi S, Valentino M and
Pollegioni L (2017) Biochemical
Properties of Human D-Amino Acid
Oxidase. *Front. Mol. Biosci.* 4:88.
doi: 10.3389/fmolb.2017.00088

D-amino acid oxidase catalyzes the oxidative deamination of D-amino acids. In the brain, the NMDA receptor coagonist D-serine has been proposed as its physiological substrate. In order to shed light on the mechanisms regulating D-serine concentration at the cellular level, we biochemically characterized human DAAO (hDAAO) in greater depth. In addition to clarify the physical-chemical properties of the enzyme, we demonstrated that divalent ions and nucleotides do not affect flavoenzyme function. Moreover, the definition of hDAAO substrate specificity demonstrated that D-cysteine is the best substrate, which made it possible to propose it as a putative physiological substrate in selected tissues. Indeed, the flavoenzyme shows a preference for hydrophobic amino acids, some of which are molecules relevant in neurotransmission, i.e., D-kynurenine, D-DOPA, and D-tryptophan. hDAAO shows a very low affinity for the flavin cofactor. The apoprotein form exists in solution in equilibrium between two alternative conformations: the one at higher affinity for FAD is favored in the presence of an active site ligand. This may represent a mechanism to finely modulate hDAAO activity by substrate/inhibitor presence. Taken together, the peculiar properties of hDAAO seem to have evolved in order to use this flavoenzyme in different tissues to meet different physiological needs related to D-amino acids.

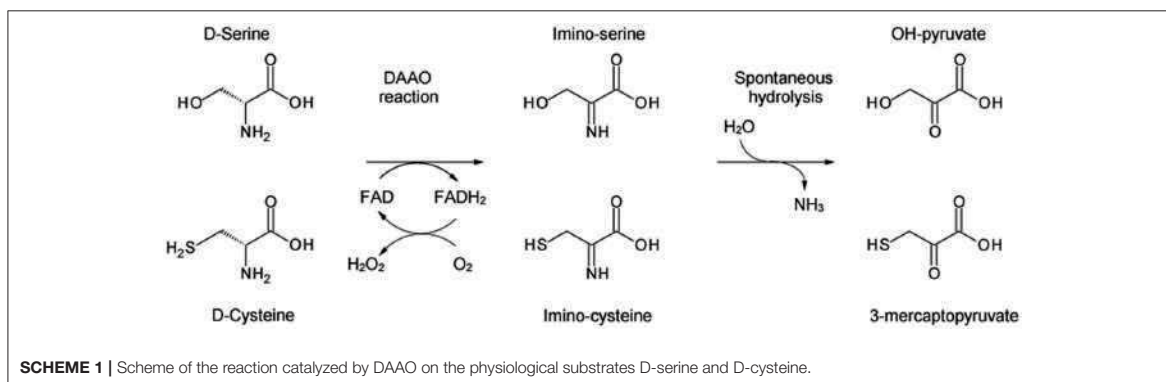
Keywords: D-serine, D-amino acid oxidase, D-cysteine, substrate specificity, structure-function relationships

INTRODUCTION

D-amino acid oxidase (DAAO, EC 1.4.3.3) is the FAD-containing enzyme that catalyzes the strictly stereospecific oxidative deamination of the D-isomer of neutral amino acids. Since its discovery in pig kidney (Krebs, 1935), DAAO has been widely studied as a prototype of FAD-dependent oxidases (Mattevi et al., 1996; Pilone, 2000). D-Amino acids are oxidized by DAAO to give the corresponding imino acids (subsequently non-enzymatically hydrolyzed to α -keto acids and ammonia) and hydrogen peroxide (which is generated during the reoxidation of FADH₂ on molecular oxygen (Scheme 1).

DAAO plays various roles in different organisms: in microorganisms it catalyzes the catabolism of D-amino acids for cell metabolism, and specific functions have been proposed in nematodes, insects, and lower vertebrates (Pollegioni et al., 2007; Saitoh et al., 2012). In higher vertebrates, it

Abbreviations: CBIO, 6-chloro-benzo(d)isoxazol-3-ol; CD, circular dichroism; DAAO, D-amino acid oxidase (EC 1.4.3.3); DOPA, 3,4-dihydroxyphenylalanine; hDAAO, human D-amino acid oxidase; L-NAC, N-acetyl-L-cysteine; NMDAR, N-methyl-D-aspartate subtype of glutamate receptor.



was thought to have a detoxifying function in catabolizing exogenous D-amino acids. In the last few years, however, a key role in the metabolism of D-amino acids with specific physiological function has come into play. In mammals, DAAO is mainly present in kidney, liver, and brain. In the latter, D-serine is the most abundant D-amino acid (Weatherly et al., 2017). D-Serine binds to N-methyl-D-aspartate-type glutamate receptor (NMDAR) - specifically at the “strychnine-insensitive glycine modulatory site” (Mothet et al., 2000). In the brain, NMDARs are involved in main physiological processes such as development, neuronal cell migration, plasticity, learning and memory (Wolosker et al., 1999, 2008; Mothet et al., 2000; Snyder and Kim, 2000; Foltyn et al., 2005; Martineau et al., 2006). In the central nervous system (CNS) DAAO gene and protein expression show an opposite content and distribution when compared with D-serine level (Horiike et al., 1994). The physiological activity of NMDAR is modulated by D-serine cellular concentration, which level is partially controlled by DAAO-induced catabolism (Sacchi et al., 2012).

An excessive production / release of D-serine has been related to acute and chronic degenerative disorders (such as stroke, amyotrophic lateral sclerosis, epilepsy, and Parkinson’s, Alzheimer’s, and Huntington’s diseases); an abnormal decrease in D-serine concentration was instead reported in psychiatric disorders (i.e., schizophrenia and bipolar disorders) (Rossi et al., 2007; Labrie and Roder, 2010; Mustafa et al., 2010; Fuchs et al., 2011; Lu et al., 2011). Here, the R199W mutation in DAAO, yielding a loss of enzymatic activity, has been associated with a familial case of amyotrophic lateral sclerosis (Mitchell et al., 2010) and association studies have linked DAAO (as well as its main modulatory partner pLG72) with schizophrenia susceptibility; (for a review, see Sacchi et al., 2012, 2016).

DAAO is mainly a peroxisomal enzyme (Horiike et al., 1994; Moreno et al., 1999) although an active DAAO form has been identified in the cytosol, both in glial cells (Sacchi et al., 2008, 2011) and neurons (Popiolek et al., 2011). Notably, DAAO was recently reported to be present in cytosol and nuclei of rat proximal tubule epithelial cells treated with propiverine (Luks et al., 2017), too, and to be secreted into the lumen by intestinal epithelial cells (Sasabe et al., 2016).

In past decades, extensive investigations were performed on pig kidney and yeast DAAOs (Pollegioni et al., 1993, 2007). Later on, recombinant human DAAO (hDAAO) expressed in *E. coli* was purified as active holoenzyme (347 residues), containing one molecule of non-covalently bound FAD per 40 kDa-protein monomer. hDAAO shows the spectral properties of the FAD-containing flavoenzymes (Molla et al., 2006). From a structural point of view, DAAO tertiary structure is made of two domains, each generated by several non-contiguous sequence regions: an interface domain made of a large, twisted, antiparallel β -sheet and a FAD-binding domain possessing the dinucleotide binding motif (Kawazoe et al., 2006).

hDAAO possesses a number of distinctive properties: (a) the weakest interaction with the flavin cofactor among known DAAOs ($K_d = 8 \times 10^{-6}$ M). In the presence of an active site ligand (such as benzoate) a 20-fold tighter interaction with FAD is apparent (Molla et al., 2006). The flavin molecule shows an elongated conformation and it is completely buried in the protein core with the only exception of the isoalloxazine ring, which is accessible to the solvent. The conformation of a short hydrophobic stretch ($^{47}\text{VAAGL}^{51}$) near the *si*-face of the isoalloxazine ring is significantly different between human and porcine DAAO and thus was considered responsible for the comparatively lower FAD affinity of hDAAO (Kawazoe et al., 2006); (b) it exists in solution as an equilibrium between the active holoenzyme and the inactive apoprotein; (c) it is a stable 80-kDa homodimer in both the holo- and the apoprotein form (Molla et al., 2006), whereas all known DAAO apoproteins are monomeric. In the homodimer, the two subunits show a head-to-head mode of interaction, as also observed in other mammalian DAAOs (Mattevi et al., 1996; Pollegioni et al., 2007; Frattini et al., 2011); however, the dimerization interface is mostly positively charged in the enzyme from pig kidney (Mattevi et al., 1996) while in hDAAO it is mainly negatively charged (Kawazoe et al., 2006); (d) its half-life (*in vitro* as well as at the cellular level) and activity are negatively affected by pLG72 binding (Sacchi et al., 2008, 2011; Cappelletti et al., 2014).

The hDAAO reaction follows a sequential kinetic mechanism. The product release from the reoxidized enzyme represents the rate-limiting step, as also observed for pig DAAO; the rate

of flavin reduction is slower for the human enzyme (Molla et al., 2006). Small, uncharged D-amino acids seem the preferred substrates for hDAAO, showing a low substrate affinity and catalytic efficiency on D-serine, the physiological substrate in the brain. The volume of hDAAO active site is $\sim 220 \text{ \AA}^3$. Tyr224 is part of the active site loop: it has been proposed that it switches during substrate binding from an open to a closed conformation and thus to allow the binding of substrates possessing large side chains (Molla et al., 2006; Kawazoe et al., 2007a,b). Indeed, the switch of this loop, which improves the efficiency of the hydride transfer reaction by increasing the hydrophobicity of the active site, represents the rate-limiting step in the kinetic cycle.

Owing to the important physiological and pathological role of hDAAO, we decided to deepen the investigation on some of the key biochemical properties of the recombinant enzyme. The novel information on hDAAO has been discussed with regard to known properties, the final aim being to highlight its peculiar characteristics.

MATERIALS AND METHODS

Enzyme Preparation

Recombinant hDAAO was expressed in *E. coli* cells and purified as reported in Molla et al. (2006) and Romano et al. (2009); 40 μM of free FAD was present during all purification steps. The final enzyme preparation was stored in 20 mM Tris-HCl buffer, pH 8.0, 100 mM NaCl, 10% (v/v) glycerol, 5 mM 2-mercaptoethanol, and 40 μM FAD. hDAAO apoprotein was prepared by overnight dialysis of the holoenzyme against 1 M KBr (Molla et al., 2006). hDAAO concentration was determined based on the extinction coefficient at 445 nm for the holoenzyme ($12.2 \text{ mM}^{-1} \text{ cm}^{-1}$) and at 280 nm for the apoprotein ($75.2 \text{ mM}^{-1} \text{ cm}^{-1}$).

Activity Assay and Kinetic Measurements

DAAO activity was assayed with an oxygen electrode at air saturation, pH 8.5 and 25°C, using 28 mM D-alanine as substrate in the presence of 0.2 mM FAD (Molla et al., 2006). The apparent kinetic parameters were calculated according to a Michaelis-Menten equation using the initial velocity values determined at increasing substrate concentrations, i.e. up to 450 mM D-cycloserine, 90 mM D-cysteine, 90 mM D,L-DOPA and 27.5 mM D-kynurenine. The effect of MgCl_2 and CaCl_2 (1 or 10 mM), of 10 μM ATP or GTP and of both divalent ions and nucleotides was assessed using the standard activity assay.

The same assay was employed to investigate the pH and the temperature effects on the enzyme activity and stability. For pH-stability, residual activity was assayed after 30 or 60 min of incubation at different pH-values in a multicomponent buffer (15 mM Tris-HCl, 15 mM Na_2CO_3 , 15 mM H_3PO_4 , 100 mM KCl, and 1% (v/v) glycerol) (Harris et al., 1999); for the effect of temperature, the incubation was carried out in 10 mM potassium phosphate buffer, pH 8.0, containing 1% (v/v) glycerol, 5 mM 2-mercaptoethanol and 40 μM FAD. The effect of temperature on the rate constant of loss of enzymatic activity was fit based on the Arrhenius equation. To investigate the pH and the temperature effect on enzyme activity, hDAAO activity was assayed at: (a) 25°C, using 200 mM D-alanine in multicomponent

buffer (Harris et al., 2001) containing 40 μM FAD at different pH-values; (b) different temperatures using 28 mM D-alanine in 75 mM sodium pyrophosphate, pH 8.5, containing 200 μM FAD. Experimental data for pH dependence were fit based on the equation for two dissociations ($Y = a + b(10^{\text{pH}-\text{pK}_{a1}})/(1 + 10^{\text{pH}-\text{pK}_{a1}}) + [b - c(10^{\text{pH}-\text{pK}_{a2}})/(1 + 10^{\text{pH}-\text{pK}_{a2}})]$) or three dissociations ($Y = a + b(10^{\text{pH}-\text{pK}_{a1}})/(1 + 10^{\text{pH}-\text{pK}_{a1}}) + [b - c(10^{\text{pH}-\text{pK}_{a2}})/(1 + 10^{\text{pH}-\text{pK}_{a2}}) + [c - d(10^{\text{pH}-\text{pK}_{a3}})/(1 + 10^{\text{pH}-\text{pK}_{a3}})]$) (Harris et al., 2001).

Spectral Measurements

Circular dichroism (CD) spectra were recorded using a Jasco J-815 spectropolarimeter (Jasco Co., Cremella, Italy) in 10 mM Tris-HCl, pH 8.0, 1% (v/v) glycerol, and 40 μM FAD. The cell path length was 0.1 cm for measurements in the 200- to 250-nm region (0.1 mg protein/mL) and 1 cm for measurements in the 250–350 nm range (0.4 mg protein/mL) (Caldinelli et al., 2010).

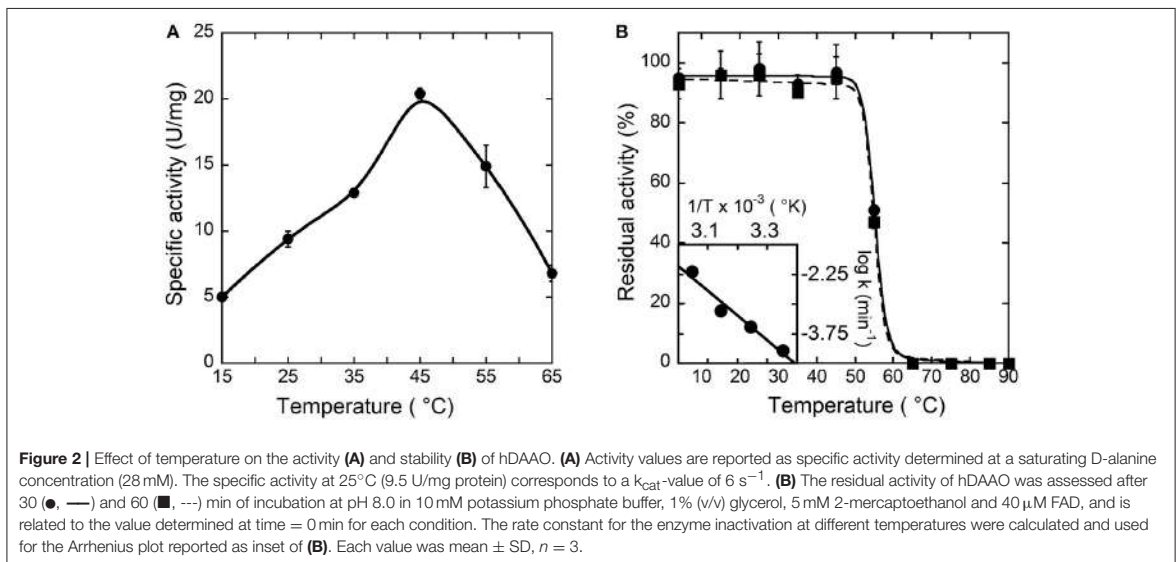
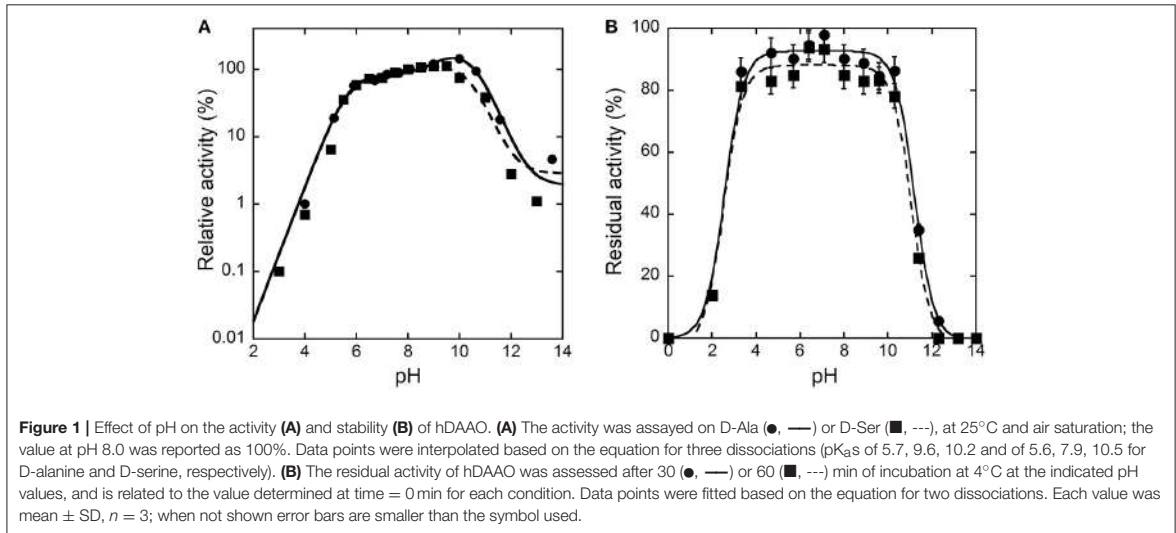
Protein fluorescence spectra were measured at 1 μM protein concentration (0.04 mg/mL) in 20 mM Tris-HCl buffer, pH 8.0, 100 mM NaCl, 10% (v/v) glycerol, 5 mM 2-mercaptoethanol, and 40 μM FAD for the holoenzyme and in 50 mM sodium pyrophosphate, pH 8.3 for the apoprotein; spectra were recorded using a Jasco FP-750 instrument and were corrected for the buffer contribution. Protein fluorescence spectra were recorded between 300 and 400 nm, with excitation at 280 nm. The ligand dissociation constants (K_d) were estimated by titrating 1 μM enzyme with increasing amounts of FAD, benzoate, or C BIO and following the protein fluorescence quenching at 330–340 nm (Molla et al., 2006). The K_d -values for FAD to the hDAAO apoprotein moiety was determined in free form and in complex with benzoate (7 or 70 μM). In all cases, K_d -values were determined using an hyperbolic plot.

RESULTS

Effect of pH and Temperature on hDAAO Activity and Stability

The activity of hDAAO on D-alanine and D-serine increases with pH, reaching a maximal value at pH 10 and 9.5, respectively, and decreases quickly at higher values (Figure 1A). Concerning the pH effect on stability, the activity values determined after 30 or 60 min show that hDAAO is fully stable in a pH range of 4–10 (Figure 1B); experimental values were fitted based on the equation for two dissociations: estimated pK_a 's were 2.5 ± 0.1 and 11.1 ± 0.1 .

To investigate the temperature dependence of the initial rate of the reaction catalyzed by hDAAO, the enzymatic activity was assayed at different temperature values on 28 mM D-alanine (a saturating substrate concentration), at pH 8.5, and in the presence of 200 μM FAD by measuring the O_2 consumption. As shown in Figure 2A, the optimal temperature of hDAAO activity is 45°C. The effect of temperature on the enzyme stability was evaluated assaying the residual activity after 30 or 60 min of incubation. The flavoenzyme was fully stable after 60 min of incubation at 45°C and fully inactivated at $\geq 65^\circ\text{C}$ (Figure 2B). Melting temperatures were 55.2 and 54.9°C after 30 and 60 min of incubation, respectively, higher than T_m 's determined from



changes in protein fluorescence (Caldinelli et al., 2010). This indicates that loss of enzymatic activity follows the alteration in secondary and tertiary structure, a behavior previously reported for DAAO from yeast (Caldinelli et al., 2004). The rates of inactivation at each temperature were determined assaying the enzyme activity up to 20 h. The Arrhenius plot reporting the logarithm of rates of inactivation ($\ln k$) plotted against inverse temperature ($1/T$) gives a straight line in the 25–55°C range (inset of Figure 2B) pointing to the absence of temperature-induced conformational transitions. From this plot, an activation energy of 119.4 kJ/mol was calculated.

Modulation of hDAAO Activity

In order to shed light on putative regulation mechanisms of hDAAO, the effect of selected physiologically relevant compounds on the flavoenzyme activity was evaluated. The activity and the far-UV CD spectrum of hDAAO are slightly modified by calcium ions at 1 or 10 mM final concentration (Figure 3A), while magnesium ions do not modify both the protein conformation and the hDAAO activity. Adding 10 μM ATP or GTP alter the far-UV CD spectrum of hDAAO, which is similarly affected by the simultaneous presence of 10 μM nucleotide triphosphate and 10 mM magnesium ions

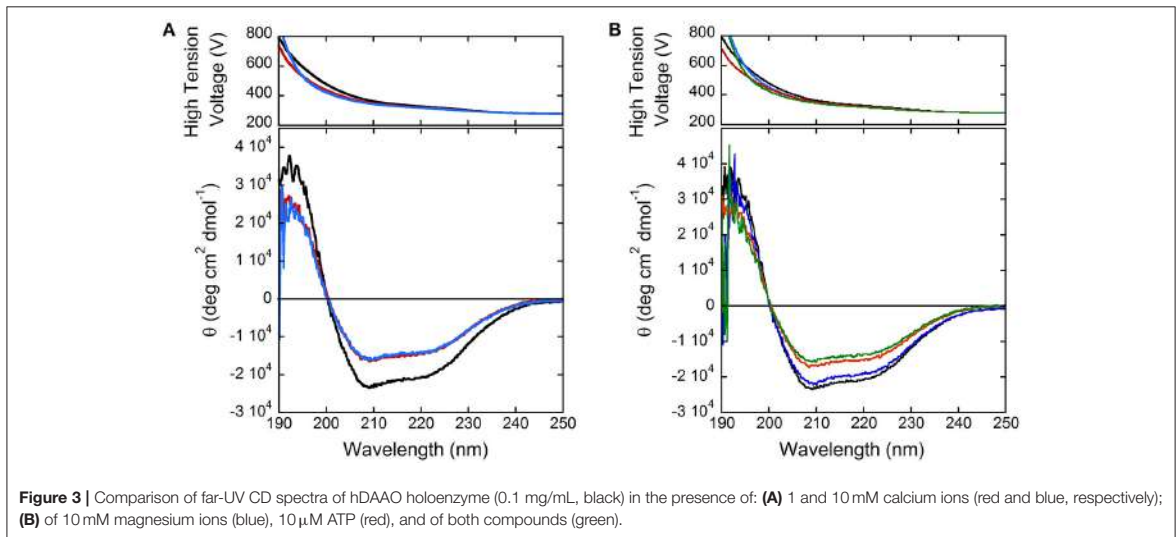


Figure 3 | Comparison of far-UV CD spectra of hDAAO holoenzyme (0.1 mg/mL, black) in the presence of: **(A)** 1 and 10 mM calcium ions (red and blue, respectively); **(B)** of 10 mM magnesium ions (blue), 10 μ M ATP (red), and of both compounds (green).

(Figure 3B). These ligands do not alter the far-UV CD spectrum of the flavoenzyme (not shown). Notably, we previously demonstrated that pLG72, the specific hDAAO modulator (Sacchi et al., 2008), also interacts with nucleotide triphosphates although no ATPase/GTPase activity was assayed (Sacchi et al., 2017). Indeed, hDAAO activity on D-alanine (at 2 or 28 mM final concentration) is not modified by the simultaneous presence of 10 mM magnesium ions and ATP or GTP (10 μ M).

The reducing agent N-acetyl-cysteine (L-NAC, a derivative of the amino acid L-cysteine, an antioxidant and anti-inflammatory agent, which has the ability to modulate NMDAR activity) (Kumar, 2015) at 1 or 10 mM concentration, does not affect hDAAO activity even when added to the enzyme preparation 60 min before the assay.

Flavin Binding

We previously set up a simple procedure to prepare the apoprotein form of hDAAO by dialysis in the presence of 1 M KBr (~70% yield) (Molla et al., 2006). From activity assays and protein fluorescence changes, a K_d -value of 8 μ M for the FAD-apoprotein complex was estimated, which is in good agreement with the value reported by Raibekas et al. (2000). Flavin interaction was significantly strengthened by benzoate binding ($K_d = 0.3 \mu$ M) (Molla et al., 2006; Caldinelli et al., 2010). Here, we decided to investigate the effect of the active-site ligand benzoate on hDAAO flavin binding by following the protein fluorescence quenching during titration of apoprotein with HPLC-purified FAD.

In the absence of an active-site ligand, the quenching in protein fluorescence intensity vs. FAD concentration is biphasic: a saturation is apparent up to $\sim 2 \mu$ M FAD, corresponding to $\sim 50\%$ of the change in fluorescence intensity, and a second saturation is evident up to $\sim 80 \mu$ M FAD (Figure 4). The corresponding dissociation constants were $0.43 \pm 0.02 \mu$ M and $>$

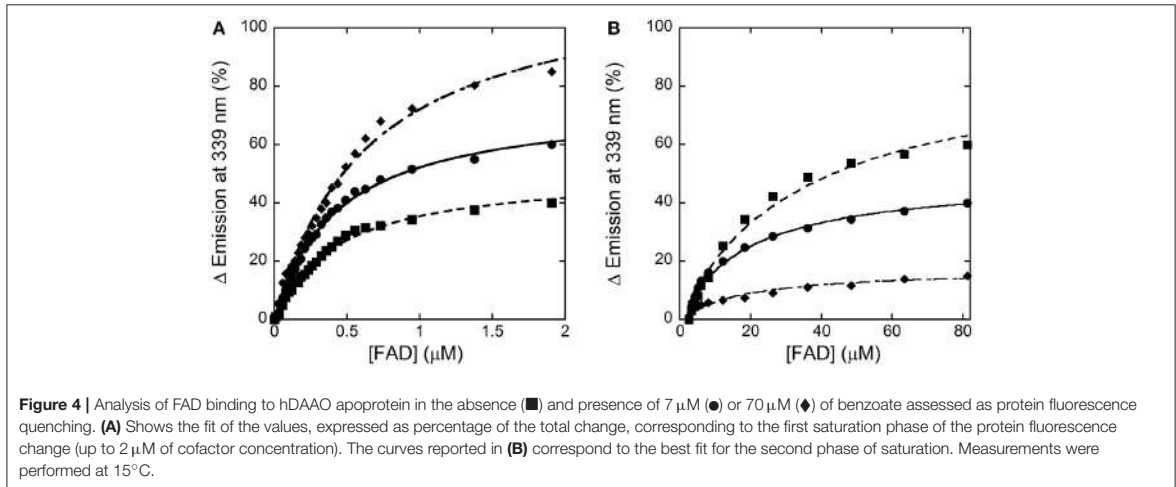
30 μ M, respectively. Using an amount of benzoate corresponding to the K_d -value for its binding to hDAAO (7 μ M), the change in fluorescence intensity was again biphasic but the first phase accounted for $>70\%$ of the total change. K_d -values of $0.43 \pm 0.02 \mu$ M and $19.1 \pm 2.8 \mu$ M were calculated for the first and the second phase, respectively. Notably, using an amount of benzoate corresponding to 10-fold the K_d for its binding to hDAAO (i.e., 70 μ M), the intensity change in fluorescence was mainly fitted using a single saturation equation with a K_d -value of $0.48 \pm 0.02 \mu$ M (Figure 4). The observed increase in the intensity amplitude associated to the first phase indicates that benzoate binding favors a protein conformation with a higher affinity for the cofactor.

The holoenzyme reconstitution process was also investigated by adding increasing concentrations of apoprotein to $\sim 1 \mu$ M of FAD and following the decrease in flavin fluorescence at 528 nm (excitation at 450 nm). In the absence of benzoate, the fluorescence change at increasing apoprotein concentration was still biphasic and yielded a $K_{d,1} = 0.67 \pm 0.07 \mu$ M (corresponding to $\sim 40\%$ of the total change) and a $K_{d,2} = 4.0 \pm 0.9 \mu$ M. In the presence of 70 μ M benzoate the fluorescence intensity change was essentially monophasic: K_d -value was estimated as $0.40 \pm 0.04 \mu$ M.

Taken together, these analyses show that the apoprotein form of hDAAO exists in solution as an equilibrium of two conformations differing in FAD binding affinity: an active-site ligand such as benzoate favors the form at higher affinity.

Substrate Specificity

All the known DAAOs show a broad substrate specificity with significant differences depending on the source (Pollegioni et al., 2007; Sacchi et al., 2012). Here, we reviewed published data and accomplished the range of investigated D-amino acids. hDAAO is mainly active on neutral, hydrophobic and



slightly polar D-amino acids: the highest catalytic efficiency was apparent with D-cysteine while the same parameter for the brain physiological substrate D-serine was 44-fold lower (see **Table 1**). The preference of hDAAO for D-cysteine is of utmost relevance (see Discussion). Glycine and D-serine are alternative coagonists that bind to the strychnine-insensitive modulatory site of NMDAR (Mothet et al., 2000). hDAAO is also able to oxidize glycine but the apparent K_m for this small substrate (~1,000-fold higher than its physiological concentration) hinders its real degradation by the flavooxidase, especially under physiological conditions.

hDAAO shows a preference for aromatic D-amino acids: the highest maximal activity was determined for D-tyrosine and was high for D-phenylalanine and D-tryptophan as well (**Table 1**). Notably, hDAAO oxidizes D-kynurenine, i.e., the D-enantiomer of the intermediate found in L-tryptophan degradation pathway: the apparent K_m -value (0.7 mM) resembles the one determined for D-cysteine. The product of hDAAO-induced D-kynurenine oxidation is kynurenic acid, which is known to inhibit NMDAR by binding to the modulatory glycine site. hDAAO also oxidizes D-cycloserine, an amino acid that acts as NMDAR modulator (Kumar, 2015). A specific argument must be made for the D-enantiomer of 3,4-dihydroxyphenylalanine (DOPA), which can be converted into the L-enantiomer (then used to synthesize dopamine) by the reactions of DAAO and a transaminase. As shown by (Kawazoe et al., 2007b), the apparent maximal activity, as well as the catalytic efficiency k_{cat}/K_m ratio, is the greatest among tested D-amino acids (**Table 1**) but the oxidation of this compound is hampered by the observed substrate inhibition effect ($K_I = 0.5$ mM). For sake of comparison, we performed the kinetics on D-DOPA preparations whose purity was evaluated by chiral HPLC: the k_{cat} -value for D-DOPA is the highest among the tested compounds and the K_m is ~6 mM, thus resulting in a lower catalytic efficiency than that of D-tyrosine. A main difference with previous results concerns the substrate inhibition effect that was observed at a significantly

TABLE 1 | Analysis of the substrate specificity of human DAAO.

	k_{cat} (s^{-1})	K_m (mM)	k_{cat}/K_m ($mM^{-1} \times s^{-1}$)
SMALL-MEDIUM SIZE AMINO ACIDS			
D-Alanine ^a	5.2 ± 0.1 [10] ^c	1.3 ± 0.2 [1] ^c	4.0
D-Serine ^a	3.0 ± 0.1 [4] ^d	7.5 ± 0.5 [1] ^c [3.9] ^d	0.4
Glycine ^a	~ 0.9	~ 180	0.005
D-Cysteine	8.6 ± 0.2	0.6 ± 0.1	14.6
D-Proline ^a	10.2 ± 0.1	8.5 ± 1.0	1.2
D-Cycloserine	0.77 ± 0.05	83.5 ± 15.0	0.009
HYDROPHOBIC AMINO ACIDS			
D-Tyrosine ^d	14.8	1.1	13.5
D-DOPA	40.5 ± 5.1 [21.7] ^d	6.0 ± 1.3 ($K_I = 41.3$) [1.5 ($K_I = 0.5$)] ^d	6.75 [14.4] ^d
D-Phenylalanine ^b	6.6 ± 0.1 [15.5] ^d	2.7 ± 0.2 [1.2] ^d	2.4
D-Tryptophan ^b	3.2 ± 0.1	1.5 ± 0.1	2.1
D-Kynurenine	0.09 ± 0.01	0.7 ± 0.4	0.14
ACIDIC AMINO ACIDS			
D-Aspartate ^a	6.7 ± 1.2	~ 2000	0.0035
D-Glutamate	b. d.	b. d.	
N-Methyl-D-aspartate	b. d.	b. d.	

^a Molla et al., 2006.

^b Frattini et al., 2011.

^c Raibekas et al., 2000.

^d Kawazoe et al., 2007b (at pH 8.3).

b. d., below detection.

The apparent kinetic parameters were determined by the oxygen-consumption assay at 21% oxygen saturation, pH 8.5, and at 25°C.

higher D-DOPA concentration ($K_I = 41.3$ mM, **Table 1**). No difference in kinetic parameters was apparent when the D,L-racemic mixture was used (not shown), suggesting that L-DOPA did not compete with the D-enantiomer for hDAAO binding.

The acidic D-amino acids NMDA and glutamate are not oxidized by hDAAO (at 100 and 500 mM final concentration) while D-aspartate is a very poor substrate: although the maximal activity is quite high (6.7 s^{-1}), the catalytic efficiency is strongly affected by the high apparent K_m (in the molar range, see **Table 1**). At physiological concentrations (0.3–0.5 mM) (Weatherly et al., 2017) the activity of hDAAO on D-Asp is negligible.

We observed that the activity of hDAAO on 100 mM D-serine (the physiological substrate in brain) is partially inhibited by the presence of the L-isomer at concentrations higher than 10 mM (not shown): half of the activity measured on D-serine only was assayed when $\sim 500 \text{ mM}$ L-serine was simultaneously present. The kinetics of D-serine oxidation by hDAAO was thus investigated at increasing L-serine concentrations: as shown by the double reciprocal plot reported in **Figure 5**, the L-isomer does not alter the apparent maximal rate but does increase the apparent K_m -value. Thus, L-serine acts as competitive inhibitor: a K_I of 26.2 mM was estimated (see the inset in **Figure 5**). At physiological concentrations ($\leq 2 \text{ mM}$ in brain tissues and in blood) (Weatherly et al., 2017), L-serine should not affect the activity of the flavoenzyme on D-serine.

The ability of L-serine to bind at the hDAAO active site like the corresponding D-enantiomer is further confirmed by the observed reduction of FAD following anaerobic addition of the L-amino acid: $14 \mu\text{M}$ of hDAAO was reduced by 1 mM L-serine in $>60 \text{ min}$. A similar behavior was apparent when employing L-alanine or L-valine (not shown) but not NMDA, which is not a substrate of hDAAO.

Ligand Binding

In past years, we focused on the ability of hDAAO to bind small-size molecules (Molla et al., 2006; Caldinelli et al., 2010). The drug chlorpromazine was demonstrated to compete with FAD for the binding to hDAAO apoprotein (Iwana et al., 2008; Sacchi et al., 2008): its binding generated a protein conformation more sensitive to thermal unfolding and proteolysis than the native holoenzyme (Caldinelli et al., 2010). Indeed, a plethora of investigations focused on identifying and characterizing substrate competitive inhibitors, in particular for their potential use as drug to treat schizophrenia and neuropathic pain (Sacchi et al., 2013). By structural bioinformatics, high-throughput screening, and three-dimensional structural studies, a number of DAAO inhibitors have been identified. These compounds have been classified into three distinct chemotypes (Lange et al., 2011): (i) hetero(bi)cyclic carboxylic acids, as 5-methylpyrazole-3-carboxylic acid, 4H-furo[3,2-b]pyrrole-5-carboxylic acid, and 4H-thieno[3,2-b]pyrrole-5-carboxylic acid; (ii) compounds based on benzo[d]isoxazol-3-ol, such as 6-chlorobenzo[d]isoxazol-3-ol (CBIO); and (iii) 3-hydroxyquinoline-2-(1H)-one (a strong hDAAO inhibitor, $IC_{50} = 4 \text{ nM}$) and its analogs. For a review focusing on properties and pharmacokinetics of DAAO's inhibitors see (Sacchi et al., 2013).

Here, we decided to investigate the ability of selected compounds to alter hDAAO conformation by following the quenching of protein fluorescence. A decrease in protein fluorescence is apparent at increasing CBIO concentrations: a K_d

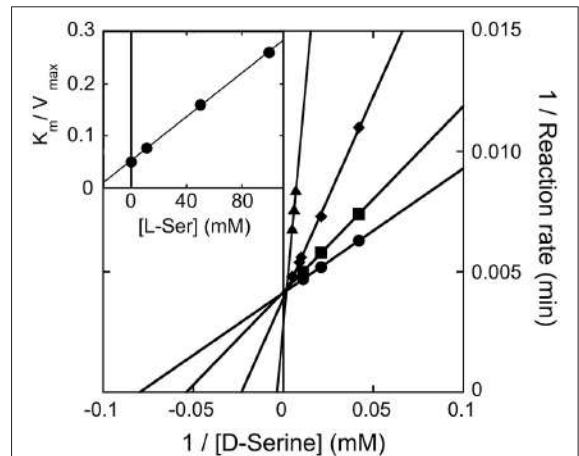


Figure 5 | Double reciprocal plot of kinetics of D-serine oxidation by hDAAO in the presence of increasing concentrations of L-serine. K_I -value for L-serine was estimated by fitting the K_m/V_{max} values calculated at different L-serine concentrations (see inset).

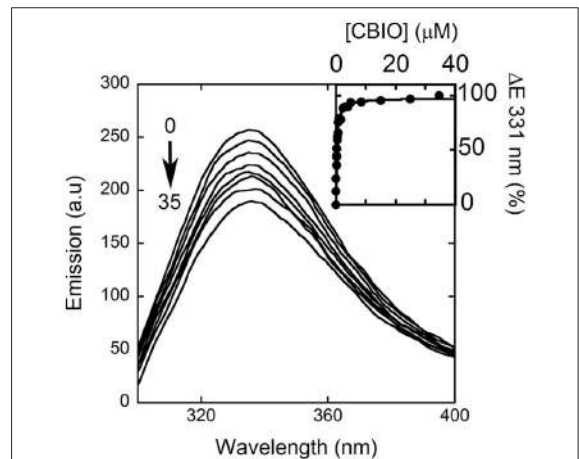


Figure 6 | Effect of CBIO binding to the fluorescence emission spectrum of hDAAO after adding increasing concentrations of ligand (up to $35 \mu\text{M}$, see arrow). The inset shows the fitting of the fluorescence intensity change at 331 nm (expressed as percentage of maximal change) vs. CBIO concentration. Measurements were performed at 15°C .

of $0.24 \pm 0.05 \mu\text{M}$ was calculated (**Figure 6**, inset), suggesting that the induced conformational changes might result in the loss of function. This value is in good agreement with the $IC_{50} = 188 \text{ nM}$ determined from enzyme's inhibition assays (Ferraris et al., 2008). Similarly, benzoate also decreased the protein fluorescence intensity at $\sim 320\text{--}340 \text{ nm}$ but a biphasic change was apparent: a first saturation is observed using low benzoate concentrations ($\leq 20 \mu\text{M}$, $K_d = 0.33 \pm 0.04 \mu\text{M}$) and a second

saturation, associated to $\sim 80\%$ of fluorescence change, was observed at higher ligand concentrations ($K_d = 2.59 \pm 0.68$ mM), see **Figure 7**. For benzoate binding, a K_d -value of $5\text{--}7\ \mu\text{M}$ was determined following the formation of a shoulder at 484 nm in the absorbance spectrum (Raibekas et al., 2000; Molla et al., 2006), a value of $9.5\ \mu\text{M}$ following the CD signal at ~ 270 nm (Caldinelli et al., 2010), and a K_i of $7\ \mu\text{M}$ following enzyme inactivation (Kawazoe et al., 2006). On the other hand, no change in protein fluorescence was observed with glycine (up to 50 mM), ATP (up to 20 mM), NMDA (up to 50 mM), or D-glutamate (up to 50 mM).

DISCUSSION

In this work, we biochemically characterized hDAAO in greater depth. Because of its relevant physiological role in the brain related to modulation of the concentration of the NMDAR coagonist D-serine, we were interested to know how hDAAO activity is modulated, taking into consideration both physical-chemical effects and ligands.

The pH and temperature dependence of hDAAO activity and stability was established. The human flavoenzyme shows a good activity on both D-alanine and D-serine in the 6–10 pH range, as well as a good stability (**Figure 1**). hDAAO is fully stable up to 45°C , a value corresponding to the optimum for the enzymatic activity (**Figure 2**). Altogether, changes in pH and temperature in the physiological range do not seem a way to modulate the function of this enzyme.

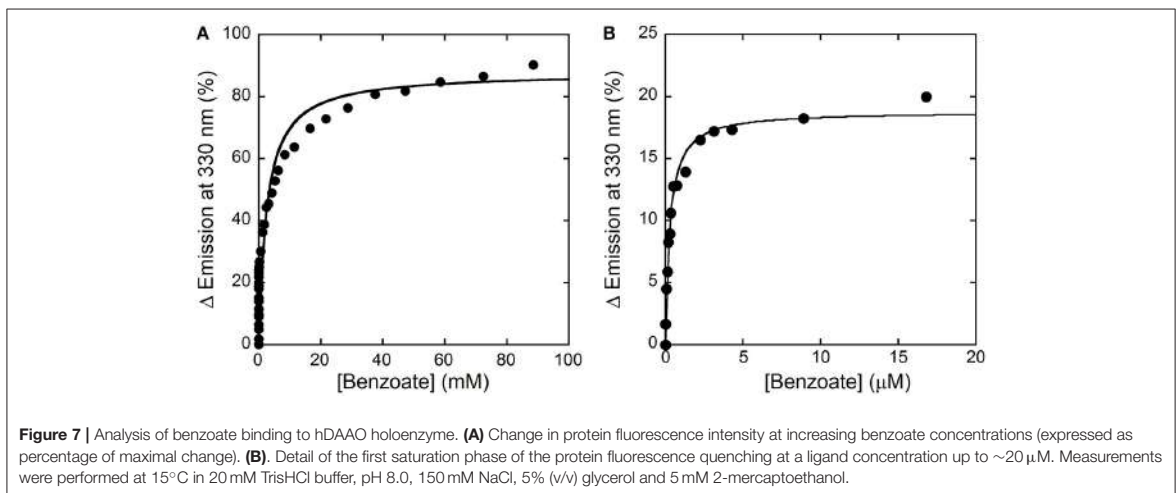
We demonstrated that the flavoenzyme activity is not altered by calcium or magnesium divalent ions and/or nucleotides as well as by the reducing agent L-NAC. In aged mice, the expression of serine racemase (the enzyme responsible for D-serine synthesis) is reduced, whereas no change in DAAO activity was observed (Sato et al., 1996): the chronic treatment of senescent rats with L-NAC to prevent oxidative damage preserved D-serine levels and

serine racemase expression, yielding to intact NMDAR activation (Haxaire et al., 2012).

We clarified the substrate acceptance of hDAAO, showing its preference for hydrophobic amino acids: some of them are molecules relevant in neurotransmission as they are intermediates of dopamine biosynthetic pathways (Kawazoe et al., 2007a,b) (see **Table 1**). Notably, the best substrate is D-cysteine: it was proposed to be converted by DAAO in brain and kidney to 3-mercaptopyruvate, which then generates pyruvate and H_2S by 3-mercaptopyruvate sulfurtransferase (Shibuya et al., 2013). H_2S plays different, main physiological roles in neuromodulation, vascular tone regulation, cytoprotection against oxidative stress, angiogenesis, and anti-inflammation; (for a review, see Kimura, 2015). D-Cysteine, originating from food (Friedman, 2010), could thus represent the physiological substrate of hDAAO in specific tissues.

D-Cycloserine is a partial agonist and positive modulator of NMDAR, which binds to the strychnine-sensitive glycine-binding modulatory site: it acts as an antagonist at high doses and as an agonist at low doses (Kumar, 2015). It is oxidized by hDAAO but with a low efficiency because of a very high K_m -value. Concerning NMDAR modulators, hDAAO is also able to oxidize both glycine and D-aspartate, but again with a very low kinetic efficiency (at least 100-fold lower than the efficiency of D-serine oxidation).

DOPA is a further molecule of relevance for neurotransmission. We confirmed that D-DOPA is oxidized by hDAAO with the highest k_{cat} -value ($\sim 40\ \text{s}^{-1}$): the K_m we determined is 4-fold higher than the value previously reported (Kawazoe et al., 2007b). Most interestingly, we demonstrated that D-DOPA is less efficient in enzyme inhibition than previously reported (K_i is 41.3 mM) and that L-DOPA does not compete with the D-form for hDAAO active-site binding. In contrast, some L-amino acids can bind in the hDAAO active site, thus acting both as competitive inhibitors (K_i for L-serine is 26.2 mM) and, with a very low efficiency,



as substrates (by slowly reducing the flavin cofactor under anaerobic conditions).

Concerning the binding of hDAAO inhibitors, a different situation is apparent for benzoate vs. CBIO. While for the latter compound the K_d -value determined following the quenching of protein fluorescence agrees with the K_d , IC_{50} , and K_i -values reported in the literature, a process characterized by two phases is apparent for benzoate binding. This observation indicates that two protein conformations in equilibrium with different affinity for the ligand or that two ligand binding sites exist. We demonstrated that benzoate interacts with both the holo- and the apoprotein forms of hDAAO (Caldinelli et al., 2009). Noteworthy, a recent investigation combining *in silico* docking simulation and labeling experiments using 4-bromo-3-nitrobenzoic acid highlighted the presence of a second ligand binding site, located in a cleft between monomers (Kohiki et al., 2017).

Concerning flavin binding, we previously demonstrated that an active-site ligand stabilizes the apoprotein-FAD interaction (Molla et al., 2006; Caldinelli et al., 2010) pushing the holoenzyme formation. Here, we clearly demonstrated that, in solution, hDAAO apoprotein exists in two alternative conformations with different flavin affinity: the equilibrium is shifted toward the one at higher avidity by the presence of the competitive inhibitor benzoate, reaching a K_d -value similar to that of rat or pig DAOs (Frattini et al., 2011). It is noteworthy that the reconstitution process leading to the active holoenzyme is a biphasic, sequential process; first, the apoprotein binds FAD and gains catalytic activity—and this step is 20-fold faster when benzoate is bound (Caldinelli et al., 2010)—and then a slower secondary conformational change follows, which stabilizes the protein (Caldinelli et al., 2009). Although no crystal structure of hDAAO in the absence of an active-site ligand has been solved, our biochemical evidence suggests that, in addition to the known conformation of the hydrophobic region ⁴⁷VAAGL⁵¹ at the *si*-face of the isoalloxazine ring of FAD observed in the hDAAO-benzoate complex, a second conformation should exist that possesses a lower affinity for the flavin cofactor. This is an important issue since the holoenzyme stability both increases the half-life of the protein and affects the cellular D-serine level (Caldinelli et al., 2010).

REFERENCES

- Caldinelli, L., Iametti, S., Barbiroli, A., Bonomi, F., Piubelli, L., Ferranti, P., et al. (2004). Unfolding intermediate in the peroxisomal flavoprotein D-amino acid oxidase. *J. Biol. Chem.* 279, 28426–28434. doi: 10.1074/jbc.M403489200
- Caldinelli, L., Molla, G., Bracci, L., Lelli, B., Pileri, S., Cappelletti, P., et al. (2010). Effect of ligand binding on human D-amino acid oxidase: implications for the development of new drugs for schizophrenia treatment. *Protein Sci.* 19, 1500–1512. doi: 10.1002/pro.429
- Caldinelli, L., Molla, G., Sacchi, S., Pilone, M. S., and Pollegioni, L. (2009). Relevance of weak flavin binding in human D-amino acid oxidase. *Protein Sci.* 18, 801–810. doi: 10.1002/pro.86
- Cappelletti, P., Campomenosi, P., Pollegioni, L., and Sacchi, S. (2014). The degradation (by distinct pathways) of human D-amino acid oxidase and its

Taken together, these findings strengthen our belief that, in the case of hDAAO, evolution adopted sophisticated regulatory strategies. Because of the weak interaction between FAD and hDAAO apoprotein and of the physiological concentration of the cofactor in human brain tissues, the flavoenzyme is largely present in the apoprotein, inactive form. The flavin binding and the kinetic properties (hDAAO possesses a low catalytic efficiency and substrate affinity) seem to be evolved to generate an enzyme that controls D-serine concentration in brain, avoiding an excessive degradation of the neuromodulator. The fact that the presence of a ligand in the active site promotes a conformational switch toward a protein form able to bind more avidly the cofactor might represent a mechanism finely modulating hDAAO activity: the free enzyme, significantly present in solution as inactive apoprotein, is rapidly turned into the flavinylated, active holoenzyme by the presence of the substrate. This, in turn, would represent an effective way to keep the concentration of specific D-amino acids in distinct tissues in the physiological range. In conclusion, hDAAO possesses a number of peculiar properties that distinguish it from homologs from diverse sources. Such properties make this flavoenzyme an interesting protein that can be used by different tissues to meet various physiological needs related to the catabolism of different D-amino acids.

AUTHOR CONTRIBUTIONS

GM performed the experiments, analyzed the data and wrote the paper; MV purified the recombinant enzyme; SS designed the study and analyzed the data; LP designed the study, analyzed the data and wrote the paper.

ACKNOWLEDGMENTS

This work was supported by grants from Fondo di Ateneo per la Ricerca to SS and LP. We thank Dr. Gianluca Molla for fruitful discussion, and the support from Consorzio Interuniversitario per le Biotecnologie to GM. GM is a Ph.D. student of the “Biotechnology, Biosciences and Surgical Technology” course at Università degli studi dell’Insubria.

- interacting partner pLG72—two key proteins in D-serine catabolism in the brain. *FEBS J.* 281, 708–723. doi: 10.1111/febs.12616
- Ferraris, D., Duvall, B., Ko, Y. S., Thomas, A. G., Rojas, G., Majer, P., et al. (2008). Synthesis and biological evaluation of D-amino acid oxidase inhibitors. *J. Med. Chem.* 51, 3357–3359. doi: 10.1021/jm800200u
- Foltyn, V. N., Bendikov, I., De Miranda, J., Panizzutti, R., Dumin, E., Shleper, M., et al. (2005). Serine racemase modulates intracellular D-serine levels through an α , β -elimination activity. *J. Biol. Chem.* 280, 1754–1763. doi: 10.1074/jbc.M405726200
- Frattini, L. F., Piubelli, L., Sacchi, S., Molla, G., and Pollegioni, L. (2011). Is rat an appropriate animal model to study the involvement of D-serine catabolism in schizophrenia? insights from characterization of D-amino acid oxidase. *FEBS J.* 278, 4362–4373. doi: 10.1111/j.1742-4658.2011.08354.x
- Friedman, M. (2010). Origin, microbiology, nutrition, and pharmacology of D-amino acids. *Chem. Biodivers.* 7, 1491–1530. doi: 10.1002/cbdv.200900225

- Fuchs, S. A., Berger, R., and de Koning, T. J. (2011). D-serine: the right or wrong isoform? *Brain Res.* 1401, 104–117. doi: 10.1016/j.brainres.2011.05.039
- Harris, C. M., Molla, G., Pilone, M. S., and Pollegioni, L. (1999). Studies on the reaction mechanism of *Rhodotorula gracilis* D-amino-acid oxidase. role of the highly conserved Tyr-223 on substrate binding and catalysis. *J. Biol. Chem.* 274, 36233–36240. doi: 10.1074/jbc.274.51.36233
- Harris, C. M., Pollegioni, L., and Ghisla, S. (2001). pH and kinetic isotope effects in D-amino acid oxidase catalysis. *FEBS J.* 268, 5504–5520. doi: 10.1046/j.1432-1033.2001.02462.x
- Haxaire, C., Turpin, F. R., Potier, B., Kervern, M., Sinet, P. M., Barbanel, G., et al. (2012). Reversal of age-related oxidative stress prevents hippocampal synaptic plasticity deficits by protecting D-serine-dependent NMDA receptor activation. *Aging Cell* 11, 336–344. doi: 10.1111/j.1474-9726.2012.00792.x
- Horiike, K., Tojo, H., Arai, R., Nozaki, M., and Maeda, T. (1994). D-amino acid oxidase is confined to the lower brain stem and cerebellum in rat brain: regional differentiation of astrocytes. *Brain Res.* 652, 297–303. doi: 10.1016/0006-8993(94)90240-2
- Iwana, S., Kawazoe, T., Park, H. K., Tsuchiya, K., Ono, K., Yorita, K., et al. (2008). Chlorpromazine oligomer is a potentially active substance that inhibits human D-amino acid oxidase, product of a susceptibility gene for schizophrenia. *J. Enzyme Inhib. Med. Chem.* 23, 901–911. doi: 10.1080/1475636070145478
- Kawazoe, T., Park, H. K., Iwana, S., Tsuge, H., and Fukui, K. (2007a). Human D-amino acid oxidase: an update and review. *Chem. Rec.* 7, 305–315. doi: 10.1002/tcr.20129
- Kawazoe, T., Tsuge, H., Imagawa, T., Aki, K., Kuramitsu, S., and Fukui, K. (2007b). Structural basis of D-DOPA oxidation by D-amino acid oxidase: alternative pathway for dopamine biosynthesis. *Biochem. Biophys. Res. Commun.* 355, 385–391. doi: 10.1016/j.bbrc.2007.01.181
- Kawazoe, T., Tsuge, H., Pilone, M. S., and Fukui, K. (2006). Crystal structure of human D-amino acid oxidase: context-dependent variability of the backbone conformation of the VAAGL hydrophobic stretch located at the si-face of the flavin ring. *Protein Sci.* 15, 2708–2717. doi: 10.1110/ps.062421606
- Kimura, H. (2015). Signaling molecules: hydrogen sulfide and polysulfide. *Antioxid. Redox Signal.* 22, 362–376. doi: 10.1089/ars.2014.5869
- Kohiki, T., Sato, Y., Nishikawa, Y., Yorita, K., Sagawa, I., Denda, M., et al. (2017). Elucidation of inhibitor-binding pocket of D-amino acid oxidase using docking simulation and N-sulfanylethylamide-based labeling technology. *Org. Biomol. Chem.* 25, 5289–5297. doi: 10.1039/C7OB00633K
- Krebs, H. A. (1935). Metabolism of amino-acids: deamination of amino-acids. *Biochem. J.* 29, 1620–1644. doi: 10.1042/bj0291620
- Kumar, A. (2015). NMDA receptor function during senescence: implication on cognitive performance. *Front. Neurosci.* 9:473. doi: 10.3389/fnins.2015.00473
- Labrie, V., and Roder, J. C. (2010). The involvement of the NMDA receptor D-serine/glycine site in the pathophysiology and treatment of schizophrenia. *Neurosci. Biobehav. Rev.* 34, 351–372. doi: 10.1016/j.neubiorev.2009.08.002
- Lange, J. H., Venhorst, J., van Dongen, M. J., Frankena, J., Bassissi, F., de Bruin, N. M., et al. (2011). Biophysical and physicochemical methods differentiate highly ligand-efficient human D-amino acid oxidase inhibitors. *Eur. J. Med. Chem.* 46, 4808–4819. doi: 10.1016/j.ejmech.2011.04.023
- Lu, M., Fan, Y., Tang, M., Qian, X., Ding, J., and Hu, G. (2011). Potentiation of D-serine involves degeneration of dopaminergic neurons in MPTP/p mouse model of Parkinson's disease. *CNS Neurosci. Ther.* 17, 796–798. doi: 10.1111/j.1755-5949.2011.00275.x
- Luks, L., Sacchi, S., Pollegioni, L., and Dietrich, D. R. (2017). Novel insights into renal d-amino acid oxidase accumulation: propiverine changes DAAO localization and peroxisomal size *in vivo*. *Arch. Toxicol.* 91, 427–437. doi: 10.1007/s00204-016-1685-z
- Martineau, M., Baux, G., and Mothet, J. P. (2006). D-serine signalling in the brain: friend and foe. *Trends Neurosci.* 29, 481–491. doi: 10.1016/j.tins.2006.06.008
- Mattevi, A., Vanoni, M. A., Todone, F., Rizzi, M., Teplyakov, A., Coda, A., et al. (1996). Crystal structure of D-amino acid oxidase: a case of active site mirror-image convergent evolution with flavocytochrome b2. *Proc. Natl. Acad. Sci. U.S.A.* 93, 7496–7501. doi: 10.1073/pnas.93.15.7496
- Mitchell, J., Paul, P., Chen, H. J., Morris, A., Payling, M., Falchi, M., et al. (2010). Familial amyotrophic lateral sclerosis is associated with a mutation in D-amino acid oxidase. *Proc. Natl. Acad. Sci. U.S.A.* 107, 7556–7561. doi: 10.1073/pnas.0914128107
- Molla, G., Sacchi, S., Bernasconi, M., Pilone, M. S., Fukui, K., and Pollegioni, L. (2006). Characterization of human D-amino acid oxidase. *FEBS Lett.* 580, 2358–2364. doi: 10.1016/j.febslet.2006.03.045
- Moreno, S., Nardacci, R., Cimini, A., and Ceru, M. P. (1999). Immunocytochemical localization of D-amino acid oxidase in rat brain. *J. Neurocytol.* 28, 169–185. doi: 10.1023/A:1007064504007
- Mothet, J. P., Parent, A. T., Wolosker, H., Brady, R. O., Linden, D. J., Ferris, C. D., et al. (2000). D-serine is an endogenous ligand for the glycine site of the N-methyl-D-aspartate receptor. *Proc. Natl. Acad. Sci. U.S.A.* 97, 4926–4931. doi: 10.1073/pnas.97.9.4926
- Mustafa, A. K., Ahmad, A. S., Zeynalov, E., Gazi, S. K., Sikka, G., Ehmsen, J. T., et al. (2010). Serine racemase deletion protects against cerebral ischemia and excitotoxicity. *J. Neurosci.* 30, 1413–1416. doi: 10.1523/JNEUROSCI.4297-09.2010
- Pilone, M. S. (2000). D-Amino acid oxidase: new findings. *Cell. Mol. Life Sci.* 57, 1732–1747. doi: 10.1007/PL00000655
- Pollegioni, L., Buto, S., Tischer, W., Ghisla, S., and Pilone, M. S. (1993). Characterization of D-amino acid oxidase from *Trigonopsis variabilis*. *Biochem. Mol. Biol. Int.* 31, 709–717.
- Pollegioni, L., Piubelli, L., Sacchi, S., Pilone, M. S., and Molla, G. (2007). Physiological functions of D-amino acid oxidases: from yeast to humans. *Cell. Mol. Life Sci.* 64, 1373–1394. doi: 10.1007/s00018-007-6558-4
- Popielek, M., Ross, J. F., Charych, E., Chanda, P., Gundelfinger, E. D., Moss, S. J., et al. (2011). D-amino acid oxidase activity is inhibited by an interaction with bassoon protein at the presynaptic active zone. *J. Biol. Chem.* 286, 28867–28875. doi: 10.1074/jbc.M111.262063
- Raibekas, A. A., Fukui, K., and Massey, V. (2000). Design and properties of human D-amino acid oxidase with covalently attached flavin. *Proc. Natl. Acad. Sci. U.S.A.* 97, 3089–3093. doi: 10.1073/pnas.97.7.3089
- Romano, D., Molla, G., Pollegioni, L., and Marinelli, F. (2009). Optimization of human D-amino acid oxidase expression in *Escherichia coli*. *Protein Exp. Purif.* 68, 72–78. doi: 10.1016/j.pep.2009.05.013
- Rossi, D. J., Brady, J. D., and Mohr, C. (2007). Astrocyte metabolism and signaling during brain ischemia. *Nat. Neurosci.* 10, 1377–1386. doi: 10.1038/nn2004
- Sacchi, S., Bernasconi, M., Martineau, M., Mothet, J. P., Ruzzeno, M., Pilone, M. S., et al. (2008). pLG72 modulates intracellular D-serine levels through its interaction with D-amino acid oxidase: effect on schizophrenia susceptibility. *J. Biol. Chem.* 283, 22244–22256. doi: 10.1074/jbc.M709153200
- Sacchi, S., Binelli, G., and Pollegioni, L. (2016). G72 primate-specific gene: a still enigmatic element in psychiatric disorders. *Cell. Mol. Life Sci.* 73, 2029–2039. doi: 10.1007/s00018-016-2165-6
- Sacchi, S., Caldinelli, L., Cappelletti, P., Pollegioni, L., and Molla, G. (2012). Structure-function relationships in human D-amino acid oxidase. *Amino Acids* 43, 1833–1850. doi: 10.1007/s00726-012-1345-4
- Sacchi, S., Cappelletti, P., Giovannardi, S., and Pollegioni, L. (2011). Evidence for the interaction of D-amino acid oxidase with pLG72 in a glial cell line. *Mol. Cell. Neurosci.* 48, 20–28. doi: 10.1016/j.mcn.2011.06.001
- Sacchi, S., Cappelletti, P., Pirone, L., Smaldone, G., Pedone, E., and Pollegioni, L. (2017). Elucidating the role of the pLG72 R30K substitution in schizophrenia susceptibility. *FEBS Lett.* 591, 646–655. doi: 10.1002/1873-3468.12585
- Sacchi, S., Rosini, E., Pollegioni, L., and Molla, G. (2013). D-amino acid oxidase inhibitors as a novel class of drugs for schizophrenia therapy. *Curr. Pharm. Des.* 19, 2499–2511. doi: 10.2174/1381612811319140002
- Saitoh, Y., Katane, M., Kawata, T., Maeda, K., Sekine, M., Furuchi, T., et al. (2012). Spatiotemporal localization of D-amino acid oxidase and D-aspartate oxidases during development in *Caenorhabditis elegans*. *Mol. Cell. Biol.* 32, 1967–1983. doi: 10.1128/MCB.06513-11
- Sasabe, J., Miyoshi, Y., Rakoff-Nahoum, S., Zhang, T., Mita, M., Davis, B. M., et al. (2016). Interplay between microbial D-amino acids and host d-amino acid oxidase modifies murine mucosal defence and gut microbiota. *Nat. Microbiol.* 1:16125. doi: 10.1038/nmicrobiol.2016.125
- Sato, E., Kurokawa, T., Oda, N., and Ishibashi, S. (1996). Early appearance of abnormality of microperoxisomal enzymes in the cerebral cortex of senescence-accelerated mouse. *Mech. Ageing Dev.* 92, 175–184. doi: 10.1016/S0047-6374(96)01832-5

- Shibuya, N., Koike, S., Tanaka, M., Ishigami-Yuasa, M., Kimura, Y., Ogasawara, Y., et al. (2013). A novel pathway for the production of hydrogen sulfide from D-cysteine in mammalian cells. *Nat. Commun.* 4:1366. doi: 10.1038/ncomms2371
- Snyder, S. H., and Kim, P. M. (2000). D-amino acids as putative neurotransmitters: focus on D-serine. *Neurochem. Res.* 25, 553–560. doi: 10.1023/A:1007586314648
- Weatherly, C. A., Du, S., Parpia, C., Santos, P. T., Hartman, A. L., and Armstrong, D. W. (2017). D-Amino acid levels in perfused mouse brain tissue and blood: a comparative study. *ACS Chem. Neurosci.* 8, 1251–1261. doi: 10.1021/acchemneuro.6b00398
- Wolosker, H., Blackshaw, S., and Snyder, S. H. (1999). Serine racemase: a glial enzyme synthesizing D-serine to regulate glutamate-N-methyl-D-aspartate neurotransmission. *Proc. Natl. Acad. Sci. U.S.A.* 96, 13409–13414. doi: 10.1073/pnas.96.23.13409
- Wolosker, H., Dumin, E., Balan, L., and Foltyn, V. N. (2008). D-amino acids in the brain: D-serine in neurotransmission and neurodegeneration. *FEBS J.* 275, 3514–3526. doi: 10.1111/j.1742-4658.2008.06515.x

Conflict of Interest Statement: The authors declare that the research was conducted in the absence of any commercial or financial relationships that could be construed as a potential conflict of interest.

Copyright © 2017 Murtas, Sacchi, Valentino and Pollegioni. This is an open-access article distributed under the terms of the Creative Commons Attribution License (CC BY). The use, distribution or reproduction in other forums is permitted, provided the original author(s) or licensor are credited and that the original publication in this journal is cited, in accordance with accepted academic practice. No use, distribution or reproduction is permitted which does not comply with these terms.



Contents lists available at ScienceDirect

BBA - Proteins and Proteomics

journal homepage: www.elsevier.com/locate/bbapap

Human D-amino acid oxidase: The inactive G183R variant

Giulia Murtas^{a,*}, Laura Caldinelli^{a,b}, Pamela Cappelletti^{a,b}, Silvia Sacchi^{a,b}, Loredano Pollegioni^{a,b}^a Dipartimento di Biotecnologie e Scienze della Vita, Università degli studi dell'Insubria, via J. H. Dunant 3, 21100 Varese, Italy^b The Protein Factory, Politecnico di Milano and Università degli studi dell'Insubria, via Mancinelli 7, 20131 Milan, Italy

ARTICLE INFO

Keywords:

D-Serine
Schizophrenia
Protein-protein interaction
D-Amino acid oxidase
Protein aggregation

ABSTRACT

In the brain, the enzyme D-amino acid oxidase (DAAO) catalyzes the oxidative deamination of D-serine, a main positive modulator of the N-methyl-D-aspartate subtype of glutamate receptors (NMDAR). Dysregulation in D-serine signaling is implicated in the NMDAR dysfunctions observed in various brain diseases, such as amyotrophic lateral sclerosis, Alzheimer's disease, schizophrenia. A strain of ddY mice lacking DAAO activity due to the G181R substitution (DAAO^{G181R} mice) and exhibiting increased D-serine concentration as compared to wild-type mice shows altered pain response, improved adaptive learning and cognitive functions, and larger hippocampal long-term potentiation. In past years, this mice line has been used to shed light on physiological and pathological brain functions related to NMDAR. Here, we decided to introduce the corresponding substitution in human DAAO (hDAAO). The recombinant G183R hDAAO is produced as an inactive apoprotein: the substitution alters the protein conformation that negatively affects the ability to bind the flavin cofactor in the orientation required for hydride-transfer during catalysis. At the cellular level, the overexpressed G183R hDAAO is not fully targeted to peroxisomes, forms protein aggregates showing a strong colocalization with ubiquitin, and significantly (7-fold) increases both the D-serine cellular concentration and the D/(D + L)-serine ratio. Taken together, our investigation warrants caution in using DAAO^{G181R} mice: the abolition of enzymatic activity is coupled to DAAO aggregation, a central process in different pathological conditions. The effect due to G181R substitution in DAAO could be misleading: the effects due to impairment of D-serine degradation overlap with those related to aggregates accumulation.

1. Introduction

D-Amino acid oxidase (DAAO, EC 1.4.3.3) is a well-known, FAD-dependent enzyme which catalyzes the stereospecific oxygen-dependent deamination of D-amino acids to give the corresponding α -keto acids, ammonia, and hydrogen peroxide [1,2]. In the human brain, the main physiological function of this flavoenzyme is degradation of D-serine. This D-amino acid binds to the glycine-modulatory site of the N-methyl-D-aspartate subtype of glutamate receptors (NMDARs) and, in addition to glutamate, conditions receptor activation [3–5]; D-Serine acts as the main endogenous coagonist in different brain areas [5–9]. Furthermore, D-serine has been proposed to be mainly synthesized and released by neurons and subsequently taken up by astrocytes. In the latter cells, which contain low levels of the enzyme serine racemase (EC 5.1.1.18, catalyzing both synthesis and degradation of D-serine), DAAO plays a central role in terminating D-serine signaling [10,11]. Accordingly, DAAO should play a main role in regulating D-serine levels and thus may affect the NMDAR-dependent physiological functions

involved in cognitive abilities, such as learning and memory [12,13]. Dysregulation in D-serine signaling is implicated in the NMDAR dysfunctions observed in various diseases: a) D-serine is increased in the spinal cord of patients affected by familial and sporadic amyotrophic lateral sclerosis (ALS): the R199W substitution in human DAAO (hDAAO) associated with familial ALS strongly affects the enzyme activity, promotes the accumulation of ubiquitinated protein aggregates, and causes primary motor neuron death [14–16]; b) D-serine level is altered in Alzheimer's disease [17,18]; c) activated astrocytes may provide D-serine to enable receptor activation and thus allodynia [19]; and d) D-serine levels are lower in the cerebrospinal fluid and serum of patients suffering from schizophrenia [20–22]: increased levels of DAAO expression and activity have been observed concomitantly [23–25].

A strain of ddY mice lacking DAAO activity in kidney homogenates was identified in 1983 [26]; the enzyme was inactivated by a single-base mutation, yielding the G181R substitution [27]. C57BL/6J mice carrying the DAAO G181R mutation (DAAO^{G181R} mice) showed a

Abbreviations: ALS, amyotrophic lateral sclerosis; CBIO, 6-chloro-benzo(d)isoxazol-3-ol; CD, circular dichroism; CPZ, chlorpromazine; DAAO, D-amino acid oxidase (EC 1.4.3.3); EYFP, enhanced yellow fluorescent protein; hDAAO, human D-amino acid oxidase; NLS, N-lauroylsarcosine; NMDAR, N-methyl-D-aspartate subtype of glutamate receptor

* Corresponding author at: Department of Biotechnology and Life Sciences, Università degli Studi dell'Insubria, via J.H. Dunant 3, 21100 Varese, Italy.

E-mail address: g.murtas@uninsubria.it (G. Murtas).

<https://doi.org/10.1016/j.bbapap.2017.12.007>

Received 25 August 2017; Received in revised form 12 December 2017; Accepted 14 December 2017

Available online 21 December 2017

1570-9639/ © 2017 Elsevier B.V. All rights reserved.

chronic reduction of DAAO activity throughout life: these mice were viable and did not demonstrate any obvious change in reproductive capacity and in NMDAR-related molecular systems but did show enhanced NMDAR activity in vivo [28]. D-Serine concentration was increased in whole brain of DAAO^{G181R} mice, as well as in different, specific brain regions (with the most significant increase in cerebellum) as compared to wild-type mice [29].

The DAAO^{G181R} mice were used for a number of behavioral tests [30–32]. DAAO inactivation in these mutant mice likely promoted adaptive learning in response to changing conditions (i.e., improved memory for a new target location in the acquisition phase following a single platform location). Indeed, DAAO^{G181R} mice showed an increase rate of extinction (a form of learning that acts to suppress, but not to erase, previously learned responses) in the Morris water maze task, similar to that observed following administration of 600 mg D-serine/kg in wild-type animals [29]. Moreover, in the *Grin1*^{D481N} mice carrying a mutation in the GluN1 subunit of NMDAR (which decreases glycine affinity), and displaying schizophrenic-related behavioral deficits, the DAAO^{G181R} mutation modestly elevated brain levels of D-serine (~20%), resulted in an improvement in social approach and spatial memory retention reversal of abnormally persistent latent inhibition and partial normalization of startle responses [33], and reversed anxiolytic effects of diminished NMDAR function [34]. Despite these intriguing findings, the effect of the G181R mutation on DAAO biochemical properties was not investigated further.

Since these mice lines are used to shed light on the role played by the catabolism of D-serine in physiological and pathological human brain functions related to NMDAR, we introduced in the human flavoenzyme the corresponding mutation that abolished enzymatic activity in the mouse counterpart, i.e., G183R substitution. This conserved residue belongs to α -helix α 9, which is close to the pyrophosphate and ribityl groups of the FAD cofactor (see Fig. 1). Here, the main biochemical properties of such a hDAAO variant were compared to those of the wild-type counterpart, and its effect on cellular D-serine levels, protein subcellular localization, and apoptosis were also investigated.

2. Materials and methods

2.1. Expression and purification of recombinant G183R hDAAO variant

The G183R hDAAO variant was generated by a mutagenesis reaction using the QuickChange Site-Directed Mutagenesis kit (Agilent Technologies, Santa Clara, CA, USA) and the pET11b-hDAAO expression vector encoding the wild-type enzyme as a template [35]. The recombinant G183R hDAAO variant was expressed in *E. coli* BL21 (DE3) Star cells (Invitrogen, Carlsbad, CA, USA), as reported for the wild-type enzyme [35]. The highest G183R hDAAO production level was obtained by growing the cells overnight at 37 °C after adding 0.6 mM IPTG at the late exponential phase of growth. The recombinant G183R hDAAO was purified from the crude extract obtained by sonication and centrifugation by a single chromatography step on a nickel-chelating column (Hi-Trap chelating HP column; GE Healthcare, Uppsala, Sweden) using the following elution buffer: 50 mM sodium pyrophosphate, pH 7.2, 0.5 M imidazole, 5% (v/v) glycerol and 5 mM 2-mercaptoethanol [35,36]. The final hDAAO preparation was equilibrated in 20 mM Tris-HCl, pH 8.0, 100 mM NaCl, 10% (v/v) glycerol, and 5 mM 2-mercaptoethanol.

In order to push holoenzyme reconstitution, the purified G183R protein (2 mg protein/mL solution added of 200 μ M FAD) was dialyzed against 20 mM Tris-HCl, pH 8.0, 100 mM NaCl, 10% (v/v) glycerol, 40 μ M FAD, and 5 mM 2-mercaptoethanol for 20 h at 4 °C, and stored in the same buffer.

The hDAAO activity was assayed on 28 mM D-alanine as substrate in 75 mM sodium pyrophosphate, pH 8.5, containing 200 μ M FAD, at air saturation and 25 °C by measuring the O₂ consumption with an oxygen electrode [35].

pLG72 was prepared as reported in [37] and stored in 20 mM Tris-HCl, pH 8.5, 100 mM NaCl, 5% (v/v) glycerol, 5 mM 2-mercaptoethanol, and 0.1% (v/v) N-lauroylsarcosine (NLS).

2.2. Spectral analysis

UV-Visible absorbance spectral analysis was performed in 20 mM Tris-HCl, pH 8.0, 100 mM NaCl, 10% (v/v) glycerol, and 5 mM 2-mercaptoethanol. The concentration of the purified enzyme was calculated using the extinction coefficient at 280 nm (72.5 mM⁻¹ cm⁻¹), which was determined by measuring the absorbance spectrum of the protein completely denatured in 6 M urea [38] and assuming an extinction coefficient as calculated by EXPASy Bioinformatic Resource Portal using the ProtParam tool (<http://web.expasy.org/protparam/>).

Circular dichroism (CD) spectra were recorded in 20 mM Tris-HCl, pH 8.0, 150 mM NaCl, 5% (v/v) glycerol, and 40 μ M FAD (for the holoenzyme form only) by using a Jasco J-815 spectropolarimeter (Jasco Co., Cremella, Italy) on a mixture containing a protein at 0.4 mg/mL for measurements above 250 nm and at 0.1 mg/mL for measurements in the 200- to 250-nm region [39].

Protein fluorescence spectra were recorded in a FP-750 instrument (Jasco Co.) at 1 μ M (0.04 mg/mL) protein concentration in 50 mM sodium pyrophosphate, pH 8.3. Protein emission fluorescence spectra were recorded between 300 and 400 nm, with excitation at 280 nm. The binding constants for FAD, chlorpromazine (CPZ), 6-chloro-benzo (*d*)isoxazol-3-ol (CBIO), benzoate, anthranilate, FMN, and riboflavin were estimated by titrating hDAAO apoprotein with increasing amounts of ligands and by analyzing the quenching of tryptophan emission at 340 nm [35]. The binding constant for FAD to the apoprotein moiety was estimated using either the free form or the benzoate-complex (obtained by adding 50 mM benzoate).

Temperature-ramp experiments (from 20 to 75 °C, at 0.5 °C/min) were performed in 20 mM Tris-HCl, pH 8.0, 100 mM NaCl, 5% (v/v) glycerol, 5 mM 2-mercaptoethanol, and 40 μ M FAD (for the holoenzyme form only), using a Peltier temperature controller and by measuring the fluorescence protein change at 340 nm or the CD signal at 220 nm, as reported in [40].

2.3. Size-exclusion chromatography

The oligomeric state of G183R hDAAO variant and its interaction with pLG72 (at 40 and 20 nmol, respectively) were investigated by size-exclusion chromatography on a Superdex 200 Increase column using an AKTA chromatographic system (GE Healthcare) in 20 mM Tris-HCl, pH 8.5, 150 mM NaCl, 5% (v/v) glycerol, 40 μ M FAD, and 5 mM 2-mercaptoethanol. In the presence of pLG72, 0.06% (v/v) NLS was added to the elution buffer [35]. The presence of pLG72 and hDAAO in the peak corresponding to the complex was confirmed by SDS-PAGE and Western blot analyses by using anti-hDAAO (1:4000; Davids Biotechnology GmbH, Regensburg, Germany) and anti-pLG72 (1:500; Santa Cruz Biotechnology Inc., Dallas, TX, USA) antibodies [41].

2.4. Expression of G183R hDAAO variant in U87 glioblastoma cells

The expression construct encoding the G183R hDAAO variant was generated using the Quickchange Site-Directed Mutagenesis kit and the pEYFP-hDAAO-C3 plasmid as template, which encodes for a chimeric hDAAO fused to the C-terminal end of the enhanced yellow fluorescent protein (EYFP) [41,42].

Human U87 glioblastoma cells (ATCC) were maintained in DMEM supplemented with 10% (w/w) fetal bovine serum, 1 mM sodium pyruvate, 2 mM L-glutamine, penicillin/streptomycin, and amphotericin B (Euroclone S.p.A., Pero, Italy) at 37 °C in a 5% CO₂ atmosphere; cells were transfected using the FuGENE HD transfection reagent (Promega Co., Madison, WI, USA) and 2 μ g of pEYFP-G183R-hDAAO-C3 construct, as reported in [41,42]. The EYFP-hDAAO expression level was

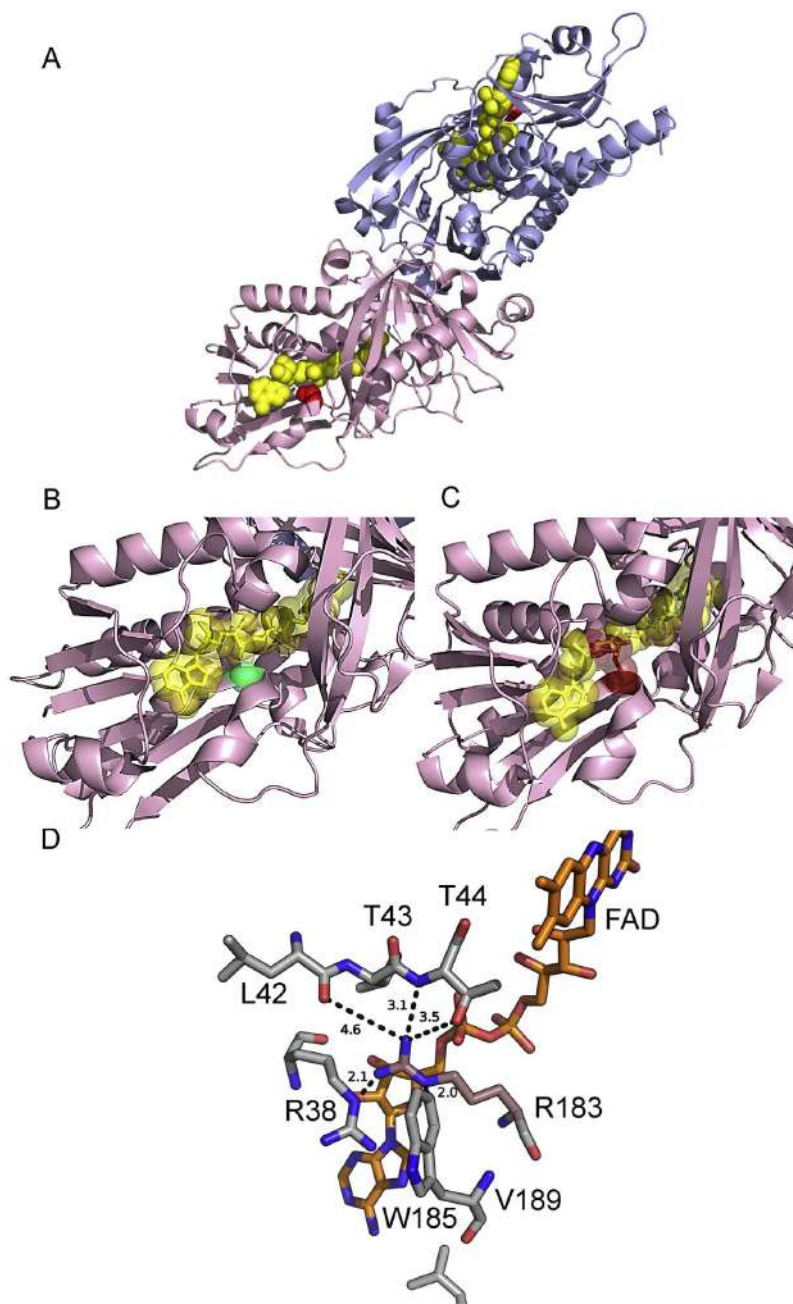


Fig. 1. Structure of human DAAO (PDB 2DU8). (A) The position of the residue G183 mutated in this work is shown in red. FAD is depicted in yellow. (B, C) Detail of the G183R substitution. The wild-type residue is shown in green (B), the mutated residue is shown in red (C). (D) Detail of the additional interactions established by R183 in the hDAAO variant. The numbers refer to the distance in Å. Figure prepared with PyMOL.

monitored by conventional epifluorescence microscopy imaging (excitation at 470 nm; Zeiss AXIOVERT 200; Zeiss, Oberkochen, Germany) and by Western blot analysis in parallel (see above). The transfected cells were used for further experiments or to select stable clones upon adding 0.4 mg/mL G418 to the growth medium.

Immunostaining and confocal analyses were performed as reported in [41,42]. U87 cells were plated on round glass coverslips (2.5×10^5 cells each), incubated for 24 h at 37 °C and 5% CO₂, and transfected with pEYFP-G183R-hDAAO-C3 construct. At 24, 48, and 72 h after transfection, the coverslips were washed with PBS (10 mM dibasic

sodium phosphate, 2 mM monobasic potassium phosphate, 137 mM NaCl, and 2.7 mM KCl, pH 7.4) and fixed with 4% (v/v) *p*-formaldehyde and 4% (w/v) sucrose in 0.1 M sodium phosphate buffer, pH 7.4, for 15 min at room temperature. The fixed cells were permeabilized and blocked in PBS supplemented with 0.2% (v/v) Triton X-100 and 4% (v/v) horse serum, and subsequently stained using primary rabbit polyclonal anti-PMP70 (peroxisomal membrane protein 70, 1:200; Sigma-Aldrich, Saint Louis, MO, USA) or mouse monoclonal anti-ubiquitin antibody (F-11, 1:150; Santa Cruz Biotechnology Inc.), followed by secondary anti-rabbit Alexa 647 and anti-mouse Alexa 546 antibodies

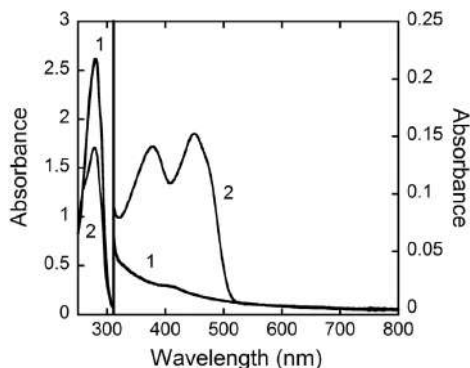


Fig. 2. Comparison of the absorbance spectrum of 35 μ M G183R hDAAO variant in apoprotein (1), as isolated at the end of the purification procedure, and in holoenzyme form (2), following incubation with a large excess of free FAD.

(1:1000; Molecular Probes, Eugene, OR, USA). Immunostained coverslips were imaged as reported in [41,42]. Immunofluorescence in U87 cells expressing the EYFP-hDAAO G183R variant was analyzed using an inverted laser-scanning confocal microscope (TCS SP5, Leica Microsystems, Wetzlar, Germany) equipped with a HCX PL APO lambda blue 63.0 \times 1.40 NA OIL UV objective. Images were acquired using the Leica TCS software in a sequential mode to avoid interference between each channel (emission windows fixed in the 520–538, 551–626 and 650–727 range for EYFP, Alexa 546 and Alexa 647, respectively) without saturating any pixel. Z-stack sections acquisition (15/cell) was carried out by selecting the optimized acquisition parameters. Controls were performed by omitting primary antibodies. The displayed images represent Z-stack projections of sections obtained with the open source image software Fiji (average intensity).

2.5. HPLC analysis

Cellular D- and L-serine levels were determined by HPLC chromatography [41,42]: 2.5×10^5 U87 cells expressing EYFP-hDAAO encoding wild-type or G183R variant were resuspended in 1 mL of ice-cold 5% (w/v) trichloroacetic acid, sonicated, and centrifuged (45 min at 13,000 rpm). The soluble fraction was extracted with ether, neutralized, and derivatized with *o*-phthalaldehyde/*N*-acetyl-L-cysteine in borate buffer. D- and L-serine were resolved by HPLC chromatography using a 5- μ m Waters C8 (4.6 \times 250 mm) reversed-phase column (Waters Co., Milford, MA, USA). Identification and quantification of D- and L-serine were based on retention times and peak areas, compared to those associated with external standards.

2.6. Caspase-Glo 3/7 assay

U87 cells were seeded in 96-well plates at a density of 10^4 cells/well, incubated for 24 h at 37 °C and 5% CO₂, and transiently transfected with 0.1 μ g of the plasmid pEYFP-hDAAO-C3 encoding wild-type, W209R [16], or G183R hDAAO variants using the FuGENE HD transfection reagent. After 48 h of incubation, caspase-3 and caspase-7 activity was measured using the Caspase-Glo 3/7 Assay kit (Promega Co., Madison, WI, USA). According to the manufacturer's instructions, 100 μ L of the Caspase-GloW 3/7 reagent was added to each well and the cells were incubated for 4 h at 25 °C. The light emission produced by the substrate cleavage, aminoluciferin release, and the subsequent luciferase reaction were measured by a plate reader (Infinite 200, Tecan, Männedorf, Switzerland): the value recorded at 2 h was used to assess caspase activity. The same measurements were performed by adding 1 mM D-serine to cells 24 h after transfection. Nontransfected U87 cells and DMEM medium were used as controls and were analyzed in

parallel.

3. Results

3.1. Expression of hDAAO G183R in *E. coli* and its purification

First, the G183R hDAAO variant was expressed in *E. coli* cells as N-terminal His-tagged protein, employing the same conditions used for the wild-type enzyme [35], but the yield in terms of purified protein was too low (1 mg/L of fermentation broth) for an in-depth biochemical characterization. In order to improve the expression level of hDAAO G183R in a soluble form, the following parameters were investigated by employing a simplified factorial design approach [43]: the growth medium (LB, 1.5x LB or TB), the OD_{600 nm} value at the moment IPTG was added (2.5 or 6), the time of cell collection (0, 1, 2, 5 or 16 h), the growth temperature after the induction of protein expression (20, 25, or 37 °C), the flask fermentation volume (350, 500, or 700 mL), and the aeration level. Best conditions in terms of protein expression are reported in Suppl. Table 1.

The G183R variant was purified by HiTrap chelating chromatography using the procedure previously set up for the wild-type enzyme [35], yielding a protein preparation with a 95% of purity as judged by SDS-PAGE analysis and an overall yield of 5.4 mg of pure protein/L of fermentation broth corresponding to 0.2 mg protein/g cells (Suppl. Table 2).

3.2. Biochemical properties of G183R hDAAO

Activity assays performed under standard conditions as well as in the presence of a large excess of exogenous FAD (200 μ M) show that purified G183R hDAAO was fully inactive (Suppl. Table 2). A similar result was obtained after incubating the enzyme for 1 or 16 h with 100 μ M FAD to push holoenzyme reconstitution before the activity assay. Indeed, the absorbance spectrum of the G183R hDAAO preparation showed that the variant was purified as apoprotein, i.e., lacking the typical absorbance peaks at 450 and 380 nm associated with the bound FAD cofactor (Fig. 2).

In order to push holoenzyme reconstitution, the purified G183R hDAAO – to which 200 μ M FAD was added – was extensively dialyzed against 40 μ M FAD: the resulting preparation showed the typical absorbance spectrum of FAD containing flavoenzymes (see spectrum 2 in Fig. 2). The activity assay performed in the presence of an excess of FAD showed that the reconstituted hDAAO G183R holoenzyme was completely inactive.

The oligomeric state of G183R hDAAO was investigated by size-exclusion chromatography. Similarly to the wild-type flavoenzyme, both the apoprotein and the reconstituted holoenzyme form of hDAAO G183R showed an elution volume corresponding to a 80-kDa homodimeric state at a protein concentration of 1 and 10 mg/mL (Suppl. Fig. 1 and Suppl. Table 2).

The protein conformation of the G183R variant was analyzed by circular dichroism spectroscopy. The far- and the near-UV CD spectra of the holoenzyme form were significantly altered for the G183R variant compared to the wild-type hDAAO (Fig. 3A, B). On the contrary, the secondary and tertiary structure of the apoprotein form was only slightly modified following the G183R substitution, as made apparent by the CD spectra in Fig. 3C, D and by the similar protein fluorescence spectra (not shown). Furthermore, the CD spectra recorded for the reconstituted holoenzyme form of G183R variant closely resembled the ones for the apoprotein form, while for the wild-type hDAAO the near-UV CD spectra significantly differed for the holo- and the apoprotein forms [39,40].

Thermal stability of hDAAO G183R was investigated by temperature-ramp experiments analyzing the changes in tryptophan fluorescence at 340 nm (for tertiary structure modifications) and in the CD signal at 220 nm (for secondary structure alterations). In all cases, the

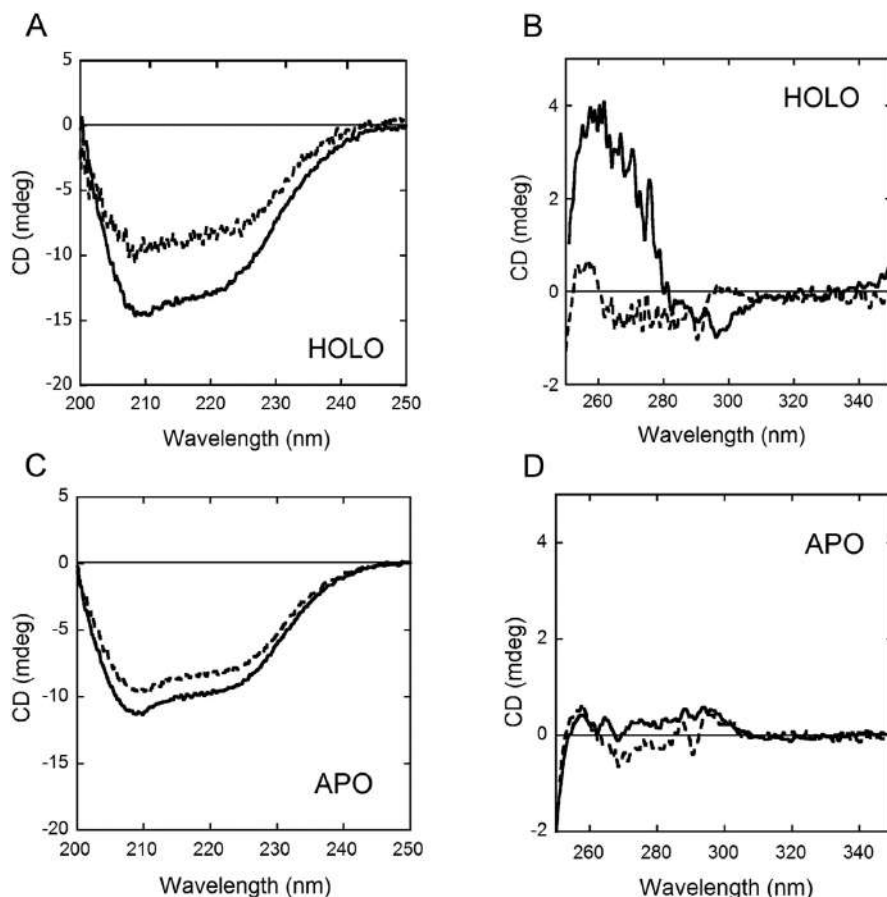


Fig. 3. Comparison of CD spectra of wild-type (—) and G183R (---) hDAAO variants. (A, C) Far-UV CD spectra of holoenzyme (A) and apoprotein (C) forms of hDAAO variants (0.1 mg/mL). (B, D) Near-UV CD spectra of holoenzyme (B) and apoprotein (D) forms of hDAAO variants (0.4 mg/mL).

Table 1
Comparison of melting temperatures of wild-type and G183R hDAAO variants as determined by different approaches.

Melting temperature (°C)	Apoprotein		Holoenzyme	
	Wild-type	G183R	Wild-type	G183R
Protein fluorescence (at 340 nm)	53.1 ± 1.0	59.1 ± 1.5	57.7 ± 0.3	61.0 ± 1.7
CD (at 220 nm)	58.8 ± 1.0	63.2 ± 0.4	57.0 ± 1.0	62.4 ± 0.3

Values are reported as mean ± SD (n = 3).

melting temperature was 3–6 °C higher for the G183R variant than for wild-type hDAAO (Table 1).

3.3. Binding properties

Dissociation constants of the apoprotein form of G183R hDAAO variant for FAD (both the free form and the benzoate complex), FMN, riboflavin, chlorpromazine (CPZ, a FAD-competitive inhibitor of hDAAO, used as an antipsychotic drug in schizophrenia treatment) [44], 6-chloro-benzo(*d*)isoxazol-3-ol (CBIO, a hDAAO inhibitor that binds to the enzyme active site) [45], benzoate (a substrate-competitive inhibitor that increases the affinity for the cofactor of the wild-type enzyme) [35], and anthranilate were estimated by titrating 1 μM of the enzyme with increasing amounts of ligand and by analyzing the quenching of tryptophan emission at 340 nm. Titration of the G183R

variant with FAD in the absence and presence of 50 mM benzoate is shown in Suppl. Fig. 2: in the latter case the emission maximum is shifted from 340 nm for the apoprotein to ~320 nm at the end of the titration.

Compared to the wild-type hDAAO, the most significant alterations in the G183R variant were apparent for the binding of FAD in the presence of benzoate (~1000-fold weaker) and for the binding of anthranilate (~150-fold weaker). K_d values are reported in Table 2.

Table 2
Comparison of binding properties of wild-type and G183R hDAAO variants. For the latter variant, the apoprotein form was used. The K_d values were determined following the quenching of protein fluorescence.

	Dissociation constant (K_d)	
	Wild-type	G183R
FAD, free form (μM)	7.9 ± 2.0 ^a	8.4 ± 1.9
Benzoate complex (μM)	0.3 ± 1.0 ^a	235.0 ± 25.9
FMN (μM)	12.0 ± 0.6	56.6 ± 4.2
Riboflavin (mM)	1.0 ± 0.1	0.8 ± 0.1
CPZ (μM)	5.0 ± 0.1 ^b	9.3 ± 0.2
Benzoate (mM)	1.8 ± 0.5	6.5 ± 0.4
CBIO (μM)	369 ± 64	628 ± 25
Anthranilate (μM)	2.7 ± 0.6	386.1 ± 30.4

Values are reported as mean ± SD (n = 3).

^a [35].

^b [41].

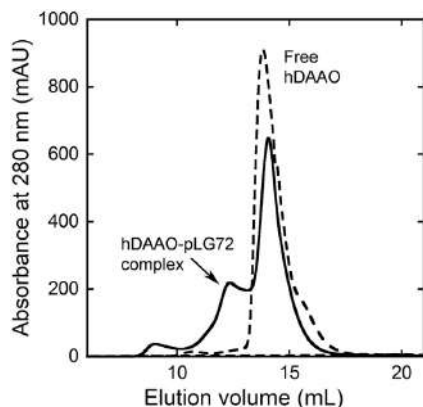


Fig. 4. Analysis of pLG72 binding to G183R hDAAO (20 and 40 nmol, respectively). Size-exclusion chromatography was used to investigate the 200 kDa hDAAO-pLG72 complex formation (—). Elution profile of G183R hDAAO (---).

Notably, after adding a large excess of benzoate or anthranilate to G183R hDAAO-reconstituted holoenzyme, no alteration of the visible absorbance spectrum was apparent, as was observed for the wild-type enzyme [35]. The alteration observed for the latter enzyme gives strong evidence of ligand binding at the active site of DAAO since it corresponds to the π - π interaction between the aromatic ring of the ligand and the isoalloxazine ring of FAD [2,46].

The interaction between G183R hDAAO and the modulator pLG72 was investigated by size-exclusion chromatography using a mixture containing a 2:1 molar ratio of hDAAO and pLG72, a condition leading to the 200-kDa complex formation for the wild-type enzyme [41]. The G183R hDAAO variant interacted with pLG72, also yielding the 200-kDa complex: in addition to the peak at an elution volume of 14.1 mL, corresponding to G183R hDAAO, a peak at 12.4 mL, corresponding to the complex, was apparent (Fig. 4).

3.4. Expression of hDAAO G183R in U87 cells

The effect of the G183R substitution in the human flavoenzyme was studied at the cellular level by analyzing its subcellular localization and by measuring cellular D-serine concentration. For this purpose the hDAAO variant was expressed in human U87 glioblastoma cells using a pEYFP-hDAAO-C3 construct that encodes for a chimeric hDAAO fused to the C-terminus of EYFP [41,42]. The subcellular localization of G183R hDAAO was analyzed in cells both stably and transiently expressing the flavoenzyme variant by immunostaining and confocal microscopy analyses. The signal for the wild-type enzyme was mainly cytosolic at 24 h from transfection and largely compartmentalized to peroxisomes at 48 and 72 h from transfection [42]. Similarly to the wild-type enzyme, in U87 cells transiently transfected EYFP-hDAAO G183R mainly showed a cytosolic distribution at 24 h from transfection; while at 48 and 72 h from transfection, differently to hDAAO wild-type, the chimeric protein fluorescence signal only partially overlapped with PMP70 one, indicating an incomplete peroxisomal targeting. Indeed, the same cells formed cytosolic protein aggregates and showed a high ubiquitin signal intensity (Fig. 5A). Notably, aggregate-containing cells often showed an altered (fused) morphology for peroxisomes, as previously observed in cells expressing the G331V hDAAO variant [36].

The images acquired from U87 cells stably expressing the G183R hDAAO variant resembled those of U87 cells 72 h after transient transfection. EYFP-hDAAO G183R was partially compartmentalized to peroxisomes: its distribution was largely cytosolic and overlapped to the signal corresponding to ubiquitin (Fig. 5B).

The effect of the G183R substitution on D-serine cellular levels was

studied on U87 cells stably expressing the wild-type or the variant hDAAO by HPLC chromatography (Suppl. Fig. 3). The D-serine cellular concentration and the D/(D + L)-serine ratio were significantly higher (~7-fold) in the selected U87 clone stably expressing the fully inactive G183R hDAAO variant than in the control clone expressing the wild-type enzyme (Table 3).

Since hDAAO is known to be partially cytosolic and that the G183R variant is prone to aggregation (see above), we investigated the activation of apoptosis induced by expression of hDAAO on U87 cells transiently expressing the wild-type, W209R (a hDAAO variant showing an improved activity) [16] or G183R variants of the flavoenzyme by assaying the activity of caspase 3 and 7. Caspase activity was lower in cells expressing the inactive G183R variant than in cells expressing the active wild-type or W209R hDAAOs (see Fig. 6, left). The level of apoptosis in cells expressing the G183R hDAAO was unchanged when exogenous 1 mM D-serine was added to the medium, while a significant decrease in luminescence signal was apparent for cells expressing the active hDAAO variants (Fig. 6, right). Taken together, the induction of apoptosis is likely related to both the activity and the aggregation ability of the overexpressed hDAAO variant.

4. Discussion

Considering the low levels of serine racemase in astrocytes, the “serine shuttle model” [10,11] indirectly assigns to DAAO a key role in regulating D-serine concentration in these cells: this flavo-oxidase exerts a neuromodulatory function by terminating D-serine signaling and thus may affect the NMDAR-dependent physiological functions involved in key cognitive abilities [12,13]. As stated in the Introduction section, a dysregulation in D-serine signaling is implicated in the NMDAR dysfunction observed in a number of pathological conditions.

Structural and functional studies have highlighted the peculiar biochemical properties of hDAAO [35,40,41,47,48]: it only weakly binds the FAD cofactor, shows a stable homodimeric state, and its activity and half-life are specifically regulated by pLG72 binding. Notwithstanding the high sequence identity with the mouse counterpart (80.6%), we propose that hDAAO evolved to tightly control D-serine concentration in the brain and thus to finely tune NMDAR-related processes.

Since the ddY mice lacking DAAO activity has been used to shed light on physiological and pathological brain functions related to NMDAR, we decided to introduce the corresponding substitution in human DAAO and to investigate the main properties of the protein variant.

The recombinant G183R hDAAO is produced as inactive apoprotein. Abolition of catalytic activity is not only due to the low binding affinity for the cofactor since the reconstituted holoenzyme did not recover the ability to oxidize D-serine. Furthermore, CD spectra of reconstituted G183R hDAAO holoenzyme resemble those recorded for the apoprotein form, and the variant protein shows a higher thermal stability than the wild-type hDAAO. By following the changes in protein fluorescence during the titration with different ligands, it was made clear that the G183R substitution only alters the binding of the FAD and its analogues FMN, riboflavin, and CPZ, as well as the substrate-competitive inhibitors benzoate and CBIO (< 3.5-fold) to a limited extent (< 4.5-fold). In any case, the absence of a perturbation in the 400- to 500-nm range of the flavin absorbance spectrum during benzoate and anthranilate titration points to ligand positioning in G183R hDAAO not parallel to the isoalloxazine ring, as usually observed for substrate-competitive aromatic inhibitors [47,48]. Taken together, the biochemical characterization indicates that the substitution of G183 with an arginine alters hDAAO conformation and negatively affects the ability to bind the flavin cofactor in the orientation required for hydride-transfer during catalysis, a conformation that is further modified when the substrate or a substrate analogue is bound in the active site [35,40]. The 25-fold tighter interaction of the apoprotein with FAD observed in the

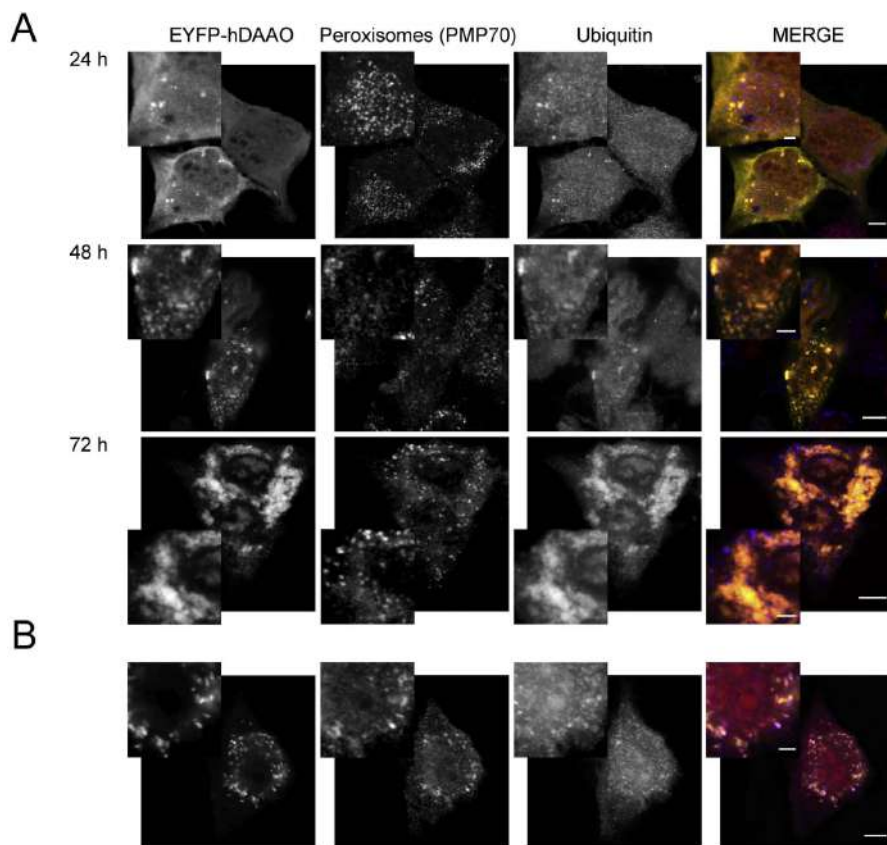


Fig. 5. Confocal analysis of the subcellular localization of EYFP-hDAAO G183R variant in transiently (A) and stably (B) transfected U87 human glioblastoma cells. The distribution pattern of EYFP-hDAAO G183R as well as the immunofluorescence of the peroxisomal marker PMP70 and ubiquitin is reported in gray scale in the single channel panels. In the merge panels the signal for chimeric protein fluorescence (yellow channel) is overlaid to the signals corresponding to peroxisomes (blue channel) and ubiquitin (red channel). Images represent Z-stack projections of 15 sections. Insets show a high magnification detail of a single cell. Scale bars correspond to 5 μm (panels) and 2 μm (insets).

Table 3

Quantitative analysis of EYFP-hDAAO G183R expression levels, D-serine levels and D/(D + L)-serine ratio in U87 cells clones stably expressing wild-type or G183R EYFP-hDAAO variants. Expression levels are reported as the pEYFP-hDAAO/actin signal intensity ratio.

	hDAAO	
	Wild-type	G183R
Relative DAAO expression (pEYFP-hDAAO/actin)	1.43	1.16
D-Serine (pmol) ^a	1.8 \pm 0.5	13.3 \pm 1.4
L-Serine (pmol) ^a	48.5 \pm 16.2	45.0 \pm 1.6
D/(D + L)-Serine (%)	3.6 \pm 0.2	28.2 \pm 8.3

^a Values refers to 2.5×10^5 cells and are reported as mean \pm SD (n = 5).

presence of benzoate for the wild-type hDAAO [35] translates into a 30-fold lower affinity in the G183R variant. The conserved G183 residue belongs to α -helix α 9, which is close to the pyrophosphate and ribityl groups of FAD (see Fig. 1A, B). By substituting it with an arginine, additional electrostatic and hydrogen bond interactions can be established with surrounding residues side chains and -CO and -NH backbone groups that are in close contact with the moiety of FAD (Fig. 1C, D). The ensuing alteration in protein conformation alters the binding and orientation of the cofactor, thus affecting the interaction of the isoalloxazine ring with the substrate/competitive inhibitor.

At the cellular level, the overexpressed G183R hDAAO is partially targeted to peroxisomes and forms protein aggregates showing a strong colocalization with ubiquitin. Indeed, its overexpression significantly increases both the D-serine cellular concentration and the D/(D + L)-serine ratio (7-fold). We demonstrated that the increase in D-serine does

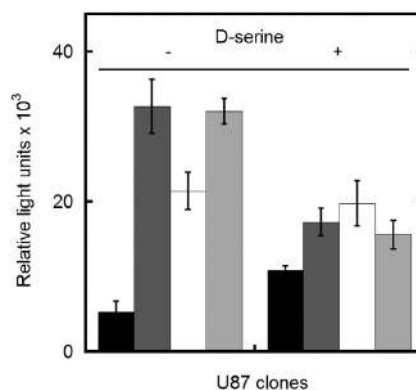


Fig. 6. Caspase activity in untransfected (black) and in transiently transfected U87 cells expressing wild-type (dark gray), G183R (white) or W209R (light gray) EYFP-hDAAOs. Caspase activity was assayed at 48 h after transient transfection of EYFP-hDAAO and compared to that detected in control cells (untransfected U87 cells). The protease activity was measured as relative light units by lysing the cells in the presence of Caspase-Glo 3/7 substrate. The samples on the right were added of 1 mM D-serine at 24 h after transfection. The values as reported as the mean \pm standard deviation.

not alter the concentration of L-serine (Table 3): in agreement with the preferential neuronal localization of serine racemase [49], in glial cells the two enantiomers cannot efficiently convert each other and thus the excess of D-serine will be stored. Notably, in contrast to what is observed for the R199W hDAAO related to ALS [15,50] and the G331V

variant related to schizophrenia susceptibility [36], where formation of protein aggregates is coupled to strong induction of apoptosis, G183R hDAAO overexpression did not result in enhanced apoptosis.

In conclusion, the ability of the G183R hDAAO to bind the FAD cofactor is strongly affected and its ability to degrade *D*-serine is fully abolished. As such, the G183R substitution resembles the effect of the R199W substitution related to a familial case of ALS [15,16,50]: the substitution altered the protein conformation, yielding loss of enzymatic activity and protein aggregation at the cellular level, which resulted in an abnormal increase in cellular *D*-serine concentration. A similar situation was observed in aged mice lacking DAAO activity, where ubiquitin-positive aggregates were observed in motoneurons of the ventral root in the spinal cord, which was associated to axonal degeneration with muscle atrophy [51].

Taken together, our investigation warrants caution in using mice lacking DAAO activity because of the G181R single-point mutation. The effect due to this substitution in hDAAO could be misleading; the effects due to impairment of *D*-serine degradation overlap with those related to aggregate accumulation.

Transparency document

The Transparency document associated with this article can be found, in online version.

Acknowledgements

This work was supported by grants from Fondo di Ateneo per la Ricerca to S.S. and L.P. We thank Dr. Gianluca Molla for fruitful discussion and help in preparation of Fig. 1, and the support from Consorzio Interuniversitario per le Biotecnologie to GM.

Appendix A. Supplementary data

Supplementary data to this article can be found online at <https://doi.org/10.1016/j.bbapap.2017.12.007>.

References

- Pollegioni, L., Piubelli, S., Sacchi, M.S., Pilone, G., Molla, Physiological functions of *D*-amino acid oxidases: from yeast to humans, *Cell. Mol. Life Sci.* 64 (2007) 1373–1394.
- Sacchi, L., Caldinelli, P., Cappelletti, L., Pollegioni, G., Molla, Structure-function relationships in human *D*-amino acid oxidase, *Amino Acids* 43 (2012) 1833–1850.
- J.P. Mothet, A.T. Parent, H. Wolosker, R.O. Brady Jr., D.J. Linden, C.D. Ferris, M.A. Rogawski, S.H. Snyder, *D*-Serine is an endogenous ligand for the glycine site of the *N*-methyl-*D*-aspartate receptor, *Proc. Natl. Acad. Sci. U. S. A.* 97 (2000) 4926–4931.
- T. Papouin, L. Lade-pêche, J. Ruel, S. Sacchi, M. Labasque, M. Hanini, L. Groc, L. Pollegioni, J.P. Mothet, S.H. Oliet, Synaptic and extrasynaptic NMDA receptors are gated by different endogenous coagonists, *Cell* 150 (2012) 633–646.
- P. Paoletti, C. Bellone, Q. Zhou, NMDA receptor subunit diversity: impact on receptor properties, synaptic plasticity and disease, *Nat. Rev. Neurosci.* 14 (2013) 383–400.
- P. Fossat, F.R. Turpin, S. Sacchi, J. Dulong, T. Shi, J.M. Rivet, J.V. Sweedler, L. Pollegioni, M.J. Millan, S.H. Oliet, J.P. Mothet, Glial *D*-serine gates NMDA receptors at excitatory synapses in prefrontal cortex, *Cereb. Cortex* 22 (2011) 595–606.
- M. LeBail, M. Martineau, S. Sacchi, N. Yatsenko, I. Radzishvsky, S. Conrod, K. Ait Ouare, H. Wolosker, L. Pollegioni, J.M. Billard, J.P. Mothet, Identity of the NMDA receptor coagonist is synapse specific and developmentally regulated in the hippocampus, *Proc. Natl. Acad. Sci. U. S. A.* 112 (2015) 204–312.
- L. Curcio, M.V. Podda, L. Leone, R. Piacentini, A. Mastrorodato, P. Cappelletti, S. Sacchi, L. Pollegioni, C. Grassi, M. D'Ascenzo, Reduced *D*-serine levels in the nucleus accumbens of cocaine-treated rats hinder the induction of NMDA receptor-dependent synaptic plasticity, *Brain* 136 (2013) 1216–1230.
- C.N. Meunier, G. Dallérac, N. Le Roux, S. Sacchi, G. Levasseur, M. Amar, L. Pollegioni, J.P. Mothet, P. Fossier, *D*-Serine and glycine differentially control neurotransmission during visual cortex critical period, *PLoS One* 11 (3) (2016) e0151233.
- H. Wolosker, Serine racemase and the serine shuttle between neurons and astrocytes, *Biochim. Biophys. Acta* 1814 (2011) 1558–1566.
- H. Wolosker, D.T. Balu, J.T. Coyle, The rise and fall of the *D*-serine-mediated gliotransmission hypothesis, *Trends Neurosci.* 39 (2016) 712–721.
- G. Morris, NMDA receptors and memory encoding, *Neuropharmacology* 74 (2013) 32–40.
- G.L. Collingridge, A. Volianskis, N. Bannister, G. France, L. Hanna, M. Mercier, P. Tidball, G. Fang, M.W. Irvine, B.M. Costa, D.T. Monaghan, Z.A. Bortolotto, E. Molnár, D. Lodge, D.E. Jane, The NMDA receptor as a target for cognitive enhancement, *Neuropharmacology* 64 (2013) 13–26.
- J. Mitchell, P. Paul, H.J. Chen, A. Morris, M. Payling, M. Falchi, J. Habgood, S. Panoutsou, S. Winkler, V. Tisato, A. Hajitou, B. Smith, C. Vance, C. Shaw, N.D. Mazarakis, J. de Bellerocche, Familial amyotrophic lateral sclerosis is associated with a mutation in *D*-amino acid oxidase, *Proc. Natl. Acad. Sci. U. S. A.* 107 (2010) 7556–7561.
- P. Paul, J. de Bellerocche, The role of *D*-amino acids in amyotrophic lateral sclerosis pathogenesis: a review, *Amino Acids* 43 (2012) 1823–1831.
- P. Cappelletti, L. Piubelli, G. Murtas, L. Caldinelli, M. Valentino, G. Molla, L. Pollegioni, S. Sacchi, Structure-function relationships in human *D*-amino acid oxidase variants corresponding to known SNPs, *Biochim. Biophys. Acta* 1854 (2015) 1150–1159.
- C. Madeira, M.V. Lourenco, C. Vargas-Lopes, C.K. Suemoto, C.O. Brandão, T. Reis, R.E.P. Leite, J. Laks, W. Jacob-Filho, C.A. Pasqualucci, L.T. Grinberg, S.T. Ferreira, R. Panizzutti, *D*-Serine levels in Alzheimer's disease: implications for novel biomarker development, *Transl. Psychiatry* 5 (2015) 561.
- Z. Li, Y. Xing, X. Guo, Y. Cui, Development of an UPLC-MS/MS method for simultaneous quantitation of 11 *D*-amino acids in different regions of rat brain: application to a study on the associations of *D*-amino acid concentration changes and Alzheimer's disease, *J. Chromatogr. B Anal. Technol. Biomed. Life Sci.* 1058 (2017) 40–46.
- L.S. Miraucourt, C. Peirs, R. Dallel, D.L. Voisin, Glycine inhibitory dysfunction turns touch into pain through astrocyte-derived *D*-serine, *Pain* 152 (2011) 1340–1348.
- K. Hashimoto, T. Fukushima, E. Shimizu, N. Komatsu, H. Watanabe, N. Shinoda, M. Nakazato, C. Kumakiri, S. Okada, H. Hasegawa, K. Imai, M. Iyo, Decreased serum levels of *D*-serine in patients with schizophrenia: evidence in support of the *N*-methyl-*D*-aspartate receptor hypofunction hypothesis of schizophrenia, *Arch. Gen. Psychiatry* 60 (2003) 572–576.
- I. Bendikov, C. Nadri, S. Amar, R. Panizzutti, J. De Miranda, H. Wolosker, G. Agam, A CSF and postmortem brain study of *D*-serine metabolic parameters in schizophrenia, *Schizophr. Res.* 90 (2007) 41–51.
- M.A. Calcia, C. Madeira, F.V. Almeida, T.C. Silva, F.M. Tannos, C. Vargas-Lopes, N. Goldenstein, M.A. Brasil, S.T. Ferreira, R. Panizzutti, Plasma levels of *D*-serine in Brazilian individuals with schizophrenia, *Schizophr. Res.* 142 (2012) 83–87.
- L. Verrall, M. Walker, N. Rawlings, I. Benzel, J.N. Kew, P.J. Harrison, P.W. Burnet, *D*-amino acid oxidase and serine racemase in human brain: normal distribution and altered expression in schizophrenia, *Eur. J. Neurosci.* 26 (2007) 1657–1669.
- C. Madeira, M.E. Freitas, C. Vargas-Lopes, H. Wolosker, R. Panizzutti, Increased brain *D*-amino acid oxidase (DAAO) activity in schizophrenia, *Schizophr. Res.* 101 (2008) 76–83.
- G. Habl, M. Zink, G. Petroianu, M. Bauer, T. Schneider-Axmann, M. von Wilmsdorff, P. Falkai, F.A. Henn, A. Schmitt, Increased *D*-amino acid oxidase expression in the bilateral hippocampal CA4 of schizophrenic patients: a post-mortem study, *J. Neural Transm.* 116 (2009) 1657–1665.
- R. Konno, Y. Yasumura, Mouse mutant deficient on *D*-amino acid oxidase activity, *Genetics* 103 (1983) 277–285.
- M. Sasaki, R. Konno, M. Nishio, A. Niwa, Y. Yushima, J. Enami, A single-base-pair substitution abolishes *D*-amino acid oxidase activity in the mouse, *Biochim. Biophys. Acta* 1139 (1992) 315–318.
- S.L. Almond, R.L. Fradley, A.J. Armstrong, R.B. Heavens, A.R. Rutter, R.J. Newman, C.S. Chiu, R. Konno, H. Hutson, R.J. Brandon, Behavioral and biochemical characterization of a mutant mouse strain lacking *D*-amino acid oxidase activity and its implications for schizophrenia, *Mol. Cell. Neurosci.* 32 (2006) 324–334.
- V. Labrie, R. Fukumura, A. Rastogi, Genetic inactivation of serine racemase produces behavioral phenotypes related to schizophrenia in mice, *Learn. Mem.* 16 (2009) 28–37.
- K. Wake, H. Yamazaki, S. Hanzawa, R. Konno, H. Sakio, A. Niwa, Y. Hori, Exaggerated responses to chronic nociceptive stimuli and enhancement of *N*-methyl-*D*-aspartate receptor-mediated synaptic transmission in mutant mice lacking *D*-amino acid oxidase, *Neurosci. Lett.* 297 (2001) 25–28.
- W. Zhao, R. Konno, X.J. Zhou, M. Yin, Y.X. Wang, Inhibition of *D*-amino acid oxidase activity induces pain relief in mice, *Cell. Mol. Neurobiol.* 28 (2008) 581–591.
- M. Maekawa, M. Watanabe, S. Yamaguchi, R. Konno, Y. Hori, Spatial learning and long-term potentiation of mutant mice lacking *D*-amino acid oxidase, *Neurosci. Res.* 53 (2005) 34–38.
- V. Labrie, W. Wang, S.W. Barger, G.B. Baker, J.C. Roder, Genetic loss of *D*-amino acid oxidase activity reverses schizophrenia-like phenotypes in mice, *Genes Brain Behav.* 9 (2010) 11–25.
- V. Labrie, S.J. Clapcote, J.C. Roder, Mutant mice with reduced NMDA-NR1 glycine affinity or lack of *D*-amino acid oxidase function exhibit altered anxiety-like behaviors, *Pharmacol. Biochem. Behav.* 91 (2009) 610–620.
- G. Molla, S. Sacchi, M. Bernasconi, M.S. Pilone, K. Fukui, L. Pollegioni, Characterization of human *D*-amino acid oxidase, *FEBS Lett.* 580 (2006) 2358–2364.
- L. Caldinelli, S. Sacchi, G. Molla, M. Nardini, L. Pollegioni, Characterization of human DAAO variants potentially related to an increased risk of schizophrenia, *Biochim. Biophys. Acta* 1832 (2013) 400–410.
- G. Molla, M. Bernasconi, S. Sacchi, M.S. Pilone, L. Pollegioni, Expression in *Escherichia coli* and in vitro refolding of the human protein pLG72, *Protein Expr. Purif.* 46 (2006) 150–155.
- L. Caldinelli, S. Iametti, A. Barbiroli, F. Bonomi, D. Fessas, G. Molla, M.S. Pilone,

- L. Pollegioni, Dissecting the structural determinants of the stability of cholesterol oxidase containing covalently bound flavin, *J. Biol. Chem.* 280 (2005) 22572–22581.
- [39] L. Caldinelli, G. Molla, L. Bracci, B. Lelli, S. Pileri, P. Cappelletti, S. Sacchi, L. Pollegioni, Effect of ligand binding on human D-amino acid oxidase: implications for the development of new drugs for schizophrenia treatment, *Protein Sci.* 19 (2010) 1500–1512.
- [40] L. Caldinelli, G. Molla, S. Sacchi, M.S. Pilone, L. Pollegioni, Relevance of weak flavin binding in human D-amino acid oxidase, *Protein Sci.* 18 (2009) 801–810.
- [41] S. Sacchi, M. Bernasconi, M. Martineau, J.P. Mothet, M. Ruzzene, M.S. Pilone, L. Pollegioni, G. Molla, pLG72 modulates intracellular D-serine levels through its interaction with D-amino acid oxidase: effect on schizophrenia susceptibility, *J. Biol. Chem.* 283 (2008) 22244–22256.
- [42] S. Sacchi, P. Cappelletti, S. Giovannardi, L. Pollegioni, Evidence for the interaction of D-amino acid oxidase with pLG72 in a glial cell line, *Mol. Cell. Neurosci.* 48 (2011) 20–28.
- [43] F. Volontè, F. Marinelli, L. Gastaldo, S. Sacchi, M.S. Pilone, L. Pollegioni, G. Molla, Optimization of glutaryl-7-aminocephalosporanic acid acylase expression in *E. coli*, *Protein Expr. Purif.* 61 (2009) 131–137.
- [44] A.A. Kurland, Chlorpromazine in the treatment of schizophrenia; a study of 75 cases, *J. Nerv. Ment. Dis.* 121 (1955) 321–329.
- [45] D. Ferraris, B. Duvall, Y.S. Ko, A.G. Thomas, G. Rojas, P. Majer, K. Hashimoto, T. Tsukamoto, Synthesis and biological evaluation of D-amino acid oxidase inhibitors, *J. Med. Chem.* 51 (2008) 3357–3359.
- [46] L. Pollegioni, S. Butò, W. Tischer, S. Ghisla, M.S. Pilone, Characterization of D-amino acid oxidase from *Trigonopsis variabilis*, *Biochem. Mol. Biol. Int.* 31 (1993) 709–717.
- [47] T. Kawazoe, H. Tsuge, M.S. Pilone, K. Fukui, Crystal structure of human D-amino acid oxidase: context-dependent variability of the backbone conformation of the VAAGL hydrophobic stretch located at the si-face of the flavin ring, *Protein Sci.* 15 (2006) 2708–2717.
- [48] C. Hopkins, M.L. Heffernan, L.D. Saraswat, C.A. Bowen, L. Melnick, L.W. Hardy, M.A. Orsini, M.S. Allen, P. Koch, K.L. Spear, R.J. Foglesong, M. Soukri, M. Chytil, Q.K. Fang, S.W. Jones, M.A. Varney, A. Panatier, S.H. Oliet, L. Pollegioni, L. Piubelli, G. Molla, M. Nardini, T.H. Large, Structural, kinetic, and pharmacodynamic mechanisms of D-amino acid oxidase inhibition by small molecules, *J. Med. Chem.* 56 (2013) 3710–3724.
- [49] H. Wolosker, I. Radzishevsky, The serine shuttle between glia and neurons: implications for neurotransmission and neurodegeneration, *Biochem. Soc. Trans.* 41 (2013) 1546–1550.
- [50] P. Paul, T. Murphy, Z. Oseni, S. Sivalokanathan, J.S. de Belleruche, Pathogenic effects of amyotrophic lateral sclerosis-linked mutation in D-amino acid oxidase are mediated by D-serine, *Neurobiol. Aging* 35 (2014) 876–885.
- [51] J. Sasabe, Y. Miyoshi, M. Suzuki, M. Mita, R. Konno, M. Matsuoka, K. Hamase, S. Aiso, D-Amino acid oxidase controls motoneuron degeneration through D-serine, *Proc. Natl. Acad. Sci. U. S. A.* 109 (2012) 627–632.



Substitution of Arginine 120 in Human D-Amino Acid Oxidase Favors FAD-Binding and Nuclear Mistargeting

Giulia Murtas*, Silvia Sacchi and Loredano Pollegioni

Dipartimento di Biotecnologie e Scienze della Vita, Università degli Studi dell'Insubria, Varese, Italy

OPEN ACCESS

Edited by:

Kornelius Zeth,
Roskilde University, Denmark

Reviewed by:

Vladimir I. Tishkov,
Lomonosov Moscow State
University, Russia
Robert Stephen Phillips,
University of Georgia, United States

*Correspondence:

Giulia Murtas
g.murtas@uninsubria.it

Specialty section:

This article was submitted to
Structural Biology,
a section of the journal
Frontiers in Molecular Biosciences

Received: 05 August 2019

Accepted: 28 October 2019

Published: 12 November 2019

Citation:

Murtas G, Sacchi S and Pollegioni L
(2019) Substitution of Arginine 120 in
Human D-Amino Acid Oxidase Favors
FAD-Binding and
Nuclear Mistargeting.
Front. Mol. Biosci. 6:125.
doi: 10.3389/fmolb.2019.00125

The peroxisomal enzyme human D-amino acid oxidase (hDAAO) is attracting attention owing to its role in degrading D-serine, the main co-agonist of N-methyl D-aspartate receptors in brain, and its involvement in brain functions and diseases. Here, we focused on arginine 120, a residue located at the protein interface, 20 Å from the assumed second ligand-binding site, showing a different orientation of the side chain in the hDAAO-benzoate complex, and corresponding to Ser119 in rat DAAO, which is part of a putative nuclear translocation signal (NTS). By substituting Arg120 in hDAAO with a glutamate (to mimic the active NTS) or a leucine (to eliminate the positive charge) the protein conformation, thermal stability, and kinetic properties are slightly altered, while the dimeric structure and the ligand-binding properties are unchanged. The most relevant alteration in Arg120 variants is the strongest interaction with FAD. Nevertheless, the activity assayed at low D-serine and FAD concentrations (resembling physiological conditions) was quite similar for wild-type and Arg120 hDAAO variants. These results resemble the ones obtained substituting another residue located at the interface region (i.e., the W209R variant), indicating that substitutions at the monomer-monomer interface mainly affects the FAD binding in hDAAO. Indeed, U87 glioblastoma cells transiently transfected for hDAAO variants show that substitution of Arg120 favors mistargeting: the increase in cytosolic localization observed for the variants promotes nuclear targeting, especially for the R120E hDAAO, without affecting cell viability. Notably, mistargeting to the nucleus is an innate process as it is apparent for the wild-type hDAAO, too: whether such a process is related to specific pathologic processes is still unknown.

Keywords: flavoprotein, D-serine, mistargeting, structure-function relationships, peroxisome

INTRODUCTION

Human D-amino acid oxidase (hDAAO, EC 1.4.3.3) is a FAD-dependent enzyme, which catalyzes the oxidative deamination of neutral D-amino acids into the corresponding α -keto acids, ammonia, and hydrogen peroxide (Pollegioni et al., 2007; Sacchi et al., 2012; Murtas et al., 2017). In the brain, the main physiological substrate of this flavoenzyme is D-serine (D-Ser). D-Ser binds the glycine site of the N-methyl-D-aspartate type of the glutamate receptors (NMDAR) regulating its activity (Mothet et al., 2000; Li et al., 2013; Le Bail et al., 2015). A number of experimental results suggests that dysregulation of processes tuning D-Ser concentrations and thus of NMDAR-dependent

neurotransmission is involved in the mechanisms that concur to trigger various diseases such as amyotrophic lateral sclerosis, Alzheimer's disease, schizophrenia, etc. (Chumakov et al., 2002; Verrall et al., 2007; Billard, 2008; Madeira et al., 2008; Wolosker et al., 2008; Collingridge et al., 2013; Curcio et al., 2013; Murtas et al., 2017). Astrocytes express DAAO, the enzyme responsible for D-Ser degradation and thus ultimately modulate NMDA-dependent physiological functions (Wolosker, 2011).

During the past few years, hDAAO structural-functional relationships have been studied in depth using the recombinant protein produced in *E. coli* (Kawazoe et al., 2006; Molla et al., 2006; Pollegioni et al., 2007; Caldinelli et al., 2009, 2010; Romano et al., 2009; Sacchi et al., 2012; Murtas et al., 2017) and cell lines overexpressing the enzyme (Sacchi et al., 2008, 2011; Li et al., 2013). Nevertheless, several aspects in the modulation of the enzyme activity remain elusive (Pollegioni et al., 2018). DAAO is known as a peroxisomal enzyme (Moreno et al., 1999; Sacchi et al., 2008; Cappelletti et al., 2014) that is targeted to this organelle due to the C-terminal PTS1 sequence. In peroxisomes, the cytotoxic product hydrogen peroxide generated by the DAAO reaction is eliminated by specific enzymes, such as catalase. U87 glioblastoma cells transiently overexpressing hDAAO showed that the flavoenzyme is cytosolic before being delivered to peroxisomes: a time course of protein import was reported in Sacchi et al. (2008, 2011). Recent reports on rats demonstrated that DAAO is present both in cytosol and nuclei of proximal tubule epithelial cells following treatment with the drug propiverine (Luks et al., 2017a). In the nucleus, DAAO is ubiquitinated, sumoylated, and degraded through the nuclear proteasomal system (Luks et al., 2017a,b). The mistargeting of the enzyme could be due to the presence of an NTS (TPx sequence corresponding to 117T-P-S119) that, after phosphorylation of Ser119, might activate the translocation to the nucleus (Chuderland et al., 2008; Luks et al., 2017a). Ser119 of rat DAAO (rDAAO) corresponds to Arg120 in the hDAAO sequence. Notably, deletion of the C-terminal peroxisomal targeting signal 1 (PTS1) in both hDAAO and rDAAO resulted in a diffused nuclear and cytosolic distribution of the flavoenzyme (Luks et al., 2017b): nuclear localization was higher for rDAAO probably because a serine is phosphorylated more frequently than an arginine or was due to the different molecular masses of the two homologous enzymes (40 vs. 80 kDa for rDAAO and hDAAO, respectively). Substitution of the putative tripeptide for nuclear translocation with the EPE sequence fully abolished nuclear import, independently of the presence of the PTS1 signal (Luks et al., 2017b).

In hDAAO, the binding of an active site ligand facilitates FAD-apoprotein interaction to yield the active holoenzyme (Caldinelli et al., 2010; Murtas et al., 2017), this representing a main regulatory mechanism of its activity. R120 is located at the monomer-monomer interface (Figure 1A) and it has been also

proposed to play a role in ligand binding. Binding of benzoate (an active site ligand) to hDAAO is a biphasic process (Murtas et al., 2017). Indeed, the FAD-binding to hDAAO apoprotein in the absence of an active site ligand is also biphasic, while a single phase of saturation is apparent in the presence of 70 μ M benzoate (Murtas et al., 2017). For both FAD and benzoate binding no evidence of cooperativity between the first and second binding process was observed, which indicates the presence of two alternative protein conformations. A second benzoate binding site located in a cleft between the monomers was proposed (Kohiki et al., 2017): it is constituted by the residues belonging to

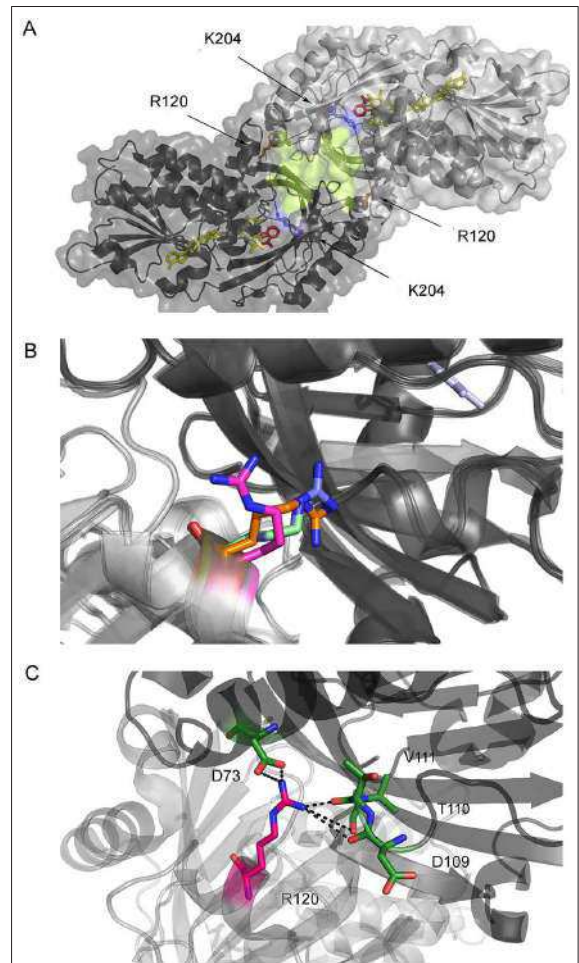


FIGURE 1 | Structure of hDAAO. **(A)** Details of the monomer-monomer interface of hDAAO. The second putative benzoate binding site proposed by Kohiki et al. (2017) is depicted in yellow. **(B)** Alternative orientations of R120 in hDAAO in the free form (blue, pdb 2E48) and in complex with benzoate (magenta, pdb 2DU8), with imino-DOPA (green, pdb 2E82), and with imino-serine (orange, pdb 2E49). **(C)** Details of the interaction of R120 with residues of the facing subunit (the two protomers are depicted in a different color).

Abbreviations: CBIO, 6-chloro-benzo(*d*)isoxazol-3-ol; CD, circular dichroism; DAAO, D-amino acid oxidase (EC 1.4.3.3); D-Ala, D-alanine; D-Cys, D-cysteine; D-Ser, D-serine; EYFP, enhanced yellow fluorescent protein; hDAAO, human D-amino acid oxidase; NMDAR, N-methyl-D-aspartate subtype of glutamate receptor; NTS, nuclear translocation signal.

the loop between β -strands 8 and 9 (residues 205–211) and those between β -strands 10 and 11 (residues 231–236); see **Figure 1A**. The overlay of the solved structures of hDAAO (in detail, 2DU8 in complex with benzoate, 2E82 in complex with imino-DOPA, 2E49 in complex with imino-serine, and 2E48, the substrate-free holoenzyme) does not show any difference in the residues belonging to the putative second binding site and pinpoints the orientation of R120 in the structure of hDAAO in complex with benzoate (**Figure 1B**) as being the only difference. R120 is located at the protein interface at 20 Å from the residues of the second binding site (**Figure 1A**).

Owing to the relevant physiological and pathological role of hDAAO, we expressed and biochemically characterized two variants at position 120 generated to mimic the activation of the NTS (by modifying the TPx sequence) and to verify its involvement in ligand binding and protein functionality.

MATERIALS AND METHODS

Preparation and Expression of hDAAO Variants in *Escherichia coli*

Mutagenesis reactions to prepare His-hDAAO R120E and R120L variants were performed on the pET11b-His-hDAAO wild-type expression plasmid (Molla et al., 2006) using the QuickChange site-directed mutagenesis kit (Stratagene, Santa Clara, CA, USA). Previous studies showed that the His-tag at the N-terminal end of hDAAO did not alter its activity or stability (Molla et al., 2006; Romano et al., 2009). Recombinant wild-type and R120 hDAAO variants were expressed in BL21 (DE3) Star *E. coli* cells and purified as reported in Molla et al. (2006) and Romano et al. (2009); 40 μ M of free FAD was present during all purification steps. The final enzyme preparations were stored at -20°C in 20 mM Tris-HCl buffer, pH 8.0, 100 mM NaCl, 10% (v/v) glycerol, 40 μ M FAD, and 5 mM 2-mercaptoethanol (added for long-term storage). Final enzyme preparations have a purify degree >95% as judged by SDS-PAGE analysis. The enzyme concentration was determined spectrophotometrically by using the extinction coefficient at 445 nm ($12.2 \text{ mM}^{-1} \text{ cm}^{-1}$) (Molla et al., 2006).

Activity Assay and Kinetic Measurements

DAAO activity was assayed with an oxygen electrode at pH 8.5, air saturation, and 25°C , using 28 mM D-alanine as the substrate in the presence of 0.2 mM FAD (Molla et al., 2000, 2006). The kinetic parameters were determined on different D-amino acids, employing increasing substrate concentrations (Molla et al., 2000, 2006). The apparent kinetic parameters were calculated using the initial reaction rate according to a Michaelis–Menten equation using the Kaleidagraph software (Synergy Software, Reading, PA, USA).

Spectral Measurements

Ligand and FAD-binding to hDAAO were investigated by following the quenching of protein fluorescence (0.3 mg protein/mL) (Molla et al., 2000; Caldinelli et al., 2009; Murtas et al., 2017). Protein fluorescence spectra were recorded between 300 and 400 nm, with excitation at 280 nm using a Jasco FP-750

instrument (excitation slit of 10 nm; emission slit of 5 nm) in 10 mM potassium phosphate, pH 8.0, 1% (v/v) glycerol, 5 mM 2-mercaptoethanol, and 40 μ M FAD.

Circular dichroism (CD) spectra were recorded in 10 mM Tris-HCl, pH 8.0, 1% (v/v) glycerol, and 40 μ M FAD by using a Jasco J-815 spectropolarimeter and analyzed employing a dedicated software (Jasco Co., Cremella, Italy). Cell path length was 1 cm for measurements above 250 nm (at 0.4 mg protein/mL) and 0.1 cm for measurements in the 190- to 250-nm region (at 0.1 mg protein/mL) (Caldinelli et al., 2009, 2010).

Temperature-ramp experiments were performed in 10 mM potassium phosphate, pH 8.0, 1% glycerol, 5 mM 2-mercaptoethanol, and 40 μ M FAD. A software-driven, Peltier-equipped fluorimeter was used to measure the fluorescence protein changes at 340 nm and Peltier-equipped CD spectropolarimeter to follow the CD signal at 220 nm: a temperature gradient of $0.5^{\circ}\text{C}/\text{min}$ (Caldinelli et al., 2009, 2010).

Oligomeric State

The molecular mass in solution of hDAAO variants (0.1–10 mg/mL protein) was investigated by means of gel-permeation chromatography on a Superdex 200 Increase column, using an Akta chromatographic system (GE Healthcare, Uppsala, Sweden), at room temperature and in 20 mM Tris-HCl, pH 8.5, 150 mM NaCl, 5% glycerol, 40 μ M FAD, and 5 mM 2-mercaptoethanol.

Cell Cultures and Transfection

Human U87 glioblastoma cells (ATCC) were cultured in DMEM supplemented with 10% fetal bovine serum, 1 mM sodium pyruvate, 2 mM L-glutamine, 1% non-essential amino acids, 1% penicillin/streptomycin, and 1% amphotericin B (Euroclone), at 37°C in 5% CO_2 . The cells were transfected either with the pEYFP-hDAAO-C3 construct (for the expression of the wild-type enzyme downstream of the enhanced yellow fluorescent protein, EYFP) (Sacchi et al., 2008, 2011), the pEYFP-hDAAO(R120L)-C3, or the pEYFP-hDAAO(R120E)-C3 expression vectors. The latter constructs were obtained by mutagenesis using the QuikChange Lightning Site-Directed Mutagenesis Kit (Agilent), and the following primers: 5'-ATTTCCGGAAGCTGACCCCGAGGAGCTGGATATGTTCCCAG-3' and 5'-CTGGGAACATATCCAGCTCCTCGGGGGTCA GCTTCCGAAAT-3' for the R120E substitution, and 5-TTCGGAAGCTGACCCCTTAGAGCTGGATATGTTCC-3' and 5'-GGAACATATCCAGCTCTAAGGGGGTCAAGCTTCCC AA-3' for the R120L substitution.

For transient transfection, 2×10^4 cells were seeded into eight-well chamber slides (Sarstedt). At 24 h after seeding, cells were transfected with 2 μ g plasmid DNA using a 4:1 ratio of FuGENE transfection reagent (Promega) to DNA. Then, 12.5 μ L of transfection mix was added to 500 μ L medium per well. Protein expression levels were monitored by using a fluorescence microscope (Olympus IX51) equipped with a FITC filter and by Western blot analysis using an anti-hDAAO antibody (Davids Biotechnologie) (Sacchi et al., 2008, 2011).

Immunostaining and Confocal Microscopy

At 24, 48, and 72 h after transfection, cells were washed twice with PBS and fixed with ice-cold 4% p-formaldehyde and 4% sucrose for 10 min at room temperature. After fixation, cells were washed twice with PBS and blocked by incubation in PBS supplemented with 0.2% Triton X-100 and 4% horse serum for 30 min at room temperature. Peroxisomes were stained using rabbit polyclonal anti-PMP70 (peroxisomal membrane protein 70, Sigma), diluted 1:500 in PBS, 0.1% Triton X-100, and 4% horse serum overnight at 4°C; they were then washed twice in PBS and 1% horse serum and incubated for 1 h at room temperature (light protected) with goat anti-rabbit Dylight 550 secondary antibodies (Abcam) diluted 1:400 in PBS, 0.1% Triton X-100, and 1.5% horse serum. Cells were then extensively washed in PBS and nuclei were stained with DRAQ5TM (Thermo Scientific) and diluted 1:500 in PBS for 10 min at room temperature in the dark. Cells were washed three times with PBS and stored in PBS at 4°C until imaging.

Immunostained cells were imaged using an inverted laser scanning confocal microscope (TCS SP5, Leica Microsystems), equipped with a 63.0 × 1.25 NA plan apochromatic oil immersion objective. Confocal image stacks were acquired using the Leica TCS software with a sequential mode to avoid interference between each channel and without saturating any pixel. Cells in 10–15 non-magnified optical fields were analyzed for each condition (i.e., different EYFP-hDAAO expression constructs at different times after transfection). The fluorescence signal corresponding to the overexpressed EYFP-hDAAO variants was monitored by excitation at 514 nm (yellow channel); the peroxisomal and nuclear cellular compartments were imaged by excitation at 546 nm (red channel) and 647 nm (blue channel), respectively.

RESULTS

Design of R120 hDAAO Variants

Analysis of the hDAAO primary sequence for nuclear localization (e.g., by NucPred or cNL Mapper) and for the presence of nuclear localization sequences (e.g., by Moseslab, NLSdb by RostLab, or SeqNLS) does not predict hDAAO targeting to the nucleus. A putative nuclear translocation signal for rDAAO (I17T-P-S119) was recently proposed (Luks et al., 2017b): this might facilitate nuclear import through importin 7 after phosphorylation of such a sequence. In hDAAO, this tripeptide corresponds to the I18T-P-R120 sequence.

R120 belongs to α -helix 6 and is involved in electrostatic interactions with the carboxylic group of D73 (α -helix 3) and hydrogen-bonded to the backbone C=O groups of D109 (α -helix 5), T110, and V111 (loop between α -helix 5 and β -strand 4) located at the interface of the opposite monomer (Figure 1C). Indeed, and as stated in the Introduction section, the R120 side chain possesses two alternative orientations, one of which is observed in the benzoate-bound complex only. R120 is located at the monomer-monomer interface (Figure 1B); therefore, a connection between protomer interaction and the binding of the ligand and/or the cofactor is feasible.

Based on these considerations, and to shed light on benzoate binding, monomer-monomer interaction, and nuclear translocation, we designed two hDAAO variants differing at position 120 aimed at eliminating the positive charge (introducing a Leu) or at mimicking the negative charge of a phosphorylated serine present at the active NTS in rDAAO (introducing a glutamate). A serine at position 120 was not introduced since no evidence is reported of phosphorylation in hDAAO (Murtas et al., 2017).

Biochemical Properties of R120E and R120L hDAAO Variants

hDAAO R120E and R120L variants were expressed in *E. coli* following the same conditions used for expressing the wild-type enzyme and were purified by HiTrap chelating chromatography as previously reported (Molla et al., 2006). The protein preparations have a purity degree of 95% and the overall purification yield is 2.5- to 4-fold lower than the wild-type hDAAO (Table 1).

The R120E and R120L hDAAO variants show the typical absorbance spectrum of FAD-containing flavoenzymes in the oxidized form (Figure 2A): absorbance maxima at 448, 384, and 279 nm and an Abs_{279nm}/Abs_{448nm} ratio of 10.4 and 11.2 for R120E and R120L variants, respectively, which are close to the value of 10.6 reported for the wild-type enzyme (Molla et al., 2006).

The far-UV CD spectra show a different signal for hDAAO R120E as compared to the wild-type enzyme and the R120L variant, indicating a lower α -helix content (Figure 2B). Concerning the tertiary structure, the near-UV CD spectra of hDAAO R120E and R120L are slightly altered in the 250- to 290-nm region, corresponding to the signal for aromatic residues, in comparison to the wild-type enzyme (Figure 2C). Accordingly, the protein fluorescence spectra for both of the variants at position 120 show a lower emission intensity of the peak at 330 nm, particularly for the R120E hDAAO (Figure 2D), strengthening the evidence that aromatic residue exposure has been altered.

Overall, the substitution of R120 results in a slight alteration in the conformation (secondary and tertiary structure) of hDAAO, which is most apparent for the R120E variant.

TABLE 1 | Comparison of selected properties of recombinant wild-type, R120E, and R120L hDAAO variants.

	hDAAO		
	Wild-type ^a	R120E	R120L
Protein purification			
Purified protein (mg/L fermentation broth)	7.0	2.8	1.8
Specific activity (U/mg protein)	12.0	21.0	17.6
Holoenzyme content (%)	80	100	100
Thermal stability (T_m, °C)			
CD (at 220 nm)	57.0 ± 1.0	46.1 ± 0.1	47.6 ± 0.1
Protein fluorescence (at 340 nm)	57.7 ± 0.3	52.7 ± 0.1	54.2 ± 0.1

^aMolla et al. (2006) and Caldinelli et al. (2009).

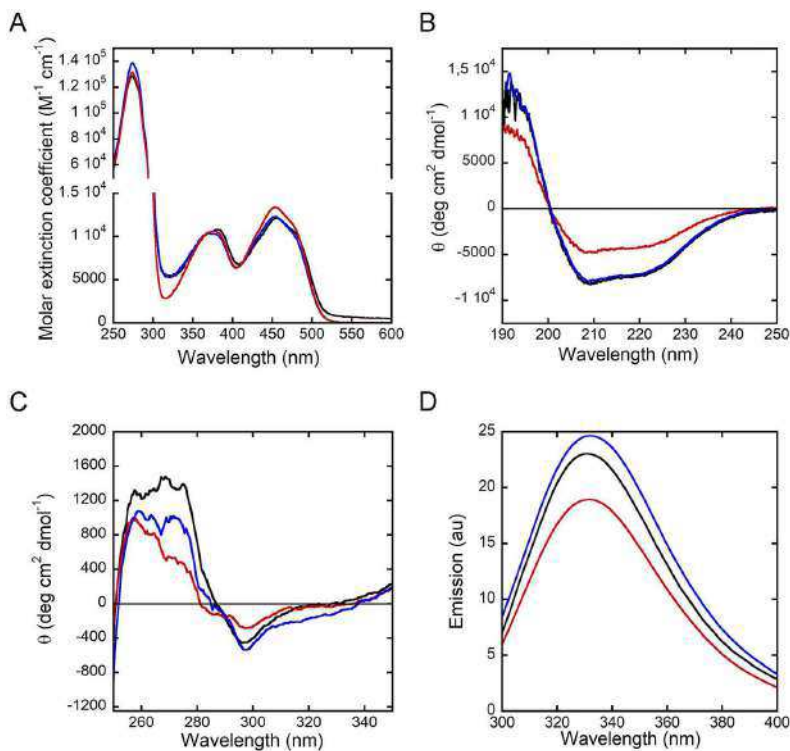


FIGURE 2 | Spectral properties of hDAAO variants in the holoenzyme form. Wild-type (black), R120E (red) and R120L (blue) hDAAO variants. Comparison of: **(A)** UV-visible absorbance spectra in the oxidized form; **(B,C)** far-UV CD spectra (0.1 mg/mL, **B**), and near-UV CD spectra (0.4 mg/mL, **C**); **(D)** protein fluorescence spectra (0.3 mg/mL).

Kinetic Properties

The activity assays performed in the absence of exogenous cofactor or the presence of an excess of FAD result in similar values indicating that purified R120E and R120L hDAAO are present in solution as holoenzyme, this being different from the wild-type enzyme, which is partially present in the apoprotein form in the absence of exogenous FAD (Table 1; see below). Notably, the R120E and R120L hDAAO variants show higher specific activity than the wild-type enzyme in the standard assay (on 28 mM D-alanine, Table 1).

The apparent kinetic parameters were calculated according to a Michaelis–Menten equation using the initial velocity values determined at increasing D-amino acid concentrations and a fixed O₂ concentration (air saturation) at pH 8.5 and 25°C, in the presence of 0.2 mM FAD to avoid apoprotein formation for wild-type hDAAO. Three D-amino acids were used: D-Ala is the reference substrate for DAAOs (Pollegioni et al., 2007), D-Ser is considered the main substrate for hDAAO in the brain (based on the concentration and physiological role) (Sacchi et al., 2012; Murtas et al., 2017; Weatherly et al., 2017), and D-Cys is the putative preferred substrate in specific tissues (Shibuya et al., 2013; Murtas et al., 2017). Both variants show a 2-fold higher

apparent kinetic efficiency (k_{cat}/K_m) for D-Ala than the wild-type hDAAO (due to a higher k_{cat} ; Table 2). On the other hand, using D-Ser as a substrate, all the enzyme variants show similar kinetic efficiency, although both apparent k_{cat} and K_m values are significantly higher in the R120-substituted variants (2.5- and 3.5-fold for the R120E and R120L, respectively; Table 2). An inhibition effect is observed at very high D-Cys concentration for both R120 variants ($K_i > 200$ mM), which is absent for wild-type hDAAO. Moreover, the kinetic efficiency of the R120L variant is 2-fold higher than the wild-type hDAAO on this substrate due to an increase in the apparent k_{cat} value.

In order to assess the effect of the kinetic properties of R120 hDAAO variants on the oxidation of D-Ser under conditions similar to the physiological ones, the enzymatic activity was assayed on 0.3 or 1 mM D-Ser in the absence of free FAD or in the presence of 2.5 μM (corresponding to the maximal estimated concentration in the brain) or 40 μM FAD (a saturating cofactor concentration) (Cappelletti et al., 2015). In all cases, the conditions affected the activity only slightly (Figure 3). At low D-Ser and FAD concentrations higher activity is measured for the R120L variant, while at 1 mM D-Ser and 40 μM FAD, the wild-type hDAAO is the most active variant.

TABLE 2 | Comparison of the apparent kinetic properties of wild-type, R120E, and R120L hDAAO variants.

hDAAO	D-Ala			D-Ser			D-Cys		
	k_{cat} (s ⁻¹)	K_m (mM)	k_{cat}/K_m (mM ⁻¹ s ⁻¹)	k_{cat} (s ⁻¹)	K_m (mM)	k_{cat}/K_m (mM ⁻¹ s ⁻¹)	k_{cat} (s ⁻¹)	K_m (mM)	k_{cat}/K_m (mM ⁻¹ s ⁻¹)
wild-type ^a	5.2 ± 0.1	1.3 ± 0.2	4.0	3.0 ± 0.1	7.5 ± 0.5	0.4	8.6 ± 0.2	0.6 ± 0.1	14.6
R120E	12.6 ± 0.1	1.4 ± 0.1	8.9	8.5 ± 0.4	17.6 ± 3.5	0.5	9.9 ± 0.5	0.6 ± 0.1	16.5
R120L	17.3 ± 0.3	2.0 ± 0.3	8.5	11.3 ± 0.4	26.7 ± 4.5	0.4	15.6 ± 0.7	0.7 ± 0.1	22.6

Conditions: air saturation, 25°C, pH 8.5.

^aMolla et al. (2006) and Murtas et al. (2017).

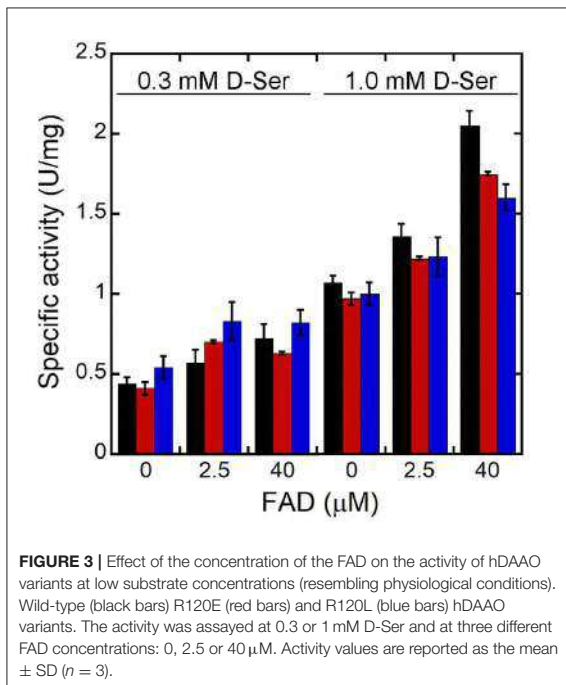


FIGURE 3 | Effect of the concentration of the FAD on the activity of hDAAO variants at low substrate concentrations (resembling physiological conditions). Wild-type (black bars) R120E (red bars) and R120L (blue bars) hDAAO variants. The activity was assayed at 0.3 or 1 mM D-Ser and at three different FAD concentrations: 0, 2.5 or 40 μM. Activity values are reported as the mean ± SD ($n = 3$).

Ligand and FAD-Binding

The interaction of R120 hDAAO variants with the classical inhibitor benzoate and with CBIO, the prototype of the new class of hDAAO inhibitors, was investigated following the protein fluorescence signal. Similar to what was observed for the wild-type hDAAO (Murtas et al., 2017), benzoate binding is a biphasic process for R120 variants. The main change observed was a ~3-fold higher K_d for the second phase of binding for the R120E variant, i.e., ~8 vs. 2.6 mM for the wild-type hDAAO (Table 3). Differently from benzoate, the binding of CBIO is a monophasic process for wild-type and variants of hDAAO.

The K_d for FAD was estimated for the R120 hDAAO variants based on the quenching of the apoprotein fluorescence during FAD titration, both in the absence and presence of the active site ligand benzoate. Similar to the wild-type enzyme, FAD-binding is a biphasic process for both R120 variants in the absence of benzoate (Figure 4A): the fluorescence intensity

TABLE 3 | Binding properties of R120E and R120L hDAAO variants compared to the wild-type enzyme.

hDAAO variants	FAD (K_d , μM)		Benzoate (K_d , μM)	CBIO (K_d , μM)
	Free form	Benzoate complex ^a		
Wild-type ^b	0.43 ± 0.02 ^c [40%] ≥30 ^d [60%]	0.48 ± 0.02	0.33 ± 0.04 ^c 2,590 ± 680 ^d	0.24 ± 0.05
R120E	0.05 ± 0.01 ^c [65%] 32 ± 3 ^d [35%]	0.61 ± 0.08 ^c [65%] ≥ 30 ^d [35%]	0.16 ± 0.01 ^c 7,985 ± 755 ^d	0.30 ± 0.05
R120L	0.05 ± 0.01 ^c [60%] 23.1 ± 1.0 ^d [40%]	0.07 ± 0.01 ^c [75%] ≥20 ^d [25%]	0.27 ± 0.12 ^c 6,205 ± 40 ^d	0.35 ± 0.04

K_d values were determined by monitoring the quenching of protein fluorescence. When the FAD binding process to the apoprotein moiety is biphasic, the amplitude of fluorescence change for each phase is reported in square parentheses.

^aIn presence of 70 μM benzoate.

^bMurtas et al. (2017).

^c K_d values corresponding to the first saturation phase.

^d K_d values corresponding to the second saturation phase.

change associated with the first phase accounts for 60–65% of the overall change. The main difference concerning the wild-type hDAAO is a 10-fold lower dissociation constant for the first phase (K_{d1}) of cofactor binding to the apoprotein of R120 variants (Table 3). Significant alterations are also apparent when FAD binding to hDAAO apoprotein is performed in the presence of a saturating benzoate concentration (i.e., 70 μM, Figure 4B): this is a monophasic process for the wild-type hDAAO and a biphasic event for the R120 variants. Indeed, a tighter binding of the first process is apparent for the R120L variant only, while similar K_d values are determined in the presence of benzoate for the wild-type and the R120E variants (Table 3).

Taken together, these findings indicate that R120 substitution modifies the interaction of hDAAO apoprotein with the flavin cofactor.

Oligomeric State and Protein Stability

Wild-type hDAAO is a stable homodimer (Molla et al., 2006). R120 is located at the interface between monomers (Figure 1A) and, therefore, the oligomeric state of hDAAO R120E and R120L holoenzymes was investigated by gel-permeation chromatography. Both variants elute as a dimer in the 0.1–10 mg/mL protein concentration range (elution volume

of ~13.7 mL, corresponding to a molecular mass of 80 kDa, not shown).

The stability of hDAAO secondary and tertiary structures was investigated by performing temperature-ramp experiments and analyzing the CD signal at 220 nm and the tryptophan fluorescence at 340 nm, respectively. The melting temperature values determined for the R120E and R120L variants are 3.5–5°C lower than those of wild-type hDAAO when the changes in tertiary structure are analyzed and ~10°C lower when the secondary structure stability is studied (Table 1).

Subcellular Localization

U87 glioblastoma cells were transiently transfected with a pEYFP-hDAAO-C3 plasmid encoding for EYFP-hDAAO chimeric proteins harboring R, E, or L at position 120 of the flavoenzyme. The presence of the fluorescence tag at the N-terminal end was previously demonstrated to not alter the activity, subcellular

distribution, or degradation pathway of wild-type hDAAO (Sacchi et al., 2008, 2011; Li et al., 2013). A similar amount of transfected cells (expressing EYFP-hDAAO protein) was obtained for all three constructs (Table 4). The percentage of cells showing a cytosolic, peroxisomal, and nuclear localization of the flavoenzyme was determined by comparing the yellow fluorescence signal of EYFP-hDAAO variants with those of the markers PMP-70 (for peroxisomes) and DRAQ5TM dye (for nuclei, Figure 5). The amount of cytosolic wild-type EYFP-hDAAO decreased with time after transfection (28% of the signal is cytosolic at 72 h vs. 94% at 24 h), as did the amount of nuclear signal (Table 4 and Figure 6). The presence of glutamate at position 120 of hDAAO to mimic a phosphorylation state favors the mistargeting by increasing the number of cells with an EYFP nuclear signal as compared to wild-type hDAAO. This is accompanied by a lower percentage of cells displaying a peroxisomal signal for the EYFP-tagged protein. Introducing an uncharged residue at position 120 (R120L variant) also

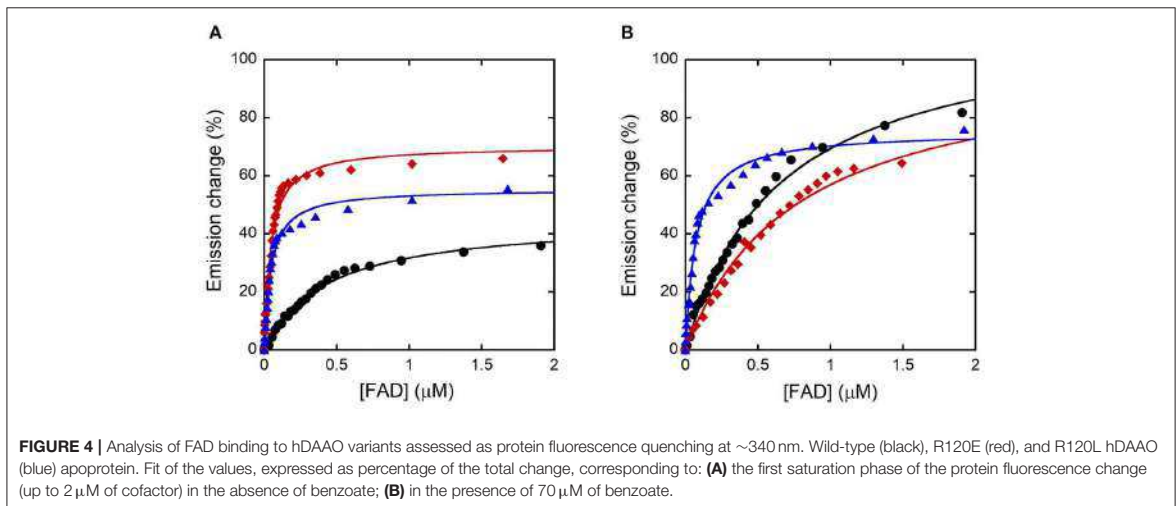
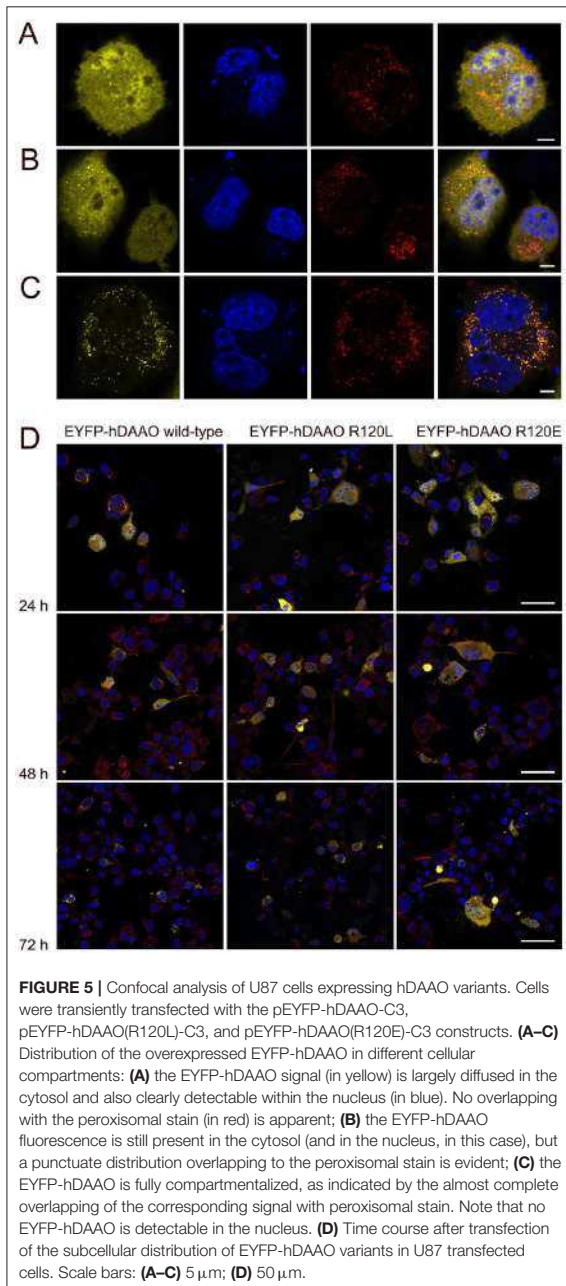


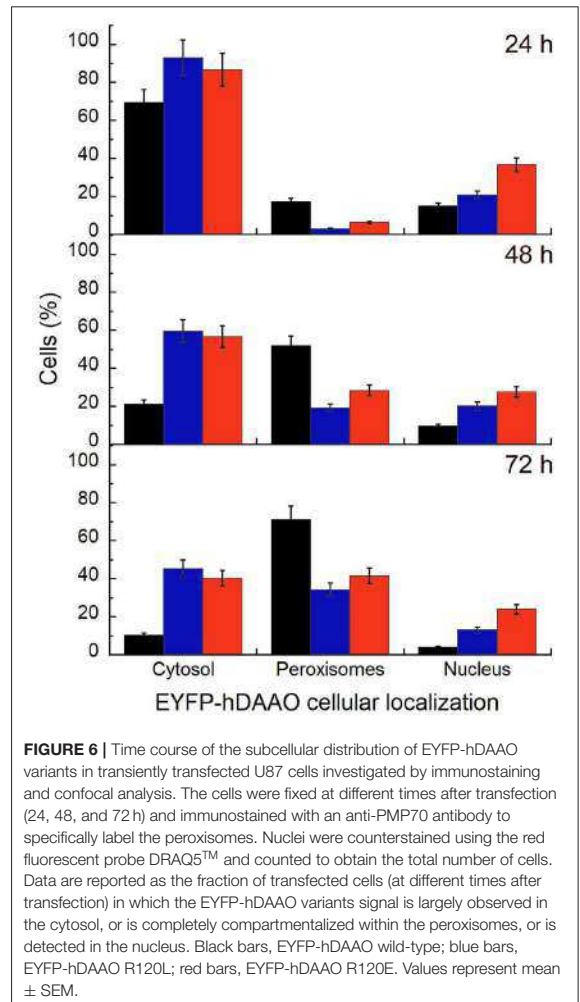
TABLE 4 | Confocal analysis of the cellular distribution of hDAAO variants in U87 cells transiently transfected with different pEYFP-hDAAO expression constructs.

hDAAO variants	Hours after transfection	Cells number	T (%)	hDAAO cellular distribution (% of transfected cells)				
				C	C/P	P	N	A
Wild-type	24	551	24.3	69.4	13.4	17.2	14.4	18.7
	48	599	17.4	21.2	26.9	51.9	9.6	15.4
	72	781	16.0	10.4	18.4	71.2	4.0	5.6
R120L	24	628	20.7	93.1	3.8	3.1	20.8	41.5
	48	497	24.9	59.7	21.0	19.4	20.2	22.6
	72	511	19.4	45.5	21.2	34.3	13.1	35.6
R120E	24	515	24.9	86.7	7.8	6.3	36.7	29.7
	48	549	24.4	56.7	14.9	28.4	27.6	31.3
	72	801	19.2	40.3	18.2	41.6	24.0	18.2

The cells were fixed at different times after transfection and peroxisomes were immunostained using an anti-PMP70 antibody. The total number of cells in each field was determined by counting the nuclei, counterstained using the DRAQ5TM far red fluorescent dye. T, transfected cells; C, cytosol; C/P, mixed, cytosol and peroxisomes; P, peroxisomes; N, nucleus; A, large cytosolic aggregates detected.



negatively affects peroxisomal targeting and modifies, to a limited extent, the percentage of cells with an EYFP-hDAAO nuclear signal as compared to the cells expressing the wild-type hDAAO (Figure 5). The substitution of R120 also appears to increase the propensity of hDAAO to form cytosolic aggregates (Table 4). Notably, in all cases, the cells showing nuclear



localization of hDAAO also possess a signal largely diffused in the cytosol.

The number of viable cells following transfection is similar for wild-type and R120 hDAAO variants, indicating that mistargeting does not affect cell viability.

DISCUSSION

The elucidation of the structure-function relationships in hDAAO represents a way to deep inside the modulation of the D-serine level in the human brain. Here we studied two enzyme variants at position 120. From a biochemical point of view, substituting R120 in hDAAO slightly alters protein conformation, kinetic properties, and ligand binding, while the dimeric quaternary structure is unchanged. The tertiary structure is largely preserved: only for the R120E hDAAO does alteration in the near-UV CD and fluorescence spectra suggest that the

orientation of aromatic residues has changed and is coupled to a decrease in the α -helix content. Indeed, both the R120E and R120L variants show a decrease in T_m , which is more evident following the signal related to the secondary structure (**Table 1**): the substitution of R120 likely alters the electrostatic interactions with the facing residues belonging to $\alpha 3$ and $\alpha 6$ and the loop connecting $\alpha 5$ and $\beta 4$ on the other monomer (**Figure 1C**). Notably, the substitution of R120 in hDAAO does not alter the affinity for the classical inhibitor benzoate (resulting in a biphasic binding process) and for CBIO (showing a monophasic process; **Table 3**). This result excludes a connection between R120 and the ligand-binding process, especially related to the second putative benzoate binding site.

Concerning the apparent kinetic properties, while both of the variants at position 120 possess a higher kinetic efficiency for D-Ala and D-Cys due to a higher k_{cat} than the wild-type enzyme, a similar kinetic efficiency value is apparent on D-Ser as the increase in maximal activity is counteracted by an increased K_m value. D-Ser is the physiological substrate of hDAAO in the brain: the low kinetic efficiency of the human flavoenzyme on this substrate seems to be evolved to control its cerebral level without resulting in a drastic decrease that could negatively affect NMDAR functionality (Caldinelli et al., 2009, 2010; Murtas et al., 2017; Pollegioni et al., 2018). The possibility that hDAAO kinetic properties could be affected by post-translational modification processes is a topic that deserves further investigations.

The most relevant change in hDAAO following the substitution of R120 is the strongest interaction with the flavin cofactor. The presence in solution of two apoprotein forms showing a different affinity for FAD is still evident for R120 variants, but the most avid form (accounting for ~ 60 – 65% of the total change in protein fluorescence following FAD-binding) possesses a 10-fold lower K_d than the corresponding form of wild-type hDAAO (**Table 3**). This could be significant at the cellular level as wild-type hDAAO at physiological FAD concentration ($\sim 2 \mu\text{M}$) is in equilibrium between the apoprotein inactive form and the active holoenzyme. In any case, the activity values for wild-type and R120 hDAAO variants were quite similar at low D-Ser and FAD concentrations, resembling the physiological conditions (**Figure 3**). Furthermore, we previously reported that benzoate binding shifts the hDAAO apoprotein into the single conformation for FAD more avidly (Caldinelli et al., 2009, 2010; Murtas et al., 2017). This ligand-induced conformation change is abolished for R120 variants: FAD-binding to hDAAO variants is biphasic both in the absence and in the presence of the active-site ligand.

The properties of W209R hDAAO, corresponding to the SNP rs11347906 (Cappelletti et al., 2015), resemble those of R120 variants: the residue W209 is also located at the monomer-monomer interface, is part of the second binding site identified by Kohiki et al. (2017), and its substitution results in an increased activity on D-Ala, a 4-fold tighter FAD-binding with no change in ligand-binding properties (Cappelletti et al., 2015). The similarity in biochemical properties between R120E/L and W209R hDAAO variants suggests that the reported alterations are due to the structure-function relationships of this specific region, which is close to the interface between monomers.

Concerning the investigation of hDAAO subcellular localization, and since phosphorylation of arginine is unusual, we substituted R120 with glutamate (to mimic the active NTS sequence) or a leucine (to eliminate the positive charge). Our studies based on U87 glioblastoma cells transiently transfected for hDAAO variants show that substitution of R120 alters the subcellular localization of the flavoenzyme; the increase in cytosolic localization, observed at all times after translocation, favors nuclear targeting, especially for the R120E hDAAO (**Figures 5, 6**). Indeed, the wild-type enzyme is also mistargeted to the nucleus, suggesting that it is a usual process for hDAAO. Nuclear passive diffusion promotes the transport of proteins of <40 kDa (corresponding to the size of DAAO monomer) although proteins at higher mass also accumulate in the nucleus (Luks et al., 2017b). R120 is located at the protein interface between monomers and electrostatically interacts with D73 on the opposite chain (**Figure 1C**). The substitution of the arginine in position 120 does not affect the generation of a soluble, dimeric holoenzyme: the altered subcellular localization of R120 hDAAO variants does not arise from a change in molecular mass. Finally, the expression of catalytically active hDAAO variants at position 120 does not alter the viability of U87 transfected cells. This is significant and can be explained in two different ways: (i) mistargeted (cytosolic and nuclear) hDAAO is inactive; (ii) no hydrogen peroxide is generated by mistargeted hDAAO because of the absence of its substrate, i.e., the D-amino acids.

Results from mutagenesis at position 120 and previous studies on the W209R hDAAO variant (Cappelletti et al., 2015) indicate that single point substitutions at the monomer-monomer interface affect biochemical properties, especially the affinity for FAD, but do not affect ligand binding. Indeed, our results reveal that mistargeting to the nucleus is an innate process, as it is apparent for the wild-type enzyme too (**Table 4**), which does not affect cell viability. Whether hDAAO mistargeting is involved in physiological processes or related to specific pathological states is still unknown (Pollegioni et al., 2018).

DATA AVAILABILITY STATEMENT

The datasets generated for this study are available on request to the corresponding author.

AUTHOR CONTRIBUTIONS

LP and SS conceived the project. GM and SS performed the experiments. All the authors analyzed the data and wrote the paper.

ACKNOWLEDGMENTS

We thank the support of Fondo di Ateneo per la Ricerca. GM is a Ph.D. student of the Biotechnology, Biosciences, and Surgical Technology course at Università degli Studi dell'Insubria. We thank the support from CIB, Consorzio Interuniversitario per le Biotecnologie.

REFERENCES

- Billard, J. M. (2008). D-serine signalling as a prominent determinant of neuronal-glial dialogue in the healthy and diseased brain. *J. Cell. Mol. Med.* 12, 1872–1884. doi: 10.1111/j.1582-4934.2008.00315.x
- Caldinelli, L., Molla, G., Bracci, L., Lelli, B., Pileri, S., Cappelletti, P., et al. (2010). Effect of ligand binding on human D-amino acid oxidase: implications for the development of new drugs for schizophrenia treatment. *Protein Sci.* 19, 1500–1512. doi: 10.1002/pro.429
- Caldinelli, L., Molla, G., Sacchi, S., Pilone, M. S., and Pollegioni, L. (2009). Relevance of weak flavin binding in human D-amino acid oxidase. *Protein Sci.* 18, 801–810. doi: 10.1002/pro.86
- Cappelletti, P., Campomenosi, P., Pollegioni, L., and Sacchi, S. (2014). The degradation (by distinct pathways) of human D-amino acid oxidase and its interacting partner pLG72—two key proteins in D-serine catabolism in the brain. *FEBS J.* 281, 708–723. doi: 10.1111/febs.12616
- Cappelletti, P., Piubelli, L., Murtas, G., Caldinelli, L., Valentino, M., Molla, G., et al. (2015). Structure-function relationships in human D-amino acid oxidase variants corresponding to known SNPs. *Biochim. Biophys. Acta* 1854, 1150–1159. doi: 10.1016/j.bbapap.2015.02.005
- Chuderland, D., Konson, A., and Seger, R. (2008). Identification and characterization of a general nuclear translocation signal in signaling proteins. *Mol. Cell.* 31, 850–861. doi: 10.1016/j.molcel.2008.08.007
- Chumakov, I., Blumenfeld, M., Guerassimenco, O., Cavarec, L., Palicio, M., Abderrahim, H., et al. (2002). Genetic and physiological data implicating the new human gene G72 and the gene for D-amino acid oxidase in schizophrenia. *Proc. Natl. Acad. Sci. U.S.A.* 99, 13675–13680. doi: 10.1073/pnas.182412499
- Collingridge, G. L., Volianskis, A., Bannister, N., France, G., Hanna, L., Mercier, M., et al. (2013). The NMDA receptor as a target for cognitive enhancement. *Neuropharmacology* 64, 13–26. doi: 10.1016/j.neuropharm.2012.06.051
- Curcio, L., Podda, M. V., Leone, L., Piacentini, R., Mastrodonato, A., Cappelletti, P., et al. (2013). Reduced D-serine levels in the nucleus accumbens of cocaine-treated rats hinder the induction of NMDA receptor-dependent synaptic plasticity. *Brain* 136(Pt 4), 1216–1230. doi: 10.1093/brain/awt036
- Kawazoe, T., Tsuge, H., Pilone, M. S., and Fukui, K. (2006). Crystal structure of human D-amino acid oxidase: context-dependent variability of the backbone conformation of the VAAGL hydrophobic stretch located at the si-face of the flavin ring. *Protein Sci.* 15, 2708–2717. doi: 10.1110/ps.062421606
- Kohiki, T., Kato, Y., Nishikawa, Y., Yorita, K., Sagawa, I., Denda, M., et al. (2017). Elucidation of inhibitor-binding pockets of D-amino acid oxidase using docking simulation and N-sulfanylethylamide-based labeling technology. *Org. Biomol. Chem.* 15, 5289–5297. doi: 10.1039/C7OB00633K
- Le Bail, M., Martineau, M., Sacchi, S., Yatsenko, N., Radzishewsky, I., Conrod, S., et al. (2015). Identity of the NMDA receptor coagonist is synapse specific and developmentally regulated in the hippocampus. *Proc. Natl. Acad. Sci. U.S.A.* 112, E204–E213. doi: 10.1073/pnas.1416668112
- Li, Y., Sacchi, S., Pollegioni, L., Basu, A. C., Coyle, J. T., and Bolshakov, V. Y. (2013). Identity of endogenous NMDAR glycine site agonist in amygdala is determined by synaptic activity level. *Nat. Commun.* 4:1760. doi: 10.1038/ncomms2779
- Luks, L., Maier, M. Y., Sacchi, S., Pollegioni, L., and Dietrich, D. R. (2017a). Understanding renal nuclear protein accumulation: an *in vitro* approach to explain an *in vivo* phenomenon. *Arch. Toxicol.* 91, 3599–3611. doi: 10.1007/s00204-017-1970-5
- Luks, L., Sacchi, S., Pollegioni, L., and Dietrich, D. R. (2017b). Novel insights into renal D-amino acid oxidase accumulation: propiverine changes DAAO localization and peroxisomal size *in vivo*. *Arch. Toxicol.* 91, 427–437. doi: 10.1007/s00204-016-1685-z
- Madeira, C., Freitas, M. E., Vargas-Lopes, C., Wolosker, H., and Panizzutti, R. (2008). Increased brain D-amino acid oxidase (DAAO) activity in schizophrenia. *Schizophr. Res.* 101, 76–83. doi: 10.1016/j.schres.2008.02.002
- Molla, G., Porrini, D., Job, V., Motteran, L., Vegezzi, C., Campaner, S., et al. (2000). Role of arginine 285 in the active site of *Rhodotorula gracilis* D-amino acid oxidase. A site-directed mutagenesis study. *J. Biol. Chem.* 275, 24715–24721. doi: 10.1074/jbc.M908193199
- Molla, G., Sacchi, S., Bernasconi, M., Pilone, M. S., Fukui, K., and Pollegioni, L. (2006). Characterization of human D-amino acid oxidase. *FEBS Lett.* 580, 2358–2364. doi: 10.1016/j.febslet.2006.03.045
- Moreno, S., Nardacci, R., Cimini, A., and Cerù, M. P. (1999). Immunocytochemical localization of D-amino acid oxidase in rat brain. *J. Neurocytol.* 28, 169–185. doi: 10.1023/A:1007064504007
- Mothet, J. P., Parent, A. T., Wolosker, H., Brady, R. O. Jr., Linden, D. J., Ferris, C. D., et al. (2000). D-serine is an endogenous ligand for the glycine site of the N-methyl-D-aspartate receptor. *Proc. Natl. Acad. Sci. U.S.A.* 97, 4926–4931. doi: 10.1073/pnas.97.9.4926
- Murtas, G., Sacchi, S., Valentino, M., and Pollegioni, L. (2017). Biochemical properties of human D-amino acid oxidase. *Front. Mol. Biosci.* 4:88. doi: 10.3389/fmolb.2017.00088
- Pollegioni, L., Piubelli, L., Sacchi, S., Pilone, M. S., and Molla, G. (2007). Physiological functions of D-amino acid oxidases: from yeast to humans. *Cell. Mol. Life Sci.* 64, 1373–1394. doi: 10.1007/s00018-007-6558-4
- Pollegioni, L., Sacchi, S., and Murtas, G. (2018). Human D-amino acid oxidase: structure, function, and regulation. *Front. Mol. Biosci.* 28:107. doi: 10.3389/fmolb.2018.00107
- Romano, D., Molla, G., Pollegioni, L., and Marinelli, F. (2009). Optimization of human D-amino acid oxidase expression in *Escherichia coli*. *Protein Expr. Purif.* 68, 72–78. doi: 10.1016/j.pep.2009.05.013
- Sacchi, S., Bernasconi, M., Martineau, M., Mothet, J. P., Ruzzeno, M., Pilone, M. S., et al. (2008). pLG72 modulates intracellular D-serine levels through its interaction with D-amino acid oxidase: effect on schizophrenia susceptibility. *J. Biol. Chem.* 283, 22244–22256. doi: 10.1074/jbc.M709153200
- Sacchi, S., Caldinelli, L., Cappelletti, P., Pollegioni, L., and Molla, G. (2012). Structure-function relationships in human D-amino acid oxidase. *Amino Acids.* 43, 1833–1850. doi: 10.1007/s00726-012-1345-4
- Sacchi, S., Cappelletti, P., Giovannardi, S., and Pollegioni, L. (2011). Evidence for the interaction of D-amino acid oxidase with pLG72 in a glial cell line. *Mol. Cell. Neurosci.* 48, 20–28. doi: 10.1016/j.mcn.2011.06.001
- Shibuya, N., Koike, S., Tanaka, M., Ishigami-Yuasa, M., Kimura, Y., Ogasawara, Y., et al. (2013). A novel pathway for the production of hydrogen sulphide from D-cysteine in mammalian cells. *Nat. Commun.* 4:1366. doi: 10.1038/ncomms2371
- Verrall, L., Walker, M., Rawlings, N., Benzil, I., Kew, J. N., Harrison, P. J., et al. (2007). D-Amino acid oxidase and serine racemase in human brain: normal distribution and altered expression in schizophrenia. *Eur. J. Neurosci.* 26, 1657–1669. doi: 10.1111/j.1460-9568.2007.05769.x
- Weatherly, C. A., Du, S., Parpia, C., Santos, P. T., Hartman, A. L., and Armstrong, D. W. (2017). D-Amino acid levels in perfused mouse brain tissue and blood: a comparative study. *ACS Chem. Neurosci.* 8, 1251–1261. doi: 10.1021/acscchemneuro.6b00398
- Wolosker, H. (2011). Serine racemase and the serine shuttle between neurons and astrocytes. *Biochim. Biophys. Acta.* 1814, 1558–1566. doi: 10.1016/j.bbapap.2011.01.001
- Wolosker, H., Dumin, E., Balan, L., and Foltyn, V. N. (2008). D-amino acids in the brain: D-serine in neurotransmission and neurodegeneration. *FEBS J.* 275, 3514–3526. doi: 10.1111/j.1742-4658.2008.06515.x

Conflict of Interest: The authors declare that the research was conducted in the absence of any commercial or financial relationships that could be construed as a potential conflict of interest.

Copyright © 2019 Murtas, Sacchi and Pollegioni. This is an open-access article distributed under the terms of the Creative Commons Attribution License (CC BY). The use, distribution or reproduction in other forums is permitted, provided the original author(s) and the copyright owner(s) are credited and that the original publication in this journal is cited, in accordance with accepted academic practice. No use, distribution or reproduction is permitted which does not comply with these terms.

Paper in preparation

Antimicrobial D-amino acid oxidase-derived peptides specify gut microbiota

Giulia Murtas¹, Silvia Sacchi¹, Gabriella Tedeschi², Elisa Maffioli², Eugenio Notomista³, Valeria Cafaro³, Monica Abbondi^{4,5}, Jean-Pierre Mothet⁶, Loredano Pollegioni^{1,5}

¹ Department of Biotechnology and Life Sciences, University of Insubria, Varese, Italy

² Department of Veterinary Medicine, University of Milan, Milan, Italy

³ Department of Biology, University of Naples Federico II, Naples, Italy

⁴ Fondazione Istituto Insubrico Ricerca per la Vita (FIIRV), Gerenzano, Italy

⁵ DAAIR, D-Amino Acid International Research Center, Gerenzano, Italy

⁶ Centre de Recherche en Neurobiologie et Neurophysiologie de Marseille UMR7286 CNRS, Aix Marseille University, Marseille, France

Introduction

The FAD-dependent enzyme D-amino acid oxidase (DAAO, EC 1.4.3.3) catalyzes the oxidative deamination of uncharged and basic D-amino acids [Pollegioni et al., 2007]. In mammals DAAO is widely distributed in different organs and is expressed by many cell types. The highest expression is apparent in proximal tubules of the kidney, while it is also present in the hepatocytes, in astrocytes of the hindbrain, in neutrophils, and in the goblet cells and enterocytes of the small intestine; for a review see [Pollegioni et al., 2007; Koga et al., 2017]. Accordingly, DAAO plays different roles.

In the central nervous (CNS) system DAAO regulates the level of D-serine (D-Ser), the main co-agonist of synaptic N-methyl-D-aspartate type of glutamate receptors (NMDAR) [Mothet et al., 2000; Collingridge et al., 2013]. NMDAR dysfunction due to alteration in D-Ser levels concurs to the development of various neurological and psychiatric disorders including

amyotrophic lateral sclerosis, Alzheimer's disease, schizophrenia, drug abuse [Lin et al., 2018; Billard 2008; Madeira et al., 2008; Wolosker et al., 2008; Wolosker 2011; Collingridge et al., 2013]. In liver and kidney, DAAO is responsible for the detoxification and degradation of D-amino acids originating from the cell wall of intestinal bacteria, from diet and endogenous racemization. In kidney the enzyme is expressed in proximal tubule cells and is associated with renal damage due to the nephrotoxicity caused by the production of H₂O₂ during the elimination of D-Ser and D-propargylglycine mediated by DAAO [Konno et al., 2000, Maekawa et al., 2005; Nakade et al., 2018]. In kidney and brain, it has been recently proposed that DAAO could take part in a new pathway (DAAO/3-MST) linked to hydrogen sulfide (H₂S) production [Shibuya et al., 2013]. In neutrophils and intestinal mucosa, DAAO shows an antimicrobial activity by generating hydrogen peroxide from the deamination of D-amino acids originating from bacteria [Sasabe et al., 2016; Sasabe and Suzuki, 2018].

In the intestine, it has been suggested that goblet cells secrete a processed form of the mouse DAAO, likely due to the presence of a signal peptide and a predicted cleavage site near the N-terminus [Sasabe et al., 2016]. DAAO could thus control the homeostasis of gut microbiota [Sasabe et al., 2016]: DAAO protein and activity were detected in the proximal and middle small intestine of mice and humans, associated to the villus epithelium [Sasabe et al., 2016]. This investigation proposed that the selection of dangerous microbes such as *Staphylococcus aureus* and *Vibrio cholera* is due to the hydrogen peroxide generated by DAAO activity on intestinal D-amino acids, originating from food or microbial cell wall.

Based on structural details suggesting that DAAO could not properly fold and maintain its enzymatic activity following the elimination of the N-terminal sequence which is part of the Rossman fold, i.e. the motif required for flavin binding, in this work we employed biochemical, microbial, cellular and tissue analyses to re-evaluate the role of the flavoenzyme in antibacterial activity and gut homeostasis. We here report that the microbiota selection ability of DAAO is mainly due to the generation of specific antimicrobial

peptides and not by the generation of hydrogen peroxide, as previously proposed.

Materials and Methods

Bioinformatics analysis

The sequences of mammalian DAAOs (from human, mouse, rat and porcine) were analyzed with different bioinformatics servers for the presence of a signal peptide and a cleavage site for protein secretion:

- i) SignalP 3.0 Server, which predicts the presence and location of signal peptide cleavage sites in amino acid sequences based on a combination of several artificial neural networks and hidden Markov models [Bendsten et al., 2004a];
- ii) SignalP 4.1 Server, an improved version of the previous server, which does not consider the hidden Markov model and is able to discriminate between signal peptides and transmembrane regions [Petersen et al., 2011];
- iii) SecretomeP 2.0 Server, which produces *ab initio* predictions of non-classical, not signal-peptide triggered protein secretion. The method queries many other feature prediction servers to obtain information on various post-translational and localization aspects of the protein, which are integrated into the final secretion prediction [Bendsten et al., 2004b];
- iv) Signal-3L server, which determines the presence of a signal peptide and cleavage site and selects a final unique site in concertation with its evolution conservation score [Shen and Chou, 2007];
- v) Signal-3L 2.0 Server, an improved version of the previous server [Zhang et al., 2017].

Molecular dynamics of hDAAO

The 3D structure of the substrate-free form of the human DAAO (PDB 2E48) was used as a starting point for molecular dynamics (MD) simulation performed using the GROMACS package, version 4.6.7. The deleted variant was obtained from the-structure of full-length hDAAO through the deletion of the first N-terminal 16 residues. For the full length hDAAO, the system was

solvated in a cubic box (volume equal to 670 nm^3 , $8.5 \text{ nm} \times 7.5 \text{ nm} \times 10.5 \text{ nm}$) with 20000 water molecules, while for the deleted form a dodecahedral box was used (volume of 610 nm^3) and solvated with 18000 water molecules, with the aim to decrease the system dimensions and to increase the rate of the simulation. To neutralize the overall charge, an adequate number of Na^+ ions was added. The system was minimized again with the Steepest Descent method, followed by equilibration of the restrained protein ($1000 \text{ kJ mol}^{-1} \text{ nm}^{-2}$ isotropic force applied to each heavy atom of the protein) in the NVT ensemble (up to 200 ps). In each system the equilibration phase was composed of an inverted simulated annealing starting with an initial temperature of 10 K and rising up to 300 K in 200 ps, keeping the heavy atoms of protein restrained in the same way as in the apoprotein systems. In production phase, each system was simulated for 100 ns in unrestrained conditions in NVT ensemble. Electrostatics was treated with the cutoff method for short-range interactions and with the Particle Mesh Ewald method for the long-range ones ($r_{\text{list}} = 1.1 \text{ nm}$, cutoff distance = 1.1 nm , VdW distance = 1.1 nm , PME order = 4). A time step of 2 fs was set using bonds-constraining algorithm LINKS. The constant temperature conditions were provided by using V-rescale thermostat, which is a modification from Berendsen's coupling algorithm. The AMBER99SB-ILDN force field was used for the simulations.

The Root Mean Square Deviation of atomic positions (RMSD, the measure of the average distance between the atoms) was used as a quantitative measure of similarity to compare the stability of the systems (full-length vs. deleted variant) in presence or in absence of the flavin cofactor with respect to the initial reference structure. The Root Mean Square Fluctuation (RMSF, the measure of the deviation between the positions of a residue averaged over time) was calculated to compare the fluctuations of every single residues in the systems.

Antimicrobial peptides

The sequences of murine and human DAAO were analyzed by an *in silico* tool

[Pane et al., 2017] which allows to detect the presence and the accurate position of a potential cryptic antimicrobial peptide (CAMP) inside a protein, based on antimicrobial “Absolute Scores” (AS) which depend on hydrophobicity, net charge and length of a peptide. Putative antimicrobial peptides identified inside the sequence of mouse DAAO, ²⁵⁷IWKSCCKLEPTLKNARIVGELTGFRPVRPQVRL²⁸⁹ (IWK) and ³¹³GLTIHWGCAMEAANLFGKILEEKLSRLPPSHL³⁴⁵ (GLT) were synthesized by Aurogene s.r.l. (Roma, Italy).

Far-UV circular dichroism (CD) spectra of DAAO-generated peptides were recorded in 10 mM sodium phosphate buffer pH 7.0 by using a Jasco J-815 spectropolarimeter (Jasco Co., Cremella, Italy). The cell path length was 0.1 cm for measurements in the 190 to 250 nm region (0.1 mg peptide/mL), as reported in [Caldinelli et al., 2009]. The effect of sodium dodecyl sulphate (SDS, 0.1-40 mM), 2,2,2-trifluoroethanol (TFE, 5-50% v/v) and lipopolysaccharides from *E. coli* (LPS, 0.1-1 mg/mL) was analyzed by titrating the peptides with increasing concentrations of these compounds and recording the far-UV CD spectra. CD-spectra were analyzed using the Selcon3 method by DichroWeb [Whitmore and Wallace, 2008] to estimate secondary structure content.

MIC (Minimum Inhibitory Concentration) analyses were performed on Gram-positive and Gram-negative bacteria by broth microdilution method for antimicrobial peptides previously described [Pane et al., 2017] with minor modifications. In details, assays were carried out in Nutrient Broth 0.5x (Difco, Detroit, Mich.) using sterile 96-well polypropylene microtiter plates (cat. 3879, Costar Corp., Cambridge, MA). Bacterial strains were grown in Luria-Bertani (LB) medium (Becton, Dickinson) overnight at 37 °C and then diluted in Nutrient Broth at a final concentration of $\sim 5 \times 10^5$ CFU/mL per well. IWK and GLT peptides were suspended in 5 mM sodium acetate buffer, pH 5. Peptide concentrations were determined by spectrophotometric analysis using the extinction coefficients calculated by the ProtParam tool (<http://web.expasy.org/protparam/>) [Gasteiger et al., 2005]. Twofold serial dilutions of peptides were carried out in the test wells to obtain

concentrations ranging from 100 μM to 0.2 μM . Plates were incubated overnight at 37 °C. MIC value was taken as the lowest concentration at which growth was inhibited. Three independent experiments were performed for each MIC value. The peptide antibiotic polymyxin B and vancomycin (Sigma, St. Louis, MO) were tested as control. MIC values were measured on: *Pseudomonas aeruginosa* PAO1, *Acinetobacter baumannii* ATCC 17878, *Escherichia coli* ATCC 25922, *Salmonella typhimurium* ATCC 14028, *Salmonella enteritidis* 706 RIVM (kindly provided by Prof. E. Veldhuizen, Utrecht University, Holland), *Staphylococcus aureus* ATCC 6538P and *Enterococcus faecalis* ATCC 29212.

The Minimum Bactericidal Concentration (MBC) was determined from the broth dilution of MIC tests by subculturing cell mixtures on agar plates. The MBC was defined as the lowest concentration of antibacterial agent that kills $\geq 99.9\%$ of bacterial cells. According to a widely accepted criterion, peptides were considered bactericidal if their MBC was no more than four times the MIC.

To assess the effect of antimicrobial peptides on lactobacilli, *Lactobacillus acidophilus* ATCC 4356, *Lactobacillus casei* ATCC 393, *Lactobacillus fermentum* ATCC 14931 and *Lactobacillus rhamnosus* ATCC 7469 (from American Type Culture Collection) were used. Before performing antimicrobial susceptibility testing, cultures were streaked on Lactobacilli MRS agar (MRS) and incubated for 24 h at 37 °C in an anaerobic chamber (BD Difco). Antimicrobial susceptibility testing was performed according to the ISO 10932/IDF 233 standard (ISO, 2010). Erythromycin and Vancomycin (Sigma-Aldrich, USA) were dissolved for preparing stock solutions of 1000 μM . IWK and GLT peptides were dissolved as above at a concentration of 400 μM . Typically, a 2-fold serial dilution of stock solutions was performed in Lactobacilli MRS broth to obtain solutions in the concentration range of 0.2–100 μM . Bacterial inocula were prepared by suspending colonies, from 24 h incubated Lactobacilli MRS agar plates, into 2 mL of 0.85% NaCl solution. Subsequently, inocula were adjusted to have an $\text{OD}_{625\text{nm}}$ of 0.25 and diluted 1:200 in Lactobacilli MRS broth for inoculation of microdilution plates by

adding 50 μ L of diluted inoculum to each well containing 50 μ L of an antibiotic solution. In these conditions, the bacterial inoculum was around $3-8 \times 10^5$ CFU/mL in the wells. After incubating the plates under anaerobic conditions at 37 °C for 48 h, MIC values were read as the lowest concentration of the antimicrobial agent at which visible growth was inhibited.

Preparation and expression of hDAAO deletion variant in *Escherichia coli*

The cDNA encoding for the N-terminal deleted variant, namely hDAAO(Δ 1-16) lacking the secretion signal peptide, was prepared by PCR using the pET11b-His-hDAAO plasmid as the template and the following primers: 5'-CACCATATGCTCTGCATCCATGAGCGC-3' (annealing downstream to the canonical starting codon, starting from the one coding for Leu17 and containing the *Nde*I restriction site, underlined) and 3'-ATGGATCCTCTTCAGAGGTGGGATGGTG-5' (annealing downstream the stop codon, in bold, and containing the *Bam*HI restriction site, underlined). The amplified insert was then subcloned in the pET11b plasmid.

For the co-expression of the N-terminal deleted variant with the His-tagged full-length hDAAO, the pET-Duet-1 vector (Novagen) was used. The His-hDAAO wild-type [Molla et al., 2006] was subcloned into the multiple cloning site 1; the PCR reaction was carried out using the pET11b-His-hDAAOwt as template and the following primers: 5'-cacCCATGGATGCATCACCATCACCATCACATG-3' (annealing downstream to the canonical starting codon of the His-hDAAO wild-type, in bold, and adding a *Nco*I restriction site, underlined) and the 3'-atAAGCTTCTTCAGAGGTGGGATGGTGGCAT-5' (annealing downstream to the canonical stop codon, in bold, and adding a *Hind*III restriction site, underlined). The amplified fragment was inserted into the pET-Duet vector between the *Nco*I-*Hind*III sites. The deleted strep-tagged hDAAO(Δ 1-16) variant was subcloned into the multiple cloning site 2; the gene was amplified using the pET11b-hDAAO(Δ 1-16) as a template using the following primers: 5'-cacCATATGCTCTGCATCCATGAGCGCTAC-3' (annealing downstream to the canonical starting codon of hDAAO(Δ 1-16), in bold, and adding a *Nde*I

restriction site, underlined) and 3'-
atCTCGAGTCTTCACTTTTCGAACTGCGGGTGGCTCCAGAGGTGGGATGGTGGCA
TTCTGGA-5' (annealing downstream to the canonical stop codon, in bold, and
adding a *Xho*I restriction site, underlined, and the strep-tag, italic). The
amplified fragment was inserted into the pET-Duet vector between *Nde*I and
*Xho*I sites.

Recombinant hDAAO wild-type and deleted variants were expressed in
BL21(DE3)Star *E. coli* cells and purified as reported in [Molla et al., 2006;
Romano et al., 2009]; 40 μ M of free FAD was present during all purification
steps. The deleted variant was purified by using the procedure previously set
up for the untagged wild-type enzyme consisting of ammonium sulfate
precipitation at 35% saturation, followed by dialysis of the pellet, and anionic
exchange chromatography on DEAE Sepharose FF at pH 8.0 (as well as using
different resins and buffers).

The co-expressed deleted variant and full-length hDAAO (which were
expected to produce heterodimers) were purified using the same protocol
set-up for the His-tagged wild-type enzyme (HiTrap Chelating
chromatography) [Molla et al., 2006] or the protocol suggested for the
purification of strep-tagged protein (Strep-Trap HP chromatography, in
TrisHCl pH 8.0 or PBS pH 7.4 using desthiobiotin in the elution buffer) for the
strep-tagged hDAAO(Δ 1-16).

The final enzyme preparations were stored in 20 mM Tris-HCl buffer, pH 8.0,
100 mM NaCl, 10% (v/v) glycerol, 40 μ M FAD and 5 mM 2-mercaptoethanol.
The enzyme concentration was determined spectrophotometrically by using
the extinction coefficient at 445 nm ($12.2 \text{ mM}^{-1} \text{ cm}^{-1}$).

DAAO activity was assayed with an oxygen electrode at pH 8.5, air saturation
and 25 °C, using 28 mM D-alanine as substrate in the presence of 0.2 mM
FAD [Molla et al., 2006].

Isolation of luminal, mucosal and epithelial layers in the small intestine

Slightly modified versions of protocol described in [Vaishnava et al., 2011]
were used to isolate luminal and mucosal layers in the small intestine of

Wistar rats (5-6 months old) and C57BL/6J mice (5-7 months old). The protocol reported in [Roche, 2001] was followed for isolation of the epithelial layer. Freshly dissected rat or mouse small intestines were partitioned into three parts: proximal, medial and distal samples. Then each part was further subdivided into three pieces: i) the 'luminal content' corresponded to the washing out with 2 mL of ice-cold sterile PBS; ii) the tissue pieces were opened longitudinally and placed in 15 mL tubes with 2 mL of ice-cold sterilized PBS. Tubes were inverted 20 times and vortexed for 10 s, the liquid was then collected in a fresh tube and defined as 'mucosal content'; iii) finally, the 'epithelial layer' was recovered. The remaining tissue pieces were cut into 3–5 mm square patches, collected in a tube with 10 mL of phosphate buffer saline (PBS) containing 0.5 mM DTT and 5 mM EDTA, and incubated with constant shaking at 37 °C for 20 min. Epithelial cells were collected by pipetting for ten times and the sample was filtered through a 70 µm cell strainer to remove tissue fragments; cells were pelleted by centrifugation at 6000 g at 4 °C for 10 min [Sasabe et al., 2016]. As negative control, we used C57BL/6J DAAO^{-/-} knock out mice which do not express the flavoenzyme [Pritchett et al., 2015].

All experiments on animals were conducted in accordance with Italian (Decr. Leg. 4.03.2014 n. 26) and French directives on animal experimentation and local ethical committee approvals and following the Directive 2010/63/EU of the European Parliament and of the Council of 22 September 2010 on the protection of animals used for scientific purposes and to the Council of Europe Convention for the Protection of Vertebrate Animals used for Experimental and other Scientific Purposes (ETS123).

Immunoprecipitation and Western blot analyses

The presence of DAAO in the different gut samples was investigated by Western blot analyses using different antibodies: anti-hDAAO, diluted 1:3000 (Davids Biotechnologie); anti-hDAAO C-terminal, diluted 1:3000 (Davids Biotechnologie); anti-hDAAO N-terminal, diluted 1:250 (Davids Biotechnologie); anti-hDAAO diluted 1:1000 (Abcam); anti-hDAAO, diluted

1:500 (Rockland); anti-mDAAO C-terminal, diluted 1:500 (Santa Cruz Biotechnology). Epithelial cells were homogenized in lysis buffer (150 mM sodium chloride, 1% NP-40, 50 mM Tris, pH 8.0, and a protease inhibitor cocktail), luminal and mucosal contents isolated from the small intestine were sonicated and centrifuged. Protein level in supernatants was quantified using Bradford reagent. A cerebellar lysate was used as a positive control for the presence of DAAO. Supernatants were subjected to SDS-PAGE and proteins were transferred to PVDF membranes. Blots were blocked in 4% skim milk in Tris-buffered saline (TBS) with 0.1% Tween-20 at 4 °C, overnight. The membranes were incubated with primary antibodies diluted in TBS with 0.05% Tween-20 and 2% skim milk at room temperature for 2 hours, subsequently washed in TBS with 0.1% Tween-20 and 4% skim milk (3 x 5 min), then incubated with secondary antibodies conjugated with horseradish peroxidase for 1 h (diluted in TBS with 0.05% Tween-20 and 2% skim milk). The membranes were washed in TBS with 0.1% Tween-20 (2 x 5 min) and TBS (2 x 5 min) and bound antibodies were detected with ECL plus WB detection solution (GE Healthcare) by a Li-Core system.

For immunoprecipitation analyses, the samples were precleared with 50 µL of mProtein A Sepharose (GE Healthcare, Chicago, Illinois, USA) for 1 hour at 4 °C with rotation. 5 µg of anti-DAAO antibodies were cross-linked to 50 µL of Dynabeads Protein G using 20 mM dimethyl pimelimidate dissolved in 0.2 mM triethanolamine, pH 8.2 (for 60 min at room temperature with rotation). The excess of cross-linker was removed and the Dynabeads were incubated for 15 min at room temperature under rotation with 50 mM Tris-HCl, pH 7.5, and then washed with PBS containing 0.1% Tween. The precleared samples were added to the Dynabeads-antibody complexes and incubated overnight at 4 °C with rotation. The supernatant (post-IP sample) was collected by separating the beads on the magnet. The beads were extensively washed with PBS and finally suspended in 50 µL of a nonreducing SDS-PAGE sample buffer (IP sample) and boiled. Subsequently, 20 µL of the IP samples were analysed by SDS-PAGE and Western blot. Recombinant hDAAO was used as positive control (added to supernatants).

nLC-MS/MS analysis

In order to verify the presence of DAAO in the small intestine, tissue samples were analysed by mass spectrometry. 160 µg (40 x 4 lanes) of total proteins from different gut fractions were separated by SDS-PAGE and stained with colloidal Coomassie; the bands of interest (i.e. at the selected molecular mass values) were cut, and stored in 5% acetic acid for the identification by nLC-MS/MS. Each band was cut and digested in situ by trypsin sequence grade upon extraction with TCA (trichloroacetic acid) and acetonitrile (CH₃CN), reduction with 45 mM dithiothreitol and malkylation with 100 mM iodoacetamide. MS/MS analysis was carried out by a LTQ-Orbitrap Velos (Thermo FisherScientific), as previously described [Dell'Orco et al., 2016]. Data Base search was performed using the Sequest search engine of Proteome Discoverer 1.4 (Thermo Fisher Scientific) against the Rodentia Uniprot sequence database. Only peptides with Xcorr 1.5 and Confidence FDR ≤ 0.05 were kept for the identification.

Native PAGE

With the aim to verify the presence and the mass of an active DAAO in the intestinal fractions, 60 µg of total proteins of the tissues were analysed by native electrophoresis (non-denaturing, 7.5% acrylamide resolving gel, 4 °C at 20 mA). Gels were stained with Blue Coomassie or for DAAO activity based on the reduction of iodinitrotetrazolium salt, i.e by incubating at 37 °C the gel in 35 mM sodium pyrophosphate, pH 8.5, 0.2 mM FAD, 28 mM D-Ala, 0.18 mM iodinitrotetrazolium dissolved in ethanol [Piubelli et al., 2003]. Controls were performed by adding the DAAO specific inhibitor CBIO in the assay solution (negative controls), as well as using the recombinant hDAAO or mice cerebellum samples (positive controls).

Results

Prediction of signal sequence in DAAO

The sequences of mammalian DAAOs (human, mouse, rat and porcine) were analyzed in silico with various bioinformatics programs, including the SignalP

3.0 used by [Sasabe et al., 2016], in order to reveal the presence of a signal peptide and a cleavage site for protein secretion, see Materials and Methods. While the SignalP 4.1 Server predicted a signal sequence and a cleavage site between positions 16 and 17 at the N-terminus of the pig DAAO only (score value of 0.455 vs. a cutoff value of 0.450), three alternative bioinformatics tools predicted the same signal peptide for all the mammalian DAAOs analyzed and the Signal-3L predicted the presence of this signal peptide in mouse and rat DAAOs only (Fig. 1A and Supplementary Data 1 and Suppl. Table 1). Accordingly, the hDAAO(Δ 1-16) variant lacking the N-terminal 16 residues was designed (see below).

The prediction analysis for the presence of antimicrobial peptides (CAMP) in the DAAO sequence suggested the presence of two cryptic cationic peptides: ²⁵⁷IWKSCCKLEPTLKNARIVGELTGFRPVRPQVRL²⁸⁹ and ³¹³GLTIHWGCAMEAANLFGKILEEKLSRLPPSHL³⁴⁵ in the murine sequence (corresponding to ²⁶⁴RLEPTLKNARIIGERTGFRPVRPQIRLEREQLR²⁹⁷ and ³¹⁵GLTIHWGCALEAAKLFGRILEEKLSRMPPSHL³⁴⁷ in the human enzyme, Fig. 1A). The antimicrobial absolute score, AS values, were calculated for all possible peptides of length between 12 and 40 residues. The highest AS was found for a 33-residues long peptide starting at position 257 (²⁵⁷IWKSCCKLEPTLKNARIVGELTGFRPVRPQVRL²⁸⁹, named IWK). The plot in Suppl. Fig. 1, shows the AS values for all the possible peptides of 22 or 33 residues in mouse DAAO sequence and highlights that the figure for this peptide is higher than two of the three threshold scores. Downstream the potential antimicrobial region 257-289, at the C-terminus of DAAO, an additional region was observed containing two relative maxima with AS = 4.5 (for the 22 residue window) and AS = 3.3 (for the 33 residue window) corresponding to peptides ³²⁴AANLFGKILEEKLSRLPPSHL³⁴⁵ and ³¹³GLTIHWGCAMEAANLFGKILEEKLSRLPPSHL³⁴⁵, respectively. Even if the scores of these peptides are below the threshold scores, we selected peptide 313-345, named GLT, for further characterization because in the crystal structure of hDAAO this region is structured as a long and amphipathic α -helix, a feature often associated to CAMPs.

Expression of hDAAO(Δ 1-16) and strep-hDAAO(Δ 1-16) variants

At first, hDAAO(Δ 1-16) was produced in *E. coli* BL21DE3Star cells using the conditions reported for the wild-type enzyme [Molla et al., 2006]: the resulting expression level in the crude extract (< 1 mg/L fermentation broth) was too low for a biochemical characterization. In order to increase the expression yield of the soluble hDAAO variant, the following parameters were investigated: the *E. coli* strain, the cultivation broth, the OD_{600nm} at the moment of IPTG addition, the time of cell collection, the growth temperature after the induction of protein expression, the presence of the inhibitor benzoate (as active site ligand designed to stabilize the enzyme conformation) and the two-step protocol for the inhibition of protein synthesis [De Marco et al., 2007]. Best conditions are reported in Supplementary Data 2 and Suppl. Table 2.

The untagged hDAAO(Δ 1-16) variant was purified employing the procedure used for the wild-type enzyme [Molla et al., 2006]. However, about 50% of the total recombinant hDAAO variant is lost in the ammonium sulfate precipitation step and part is eluted in the flow through of the DEAE Sepharose FF column (~ 25%): the resulting overall purification yield is extremely low (< 20%) corresponding to 0.04 mg of pure hDAAO variant/L fermentation broth. Indeed, no DAAO activity was detected in the crude extract or in the final enzyme preparation also in the presence of a saturating exogenous FAD concentration, i.e. 0.2 mM.

In order to facilitate the production of the deleted variant, and since hDAAO is a stable homodimer in solution, it was co-expressed with the wild-type hDAAO using the pET-Duet plasmid as tagged proteins, i.e. His-hDAAO wild-type and strep-hDAAO(Δ 1-16). No DAAO enzymatic activity was detected in the crude extract of BL21(DE3)pLysS *E. coli* cells harbouring the pET-Duet vector. Neither a HiTrap chelating chromatography nor a StrepTrap column (using desthiobiotin in the elution buffer) allowed binding of the recombinant proteins: in both cases, the two protein forms eluted in the flow-through (not shown). None of the conditions reported in Suppl. Table 3

allow to produce a suitable amount of Δ 1-16-deleted hDAAO: the recombinant protein poorly binds to different resins and seems highly unstable and inactive. We concluded that elimination of 16 residues at the N-terminal end of hDAAO significantly hampers protein folding, FAD binding and stability.

MD simulation analysis

We next used molecular dynamics simulations to compare the stability of the tertiary structure of full-length (PDB 2E48) with the model of Δ 1-16 deleted hDAAO variant (Fig. 1B), in presence and in absence of the flavin cofactor. Actually, wild-type hDAAO exists in solution in equilibrium between the apoprotein and the holoenzyme forms because of the weak FAD binding [Molla et al., 2006; Caldinelli et al., 2009]. The Root Mean Square deviation (RMSD) during the time of simulation (100 ns) is higher for the Δ 1-16 variant compared to the full-length enzyme, in particular in the absence of FAD (Fig. 2A). The Root Mean Square Fluctuation (RMSF), calculated to compare the extent of fluctuations of each single residue of the system, is still significantly higher for the Δ 1-16 hDAAO (Fig. 2B). In the absence of the cofactor, the Δ 1-16 variant resulted more unstable than the full-length protein: the regions characterized by highest instability are those located close to the flavin cofactor (residues from 17 to 50, residues from 135 to 210 and residues from 260 to 320, Fig. 2C). Altogether, experimental and *in silico* analyses suggest that elimination of part of the Rossmann fold, and especially of the GXGXXG Wierenga sequence [Rossmann 1974, Wierenga 1983], strongly affects the overall fold of the flavoenzyme hampering FAD binding and catalytic activity.

Tissue analysis on rat and mouse intestine

At first, the presence of DAAO in tissue fractions from mouse and rat small intestine (luminal, mucosal content and epithelial layer of proximal, medial and distal small intestine) was investigated by Western blot analysis using five different commercial anti-hDAAO antibodies. In a previous investigation [Sasabe et al., 2016] an home-made produced and affinity chromatography

purified polyclonal anti-mouse DAAO antibody and an polyclonal anti-human DAAO antibody (from Everest Biotech, which is no more commercially available) were used. Among the five commercially available antibodies we here selected the two antibodies giving reproducible results in preliminary experiments and that could provide information about the lost region, i.e. the anti-N-terminal and anti-C-terminal hDAAO antibodies (from Davids Biotechnologie). The regions recognized by these antibodies are indicated in Fig. 1A. The elimination of the putative N-terminal translocation sequence should convert the 38.7-38.8 kDa full-length rat or mouse DAAO into a 37.3-37.5 kDa fragment which is still recognized by both the antibodies we used. The lack of recognition by the anti-N-terminal antibody requires the elimination of 120 residues at the N-terminal end, corresponding to a 13.5 kDa decrease in mass. The elimination of a sequence ≥ 20 residues at the C-terminus will give a DAAO form not recognized by the anti-C-terminal hDAAO antibody.

The analysis of rat intestine samples resulted in aspecific recognition patterns, see Suppl. Data 3 and Suppl. Table 4. On mice samples, the main signals recognized by anti-C-terminal hDAAO antibodies corresponds to bands at 70 kDa in mucosal proximal and distal samples, at 40 kDa in mucosal distal and luminal (proximal, median and distal) samples, and at 27 kDa in mucosal proximal and distal samples, see Table 1, Supplementary Data 4 and Suppl. Fig. 2A. The band at ~ 40 kDa, that should correspond to the full-length mice DAAO, was recognized by both anti-hDAAO antibodies in mucosal distal, and luminal medium and distal regions. Faint bands at ~ 100 kDa (in distal mucosal), 70, 45 and ~ 35 kDa (in epithelial layer samples), and at 18 kDa (in proximal and distal mucosal samples) were also observed depending on sample concentration and preparation (see the samples indicated by asterisk in Table 1). An anti-C-terminal mDAAO antibody recognized bands at 55, 35 and 27 kDa in mucosal proximal and distal samples: the band at lower molecular mass was also recognized by the anti-C-terminal hDAAO antibody (see Table 1, Supplementary Data 4 and Suppl. Fig. 3).

The main signals corresponding to anti-N-terminal antibody recognition

corresponds to bands at 40 kDa in distal samples from mucosal and luminal portions (and, with a lower intensity, from proximal and medial samples), at 35 kDa in proximal and medial samples from mucosal and luminal fractions, and at ≤ 20 kDa in epithelial samples (in details at 20 and 18 kDa in the medial and at 15 kDa in all samples of the epithelial fraction). These results should arise from a specific recognition since the apparent mass values agree with protein fragments harboring the regions recognized by the two antibodies. Notably, bands at ≤ 20 kDa are recognized only in the epithelial layer: the 20 kDa-band in proximal epithelial layer corresponds to 5.7 ng / μ g total proteins. Faint bands at 55 kDa (in mucosal samples), 45 kDa (in epithelial layer samples), 20 kDa (in medial and distal epithelial layer samples) were also detected based on sample concentration and preparation (see the samples indicated by the asterisk in Table 1).

These results differ from what is reported in [Sasabe et al., 2016]: the presence of the full-length ~ 39 kDa form of mouse DAAO in the epithelial layer samples is not apparent in our studies, while only bands at < 20 kDa molecular mass are apparent. On the other hand, the presence of a ~ 35 - 37 kDa protein form lacking the N-terminal sequence in the intestinal content is confirmed in proximal and medium regions of mucosal and luminal samples. Notably, bands at ~ 30 and 20 kDa, too small to preserve the enzymatic activity, were also apparent in the analyses reported by [Sasabe et al., 2016].

In order to confirm the presence of mouse DAAO in the most interesting samples, the bands at 40 and 35 kDa in the mucosal distal and proximal regions and the ~ 27 kDa band in the mucosal distal and proximal samples were analyzed by mass spectrometry (Fig. 3). In the band at 40 kDa of the distal mucosal content the presence of DAAO was confirmed with three different peptides (corresponding to sequences 23-33, 115-141, 233-252, equal to the 4% of the whole protein contents). No peptides derived from DAAO were identified in the ~ 35 kDa band from proximal mucosal sample. In the band at 27 kDa of the distal mucosal content four different DAAO-generated peptides (i.e. sequences 1-32, 116-141, 158-171, 233-263) were also identified. Three different peptides derived from DAAO were detected

in the ~ 27 kDa band of the proximal mucosal content, corresponding to 29% of the total amount of the proteins (i.e. sequences 101-140, 233-259, 295-335). Altogether, DAAO is released in mouse gut, where it is largely proteolyzed.

In order to verify the specificity of the recognized bands in intestinal tissues, we followed the recommendations recently reported by [Mothelet al., 2019], i.e. we performed the same Western blot analyses as above on intestinal tissues from a full DAAO null constitutive mutant mice strain (DAAO^{-/-}) [Schweimer et al., 2014]. The Western blot analysis revealed bands at 27 kDa in mucosal medial samples (and faint bands at 45 kDa in epithelial samples and at 70 and 35 kDa in proximal epithelial samples) using the anti-C-terminal hDAAO antibody (Suppl. Fig. 4A) and a band at ~ 20 kDa in proximal epithelial sample by the anti-C-terminal hDAAO antibody (Suppl. Fig. 4B). The anti-C-terminal mDAAO antibody recognized similar signals in samples isolated from wild-type and DAAO^{-/-} mice (Table 1 and Suppl. Fig. 4A). The 40 kDa, ~ 35 kDa and ~ 27 kDa bands in proximal and distal mucosal layers were subjected to MS analysis: no peptides deriving from DAAO were identified in samples from DAAO^{-/-} mice. This analysis on samples from DAAO^{-/-} mice demonstrates that DAAO's aspecific recognition is apparent in Western blot analysis of gut samples, pointing to the need of mass spectrometry to confirm the presence of the flavoenzyme.

Despite the purified recombinant hDAAO was immunoprecipitated with the tested antibodies, endogenous DAAO was not isolated from the mouse intestinal samples. Notably, zymograms performed following native-PAGE on whole mice gut tissue show a band at low electrophoretic mobility, significantly different from the one corresponding to the reference recombinant hDAAO and from the signal observed using a mice cerebellum sample (Suppl. Fig. 5) Indeed, this band is present even when the gel was incubated in the presence of the 6-chloro-1,2-benzisoxazol-3(2H)-one (CBIO), an inhibitor of hDAAO. The altered migration of hDAAO in native-PAGE of crude samples is probably due to its composition since also the recombinant hDAAO added to mucosal proximal mouse intestine sample did not migrate

as the pure protein alone. Anyway, the lack of inhibition of activity signal by CBIO points to the presence of aspecific signals.

Antimicrobial peptides

Investigating the primary structure of mDAAO using the method described in [Pane et al., 2017] suggests the presence of two antimicrobial peptides corresponding to 257-289 (IWK) and 315-347 (GLT) regions, see Fig. 1A. Conformation of DAAO antimicrobial peptides was analyzed by far-UV CD. Both the peptides are mostly unstructured and show slightly different spectra (Fig. 4, black lines): notably, they assume an ordered helical conformation (minima at around 210 and 220 nm) in the presence of SDS (1 mM) or TFE (30% v/v), two membrane mimicking agents, and of LPS from *E. coli* (0.1 and 0.25 mg/mL for GLT and IWK, respectively) (Fig. 4). DichroWeb confirmed the experimental results: both the peptides are initially “unordered” and assume an helical conformation during the titration (α -helix content > 70%).

In order to shed light on their putative role in the observed microbial selection in the gut, the antimicrobial activity of the two polypeptides and of a mixture containing both peptides at 1:1 a molar ratio was tested on two Gram-positive and five Gram-negative bacteria (Table 2). Both peptides showed bactericidal or bacteriostatic activity on the tested bacteria, the only exception was *S. enteritidis*. Notably, in some cases an additive effect of the two peptides is apparent (Table 2) reaching MIC values in the low micromolar range. Noteworthy, both peptides show a strong and additive bacteriostatic activity on *E. faecalis* with the mixture of the two peptides being already active at about 3 μ M.

Four lactic acid bacteria (LAB) strains belonging to species *Lactobacillus acidophilus*, *Lactobacillus casei*, *Lactobacillus fermentum*, *Lactobacillus rhamnosus* were tested for their susceptibility to IWK and GLT peptides. The results of antimicrobial susceptibility testing of four *Lactobacillus* strains using broth microdilution are listed in Table 3. The tested strains do not show any significant difference in their antibiotic resistance profile. All strains were

resistant to vancomycin and susceptible to erythromycin. None of the four lactobacilli tested showed susceptibility to IWK and GLT peptides *in vitro* at the highest tested concentration of 100 μ M.

Conclusions

We are aware that, despite the key role played by hDAAO in some important physiological processes, much remains to be unraveled concerning the modulation of its functional properties; a fine and careful regulation through post-translational modification(s) and alternative subcellular targeting is expected and not yet proved. DAAO is known to be largely peroxisomal [Moreno 1999, Sacchi 2008, Cappelletti 2014] even if a cytosolic form has been observed [Sacchi 2008, Sacchi 2011], largely corresponding to the neo-synthesized protein which is cytosolic before reaching the peroxisomes. Recent reports on rats demonstrated that DAAO is present both in cytosol and nuclei of proximal tubule epithelial cells following treatment with the drug propiverine [Luks et al., 2018]. Indeed DAAO was also reported to be secreted in the intestine: it has been proposed that the flavoenzyme might play a role in controlling the homeostasis of gut microbiota through the production of H₂O₂ [Sasabe et al., 2016]. DAAO protein and activity were detected in the epithelium of proximal and middle small intestine of mice and humans. A processed form of the protein appeared to be secreted in the lumen by goblet cells, due to the presence of a signal peptide and a predicted cleavage site near the N-terminus [Sasabe et al., 2016].

However, despite bioinformatics analysis by several softwares (Suppl. Table 1) confirm the presence of the signal peptide, the fact that the putative signal peptide belongs to the Rossmann fold motif, which contains the Wierenga sequence (GxGxxG) required for the binding to the cofactor (Fig. 1B), suggests that the processed enzyme might not be folded and active. Our experiments on recombinant hDAAO show that the enzyme form lacking the residues from 1 to 16 is unstable and inactive. This conclusion is supported by molecular dynamics studies, highlighting a higher instability of the deleted hDAAO, especially in the absence of FAD, compared to the full-length counterpart.

Accordingly, we propose that any active hDAAO present in the lumen might retain the N-terminal sequence required for cofactor binding and essential for the enzymatic activity. Native-PAGE does not suggest the presence of an active DAAO in the mice gut: the band identified in the zymogram shows a low electrophoretic mobility and is not inhibited by a strong DAAO inhibitor (see Suppl. Fig. 5). Notably, our results agree with a recent assay of DAAO activity in mice tissues which did not identify any enzymatic activity in small intestine (whole intestine as well as proximal, middle and distal fractions) [Kim et al., 2019].

In order to clarify this issue (and the putative secretion pattern), Western blot analyses were performed on small intestine samples from rat and mouse using different antibodies. We excluded three commercial anti-hDAAO antibodies as well as the results gathered on the rat tissues since the recognized bands seem largely due to unspecific recognition. By using anti-N-terminal and anti-C-terminal hDAAO antibodies (from Davids Biotechnologies), bands at 40 and 35 kDa were apparent in the mucosal and luminal content of mouse small intestine, as well as bands at lower molecular mass which can arise from processing of the full-length enzyme (Table 1). Concerning the bands at 40 (in mucosal distal fraction) and at ~ 27 kDa (in mucosal distal and proximal fractions) both contains DAAO-originating peptides, Fig. 3. The 27 kDa-band arises from cleavage of ~ 100 residues at the N-terminus of DAAO. The same analysis were performed on DAAO^{-/-} mice tissues as a negative control: again bands at 40, 35 and at lower molecular mass were apparent in Western blot, but MS analysis did not identify DAAO-generated peptides. We conclude that i) commercial anti-DAAO antibodies recognize aspecific bands in gut samples; ii) DAAO is present in the mucosal fraction of mouse gut, where it is largely proteolyzed. We can not exclude that the use of Germ Free C57BL/6 mice [Sasabe et al., 2016] instead of untreated C57BL/6 mice, as in our case, can induce a different expression of DAAO.

The antimicrobial AS score, a tool that has already allowed the identification of several cryptic CAMPs inside human, plant and archaeal proteins [Bosso et

al., 2017; Gaglione et al., 2017; Notomista et al., 2015; Pane et al., 2016; Pane et al., 2018; Pizzo et al., 2018], identified two internal regions in DAAO sequence as CAMP (see Table and Fig. 1A). The corresponding peptides showed antimicrobial activity on various Gram-positive and Gram-negative bacteria (Table 2), but not on Lactobacilli species which represent the commensal microbiota (Table 3). Interestingly, these peptides assumed a secondary structure in presence of detergents and LPS from *E. coli*.

Our study confirms that hDAAO activity is finely tuned through post-translational modifications to fulfil different physiological functions in different tissues. At the same time, our results modify the mechanism by which DAAO is able to select the gut microbiota. DAAO seems to act indirectly, by the generation of antimicrobial peptides, instead of a direct action due to its catalytic activity and mediated by H₂O₂.

References

- Bendtsen JD, Jensen LJ, Blom N, Von Heijne G, Brunak S. Feature-based prediction of non-classical and leaderless protein secretion. *Protein Eng Des Sel.* 2004 Apr; 17(4):349-56.
- Bendtsen JD, Nielsen H, von Heijne G, Brunak S. Improved prediction of signal peptides: SignalP 3.0. *J Mol Biol.* 2004 Jul 16; 340(4):783-95.
- Billard JM. D-serine signalling as a prominent determinant of neuronal-glia dialogue in the healthy and diseased brain. *J Cell Mol Med.* 2008 Oct; 12(5B):1872-84.
- Bosso A, Pirone L, Gaglione R, Pane K, Del Gatto A, Zaccaro L, Di Gaetano S, Diana D, Fattorusso R, Pedone E, Cafaro V, Haagsman HP, van Dijk A, Scheenstra MR, Zanfardino A, Crescenzi O, Arciello A, Varcamonti M, Veldhuizen EJA, Di Donato A, Notomista E, Pizzo E. A new cryptic host defense peptide identified in human 11-hydroxysteroid dehydrogenase-1 β -like: from in silico identification to experimental evidence. *Biochim Biophys Acta Gen Subj.* 2017 Sep; 1861(9):2342-2353.
- Caldinelli L, Molla G, Sacchi S, Pilone MS, Pollegioni L. Relevance of weak flavin binding in human D-amino acid oxidase. *Protein Sci.* 2009 Apr; 18(4):801-10.
- Cappelletti P, Campomenosi P, Pollegioni L, Sacchi S. The degradation (by distinct pathways) of human D-amino acid oxidase and its interacting partner pLG72--two key proteins in D-serine catabolism in the brain. *FEBS*

- J. 2014 Feb; 281(3):708-23.
- Collingridge GL, Volianskis A, Bannister N, France G, Hanna L, Mercier M, Tidball P, Fang G, Irvine MW, Costa BM, Monaghan DT, Bortolotto ZA, Molnár E, Lodge D, Jane DE. The NMDA receptor as a target for cognitive enhancement. *Neuropharmacology*. 2013 Jan; 64:13-26.
- De Marco A, Deuerling E, Mogk A, Tomoyasu T, Bukau B. Chaperone-based procedure to increase yields of soluble recombinant proteins produced in *E. coli*. *BMC Biotechnol*. 2007 Jun 12; 7:32.
- Dell'Orco M, Milani P, Arrigoni L, Pansarasa O, Sardone V, Maffioli E, Polveraccio F, Bordoni M, Diamanti L, Ceroni M, Peverali FA, Tedeschi G, Cereda C. Hydrogen peroxide-mediated induction of SOD1 gene transcription is independent from Nrf2 in a cellular model of neurodegeneration. *Biochim Biophys Acta*. 2016 Feb; 1859(2):315-23.
- Gaglione R, Dell'Olmo E, Bosso A, Chino M, Pane K, Ascione F, Itri F, Caserta S, Amoresano A, Lombardi A, Haagsman HP, Piccoli R, Pizzo E, Veldhuizen EJA, Notomista E, Arciello A. Novel human bioactive peptides identified in Apolipoprotein B: Evaluation of their therapeutic potential. *Biochem Pharmacol*. 2017 Apr 15; 130:34-50.
- Gasteiger E, Hoogland C, Gattiker A, Duvaud S, Wilkins MR, Appel RD, Bairoch A. Protein identification and analysis tools on the ExPASy server. *The Proteomics Protocols Handbook Humana Press* 2005. p. 571–607.
- Kim SH, Shishido Y, Sogabe H, Rachadech W, Yorita K, Kato Y, Fukui K. Age- and gender-dependent D-amino acid oxidase activity in mouse brain and peripheral tissues: implication for aging and neurodegeneration. *J Biochem*. 2019 Aug 1; 166(2):187-196.
- Koga R, Miyoshi Y, Sakaue H, Hamase K, Konno R. Mouse D-amino-acid oxidase: distribution and physiological substrates. *Front Mol Biosci*. 2017 Dec 4; 4:82.
- Konno R, Ikeda M, Yamaguchi K, Ueda Y, Niwa A. Nephrotoxicity of D-propargylglycine in mice. *Arch Toxicol*. 2000 Oct; 74(8):473-9.
- Lin CH. Sodium Benzoate, a D-amino acid oxidase inhibitor, added to clozapine for the treatment of schizophrenia: a randomized, double-blind, placebo-controlled trial. *Biol Psychiatry*. 2018 Sep 15;84(6):422-432.
- Luks L, Maier MY, Sacchi S, Pollegioni L, Dietrich DR. Understanding renal nuclear protein accumulation: an in vitro approach to explain an in vivo phenomenon. *Arch Toxicol*. 2017 Nov; 91(11):3599-3611.
- Madeira C, Freitas ME, Vargas-Lopes C, Wolosker H, Panizzutti R. Increased brain D-amino acid oxidase (DAAO) activity in schizophrenia. *Schizophr Res*. 2008 Apr; 101(1-3):76-83.

- Maekawa M, Okamura T, Kasai N, Hori Y, Summer KH, Konno R. D-amino-acid oxidase is involved in D-serine-induced nephrotoxicity. *Chem Res Toxicol*. 2005 Nov; 18(11):1678-82.
- Molla G, Sacchi S, Bernasconi M, Pilone MS, Fukui K, Polegioni L. Characterization of human D-amino acid oxidase. *FEBS Lett*. 2006 Apr 17; 580(9):2358-64..
- Moreno S, Nardacci R, Cimini A, Cerù MP. Immunocytochemical localization of D-amino acid oxidase in rat brain. *J Neurocytol*. 1999 Mar; 28(3):169-85.
- Mothet JP, Parent AT, Wolosker H, Brady RO Jr, Linden DJ, Ferris CD, Rogawski MA, Snyder SH. D-serine is an endogenous ligand for the glycine site of the N-methyl-D-aspartate receptor. *Proc Natl Acad Sci U S A*. 2000 Apr 25; 97(9):4926-31.
- Nakade Y, Iwata Y, Furuichi K, Mita M, Hamase K, Konno R, Miyake T, Sakai N, Kitajima S, Toyama T, Shinozaki Y, Sagara A, Miyagawa T, Hara A, Shimizu M, Kamikawa Y, Sato K, Oshima M, Yoneda-Nakagawa S, Yamamura Y, Kaneko S, Miyamoto T, Katane M, Homma H, Morita H, Suda W, Hattori M, Wada T. Gut microbiota-derived D-serine protects against acute kidney injury. *JCI Insight*. 2018 Oct 18; 3(20).
- Notomista E, Falanga A, Fusco S, Pirone L, Zanfardino A, Galdiero S, Varcamonti M, Pedone E, Contursi P. The identification of a novel *Sulfolobus islandicus* CAMP-like peptide points to archaeal microorganisms as cell factories for the production of antimicrobial molecules. *Microb Cell Fact*. 2015 Sep 4; 14:126.
- Pane K, Sgambati V, Zanfardino A, Smaldone G, Cafaro V, Angrisano T, Pedone E, Di Gaetano S, Capasso D, Haney EF, Izzo V, Varcamonti M, Notomista E, Hancock RE, Di Donato A, Pizzo E. A new cryptic cationic antimicrobial peptide from human apolipoprotein E with antibacterial activity and immunomodulatory effects on human cells. *FEBS J*. 2016 Jun; 283(11):2115-31.
- Pane K, Cafaro V, Avitabile A, Torres MT, Vollaro A, De Gregorio E, Catania MR, Di Maro A, Bosso A, Gallo G, Zanfardino A, Varcamonti M, Pizzo E, Di Donato A, Lu TK, de la Fuente-Nunez C, Notomista E. Identification of novel cryptic multifunctional antimicrobial peptides from the human stomach enabled by a computational-experimental platform. *ACS Synth Biol*. 2018 Sep 21; 7(9):2105-2115.
- Pane K, Durante L, Crescenzi O, Cafaro V, Pizzo E, Varcamonti M, Zanfardino A, Izzo V, Di Donato A, Notomista E. Antimicrobial potency of cationic antimicrobial peptides can be predicted from their amino acid composition: application to the detection of "cryptic" antimicrobial

- peptides. *J Theor Biol.* 2017 Apr 21; 419:254-265.
- Petersen TN, Brunak S, von Heijne G, Nielsen H. SignalP 4.0: discriminating signal peptides from transmembrane regions. *Nat Methods.* 2011 Sep 29; 8(10):785-6.
- Piubelli L, Molla G, Caldinelli L, Pilone MS, Pollegioni L. Dissection of the structural determinants involved in formation of the dimeric form of D-amino acid oxidase from *Rhodotorula gracilis*: role of the size of the betaF5-betaF6 loop. *Protein Eng.* 2003 Dec; 16(12):1063-9.
- Pizzo E, Pane K, Bosso A, Landi N, Ragucci S, Russo R, Gaglione R, Torres MDT, de la Fuente-Nunez C, Arciello A, Di Donato A, Notomista E, Di Maro A. Novel bioactive peptides from PD-L1/2, a type 1 ribosome inactivating protein from *Phytolacca dioica* L. Evaluation of their antimicrobial properties and anti-biofilm activities. *Biochim Biophys Acta Biomembr.* 2018 Jul; 1860(7):1425-1435.
- Pollegioni L, Piubelli L, Sacchi S, Pilone MS, Molla G. Physiological functions of D-amino acid oxidases: from yeast to humans. *Cell Mol Life Sci.* 2007 Jun; 64(11):1373-94.
- Pritchett D, Hasan S, Tam SK, Engle SJ, Brandon NJ, Sharp T, Foster RG, Harrison PJ, Bannerman DM, Peirson SN. D-amino acid oxidase knockout (Dao^{-/-}) mice show enhanced short-term memory performance and heightened anxiety, but nosleep or circadian rhythm disruption. *Eur J Neurosci.* 2015 May; 41(9):1167-79.
- Roche JK. Isolation of a purified epithelial cell population from human colon. *Methods Mol Med.* 2001; 50:15-20.
- Romano D, Molla G, Pollegioni L, Marinelli F. Optimization of human D-amino acid oxidase expression in *Escherichia coli*. *Protein Expr Purif.* 2009 Nov; 68(1):72-8.
- Rossmann MG, Moras D, Olsen KW. Chemical and biological evolution of nucleotide-binding protein. *Nature.* 1974 Jul 19; 250(463):194-9.
- Sacchi S, Bernasconi M, Martineau M, Mothet JP, Ruzzene M, Pilone MS, Pollegioni L, Molla G. pLG72 modulates intracellular D-serine levels through its interaction with D-amino acid oxidase: effect on schizophrenia susceptibility. *J Biol Chem.* 2008 Aug 8; 283(32):22244-56.
- Sacchi S, Cappelletti P, Giovannardi S, Pollegioni L. Evidence for the interaction of D-amino acid oxidase with pLG72 in a glial cell line. *Mol Cell Neurosci.* 2011 Sep; 48(1):20-8.
- Sasabe J, Miyoshi Y, Rakoff-Nahoum S, Zhang T, Mita M, Davis BM, Hamase K, Waldor MK. Interplay between microbial D-amino acids and host D-amino acid oxidase modifies murine mucosal defence and gut microbiota.

- Nat Microbiol. 2016 Jul 25; 1(10):16125.
- Sasabe J, Suzuki M. Emerging role of D-amino acid metabolism in the innate defense. *Front Microbiol.* 2018 May 9; 9:933.
- Schweimer JV, Coullon GS, Betts JF, Burnet PW, Engle SJ, Brandon NJ, Harrison PJ, Sharp T. Increased burst-firing of ventral tegmental area dopaminergic neurons in D-amino acid oxidase knockout mice in vivo. *Eur J Neurosci.* 2014 Oct; 40(7):2999-3009.
- Shen HB, Chou KC. Signal-3L: A 3-layer approach for predicting signal peptides. *Biochem Biophys Res Commun.* 2007 Nov 16; 363(2):297-303.
- Shibuya N, Koike S, Tanaka M, Ishigami-Yuasa M, Kimura Y, Ogasawara Y, Fukui K, Nagahara N, Kimura H. A novel pathway for the production of hydrogen sulfide from D-cysteine in mammalian cells. *Nat Commun.* 2013; 4:1366.
- Vaishnava S, Yamamoto M, Severson KM, Ruhn KA, Yu X, Koren O, Ley R, Wakeland EK, Hooper LV. The antibacterial lectin RegIIIgamma promotes the spatial segregation of microbiota and host in the intestine. *Science.* 2011 Oct 14; 334(6053):255-8.
- Whitmore L, Wallace BA. Protein secondary structure analyses from circular dichroism spectroscopy: methods and reference databases. *Biopolymers.* 2008 May; 89(5):392-400.
- Wierenga RK, Terpstra P, Hol WG. Prediction of the occurrence of the ADP-binding beta alpha beta-fold in proteins, using an amino acid sequence fingerprint. *J Mol Biol.* 1986 Jan 5; 187(1):101-7.
- Wolosker H, Dumin E, Balan L, Foltyn VN. D-amino acids in the brain: D-serine in neurotransmission and neurodegeneration. *FEBS J.* 2008 Jul; 275(14):3514-26.
- Wolosker H. Serine racemase and the serine shuttle between neurons and astrocytes. *Biochim Biophys Acta.* 2011 Nov; 1814(11):1558-66.
- Zhang YZ, Shen HB. Signal-3L 2.0: A hierarchical mixture model for enhancing protein signal peptide prediction by incorporating residue-domain cross-level features. *J Chem Inf Model.* 2017 Apr 24; 57(4):988-999.

A

Mouse	MRVAVIGAGVIGLSTALCIHERYHP-TQPLHMKIYADRFPFTTSDVAAGLWQPYLSDPS	59
Rat	MRVAVIGAGVIGLSTALCIHERYHP-AQPLHMKIYADRFPFTTSDVAAGLWQPYLSDPS	59
Human	MRVVVIGAGVIGLSTALCIHERYHSLQPLDIKVYADRFTPLTTTDDVAAGLWQPYLSDPN	60
Porcine	MRVVVIGAGVIGLSTALCIHERYHSLQPLDVKVYADRFPFTTTDDVAAGLWQPYTSEPS	60
	,** ***,*:*:*****:**:***** *:*	
Mouse	NPQEAEWQQTFDYLLSCLHSPNAEKMGLALISGYNLFREVPDPFWK NAVLGFRKLTPS	119
Rat	NPQEAEWQQTFDHLQSC L HSPNAEKMGLALISGYNLFREVPDPFWKSTVLGFRKLTPS	119
Human	NPQEAADWSQQTFDYLLSHVHSPNAENLGLFLISGYNLFHEAI PDPSWKDVTVLGFRKLTPR	120
Porcine	NPQEANWNQQTFNYLLSHIGSPNAANMGLTPVSGYNLFREAVPDPYWKDMVLGFRKLTPR	120
	*****:*:*****:* * : **** ::* :*****: :*** ** *****	
Mouse	EMLDFPDYGYGWFNTSLLEGGKSYLPWLTERTLTERGVKLIHRKVESLEEVAR-GVDVIIN	178
Rat	E LDMFPDYSYGFNTSLLEGGKSYLSWLTERLTERGVKFIHRKVASFEVVRGGVDVIIN	179
Human	E LDMFPDYGWGFNTSLLEGGKSYLQWLTERLTERGVKFFQRKVESFEVAREGADVIIN	180
Porcine	E LDMFPDYRYGWFNTSLILEGRKYLQWLTERLTERGVKFFLRKVESFEVARGGADVIIN	180
	::*** **:*:***:**:*:* *****: : ** *:*:* * *:*:*	
Mouse	CTGVWAGALQADASLQPRGQIIQVEAPWIKHFILTHDPSLGIYNSPYIIPGSK TVTLGG	238
Rat	CTGVWAGALQADASLQPRGQIIQVEAPWIKHFILTHDPSLGIYNSPYIIPGSKT VTLGG	239
Human	CTGVWAGALQRDPLLQPRGQIMKVDAPWMKHFILTHDPERGIYNSPYIIPGT QVTLGG	240
Porcine	CTGVWAGVLQDPDLLQPRGQIIKVDAPWLKNFIITHDLERGIYNSPYIIPGLQ AVTLGG	240
	***** ** * *****:~*:*:*:*:* ***** :***** :*****	
Mouse	IFQLGNWSGLNSVRDHNTIWKSCCKLEPTLKNARIVGELTGFRPVRPQVRLEREWLHFGS	298
Rat	VFQLGNWSELNSVHDHNTIWKSCCQLEPTLKNARIMGELTGFRPVRPQVRLERERLRFGS	299
Human	IFQLGNWSELNNIQDHNTIWEGCCREPTLKNARIIGERTGFRPV RQVRLEREQLR TGP	300
Porcine	TFQVGNWNEINNIQDHNTIWEGCCREPTLKDIAIVGEYTGFRPVRPQVRLEREQLRFGS	300
	::*** :*:*:*****:**:*****:**:* *****:***** ** *	
Mouse	SSAEVIHNYGHGGYGLTIHWGCAMEAANLFGKILEEKLSRLPPSHL	345
Rat	SSAEVIHNYGHGGYGLTIHWGCAMEAANLFGKILEEKNLSRMPPSHL	346
Human	SNTEVIHNYGHGGYGLTIHWGC AL EAAKLFGRILEEKLSRMPP SHL	347
Porcine	SNTEVIHNYGHGGYGLTIHWGCAL EVAKLFGKIVLEERNLLTMPP SHL	347
	::*****:*****:**:*****:** * *****	

B

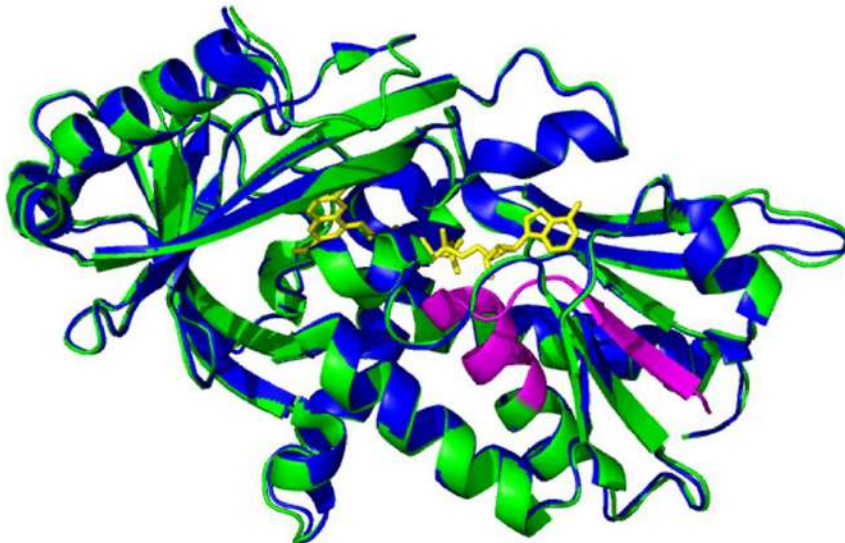


Fig. 1. A) Comparison of primary structure of mouse, rat, porcine and human DAAO. The putative secretion signal is marked in red, the regions recognized by anti-N-terminal and anti-C-terminal hDAAO antibodies are in violet and underlined, and

putative antimicrobial sequences are in light blue and green. The regions recognized by the anti-DAAO antibodies used in [Sasabe et al., 2016] are highlighted in green and yellow. The peptides identified by MS analysis following SDS-PAGE are highlighted in grey. B) Comparison of the structure of full-length hDAAO (PDB 2DU8, green) and of the model of the Δ 1-16 hDAAO variant (blue). The deleted N-terminal sequence is coloured in magenta.

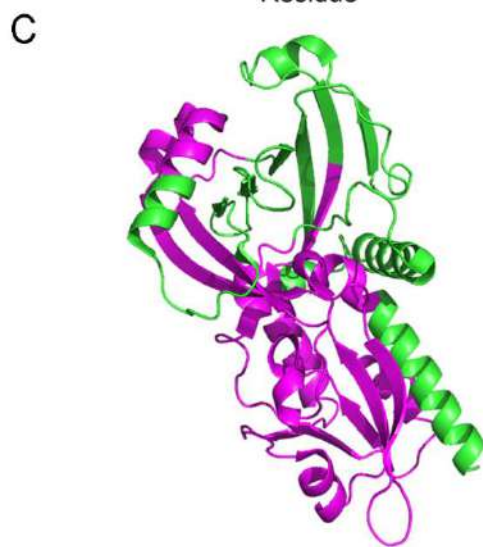
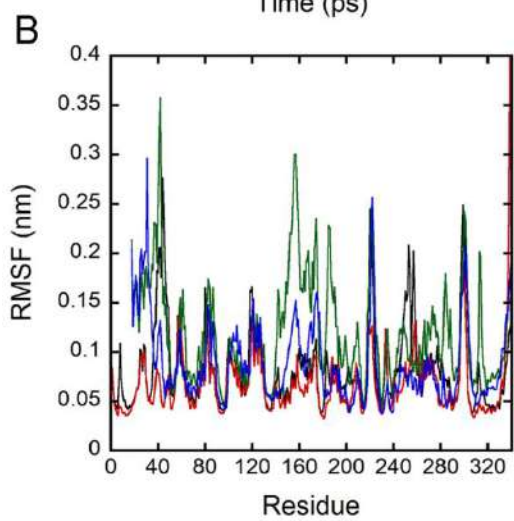
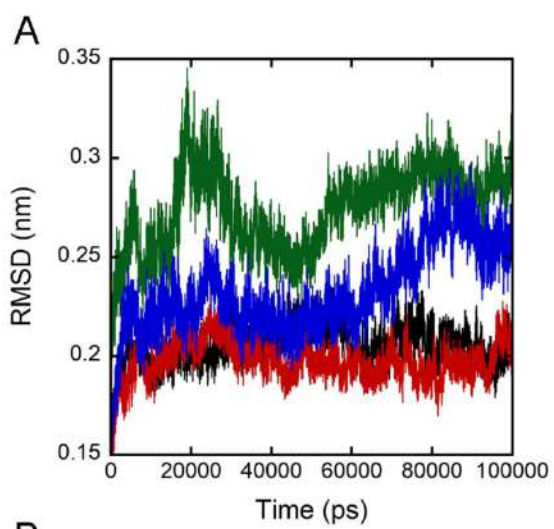


Fig. 2. A) Protein RMSD from the starting structure are represented as a function of simulation time: full-length wild-type hDAAO in absence and in presence of FAD (in black and red) and $\Delta 1-16$ deleted variant in absence and in presence of the cofactor (in green and blue). B) The per residue RMSF are represented as a function of the residue number (same colours as in panel A). C) Model of the 3D structure of the $\Delta 1-16$ deleted variant without FAD. The sequences characterized by highest instability are colored in magenta.

A) Distal mucosal

Anti-N-terminal:



Anti-C-terminal:



B) Proximal mucosal

Anti-C-terminal:



Fig. 3. Western blot and MS analysis of distal (A) and proximal (B) mucosal contents of mouse intestinal samples. The bands recognized by two different antibodies were analysed by MS for the presence of DAAO: the peptides identified are reported (right side). The sequence belonging to the antimicrobial peptides are shown in bold.

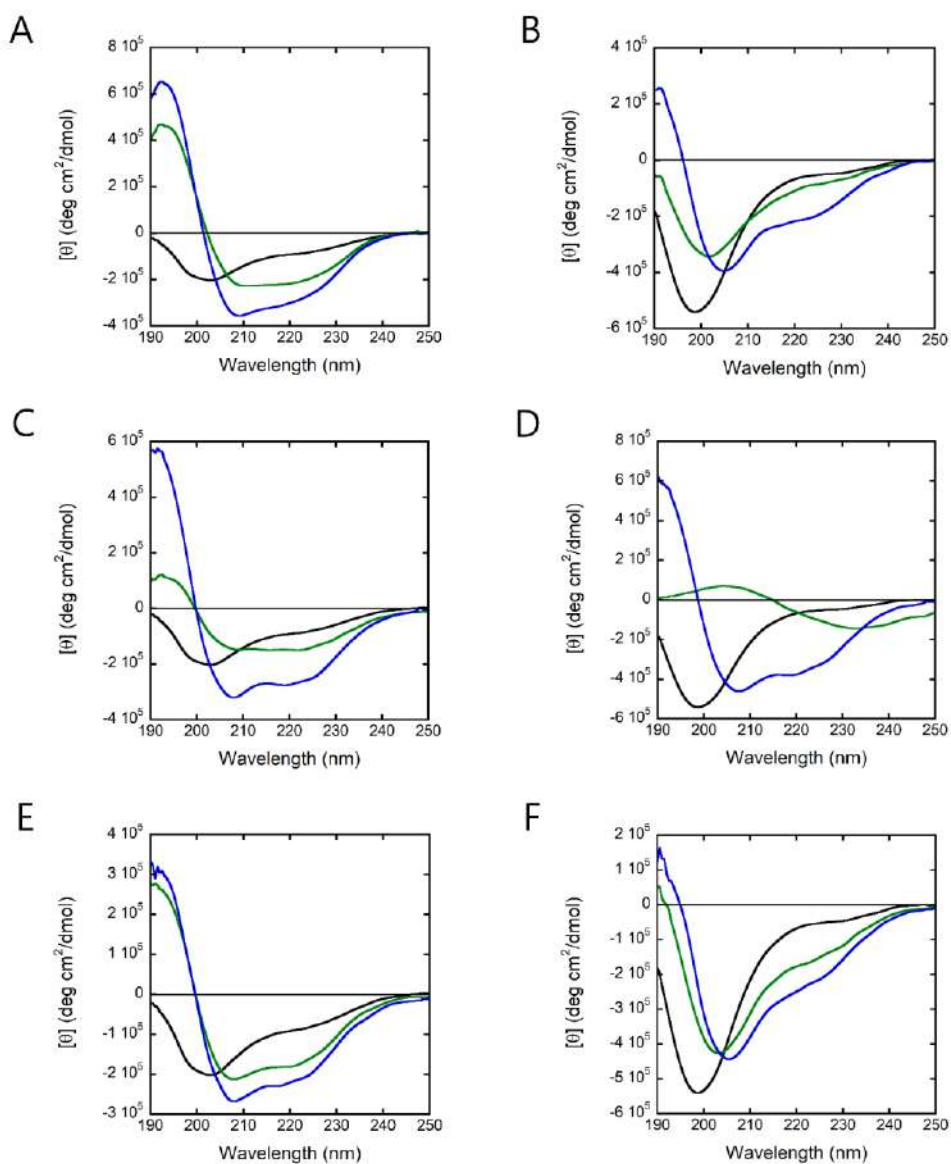


Fig. 4. Comparison of far-UV CD spectra of DAAO antimicrobial peptides: GLT (A, C, E) and IWK (B, D, F) peptides (0.1 mg/mL, black) in the presence of: (A, B) 0.1 and 1 mM SDS (green and blue, respectively); (C, D) of 5 and 30% TFE (green and blue, respectively), (E, F) 0.1 and 0.25 mg/mL LPS (green and blue respectively). In green is shown the spectrum at the lowest concentration added during the titration; in blue is reported the spectrum at the concentration at which the peptides show secondary structure.

Table 1: Schematic recognition pattern obtained using different antibodies in Western blot analyses on mouse intestinal tissues (see Suppl. Data 4). The bands indicated in bold have been analyzed by MS: the underlined samples contain DAAO-derived peptides (see Fig. 3).

Model	MW (kDa)	α -hDAAO-Nterm (DaBio)		α -hDAAO-Cterm (DaBio) [α -mDAAO-Cterm (Santa Cruz)]	
Mouse wild-type	100			mucosal distal	*
	70			mucosal proximal mucosal medial mucosal distal epithelial layer (proximal, medial, distal)	** ***** ** *
	55	mucosal (proximal, medial, distal)	*	[mucosal distal] [mucosal proximal]	[**] [***]
	45	epithelial proximal epithelial (medial, distal)	** *	epithelial layer (proximal, medial, distal)	*
	40	<u>mucosal distal</u> luminal medial, proximal luminal distal	** */** ***	<u>mucosal distal</u> luminal (proximal, medial, distal)	** */**
	~ 35	<u>mucosal proximal</u> mucosal medial luminal proximal luminal medial	**/** */** ** *	epithelial layer (proximal, medial, distal) [mucosal distal, proximal]	* [**]
	27			<u>mucosal proximal</u> <u>mucosal distal</u>	**/**/[**] ***/***/[**]
	20	epithelial layer proximal epithelial layer (medial, distal)	*** *		
	18	epithelial layer distal	***	mucosal (proximal, distal)	*

	15	epithelial layer (proximal, medial, distal)	*		
Mouse DAAO-/-	70				epithelial proximal *
	55				[mucosal proximal, distal] [**]
	45	mucosal distal	*		epithelial layer (proximal, medial, distal) *
	40	mucosal distal mucosal proximal	* *		
	~ 35	mucosal proximal mucosal distal	* *		mucosal distal [mucosal proximal] ***/[*] [*]
	27	mucosal distal epithelial layer proximal	* ***		[mucosal proximal] [mucosal distal] [*] [***]
	18	mucosal distal	*		
	15	mucosal distal	*		

Relative amount:

* < 0.1 ng DAAO/μg total proteins

** 0.1-0.5 ng DAAO/μg total proteins

*** 0.5-1 ng DAAO/μg total proteins

**** > 1 ng DAAO/μg total proteins

Table 2: Antimicrobial activity expressed as MIC and MBC values of two putative CAMPs derived from mouse DAAO.

Bacterial strain	Peptide/Antibiotic	MIC (μM)	MBC (μM)	MBC/MIC	Bactericidal activity	Bacteriostatic activity	MIC ($\mu\text{g/mL}$)
Gram-negative							
<i>Pseudomonas aeruginosa</i> PAO1	IWK	25	50	2	x		
	GLT	100	>100	-			
	IWK+GLT	12.5	50	4	x		
	Polymyxin B						0.25
<i>Acinetobacter baumannii</i> ATCC 17878	IWK	12.5	12.5	1	x		
	GLT	50	50	1	x		
	IWK+GLT	12.5	25	2	x		
	Polymyxin B						0.5
<i>Escherichia coli</i> ATCC 25922	IWK	12.5	12.5	1	x		
	GLT	50	>100	-			
	IWK+GLT	12.5	100	8		x	
	Polymyxin B						0.5
<i>Salmonella typhimurium</i> ATCC 14028	IWK	25	50	2	x		
	GLT	25	>100	>4		x	
	IWK+GLT	6.25	100	16		x	
	Polymyxin B						0.12
<i>Salmonella enteritidis</i> 706 RIVM	IWK	100	-	-			
	GLT	100	-	-			
	IWK+GLT	50	-	-			
	Polymyxin B						0.5
Gram-positive							
<i>Staphylococcus aureus</i> ATCC 6538P	IWK	25	50	2	x		
	GLT	>100	-	-			
	IWK+GLT	25	50	2	x		
	Vancomycin						0.5
<i>Enterococcus faecalis</i> ATCC 29212	IWK	12.5	>100	>4		x	
	GLT	6.25	>100	>4		x	
	IWK+GLT	3.12	>100	>4		x	
	Vancomycin						2

Table 3. Minimum inhibitory concentration (MIC) values of DAAO-derived antimicrobial peptides on Lactobacilli determined by the microdilution method.

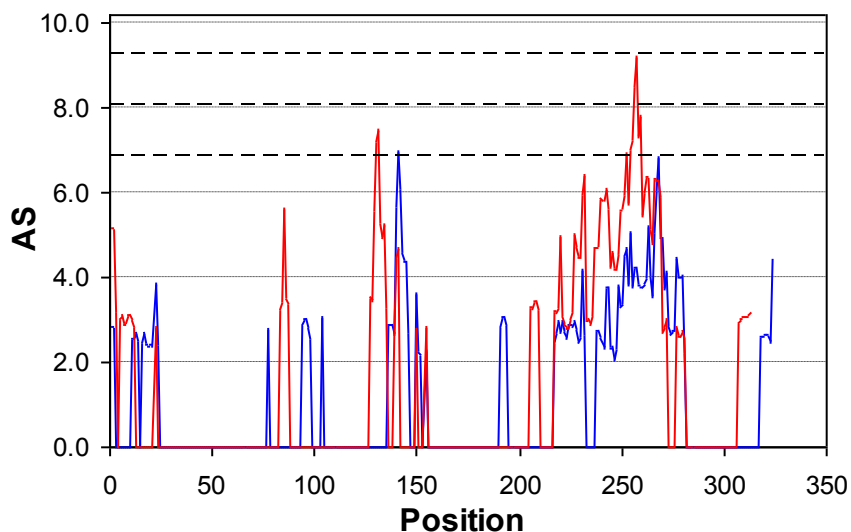
MIC (μM)				
	<i>L. fermentum</i> ATCC 14931	<i>L. casei</i> ATCC 393	<i>L. rhamnosus</i> ATCC 7469	<i>L. acidophilus</i> ATCC 4356
IWK	> 110	> 110	> 110	> 110
GLT	> 100	> 100	> 100	> 100
Erythromycin	1.4	2.8	0.7	0.7
Vancomycin	> 100	> 100	> 100	> 100

Supplemental Data 1. In silico analysis of DAAO sequences

Suppl. Table 1: Prediction of N-terminal signal sequence for secretion in DAAOs from different sources.

	SignalP 3.0	SignalP 4.1	SecretomeP 2.0	Signal-3L	Signal-3L 2.0
Human	0.749	0.447	0.782	yes	no
Mouse	0.700	0.415	0.693	yes	yes
Rat	0.699	0.415	0.685	yes	yes
Porcine	0.756	0.455	0.667	yes	no

Cutoff values: 0.430 for SignalP 3.0; 0.450 for SignalP 4.1; 0.600 for SecretomeP 2.0



Suppl. Fig. 1. Sliding window analysis of mouse DAAO sequence. AS values were calculated using parameters optimized for *S. aureus* strain C623 and the hydrophobicity scale “Parker-Arg0”. Plots were obtained using window lengths of 22 (blue line) and 33 residues (red line). Dotted lines indicate AS values corresponding approximately to hypothetical MIC values of 100 (bottom), 10 and 1 (top) μM.

Supplementary Data 2. Production of $\Delta 1-16$ DAAO

Suppl. Table 2: Comparison of the best fermentation conditions used for the expression of the wild-type and deleted variant of hDAAO (and for co-expression).

Conditions	hDAAO variant		
	$\Delta 1-16$	$\Delta 1-16$ /wild-type	wild-type
Strain	BL21 (DE3) Star	BL21 (DE3) pLysS	BL21 (DE3) Star
Cultivation broth	TB	LB	TB
IPTG (mM)	0.1	1	0.1
Temperature after induction ($^{\circ}\text{C}$)	25	37	37
Time of cell collection after induction (h)	6	3	4
OD _{600nm} at induction	0.8	0.6	8
Expression level (mg/L) in the crude extract	2.1	0.8	7

Suppl. Table 3: Purification trials for $\Delta 1-16$ hDAAO and for His-hDAAO wild-type/hDAAO $\Delta 1-16$ -strep tag.

	pET11b-hDAAO($\Delta 1-16$) (no tag)	pETDuet-His-hDAAO wild-type/strep-hDAAO($\Delta 1-16$)
Type	Ion-exchange chromatography	Affinity chromatography
Column/Resin	Anionic and cationic (DEAE, SP FF, Q FF)	HiTrap chelating (Ni^{2+}), Strep-trap
Buffer	Tris, BisTris-propane, MES	Na pyrophosphate, PBS, Tris
pH	6, 8, 8.7, 9.2	7.2, 7.4, 8.0

Supplementary Data 3. Western blot analyses of rat intestine samples

As summarized in Suppl. Table 4, different bands were recognized by anti-N-terminal and anti-C-terminal hDAAO antibodies in rat tissues. In details, two bands at a molecular mass higher than wild-type DAAO have been recognized by the anti-N-terminal hDAAO antibody, namely at 100 and 55 kDa, which are apparent in both mucosal and luminal layers: these bands most likely should correspond to aspecific signals. Both the antibodies recognized a band at 40 kDa, but in different samples. Indeed, the anti-N-terminal antibody recognized bands at 35, 25 and ~ 10 kDa while the anti-C-terminal antibody recognized bands at 30 and 20 kDa that most likely derived from elimination of an N-terminal region. Notably, the fragments of > 25 kDa mass should be recognized by both antibodies but this was not observed. Altogether, the employed antibodies seem to detect aspecific signals in rat intestinal samples.

Suppl. Table 4: Schematic recognition pattern obtained using different antibodies in Western blot analyses on rat intestinal tissues.

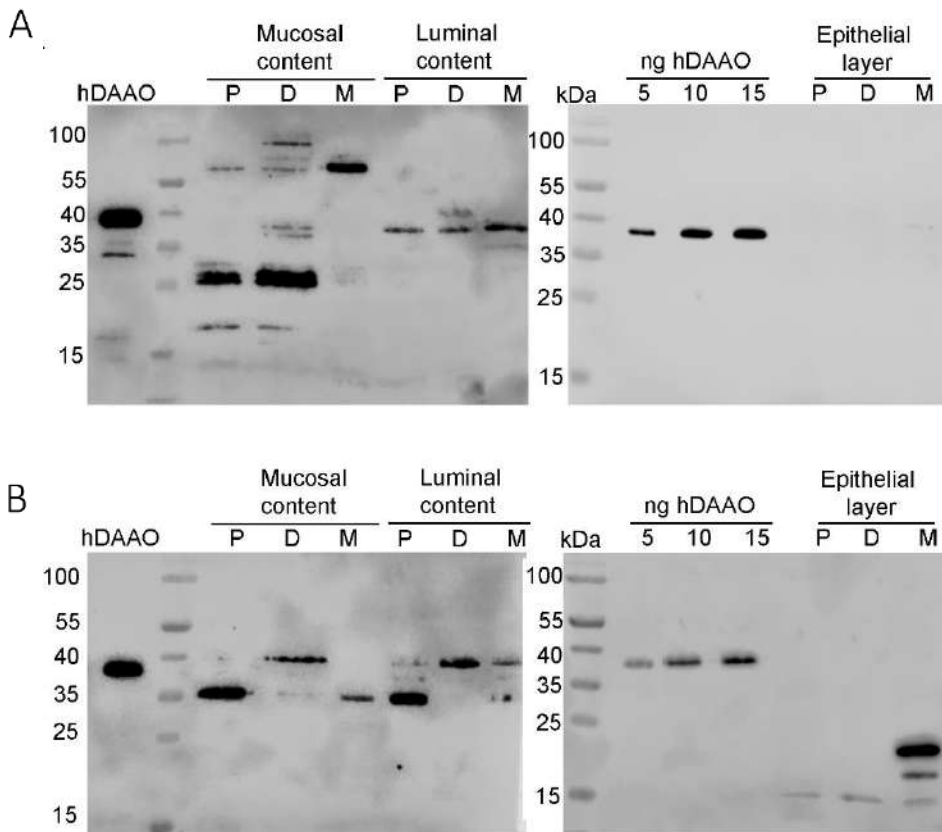
MW (kDa)	α -hDAAO-Nterm (DaBio)		α -hDAAO-Cterm (DaBio)	
100	mucosal (proximal, medium, distal)	**		
	luminal proximal	***		
	luminal medial	*		
55	mucosal distal	**		
	mucosal proximal	***		
~ 40	mucosal (proximal, medial, distal)	**/**	EP layer medial	*
~ 35	luminal distal	**		
30			mucosal (proximal, medium, distal)	**
			luminal distal	*
			EP layer distal	*
25	mucosal distal	**		
	mucosal proximal	**		
20			mucosal medial	**
~ 10	mucosal proximal	**		
	luminal proximal	****		
	luminal medium	**		

Relative amount:

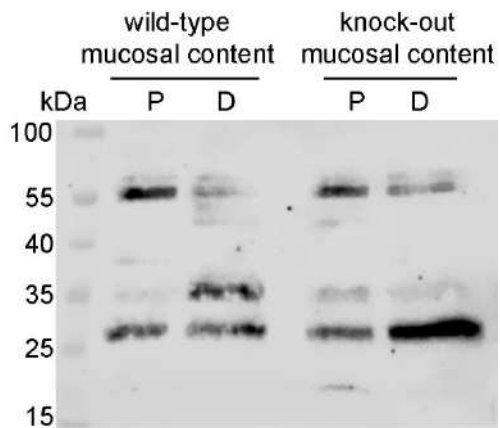
* < 0.1 ng DAAO/ μ g total proteins

** 0.1-0.5 ng DAAO/ μ g total proteins
*** 0.5-1 ng DAAO/ μ g total proteins
**** > 1 ng DAAO/ μ g total proteins

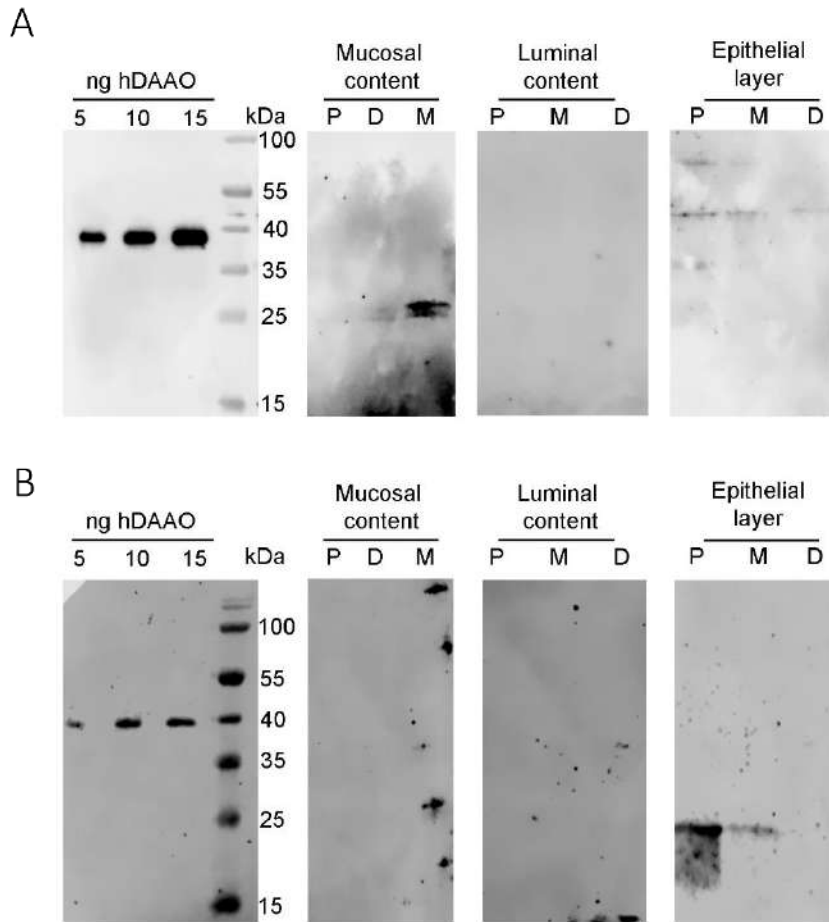
Supplementary Data 4. Western blot analyses of mouse intestine samples



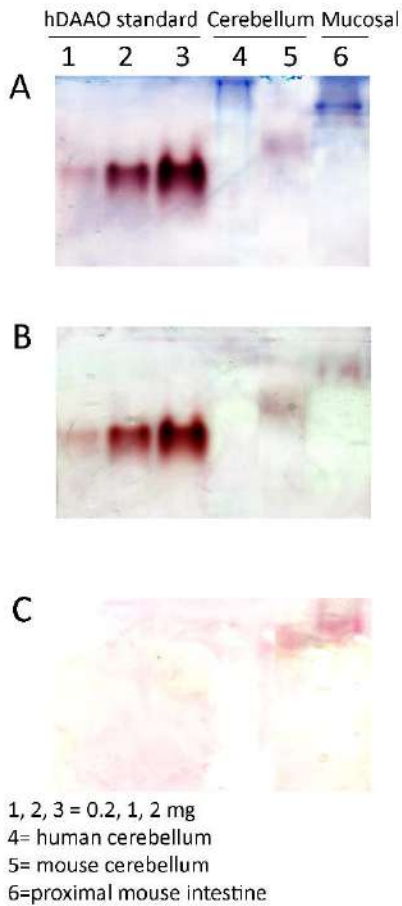
Supplementary Fig. 2. Western blot analysis of mouse intestine samples using anti-C-terminal (panel A) or anti-N-terminal hDAAO antibodies (panel B). In each lane an amount corresponding to 30 μ g of total proteins was loaded.



Supplementary Fig. 3. Western blot analysis of proximal and distal mucosal samples from wild-type or $\text{DAAO}^{-/-}$ mice using an anti-C-terminal mDAAO antibody. In each lane an amount corresponding to 40 μg of total proteins was loaded.



Supplementary Fig. 4. Western blot analysis of DAAO^{-/-} mouse intestine samples using anti-C-terminal (panel A) or anti-N-terminal hDAAO antibodies (panel B). In each lane an amount corresponding to 40 μg of total proteins was loaded.



Suppl. Fig. 5. Coomassie (A) and native-PAGE (B) of proximal mucosal sample (lane 6). Different amount of recombinant hDAAO was used as reference (0.2, 1 and 2 μ g, corresponding to lanes 1, 2 and 3, respectively). Human (lane 4) and mouse (lane 5) cerebellum was used as positive control. The specificity of the activity signal observed was verified using the specific DAAO inhibitor CBIO (C).

4. Discussion

D-amino acid oxidase (DAAO, EC 1.4.3.3) is a peroxisomal, hydrogen peroxide-generating flavoenzyme which catalyzes the degradation of uncharged D-AAAs (Pollegioni et al., 2007; Saitoh et al., 2012). DAAO plays different roles in several organisms: in mammals, the flavoenzyme is mainly expressed in kidney, liver, and brain (Pollegioni et al., 2007). In the first two organs it plays a detoxifying role by catabolizing exogenous D-AAAs, while in the latter one DAAO degrades D-Ser, which acts as co-agonist of glutamate by binding to the “strychnine-insensitive glycine modulatory site” of NMDAR: in the brain, D-Ser plays a key role in main physiological processes such as synaptic plasticity, learning and memory (Mothet et al., 2000). The glycine modulatory site is not saturated under normal conditions, thus, even small alterations in D-Ser concentration may affect NMDAR functionality.

A model of D-Ser metabolism, the “serine shuttle model” (Wolosker, 2011) proposes that this neuromodulator is synthesized in neurons by the PLP-dependent enzyme serine racemase (SR) that can also degrade the D-AA. D-Ser is then released by neurons and taken up by astrocytes. Considering the low levels of SR in astrocytes, DAAO should play a key role in D-Ser catabolism in these cells. Indeed, the flavoenzyme activity, through the regulation of D-Ser cellular levels (and release), may affect the NMDAR-dependent physiological functions. A relationship between D-Ser signaling deregulation, NMDAR dysfunction and CNS diseases is presumed (Billard, 2008). In particular, decreased concentration of synaptic D-Ser, which induces a hypoactivation of NMDAR, has been associated to psychiatric disorders, such as schizophrenia and bipolar disorder (Verrall et al., 2007; Madeira et al., 2008; Collingridge et al., 2013). On the other hand, an increase in D-Ser levels is responsible of hyperactivation of NMDAR and induces excitotoxicity: it has been related to the onset of neurodegenerative diseases, such as amyotrophic lateral sclerosis, ALS (Wolosker et al., 2008). Actually, the substitution of R199 with a tryptophan in hDAAO has been correlated to familial ALS (Mitchell et al., 2010).

In 2006, the recombinant human DAAO (hDAAO) was expressed in *E. coli* and purified as active holoenzyme and the crystallographic structure was solved

(Kawazoe et al., 2006; Molla et al., 2006). hDAAO exhibits the well-known properties of FAD-containing flavooxidases: it stabilizes the anionic semiquinone species, it is able to covalently bind sulfite, it is fully converted into the reduced form in anaerobic conditions and in the presence of the substrate, a form which is highly reactive with oxygen (Curti et al., 1992; Molla et al., 2006).

However, the human enzyme shows some peculiar features that distinguish it from other DAAOs: i) hDAAO shows a head-to-head mode of monomer-monomer interaction and it is a dimer in both apoprotein and holoenzyme forms. The stable mode of interaction between monomers is due to the composition of the region located at the interface of the two subunits, which, differently from all other DAAOs, is negatively charged (Kawazoe et al., 2007; Kawazoe et al., 2006; Molla et al., 2006); ii) the human enzyme binds FAD very weakly (the K_d value is the highest among known DAAOs): the sole difference between human and pig DAAOs is the conformation of the 47-VAAGL-51 hydrophobic stretch, which, in the previous enzyme is shifted away from the FAD. Due to the low cofactor binding affinity, a significant fraction of hDAAO is present in solution as inactive apoprotein that shows a more “relaxed” and less stable conformation. The addition of exogenous FAD protects the enzyme from proteolytic cleavage, suggesting that binding or dissociation of the cofactor might represent a mechanism regulating hDAAO activity. Notably, the presence of a ligand in the active site induces an increase in the cofactor binding affinity (Kawazoe et al., 2006; Kawazoe, et al., 2007; Caldinelli et al., 2010); iii) the activity and the half-life of hDAAO are affected by pLG72 binding (Sacchi et al., 2008; Pollegioni et al., 2018).

Despite the key role played by hDAAO in some important physiological processes, much remains to be unraveled concerning the modulation of its functional properties. This PhD project was aimed to deep into the characterization of hDAAO.

At first, we focused on determination of the biochemical properties of hDAAO. At conditions resembling the physiological ones (37 °C, pH 7-8),

hDAAO is stable but not fully active: since the peroxisomal pH value is between 7.1 and 8.2 (Jankowski et al., 2001), the enzyme activity represents 70% of its maximal value. Moreover, we studied the effect of various divalent ions and/or nucleotides (Ca^{2+} , Mg^{2+} , ATP and GTP) on the functional and structural properties of hDAAO. These molecules are present at significant levels in the brain and are involved in the regulation of D-Ser metabolism: indeed, it has been shown that the oligomeric state and the activity of serine racemase are influenced by divalent cations like calcium, magnesium and manganese, as well as by nucleotides like ATP, ADP or GTP. (Baumgart and Rodriguez-Crespo., 2008; Bruno et al., 2017). However, the DAAO activity is not affected by these molecules, which also alter to a slight extent its secondary structure.

The substrate specificity profile of hDAAO was clarified: the human enzyme prefers hydrophobic amino acids. Interestingly, some DAAO substrates are molecules playing a role in neurotransmission. D-cysteine seems the best substrate. It could represent the physiological substrate of DAAO in specific tissues: in brain and kidney, it was recently proposed to be converted to H_2S by DAAO and 3-mercaptopyruvate sulfurtransferase (Shibuya et al., 2013). Also, DOPA is a relevant molecule in neurotransmission: the oxidation of this substrate by hDAAO is confirmed. Some discrepancies with previous results are apparent: hDAAO shows on D-DOPA the highest apparent k_{cat} value, but the apparent substrate affinity and inhibition are lower than those reported by (Kawazoe et al., 2007). L-DOPA does not compete with the D-form for the binding to the hDAAO active site, while other L-amino acids can bind the active site of the enzyme, although with a very low efficiency (L-Ser shows a $K_i = 26.2$ mM vs. a physiological concentration of 0.1 mM).

The binding of substrate competitive inhibitors was determined following the quenching of protein fluorescence. The K_d value for CBIO is similar to the K_d , IC_{50} and K_i values reported in literature (Ferraris et al., 2008). Notably, for benzoate a biphasic binding process is apparent pointing to the presence of two different protein conformations in equilibrium (with different affinity for the ligand) or of two different binding pockets for benzoate (as reported in

Kohiki et al., 2017) (Fig. 9A), suggesting that a ligand bound in the second pocket located at protein interface could influence the structural and functional properties of the active site.

Concerning flavin binding, it has been previously demonstrated that the interaction between the apoprotein and FAD is stabilized by an active site ligand (Caldinelli et al., 2010; Molla et al., 2006) boosting the holoenzyme reconstitution process (Figure 17).

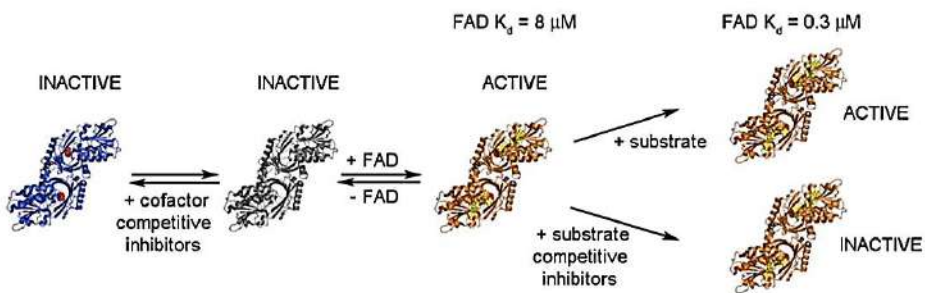


Figure 17. Scheme of the different forms of hDAAO observed *in vitro* and effect of several molecules on hDAAO structure.

Here, we demonstrated that in solution hDAAO apoprotein exists in two alternative conformations with different affinity for the cofactor: the equilibrium is shifted towards the one at higher affinity by the presence of an active site ligand. The presence of the competitive inhibitor benzoate favors the conformation at higher affinity for the flavin cofactor, reaching a K_d value like that of rat or pig DAAOs (Frattini et al., 2011). Altogether, these findings suggest that the binding of an active site ligand could represent a mechanism for the regulation of the enzyme activity: the free enzyme, largely present in solution as inactive apoprotein, is rapidly turned into the active holoenzyme in the presence of the substrate (Figure 18). Thus, at physiological level, the presence of the substrate itself should push the formation of the active holoenzyme, a way to finely regulate its concentration.

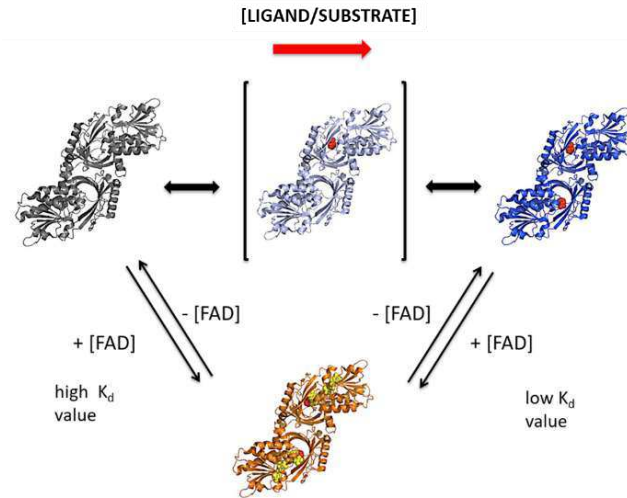


Figure 18. Scheme of the different conformations of hDAAO apoprotein observed *in vitro*.

Subsequently, the investigations focused on the effect of single positions in the functionality of the enzyme. In previous studies the role of D31, R199, W209, R279 and G331 related to known SNPs were studied (Caldinelli et al., 2013; Cappelletti et al., 2015). These hDAAO variants were classified into two classes, based on their biochemical properties and on their effect on hDAAO functionality: i) hypoactive and ii) hyperactive (Sacchi et al., 2018). Here, we focused on G183R hDAAO variant, the human counterpart of the natural single-base mutation (yielding the G181R substitution) that in ddY mice inactivates the enzyme, yielding an increased D-Ser concentration and consequent altered NMDAr functions (Labrie et al., 2010). This mouse model was used to perform behavioral tests, which concur to clarify the role of DAAO in the mechanisms related to NMDAr transmission. Despite this, no characterization of the protein variant and of the way by which G181R substitution impacts on the enzyme functionality was carried out. Thus, we introduced the corresponding substitution in human DAAO and investigated the main properties of the protein variant. The recombinant G183R hDAAO variant was expressed in *E. coli* and fully purified as inactive apoprotein. Also after an extensive dialysis to push the reconstitution of the holoenzyme, the

recombinant G183R variant resulted inactive. The substitution of G183 resulted in a significant alteration in the binding to the cofactor in presence of an active site ligand: the arginine in position 183, located close to the cofactor, might create new interactions with surrounding residues, negatively affecting the ability to bind FAD in the correct orientation for the catalysis.

Notably, when expressed in the U87 cell line, G183R hDAAO is not fully targeted to peroxisomes and forms protein aggregates showing a strong colocalization with ubiquitin. According to its impaired activity, its overexpression significantly (7-fold) increases D-Ser cellular concentration, although did not result in enhanced apoptosis. These results warn about the use of mice lacking DAAO activity because of the G181R single point mutation. The consequence of this substitution in DAAO are complex and possibly misleading: the effects due to impairment of D-Ser degradation overlaps with the ones related to aggregates accumulation.

Moreover, we focused on the role of R120, a residue located at protein interface and thus putatively affecting the oligomerization state. Indeed, R120 has been also proposed to play a role in ligand and FAD binding: the overlay of the structures of hDAAO (in complex with benzoate, imino-DOPA, imino-serine and the substrate-free) did not show any difference in the conformations of the residues of the putative second binding-site, pointing to the side chain of R120 in the structure of hDAAO in complex with benzoate as the only difference. Moreover, R120 belongs to a NTS that, after phosphorylation, might activate the translocation of the protein to the nucleus (TPx sequence; in rat DAAO this signal is 117-TPS-119 corresponding to the 118-TPR-120 sequence in the human enzyme) (Chuderland et al., 2008; Luks et al., 2017). Indeed, it has been recently suggested that rat DAAO is present in both cytosol and nucleus of proximal tubule epithelial cells following treatment with the drug propiverine (Luks et al., 2017). Thus, two variants at position 120 (R120E and R120L) were designed and characterized to mimic the activation of NTS and to verify the involvement of this residue in ligand binding process and enzyme functionality.

The R120 hDAAO variants, produced as soluble holoenzymes, possess an altered tertiary structure. In particular, the R120E variant shows a significant alteration of the near-UV CD and fluorescence spectra, suggesting a change in the exposure of aromatic residues. Moreover, for both the R120E and R120L variants, a significant decrease in T_m was observed, pointing to an alteration in protein flexibility. Structural data indicated that the substitution of R120 alters the electrostatic interactions with the facing residues on the other monomer, without affecting the oligomerization state of the protein, always present in solution as a dimer. Concerning the kinetic properties, while both the variants show a 2-fold higher kinetic efficiency than the wild-type enzyme for D-Ala (due to a higher k_{cat}), the kinetic efficiency on D-Ser is similar to the value reported for the wild-type enzyme. Considering the level of D-Ser in the brain (0.3 mM) and in kidney (0.14 mM) (Hashimoto et al., 1993; Huang et al., 1998), R120 hDAAO variants show a low ability to degrade D-Ser, as the *wild-type* enzyme is. This could be a way to finely tune D-Ser concentrations, avoiding an excessive degradation. Concerning D-Cys, the R120L variant shows an increased k_{cat} value, resulting in a slightly higher kinetic efficiency for this substrate. Interestingly, at high D-Cys concentration an inhibition effect is apparent for both the variants, which is absent for the wild-type hDAAO (the *in vivo* concentration of this D-amino acid is approximately 0.2 mM) (Stipanuk et al., 2006). The substitution of R120 does not alter the ability to bind classical hDAAO inhibitors, thus excluding a connection between R120 and the binding process related to the second putative ligand binding site.

The most relevant change following the R120 substitution is the tighter binding of FAD. R120 hDAAO variants exist in solution in two apoprotein forms, with the first one showing a K_d for the flavin cofactor 10-fold lower than the wild-type enzyme. Moreover, and differently from the wild-type counterpart, the presence of an active site ligand does not favour the apoprotein form at higher affinity: FAD binding to R120 hDAAO variants is biphasic both in the absence and in the presence of benzoate. The activity values at low FAD and D-Ser concentrations (resembling the physiological

conditions) for R120 hDAAO variants are similar to those of the wild-type enzyme, probably because of the higher K_m for this substrate.

Altogether, R120 hDAAO variants can be classified among the hyperactive hDAAO variants group, showing an improved catalytic efficiency and FAD affinity (Sacchi et al., 2018). The alterations related to R120 substitution seem to be due to the structure-function relationships of the specific region close to the interface between monomers. Actually, the properties of R120 hDAAO variants resemble those of W209R hDAAO (SNP rs11347906) (Cappelletti et al., 2015): W209 is also located at the monomer-monomer interface, is part of the second (putative) binding site (Kohiki et al., 2017), and its substitution results in an increased activity on D-Ala and a tighter FAD binding, with no change in ligand binding properties.

Immunolocalization analysis on U87 glioblastoma cells transiently transfected for R120 variants revealed that R120 substitution alters the subcellular localization of the enzyme: the substitution of R120 favors the mistargeting to the nucleus, in particular in the presence of a glutamate at position 120. Moreover, R120 hDAAO variants also shows an increased propensity to form cytosolic aggregates. Interestingly, the expression of hDAAO variants at position R120 does not alter cell viability, suggesting that the mistargeted (nuclear) variants should be inactive, e.g. for the absence of the substrate. This is a relevant observation since the oxidative stress induced by H_2O_2 generated by hDAAO reaction would lead to cell death by inducing DNA fragmentation and telomeric damage by oxidizing nucleobases and cleaving sugar-phosphate backbone (Richter-Landsberg & Vollgraf, 1998; Veal et al., 2007; Coluzzi et al., 2014).

Notably, also SR was previously demonstrated to be mistargeted to the nucleus and inactivated under stress conditions (Kolodney et al., 2015), suggesting that the nuclear translocation of the enzymes related to D-Ser metabolism may represent an elegant regulation mechanism of this D-AA levels.

Despite the fact that DAAO has always been considered a peroxisomal protein, recently its localization has held some surprises: in addition to its presence at the cytosolic, nuclear and extrasynaptic levels (Sacchi et al., 2008; Popiolek et al., 2011; Luks et al., 2017), DAAO protein and activity were previously detected in the epithelium of proximal and middle small intestine of mice and humans (Sasabe et al., 2016). Indeed, it has been proposed that the flavoenzyme might play a role in controlling the homeostasis of gut microbiota through the production of H₂O₂ (Sasabe et al., 2016). A 37 kDa processed form of the protein appeared to be secreted in the lumen by goblet cells, due to the presence of a signal peptide and a predicted cleavage site near the N-terminus (Sasabe et al., 2016). However, despite bioinformatic analyses by several softwares confirm the presence of the putative signal peptide, the fact that it belongs to the Rossmann fold motif, which contains the Wierenga sequence (GxGxxG) required for cofactor binding, suggests that the processed enzyme might not be folded and active. Indeed, the molecular dynamics simulations indicate that the overall structure of the variant lacking the N-terminal sequence should be less stable than the full-length enzyme.

The experiments on the recombinant hDAAO variant confirm the computational analysis, showing that the enzyme form lacking the residues from 1 to 16 is unstable and inactive; accordingly, the presence of an active enzyme in the lumen requires a hDAAO possessing the N-terminal sequence required for cofactor binding and essential for the activity. Notably, a recent assay of DAAO activity in mice tissues did not identify any enzymatic activity in small intestine (whole as well as proximal, middle and distal fractions) (Kim et al., 2019). These evidences do not exclude that an alternative secretion pattern should be active for hDAAO.

The analysis of the primary sequence of the enzyme by a specific *in silico* tool suggests the presence of two potential cryptic antimicrobial peptides, pointing to an alternative mechanism of action of hDAAO in the gut, not based on hDAAO-produced H₂O₂. In order to clarify this issue (and the putative secretion pattern) Western blot analyses were performed on small

intestine samples from rat and mouse using different antibodies. By using three commercial anti-hDAAO antibodies, bands at different mass values were recognized, largely due to unspecific recognition. Actually, bands at 40, 35 and 27 kDa were observed in the mucosal and luminal content of mouse small intestine using anti-N-terminal and anti-C-terminal hDAAO antibodies. MS analysis detected the presence of hDAAO-derived peptides in the 40 and 27 kDa bands, suggesting the presence of a processed form of the enzyme in the latter band. The same analysis were performed on DAAO^{-/-} mice tissues as a negative control: again bands at 40, 35 and at lower molecular mass were apparent, but MS analysis did not identify DAAO-generated peptides. Notably, the two peptides corresponding to the putative antimicrobial sequences inside DAAO sequence (namely ²⁵⁷IWKSCCKLEPTLKNARIVGELTGFRPVRPQVRL²⁸⁹ and ³¹³GLTIHWGCAMEAANLFGKILEEKLSRLPPSHL³⁴⁵) were found to be able to assume a secondary structure in presence of membrane-mimic detergents and LPS from *E. coli* and showed antibacterial and bactericidal activity on both Gram-positive and Gram-negative pathogenic bacteria, but not on *Lactobacilli species*, which represent the commensal microbiota. These results point to the ability of hDAAO to select the gut microbiota mainly by generating antibacterial peptides following extracellular proteolytic digestion.

In conclusion, these studies demonstrate that hDAAO activity is finely tuned through ligand/flavin binding. The subcellular targeting of hDAAO also seems a way to modulate hDAAO functionality. If the flavoenzyme is active in the nucleus and whether hDAAO mistargeting is related to specific pathological states or involved in physiological processes is still unknown and should be clarified. These modulations allow hDAAO to fulfil different physiological functions, such as the control of D-Ser levels in the brain and of other D-AAAs in different tissues or the selection of microbiota in the gut.

A main issue that remain to be clarified is the mechanism of antibacterial peptides production and their physiological relevance. A system that can

reproduce the intestinal conditions will be required to investigate the secretion of the flavoenzyme, the generation of AMPs and their efficacy. A full elucidation of the regulation mechanisms of this human flavoenzyme, especially related to its role in different tissues, will allow the understanding of important physiological processes as well as the development of novel targeted therapies to relevant human diseases.

References

Abe K, Kimura H. The possible role of hydrogen sulfide as an endogenous neuromodulator. *J Neurosci*. 1996 Feb 1; 16(3):1066-71.

Adage T, Trillat AC, Quattropani A, Perrin D, Cavarec L, Shaw J, Guerassimenko O, Giachetti C, Gréco B, Chumakov I, Halazy S, Roach A, Zaratin P. In vitro and in vivo pharmacological profile of AS057278, a selective D-amino acid oxidase inhibitor with potential anti-psychotic properties. *Eur Neuropsychopharmacol*. 2008 Mar; 18(3):200-14

Anderson LL. Discovery of the 'porosome'; the universal secretory machinery in cells. *J Cell Mol Med*. 2006 Jan-Mar; 10(1):126-31.

Audagnotto M, Dal Peraro M. Protein post-translational modifications: In silico prediction tools and molecular modeling. *Comput Struct Biotechnol J*. 2017 Mar 31; 15:307-319.

Baumgart F, Rodríguez-Crespo I. D-amino acids in the brain: the biochemistry of brain serine racemase. *FEBS J*. 2008 Jul; 275(14):3538-45.

Billard JM. D-serine signalling as a prominent determinant of neuronal-glia dialogue in the healthy and diseased brain. *J Cell Mol Med*. 2008 Oct; 12(5B):1872-84.

Billard JM. Changes in Serine Racemase-Dependent Modulation of NMDA Receptor: Impact on Physiological and Pathological Brain Aging. *Front Mol Biosci*. 2018 Nov 28;5:106.

Birolo L, Sacchi S, Smaldone G, Molla G, Leo G, Caldinelli L, Pirone L, Eliometri P, Di Gaetano S, Orefice I, Pedone E, Pucci P, Pollegioni L. Regulating levels of the neuromodulator d-serine in human brain: structural insight into pLG72 and D-amino acid oxidase interaction. *FEBS J*. 2016 Sep; 283(18):3353-70.

Bruno S, Margiotta M, Marchesani F, Paredi G, Orlandi V, Faggiano S, Ronda L, Campanini B, Mozzarelli A. Magnesium and calcium ions differentially affect human serine racemase activity and modulate its quaternary equilibrium toward a tetrameric form. *Biochim Biophys Acta Proteins Proteom*. 2017 Apr; 1865(4):381-387.

Burnet PW, Eastwood SL, Bristow GC, Godlewska BR, Sikka P, Walker M, Harrison PJ. D-amino acid oxidase activity and expression are increased in schizophrenia. *Mol Psychiatry*. 2008 Jul; 13(7):658-60.

Caldinelli L, Molla G, Bracci L, Lelli B, Pileri S, Cappelletti P, Sacchi S, Pollegioni L. Effect of ligand binding on human D-amino acid oxidase: implications for the development of new drugs for schizophrenia treatment. *Protein Sci*. 2010 Aug; 19(8):1500-12.

Caldinelli L, Sacchi S, Molla G, Nardini M, Pollegioni L. Characterization of human DAAO variants potentially related to an increased risk of schizophrenia. *Biochim Biophys Acta*. 2013 Mar; 1832(3):400-10.

Cappelletti P, Campomenosi P, Pollegioni L, Sacchi S. The degradation (by distinct pathways) of human D-amino acid oxidase and its interacting partner pLG72--two key proteins in D-serine catabolism in the brain. *FEBS J*. 2014 Feb; 281(3):708-23.

Cappelletti P, Piubelli L, Murtas G, Caldinelli L, Valentino M, Molla G, Pollegioni L, Sacchi S. Structure-function relationships in human D-amino acid oxidase variants corresponding to known SNPs. *Biochim Biophys Acta*. 2015 Sep; 1854(9):1150-9.

Chuderland D, Konson A, Seger R. Identification and characterization of a general nuclear translocation signal in signaling proteins. *Mol Cell*. 2008 Sep 26; 31(6):850-61.

Chumakov I, Blumenfeld M, Guerassimenko O, Cavarec L, Palicio M, Abderrahim H, Bougueleret L, Barry C, Tanaka H, La Rosa P, Puech A, Tahri N, Cohen-Akenine A, Delabrosse S, Lissarrague S, Picard FP, Maurice K, Essioux L, Millasseau P, Grel P, Debailleul V, Simon AM, Caterina D, Dufaure I, Malekzadeh K, Belova M, Luan JJ, Bouillot M, Sambucy JL, Primas G, Saumier M, Boubkiri N, Martin-Saumier S, Nasroune M, Peixoto H, Delaye A, Pinchot V, Bastucci M, Guillou S, Chevillon M, Sainz-Fuertes R, Meguenni S, Aurich-Costa J, Cherif D, Gimalac A, Van Duijn C, Gauvreau D, Ouellette G, Fortier I, Raelson J, Sherbatich T, Riazanskaia N, Rogaev E, Raeymaekers P, Aerssens J, Konings F, Luyten W, Macchiardi F, Sham PC, Straub RE, Weinberger DR, Cohen N, Cohen D. Genetic and physiological data implicating the new human gene

G72 and the gene for D-amino acid oxidase in schizophrenia. *Proc Natl Acad Sci U S A*. 2002 Oct 15; 99(21):13675-80.

Cirulli ET, Lasseigne BN, Petrovski S, Sapp PC, Dion PA, Leblond CS, Couthouis J, Lu YF, Wang Q, Krueger BJ, Ren Z, Keebler J, Han Y, Levy SE, Boone BE, Wimbish JR, Waite LL, Jones AL, Carulli JP, Day-Williams AG, Staropoli JF, Xin WW, Chesi A, Raphael AR, McKenna-Yasek D, Cady J, Vianney de Jong JM, Kenna KP, Smith BN, Topp S, Miller J, Gkazi A; FALS Sequencing Consortium, Al-Chalabi A, van den Berg LH, Veldink J, Silani V, Ticozzi N, Shaw CE, Baloh RH, Appel S, Simpson E, Lagier-Tourenne C, Pulst SM, Gibson S, Trojanowski JQ, Elman L, McCluskey L, Grossman M, Shneider NA, Chung WK, Ravits JM, Glass JD, Sims KB, Van Deerlin VM, Maniatis T, Hayes SD, Ordureau A, Swarup S, Landers J, Baas F, Allen AS, Bedlack RS, Harper JW, Gitler AD, Rouleau GA, Brown R, Harms MB, Cooper GM, Harris T, Myers RM, Goldstein DB. Exome sequencing in amyotrophic lateral sclerosis identifies risk genes and pathways. *Science*. 2015 Mar 27; 347(6229):1436-41.

Collingridge GL, Volianskis A, Bannister N, France G, Hanna L, Mercier M, Tidball P, Fang G, Irvine MW, Costa BM, Monaghan DT, Bortolotto ZA, Molnár E, Lodge D, Jane DE. The NMDA receptor as a target for cognitive enhancement. *Neuropharmacology*. 2013 Jan; 64:13-26.

Coluzzi E, Colamartino M, Cozzi R, Leone S, Meneghini C, O'Callaghan N, Sgura A. Oxidative stress induces persistent telomeric DNA damage responsible for nuclear morphology change in mammalian cells. *PLoS One*. 2014 Oct 29; 9(10):e110963.

Coyle JT. Glutamate and schizophrenia: beyond the dopamine hypothesis. *Cell Mol Neurobiol*. 2006 Jul-Aug; 26(4-6):365-84.

Coyle JT, Tsai G, Goff D. Converging evidence of NMDA receptor hypofunction in the pathophysiology of schizophrenia. *Ann N Y Acad Sci*. 2003 Nov; 1003:318-27.

Fairbank M, Huang K, El-Husseini A, Nabi IR. RING finger palmitoylation of the endoplasmic reticulum Gp78 E3 ubiquitin ligase. *FEBS Lett*. 2012 Jul 30; 586(16):2488-93.

Ferraris D, Duvall B, Ko YS, Thomas AG, Rojas C, Majer P, Hashimoto K, Tsukamoto T. Synthesis and biological evaluation of D-amino acid oxidase inhibitors. *J Med Chem.* 2008 Jun 26; 51(12):3357-9.

Foltyn VN, Bendikov I, De Miranda J, Panizzutti R, Dumin E, Shleper M, Li P, Toney MD, Kartvelishvily E, Wolosker H. Serine racemase modulates intracellular D-serine levels through an alpha,beta-elimination activity. *J Biol Chem.* 2005 Jan 21; 280(3):1754-63.

Frattini LF, Piubelli L, Sacchi S, Molla G, Pollegioni L. Is rat an appropriate animal model to study the involvement of D-serine catabolism in schizophrenia? Insights from characterization of D-amino acid oxidase. *FEBS J.* 2011 Nov; 278(22):4362-73.

Fuchs SA, Berger R, Klomp LW, de Koning TJ. D-amino acids in the central nervous system in health and disease. *Mol Genet Metab.* 2005 Jul; 85(3):168-80.

Fuchs SA, Berger R, de Koning TJ. D-serine: the right or wrong isoform? *Brain Res.* 2011 Jul 15; 1401:104-17.

Fukui K, Miyake Y. Molecular cloning and chromosomal localization of a human gene encoding D-amino-acid oxidase. *J Biol Chem.* 1992 Sep 15; 267(26):18631-8.

Ghosh D, Berg JM. A proteome-wide perspective on peroxisome targeting signal 1(PTS1)-Pex5p affinities. *J Am Chem Soc.* 2010 Mar 24; 132(11):3973-9.

Gilson MK, Liu T, Baitaluk M, Nicola G, Hwang L, Chong J. BindingDB in 2015: A public database for medicinal chemistry, computational chemistry and systems pharmacology. *Nucleic Acids Res.* 2016 Jan 4; 44(D1):D1045-53.

Hashimoto A, Nishikawa T, Oka T, Takahashi K, Hayashi T. Determination of free amino acid enantiomers in rat brain and serum by high-performance liquid chromatography after derivatization with N-tert.-butyloxycarbonyl-L-cysteine and o-phthaldialdehyde. *J Chromatogr.* 1992 Nov 6; 582(1-2):41-8.

Hashimoto A, Nishikawa T, Konno R, Niwa A, Yasumura Y, Oka T, Takahashi K. Free D-serine, D-aspartate and D-alanine in central nervous system and serum in mutant mice lacking D-amino acid oxidase. *Neurosci Lett*. 1993 Apr 2; 152(1-2):33-6.

Hashimoto A, Nishikawa T, Oka T, Takahashi K. Endogenous D-serine in rat brain: N-methyl-D-aspartate receptor-related distribution and aging. *J Neurochem*. 1993 Feb; 60(2):783-6

Heresco-Levy U, Javitt DC, Ebstein R, Vass A, Lichtenberg P, Bar G, Catinari S, Ermilov M. D-serine efficacy as add-on pharmacotherapy to risperidone and olanzapine for treatment-refractory schizophrenia. *Biol Psychiatry*. 2005 Mar 15; 57(6):577-85.

Horiike K, Tojo H, Arai R, Nozaki M, Maeda T. D-amino-acid oxidase is confined to the lower brain stem and cerebellum in rat brain: regional differentiation of astrocytes. *Brain Res*. 1994 Aug 1; 652(2):297-303.

Huang Y, Nishikawa T, Satoh K, Iwata T, Fukushima T, Santa T, Homma H, Imai K. Urinary excretion of D-serine in human: comparison of different ages and species. *Biol Pharm Bull*. 1998 Feb; 21(2):156-62.

Hunter T. Tyrosine phosphorylation: thirty years and counting. *Curr Opin Cell Biol*. 2009 Apr; 21(2):140-6.

Ikonomidou C, Bosch F, Miksa M, Bittigau P, Vöckler J, Dikranian K, Tenkova TI, Stefovská V, Turski L, Olney JW. Blockade of NMDA receptors and apoptotic neurodegeneration in the developing brain. *Science*. 1999 Jan 1; 283(5398):70-4.

Inanobe A, Furukawa H, Gouaux E. Mechanism of partial agonist action at the NR1 subunit of NMDA receptors. *Neuron*. 2005 Jul 7; 47(1):71-84.

Jagannath V, Marinova Z, Monoranu CM, Walitza S, Grünblatt E. Expression of D-amino acid oxidase (DAO/DAAO) and D-amino acid oxidase activator (DAOA/G72) during development and aging in the human post-mortem brain. *Front Neuroanat*. 2017 Apr 6; 11:31.

Jankowski A, Kim JH, Collins RF, Daneman R, Walton P, Grinstein S. In situ measurements of the pH of mammalian peroxisomes using the fluorescent protein pHluorin. *J Biol Chem*. 2001 Dec 28; 276(52):48748-53.

Johnson JW, Ascher P. Glycine potentiates the NMDA response in cultured mouse brain neurons. *Nature*. 1987 Feb 5-11; 325(6104):529-31.

Kapoor R, Lim KS, Cheng A, Garrick T, Kapoor V. Preliminary evidence for a link between schizophrenia and NMDA-glycine site receptor ligand metabolic enzymes, D-amino acid oxidase (DAAO) and kynurenine aminotransferase-1 (KAT-1). *Brain Res*. 2006 Aug 23; 1106(1):205-210.

Kapp K, Schrepf S, Lemberg MK, et al. Post-targeting functions of signal peptides. In: *Madame Curie Bioscience Database* [Internet]. Austin (TX): Landes Bioscience; 2000-2013. Available from: <https://www.ncbi.nlm.nih.gov/books/NBK6322/>

Katane M, Osaka N, Matsuda S, Maeda K, Kawata T, Saitoh Y, Sekine M, Furuchi T, Doi I, Hirono S, Homma H. Identification of novel D-amino acid oxidase inhibitors by in silico screening and their functional characterization in vitro. *J Med Chem*. 2013 Mar 14; 56(5):1894-907.

Kawazoe T, Tsuge H, Piloni MS, Fukui K. Crystal structure of human D-amino acid oxidase: context-dependent variability of the backbone conformation of the VAAGL hydrophobic stretch located at the si-face of the flavin ring. *Protein Sci*. 2006 Dec; 15(12):2708-17.

Kawazoe T, Park HK, Iwana S, Tsuge H, Fukui K. Human D-amino acid oxidase: an update and review. *Chem Rec*. 2007; 7(5):305-15.

Kawazoe T, Tsuge H, Imagawa T, Aki K, Kuramitsu S, Fukui K. Structural basis of D-DOPA oxidation by D-amino acid oxidase: alternative pathway for dopamine biosynthesis. *Biochem Biophys Res Commun*. 2007 Apr 6; 355(2):385-91.

Kemp JA, McKernan RM. NMDA receptor pathways as drug targets. *Nat Neurosci*. 2002 Nov; 5 Suppl:1039-42.

Kim SH, Shishido Y, Sogabe H, Rachadech W, Yorita K, Kato Y, Fukui K. Age- and gender-dependent D-amino acid oxidase activity in mouse brain and peripheral tissues: implication for aging and neurodegeneration. *J Biochem.* 2019 Aug 1; 166(2):187-196.

Kohiki T, Kato Y, Nishikawa Y, Yorita K, Sagawa I, Denda M, Inokuma T, Shigenaga A, Fukui K, Otaka A. Elucidation of inhibitor-binding pockets of D-amino acid oxidase using docking simulation and N-sulfanylethylanilide-based labeling technology. *Org Biomol Chem.* 2017 Jun 27; 15(25):5289-5297.

Koibuchi N, Konno R, Matsuzaki S, Ohtake H, Niwa A, Yamaoka S. Localization of D-amino acid oxidase mRNA in the mouse kidney and the effect of testosterone treatment. *Histochem Cell Biol.* 1995 Nov; 104(5):349-55.

Kolodney G, Dumin E, Safory H, Rosenberg D, Mori H, Radzishevsky I, Wolosker H. Nuclear compartmentalization of serine racemase regulates D-serine production: implications for N-methyl-D-aspartate (NMDA) receptor activation. *J Biol Chem.* 2015 Dec 25; 290(52):31037-50.

Kondori NR, Paul P, Robbins JP, Liu K, Hildyard JCW, Wells DJ, de Belleruche JS. Characterisation of the pathogenic effects of the in vivo expression of an ALS-linked mutation in D-amino acid oxidase: Phenotype and loss of spinal cord motor neurons. *PLoS One.* 2017 Dec 1; 12(12):e0188912.

Konno R, Yasumura Y. Mouse mutant deficient in D-amino acid oxidase activity. *Genetics.* 1983 Feb; 103(2):277-85.

Konno R, Ikeda M, Yamaguchi K, Ueda Y, Niwa A. Nephrotoxicity of D-propargylglycine in mice. *Arch Toxicol.* 2000 Oct; 74(8):473-9.

Konno R. Assignment of D-amino-acid oxidase gene to a human and a mouse chromosome. *Amino Acids.* 2001; 20(4):401-8.

Krebs HA. Metabolism of amino-acids: Deamination of amino-acids. *Biochem J.* 1935 Jul; 29(7):1620-44.

Krug AW, Völker K, Dantzler WH, Silbernagl S. Why is D-serine nephrotoxic and alpha-aminoisobutyric acid protective? *Am J Physiol Renal Physiol*. 2007 Jul; 293(1):F382-90.

Kvajo M, Dhillia A, Swor DE, Karayiorgou M, Gogos JA. Evidence implicating the candidate schizophrenia/bipolar disorder susceptibility gene G72 in mitochondrial function. *Mol Psychiatry*. 2008 Jul; 13(7):685-96.

Labrie V, Wang W, Barger SW, Baker GB, Roder JC. Genetic loss of D-amino acid oxidase activity reverses schizophrenia-like phenotypes in mice. *Genes BrainBehav*. 2010 Feb; 9(1):11-25.

Luks L, Maier MY, Sacchi S, Pollegioni L, Dietrich DR. Understanding renal nuclear protein accumulation: an in vitro approach to explain an in vivo phenomenon. *Arch Toxicol*. 2017a Nov; 91(11):3599-3611.

Luks L, Sacchi S, Pollegioni L, Dietrich DR. Novel insights into renal D-amino acid oxidase accumulation: propiverine changes DAAO localization and peroxisomal size in vivo. *Arch Toxicol*. 2017b Jan; 91(1):427-437.

Madeira C, Freitas ME, Vargas-Lopes C, Wolosker H, Panizzutti R. Increased brain D-amino acid oxidase (DAAO) activity in schizophrenia. *Schizophr Res*. 2008 Apr; 101(1-3):76-83.

Madeira C, Lourenco MV, Vargas-Lopes C, Suemoto CK, Brandão CO, Reis T, Leite RE, Laks J, Jacob-Filho W, Pasqualucci CA, Grinberg LT, Ferreira ST, Panizzutti R. D-serine levels in Alzheimer's disease: implications for novel biomarker development. *Transl Psychiatry*. 2015 May 5; 5:e561.

Maeda A, Okano K, Park PS, Lem J, Crouch RK, Maeda T, Palczewski K. Palmitoylation stabilizes unliganded rod opsin. *Proc Natl Acad Sci U S A*. 2010 May 4; 107(18):8428-33.

Maekawa M, Okamura T, Kasai N, Hori Y, Summer KH, Konno R. D-amino-acid oxidase is involved in D-serine-induced nephrotoxicity. *Chem Res Toxicol*. 2005 Nov; 18(11):1678-82.

Massey V, Palmer G, Bennett R. The purification and some properties of D-amino acid oxidase. *Biochim Biophys Acta*. 1961 Mar 18; 48:1-9.

Matsumoto M, Kunisawa A, Hattori T, Kawana S, Kitada Y, Tamada H, Kawano S, Hayakawa Y, Iida J, Fukusaki E. Free D-amino acids produced by commensal bacteria in the colonic lumen. *Sci Rep*. 2018 Dec 17; 8(1):17915.

Mattevi A, Vanoni MA, Todone F, Rizzi M, Teplyakov A, Coda A, Bolognesi M, Curti B. Crystal structure of D-amino acid oxidase: a case of active site mirror-image convergent evolution with flavocytochrome b2. *Proc Natl Acad Sci USA*. 1996 Jul 23; 93(15):7496-501.

McBain CJ, Kleckner NW, Wyrick S, Dingledine R. Structural requirements for activation of the glycine coagonist site of N-methyl-D-aspartate receptors expressed in *Xenopus* oocytes. *Mol Pharmacol*. 1989 Oct; 36(4):556-65.

Meinecke M, Cizmowski C, Schliebs W, Krüger V, Beck S, Wagner R, Erdmann R. The peroxisomal importomer constitutes a large and highly dynamic pore. *Nat Cell Biol*. 2010 Mar; 12(3):273-7.

Mitchell J, Paul P, Chen HJ, Morris A, Payling M, Falchi M, Habgood J, Panoutsou S, Winkler S, Tisato V, Hajitou A, Smith B, Vance C, Shaw C, Mazarakis ND, de Belleruche J. Familial amyotrophic lateral sclerosis is associated with a mutation in D-amino acid oxidase. *Proc Natl Acad Sci USA*. 2010 Apr 20; 107(16):7556-61.

Mizutani H, Miyahara I, Hirotsu K, Nishina Y, Shiga K, Setoyama C, Miura R. Three-dimensional structure of porcine kidney D-amino acid oxidase at 3.0 Å resolution. *J Biochem*. 1996 Jul; 120(1):14-7.

Molla G, Sacchi S, Bernasconi M, Pilone MS, Fukui K, Pollegioni L. Characterization of human D-amino acid oxidase. *FEBS Lett*. 2006 Apr 17; 580(9):2358-64.

Molla G. Competitive inhibitors unveil structure/function relationships in human D-amino acid oxidase. *Front Mol Biosci*. 2017 Nov 27; 4:80.

Momoi K, Fukui K, Watanabe F, Miyake Y. Molecular cloning and sequence analysis of cDNA encoding human kidney D-amino acid oxidase. *FEBS Lett*. 1988 Sep 26; 238(1):180-4.

Montilla-Martinez M, Beck S, Klümper J, Meinecke M, Schliebs W, Wagner R, Erdmann R. Distinct Pores for Peroxisomal Import of PTS1 and PTS2 Proteins. *Cell Rep*. 2015 Dec 15; 13(10):2126-34.

Moreno S, Nardacci R, Cimini A, Cerù MP. Immunocytochemical localization of D-amino acid oxidase in rat brain. *J Neurocytol*. 1999 Mar; 28(3):169-85.

Mothet JP, Parent AT, Wolosker H, Brady RO Jr, Linden DJ, Ferris CD, Rogawski MA, Snyder SH. D-serine is an endogenous ligand for the glycine site of the N-methyl-D-aspartate receptor. *Proc Natl Acad Sci USA*. 2000 Apr 25; 97(9):4926-31.

Nagai Y, Tsugane M, Oka J, Kimura H. Hydrogen sulfide induces calcium waves in astrocytes. *FASEB J*. 2004 Mar; 18(3):557-9.

Nagata Y. Involvement of D-amino acid oxidase in elimination of D-serine in mouse brain. *Experientia*. 1992 Aug 15; 48(8):753-5.

Nagata Y, Masui R, Akino T. The presence of free D-serine, D-alanine and D-proline in human plasma. *Experientia*. 1992 Oct 15; 48(10):986-8.

Nakamura H, Fang J, Maeda H. Protective role of D-amino acid oxidase against *Staphylococcus aureus* infection. *Infect Immun*. 2012 Apr; 80(4):1546-53.

Neims AH, Zieverink WD, Smilack JD. Distribution of D-amino acid oxidase in bovine and human nervous tissues. *J Neurochem*. 1966 Mar; 13(3):163-8.

Ono K, Shishido Y, Park HK, Kawazoe T, Iwana S, Chung SP, Abou El-Magd RM, Yorita K, Okano M, Watanabe T, Sano N, Bando Y, Arima K, Sakai T, Fukui K. Potential pathophysiological role of D-amino acid oxidase in schizophrenia: immunohistochemical and in situ hybridization study of the expression in human and rat brain. *J Neural Transm (Vienna)*. 2009 Oct; 116(10):1335-47.

Paul P, de Belleruche J. The role of D-amino acids in amyotrophic lateral sclerosis pathogenesis: a review. *Amino Acids*. 2012 Nov; 43(5):1823-31.

Paul P, Murphy T, Oseni Z, Sivalokanathan S, de Bellerocche JS. Pathogenic effects of amyotrophic lateral sclerosis-linked mutation in D-amino acid oxidase are mediated by D-serine. *Neurobiol Aging*. 2014 Apr; 35(4):876-85.

Pigino, Gustavo & Morfini, Gerardo & Brady, Scott. Intracellular Trafficking. 2012. 10.1016/B978-0-12-374947-5.00007-9.

Pilone Simonetta M, Pollegioni L, Casalin P, Curti B, Ronchi S. Properties of D-amino-acid oxidase from *Rhodotorula gracilis*. *Eur J Biochem*. 1989 Mar 1; 180(1):199-204.

Pilone MS. D-Amino acid oxidase: new findings. *Cell Mol Life Sci*. 2000 Nov; 57(12):1732-47.

Pollegioni L, Piubelli L, Sacchi S, Pilone MS, Molla G. Physiological functions of D-amino acid oxidases: from yeast to humans. *Cell Mol Life Sci*. 2007 Jun; 64(11):1373-94.

Pollegioni L, Sacchi S. Metabolism of the neuromodulator D-serine. *Cell Mol Life Sci*. 2010 Jul; 67(14):2387-404.

Pollegioni L, Piubelli L, Molla G, Rosini E. D-amino acid oxidase-pLG72 interaction and D-serine modulation. *Front Mol Biosci*. 2018 Jan 24; 5:3.

Pollegioni L, Sacchi S, Murtas G. Human D-amino acid oxidase: structure, function, and regulation. *Front Mol Biosci*. 2018 Nov 28; 5:107.

Popiolek M, Ross JF, Charych E, Chanda P, Gundelfinger ED, Moss SJ, Brandon NJ, Pausch MH. D-amino acid oxidase activity is inhibited by an interaction with bassoon protein at the presynaptic active zone. *J Biol Chem*. 2011 Aug 19; 286(33):28867-75.

Prybylowski K, Wenthold RJ. N-Methyl-D-aspartate receptors: subunit assembly and trafficking to the synapse. *J Biol Chem*. 2004 Mar 12; 279(11):9673-6.

Rabouille C. Pathways of Unconventional Protein Secretion. *Trends Cell Biol*. 2017 Mar; 27(3):230-240.

Raibekas AA, Fukui K, Massey V. Design and properties of human D-amino acid oxidase with covalently attached flavin. *Proc Natl Acad Sci USA*. 2000 Mar 28; 97(7):3089-93.

Raje M, Hin N, Duvall B, Ferraris DV, Berry JF, Thomas AG, Alt J, Rojas C, Slusher BS, Tsukamoto T. Synthesis of kojic acid derivatives as secondary binding site probes of D-amino acid oxidase. *Bioorg Med Chem Lett*. 2013 Jul 1; 23(13):3910-3.

Richter-Landsberg C, Vollgraf U. Mode of cell injury and death after hydrogen peroxide exposure in cultured oligodendroglia cells. *Exp Cell Res*. 1998 Oct 10; 244(1):218-29.

Robinson JM, Briggs RT, Karnovsky MJ. Localization of D-amino acid oxidase on the cell surface of human polymorphonuclear leukocytes. *J Cell Biol*. 1978 Apr; 77(1):59-71.

Romano D, Molla G, Pollegioni L, Marinelli F. Optimization of human D-amino acid oxidase expression in *Escherichia coli*. *Protein Expr Purif*. 2009 Nov; 68(1):72-8.

Sacchi S, Bernasconi M, Martineau M, Mothet JP, Ruzzene M, Pilone MS, Pollegioni L, Molla G. pLG72 modulates intracellular D-serine levels through its interaction with D-amino acid oxidase: effect on schizophrenia susceptibility. *J Biol Chem*. 2008 Aug 8; 283(32):22244-56.

Sacchi S, Cappelletti P, Giovannardi S, Pollegioni L. Evidence for the interaction of D-amino acid oxidase with pLG72 in a glial cell line. *Mol Cell Neurosci*. 2011 Sep; 48(1):20-8.

Sacchi S, Caldinelli L, Cappelletti P, Pollegioni L, Molla G. Structure-function relationships in human D-amino acid oxidase. *Amino Acids*. 2012 Nov; 43(5):1833-50.

Sacchi S, Rosini E, Pollegioni L, Molla G. D-amino acid oxidase inhibitors as a novel class of drugs for schizophrenia therapy. *Curr Pharm Des*. 2013; 19(14):2499-511.

Sacchi S, Binelli G, Pollegioni L. G72 primate-specific gene: a still enigmatic element in psychiatric disorders. *Cell Mol Life Sci.* 2016 May; 73(10):2029-39.

Sacchi S, Cappelletti P, Pirone L, Smaldone G, Pedone E, Pollegioni L. Elucidating the role of the pLG72 R30K substitution in schizophrenia susceptibility. *FEBS Lett.* 2017 Feb; 591(4):646-655.

Sacchi S, Cappelletti P, Murtas G. Biochemical properties of human D-amino acid oxidase variants and their potential significance in pathologies. *Front Mol Biosci.* 2018 Jun 12; 5:55.

Saitoh Y, Katane M, Kawata T, Maeda K, Sekine M, Furuchi T, Kobuna H, Sakamoto T, Inoue T, Arai H, Nakagawa Y, Homma H. Spatiotemporal localization of D-amino acid oxidase and D-aspartate oxidases during development in *Caenorhabditis elegans*. *Mol Cell Biol.* 2012 May; 32(10):1967-83.

Sasabe J, Miyoshi Y, Suzuki M, Mita M, Konno R, Matsuoka M, Hamase K, Aiso S. D-amino acid oxidase controls motoneuron degeneration through D-serine. *Proc Natl Acad Sci USA.* 2012 Jan 10; 109(2):627-32.

Sasabe J, Suzuki M, Imanishi N, Aiso S. Activity of D-amino acid oxidase is widespread in the human central nervous system. *Front Synaptic Neurosci.* 2014 Jun 10; 6:14.

Sasabe J, Suzuki M, Miyoshi Y, Tojo Y, Okamura C, Ito S, Konno R, Mita M, Hamase K, Aiso S. Ischemic acute kidney injury perturbs homeostasis of serine enantiomers in the body fluid in mice: early detection of renal dysfunction using the ratio of serine enantiomers. *PLoS One.* 2014 Jan 29; 9(1):e86504.

Sasabe J, Miyoshi Y, Rakoff-Nahoum S, Zhang T, Mita M, Davis BM, Hamase K, Waldor MK. Interplay between microbial d-amino acids and host D-amino acid oxidase modifies murine mucosal defence and gut microbiota. *Nat Microbiol.* 2016 Jul 25; 1(10):16125.

Schell MJ, Molliver ME, Snyder SH. D-serine, an endogenous synaptic modulator: localization to astrocytes and glutamate-stimulated release. *Proc Natl Acad Sci USA.* 1995 Apr 25; 92(9):3948-52.

Shibuya N, Kimura H. Production of hydrogen sulfide from D-cysteine and its therapeutic potential. *Front Endocrinol (Lausanne)*. 2013a Jul 16;4:87.

Shibuya N, Koike S, Tanaka M, Ishigami-Yuasa M, Kimura Y, Ogasawara Y, Fukui K, Nagahara N, Kimura H. A novel pathway for the production of hydrogen sulfide from D-cysteine in mammalian cells. *Nat Commun*. 2013b; 4:1366.

Shoji K, Mariotto S, Ciampa AR, Suzuki H. Mutual regulation between serine and nitric oxide metabolism in human glioblastoma cells. *Neurosci Lett*. 2006a Feb 20; 394(3):163-7.

Shoji K, Mariotto S, Ciampa AR, Suzuki H. Regulation of serine racemase activity by D-serine and nitric oxide in human glioblastoma cells. *Neurosci Lett*. 2006 bJan 9; 392(1-2):75-8.

Spalloni A, Nutini M, Longone P. Role of the N-methyl-D-aspartate receptors complex in amyotrophic lateral sclerosis. *Biochim Biophys Acta*. 2013 Feb; 1832(2):312-22.

Stipanuk MH, Dominy JE Jr, Lee JI, Coloso RM. Mammalian cysteine metabolism: new insights into regulation of cysteine metabolism. *J Nutr*. 2006 Jun; 136(6 Suppl):1652S-1659S.

Tannenbergs RK, Scott HL, Westphalen RI, Dodd PR. The identification and characterization of excitotoxic nerve-endings in Alzheimer disease. *Curr Alzheimer Res*. 2004 Feb; 1(1):11-25.

Terry-Lorenzo RT, Chun LE, Brown SP, Heffernan ML, Fang QK, Orsini MA, Pollegioni L, Hardy LW, Spear KL, Large TH. Novel human D-amino acid oxidase inhibitors stabilize an active-site lid-open conformation. *Biosci Rep*. 2014 Aug 11; 34(4).

Terry-Lorenzo RT, Masuda K, Sugao K, Fang QK, Orsini MA, Sacchi S, Pollegioni L. High-Throughput Screening Strategy Identifies Allosteric, Covalent Human D-Amino Acid Oxidase Inhibitor. *J Biomol Screen*. 2015 Dec; 20(10):1218-31.

Tran EJ, Wentz SR. Dynamic nuclear pore complexes: life on the edge. *Cell*. 2006 Jun 16; 125(6):1041-53.

Umhau S, Pollegioni L, Molla G, Diederichs K, Welte W, Pilone MS, Ghisla S. The x-ray structure of D-amino acid oxidase at very high resolution identifies the chemical mechanism of flavin-dependent substrate dehydrogenation. *Proc Natl Acad Sci USA*. 2000 Nov 7; 97(23):12463-8

Veal EA, Day AM, Morgan BA. Hydrogen peroxide sensing and signaling. *Mol Cell*. 2007 Apr 13; 26(1):1-14.

Verrall L, Walker M, Rawlings N, Benzel I, Kew JN, Harrison PJ, Burnet PW. D-Amino acid oxidase and serine racemase in human brain: normal distribution and altered expression in schizophrenia. *Eur J Neurosci*. 2007 Sep; 26(6):1657-69.

Verrall L, Burnet PW, Betts JF, Harrison PJ. The neurobiology of D-amino acid oxidase and its involvement in schizophrenia. *Mol Psychiatry*. 2010 Feb; 15(2):122-37.

Walsh CT, Garneau-Tsodikova S, Gatto GJ Jr. Protein posttranslational modifications: the chemistry of proteome diversifications. *Angew Chem Int Ed Engl*. 2005 Dec 1; 44(45):7342-72.

Wang H, Wolosker H, Pevsner J, Snyder SH, Selkoe DJ. Regulation of rat magnocellular neurosecretory system by D-aspartate: evidence for biological role(s) of a naturally occurring free D-amino acid in mammals. *J Endocrinol*. 2000 Nov; 167(2):247-52.

Wenthold RJ, Prybylowski K, Standley S, Sans N, Petralia RS. Trafficking of NMDA receptors. *Annu Rev Pharmacol Toxicol*. 2003; 43:335-58.

Wolosker H, Blackshaw S, Snyder SH. Serine racemase: a glial enzyme synthesizing D-serine to regulate glutamate-N-methyl-D-aspartate neurotransmission. *Proc Natl Acad Sci U S A*. 1999 Nov 9; 96(23):13409-14.

Wolosker H, D'Aniello A, Snyder SH. D-aspartate disposition in neuronal and endocrine tissues: ontogeny, biosynthesis and release. *Neuroscience*. 2000; 100(1):183-9.

Wolosker H, Panizzutti R, De Miranda J. Neurobiology through the looking-glass: D-serine as a new glial-derived transmitter. *Neurochem Int.* 2002 Nov; 41(5):327-32.

Wolosker H, Dumin E, Balan L, Foltyn VN. D-amino acids in the brain: D-serine in neurotransmission and neurodegeneration. *FEBS J.* 2008 Jul; 275(14):3514-26.

Wolosker H. Serine racemase and the serine shuttle between neurons and astrocytes. *Biochim Biophys Acta.* 2011 Nov; 1814(11):1558-66.

Wolosker H, Radzishovsky I. The serine shuttle between glia and neurons: implications for neurotransmission and neurodegeneration. *Biochem Soc Trans.* 2013 Dec; 41(6):1546-5.

Other publications



Biochemical Properties of Human D-amino Acid Oxidase Variants and Their Potential Significance in Pathologies

Silvia Sacchi^{1,2*}, Pamela Cappelletti^{1,2} and Giulia Murtas¹

¹ Dipartimento di Biotecnologie e Scienze della Vita, Università degli Studi dell'Insubria, Varese, Italy, ² The Protein Factory, Politecnico di Milano and Università degli Studi dell'Insubria, Milan, Italy

OPEN ACCESS

Edited by:

Jumpei Sasabe,
Keio University, Japan

Reviewed by:

Hisashi Mori,
University of Toyama, Japan
Jackie de Belleruche,
Imperial College London,
United Kingdom

*Correspondence:

Silvia Sacchi
silvia.sacchi@uninsubria.it

Specialty section:

This article was submitted to
Structural Biology,
a section of the journal
Frontiers in Molecular Biosciences

Received: 10 April 2018

Accepted: 23 May 2018

Published: 12 June 2018

Citation:

Sacchi S, Cappelletti P and Murtas G
(2018) Biochemical Properties of
Human D-amino Acid Oxidase
Variants and Their Potential
Significance in Pathologies.
Front. Mol. Biosci. 5:55.
doi: 10.3389/fmolb.2018.00055

The stereoselective flavoenzyme D-amino acid oxidase (DAAO) catalyzes the oxidative deamination of neutral and polar D-amino acids producing the corresponding α -keto acids, ammonia, and hydrogen peroxide. Despite its peculiar and atypical substrates, DAAO is widespread expressed in most eukaryotic organisms. In mammals (and humans in particular), DAAO is involved in relevant physiological processes ranging from D-amino acid detoxification in kidney to neurotransmission in the central nervous system, where DAAO is responsible of the catabolism of D-serine, a key endogenous co-agonist of N-methyl-D-aspartate receptors. Recently, structural and functional studies have brought to the fore the distinctive biochemical properties of human DAAO (hDAAO). It appears to have evolved to allow a strict regulation of its activity, so that the enzyme can finely control the concentration of substrates (such as D-serine in the brain) without yielding to an excessive production of hydrogen peroxide, a potentially toxic reactive oxygen species (ROS). Indeed, dysregulation in D-serine metabolism, likely resulting from altered levels of hDAAO expression and activity, has been implicated in several pathologies, ranging from renal disease to neurological, neurodegenerative, and psychiatric disorders. Only one mutation in *DAO* gene was unequivocally associated to a human disease. However, several single nucleotide polymorphisms (SNPs) are reported in the database and the biochemical characterization of the corresponding recombinant hDAAO variants is of great interest for investigating the effect of mutations. Here we reviewed recently published data focusing on the modifications of the structural and functional properties induced by amino acid substitutions encoded by confirmed SNPs and on their effect on D-serine cellular levels. The potential significance of the different hDAAO variants in human pathologies will be also discussed.

Keywords: D-amino acid oxidase, D-amino acids, D-serine levels, protein variants, structural-functional properties, protein conformation, human pathologies

Abbreviations: DAAO, D-amino acid oxidase; hDAAO, human DAAO; D-AAs, D-amino acids; NMDAR, N-methyl-D-aspartate type glutamate receptor; SNP, single nucleotide polymorphism; CBIO, 5-chloro-benzo[d]isoxazol-3-ol; CNS, central nervous system; ROS, reactive oxygen species.

INTRODUCTION

The peroxisomal flavoprotein D-amino acid oxidase (EC 1.4.3.3, DAAO) is characterized by a strict stereoselectivity and a broad substrate specificity. Since the first identification of the enzyme activity by Krebs in 1935 (Krebs, 1935) and the following purification of the protein from pig kidney (Yagi et al., 1967; Curti et al., 1973), it was subjected to extensive studies becoming the prototype of the dehydrogenase-oxidase class of FAD-dependent flavoenzymes (Fitzpatrick and Massey, 1982). DAAO catalyzes the oxidative deamination of most neutral and polar D-amino acids (D-AAAs) to their imino acids counterparts and concomitantly reduces the cofactor FAD. Once released, imino acids non-enzymatically hydrolyze to α -keto acids and ammonia, while the reduced flavin is concomitantly reoxidized by molecular oxygen producing hydrogen peroxide (H_2O_2 ; **Figure 1**). DAAO is therefore considered a marker enzyme associated with the generation of ROS in peroxisomes.

Despite its atypical substrates, DAAO is widespread in nature: the enzyme activity has been identified in most eukaryotic organisms, the only exception being plants. The protein from a variety of sources, ranging from microorganisms to mammals including humans, have been purified and characterized (Pollegioni et al., 2007; Khoronenkova and Tishkov, 2008). In different organisms, DAAO fulfills distinct physiological functions: it is involved in the catabolism of D-AAAs in yeasts (allowing the microorganisms to grow on these substrates as carbon, nitrogen and energy sources); while it plays important regulatory roles in higher organisms. Indeed, in mammals DAAO is implicated in relevant processes ranging from D-AA detoxification and the modulation of excretion in kidney, to neurotransmission in the central nervous system (CNS). Therefore, abnormal levels of the enzyme activity have been shown/proposed to play a significant role in pathologies. Here we provide for the first time a review of human DAAO (hDAAO) variants containing single point amino acidic substitution encoded by single nucleotide polymorphisms (SNPs) reported in the database. Their structural and functional properties, as well as their substantiated or presumed role in diseases, will be discussed.

DAAO INVOLVEMENT IN MAMMALIAN KEY PHYSIOLOGICAL PROCESSES

In mammals DAAO is mainly expressed in kidney, liver, brain and to a lesser extent in the small intestine and in neutrophilic leukocytes (Pollegioni et al., 2007, see **Table 1**). Worthy of note, until 1980s no systematic studies on DAAO from higher organisms were performed for several reasons: the enzyme content and stability were thought to be low, the levels of its substrates D-AAAs were barely detectable (their presence in tissues was even questioned) and therefore, no relevant biological functions for the enzyme had been figured out at that time. However, starting from the mid-1990s interest aroused by this enzyme has grown exponentially. Thanks to improved analytical methods based on high performances liquid chromatography (HPLC), significant levels of different D-AAAs were detected in

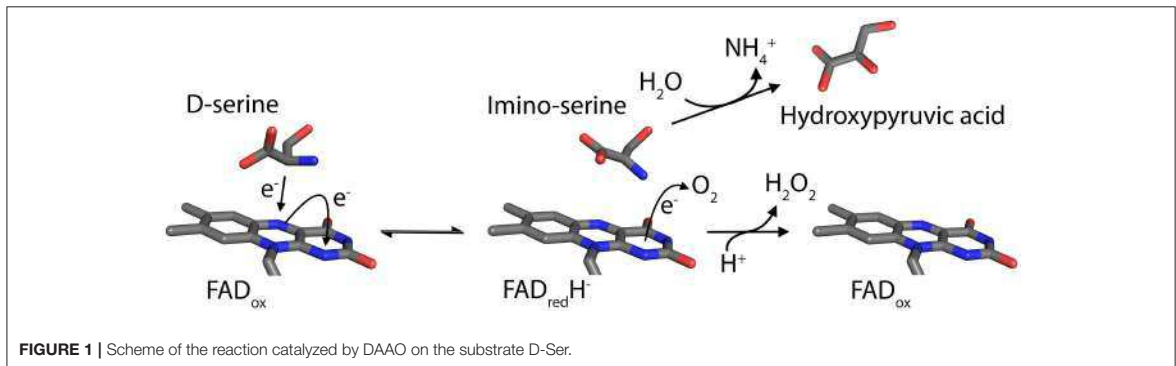
brain and other tissues (Nagata et al., 1992; Hashimoto et al., 1993; Hamase et al., 1997). Afterwards, specific physiological roles for D-isomers were demonstrated (Wang et al., 2000; Wolosker et al., 2002; Fuchs et al., 2005) and a key function of DAAO in their metabolic control was proposed (Nagata et al., 1989; Nagata, 1992).

Liver and kidney are among the most DAAO-rich organs, with the only exception for mouse liver, in which the enzyme has been shown to be absent (Konno et al., 1997). Interestingly, DAAO activity was reported in hepatocytes from mouse fetuses (Dabholkar, 1986), but it disappeared in the liver of adult animals, where DAAO mRNA and protein were undetectable (Konno et al., 1997; Wang and Zhu, 2003). The reason why mouse is the only mammal showing no expression of DAAO in the liver remains an intriguing issue. In kidney, the enzyme was observed in proximal tubule cells by the detection of the encoding transcript (Koibuchi et al., 1995) and enzyme histochemistry in mice (Sasabe et al., 2014). The identification of the mutant ddY/DAAO^{-/-} mice strain, expressing a fully inactive protein variant due to the naturally occurring substitution of a Gly by an Arg at position 181 (Konno and Yasumura, 1983), proved to be of primary importance in the elucidation of DAAO physiological functions. The urine of these animals was reported to contain abnormally high amounts of D-AAAs (originating from the cell walls of intestinal bacteria, endogenous racemization or the assumption from the diet). Thus, it was inferred that in liver and kidney (and, to a lesser extent, in the urinary apparatus and in colon) DAAO was responsible for their elimination. More recently, in kidney and brain the enzyme was shown to be involved in the metabolism of the gaseous signaling molecule hydrogen sulfide (H_2S) through the DAAO/3-MST pathway, an alternative generation pathway (Shibuya et al., 2013).

The flavoenzyme was shown to be also expressed in the granule fraction of normal mature human granulocytes. In these cells DAAO, appropriately linked to myeloperoxidase, was proposed to be part of a cellular strategy to recognize and counteract foreign phagocytized microorganisms (Cline and Lehrer, 1969).

Analogously, the role of DAAO in controlling the homeostasis of gut microbiota has been recently reported (Sasabe et al., 2016). Both enzymatic activity and protein expression were detected in the proximal and middle small intestine of mice and humans (**Table 1**), associated to the villus epithelium. Unexpectedly, a processed form of the mouse protein appeared to be secreted in the lumen by goblet cells, likely due to the presence of a signal peptide and a predicted cleavage site near the N-terminus (Sasabe et al., 2016). DAAO-mediated oxidative deamination of free D-AAAs (present as microbial products) with the consequent production of H_2O_2 , was shown to represent an important factor in host defense, and in the modulation of microbiota composition (Sasabe et al., 2016).

In the CNS, DAAO was proposed to exert an important physiological function (undoubtedly, the most investigated one). It appeared responsible for the catabolism of endogenous D-Serine (D-Ser), a key neuromodulator for the development of neural circuits, which acts as a co-agonist of N-methyl-D-aspartate receptors (NMDAR). Thus, it was suggested



that DAAO contributes to normal neuronal functioning. Consistently, D-Ser levels distribution in the CNS was found to precisely mirror DAAO expression one, both in rodents and humans. The cellular mechanisms involved in the kinetics of serine enantiomers have been the subject of a heated debate. A widely accepted scenario was summarized in the so-called “serine shuttle” model (Wolosker, 2011). According to this hypothesis, D-Ser is predominantly produced in neurons by the stereoconversion from L-serine (provided by astrocytes) catalyzed by the PLP-dependent enzyme serine racemase (SR) (Wolosker, 2011; Wolosker and Radziszewsky, 2013), and shuttled to astrocytes where it is stored and released. Here DAAO, mainly expressed in this cell type contrary to SR, is believed to exert a key role in the regulation of D-Ser cellular concentrations and release, thus indirectly modulating its availability at the synapse and affecting NMDAR activation state through the reduced occupancy of the co-agonist site.

Due to the different methodologies used to detect the presence of DAAO, complexities, and controversies were raised concerning its expression levels and distribution in the mammalian CNS, in terms of both region and cell type (Table 1 summarizes the available data on humans). In rodents, histochemistry methods based on the detection of the enzyme activity led to traditionally consider DAAO as a hindbrain enzyme, highly expressed in the cerebellum (in particular in Bergmann glia), spinal cord and brain stem (Horiike et al., 1994; Kapoor and Kapoor, 1997; Sasabe et al., 2012). On the other hand, immunohistochemistry allowed the detection of low levels of DAAO also in frontal cortex and hippocampus (Moreno et al., 1999).

Both DAAO activity and immunoreactivity was instead consistently detected in the human forebrain, albeit at only a small fraction of that seen in cerebellum (Verrall et al., 2007; Madeira et al., 2008; Table 1). A recent elegant study, performed in both human and mouse tissues, investigated the flavoenzyme distribution using a novel activity staining method based on FITC-conjugated tyramide (Sasabe et al., 2014). The authors confirmed the presence of DAAO in human forebrain regions, but differently from previous studies (Verrall et al., 2007), detected the enzyme activity only in the white matter, throughout the corticospinal tract and in the spinal gray matter,

within astrocytes mainly located in the motor pathway. The high hDAAO levels found in spinal cord (Table 1) and brain stem were consistent with its role in preventing excitotoxic cell death in these regions.

Significant levels of hDAAO activity were detected in the nigrostriatal system (Table 1; Sasabe et al., 2014), suggesting that the flavoenzyme might affect not only glutamatergic but also dopaminergic neurons. Intriguingly, hDAAO was shown to efficiently metabolize D-DOPA: it is converted to dihydroxyphenylpyruvic acid, which is then transaminated to L-DOPA via what is known as the alternative pathway for dopamine biosynthesis (Kawazoe et al., 2007a,b; and reference therein). These findings suggested that D-DOPA might be the preferential substrate of hDAAO in the nigrostriatal system instead of D-Ser, and that the enzyme could be implicated in the metabolism of dopamine, norepinephrine, and epinephrine.


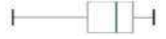
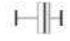





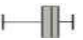
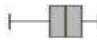



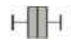


Other roles of DAAO, exerted through the degradation of D-Ser or other D-AAs, might be envisaged. Indeed, D-Ser may also modulate glycinergic transmission by antagonizing NR1/NR3A or NR1/NR3B receptors, which are insensitive to glutamate and activated by glycine (Chatterton et al., 2002; Takarada et al., 2009). On the other hand, the alternative DAAO substrate D-proline can activate glycine receptors (Hamasu et al., 2010), whereas D-leucine is a potent regulator of the blood–brain barrier enkephalin transport system (Banks and Kastin, 1991). It is still not known, whether these various additional actions of D-AAs may effectively be regulated by DAAO and have any significance with regard to its involvement in pathologies.

DAAO AND PATHOLOGIES: PROPOSED ROLES AND IMPLICATIONS

Kidney Diseases

Experimental evidence pointed out a role of DAAO in some chronic renal pathologic damages, such as D-Ser and D-propargylglycine induced nephrotoxicity (Konno et al., 2000; Maekawa et al., 2005), due to the intracellular DAAO-mediated generation of H_2O_2 , which in turn can produce even more aggressive ROS (Krug et al., 2007). Accordingly, renal ROS levels exhibits strong dependence on DAAO activity. On the other hand, a more recent study performed in rats reported that

TABLE 1 | DAO gene and protein expression in humans.

Tissue	Region	Gene expression* (Log ₁₀ TPM)	Protein expression**	Cell type	Main indicated function(s)
Liver			+++	Hepatocytes	Detoxification of DAAs
Kidney	Cortex		+++	Tubule cells	Detoxification of DAAs, H ₂ S generation
Testis			nd		
Colon	Transverse		nd		
Pituitary gland			nd		
Spleen			nd		
Whole blood			nd		
Small intestine			+	Enterocytes	Host defense, controls microbiota composition
Brain	Cerebellum		+++	Astrocytes	D-Ser catabolism
	Spinal cord (c-1)		++	Motor neurons	D-Ser catabolism
	Substantia nigra		++		D-Ser catabolism, D-DOPA metabolism
	Hypothalamus		nd		
	Hippocampus		nd		
	Frontal cortex		+	Neurons	D-Ser catabolism
	Nucleus accumbens		nd		
	Caudate		nd		

*Box plot of DAO gene transcripts levels in different human tissues. Values are shown in TPM (transcripts per kilobase million). Box represent the median and 25 and 75th percentiles. The data presented in this column were obtained from the Genotype-Tissue Expression (GTEx) Project Portal, dbGaP accession number phs000424, v7.p2 on 15/02/2018 (<https://www.gtexportal.org/home/gene/DAO>).

**Expression data as reported on the human protein atlas site (<https://www.proteinatlas.org/ENSG00000110887-DAO/tissue>) and in the literature cited in this review. + low expression; ++ medium expression, +++ high expression; nd, not detected.

renal ischemia-reperfusion injury, a major cause of acute kidney injury, substantially reduced renal DAAO activity (Zhang et al., 2012). The proposed underlying pathophysiological mechanism appeared very complex, involving among others ATP depletion, calcium overload, ROS generation, apoptotic and inflammatory responses (Eltzschig and Eckle, 2011). The observed change in the local level of DAAO activity was attributed to the markedly reduced pH value in kidney upon ischemia (Garcia et al., 2007; Prathapasinghe et al., 2008).

Emerging evidence suggested that H₂S also actively regulates renal function and is implicated in numerous acute and chronic kidney diseases. The broad renal protective effect of exogenous H₂S has been recently reviewed (Cao and Bian, 2016), but the

systemically administration of H₂S raised matter of concern due to its well-known toxicity (Guidotti, 2010). Considering the role of DAAO in the DAAO/3-MST H₂S generation pathway, its targeting by D-cysteine administration has been proposed as a way to safely deliver H₂S to the kidney (Shibuya et al., 2013).

Chronic Pain and Related Diseases

Neuropathic pain that arises after nerve injury is characterized by ongoing neurotransmission of pain signals through spinal circuits via the dorsal root ganglion and dorsal horn neurons (Basbaum et al., 2009). NMDARs are expressed in spinal cord neurons and play a key role in the development of ongoing pain

states via central sensitization (Latremliere and Woolf, 2009). A pioneering study reported that tonic pain-related behavior was exaggerated in the *ddY/DAAO^{-/-}* mice lacking DAAO activity (Wake et al., 2001), indicating that the resulting increased D-Ser levels potentiated NMDARs activation leading to a buildup in the second phase of the formalin response. More recent investigations (Zhao et al., 2010; Gong et al., 2011), further confirmed that DAAO in the spinal cord acts as a pronociceptive factor and demonstrated the efficacy of DAAO inhibitors in models of tonic and chronic pain, generally believed to be mediated by central sensitization. In this context, the systemic administration of the DAAO inhibitor 4H-furo[3,2-b]pyrrole-5-carboxylic acid was shown to reverse pain-related behaviors in rat models of neuropathic and inflammatory pain, with a reduction in the electrophysiological activity in spinal cord dorsal horn neurons and peripheral afferent inputs (Hopkins et al., 2013).

It cannot be excluded that the role of DAAO in chronic pain involves other mechanisms, independent from NMDAR modulation. Indeed, conditions of nerve injury may include changes in local concentrations of ROS, as it has been reported for formalin-induced pain (Lu et al., 2012). The inhibition of DAAO activity was observed to reduce the spinal H_2O_2 level (Lu et al., 2012; Gong et al., 2014) and to increase D-Ser levels in the brain and plasma (Adage et al., 2008; Duplantier et al., 2009; Hopkins et al., 2013).

Interestingly, spinal DAAO has been reported to contribute to pain hypersensitivity induced by perturbation of the sleep-regulating circuitries in the CNS (i.e., a “physiological” process) through the deprivation of sleep, that produces pain hypersensitivity without an accompanying nerve or tissue injury (Wei et al., 2013). Also in this case, the role of DAAO has been suggested to be related to the production of ROS species. H_2O_2 produced by the enzyme could act on the pronociceptive TRPA1 channel expressed by central terminals of primary afferent nerve fibers in the spinal dorsal horn.

Neurodegenerative and Neuropsychiatric Disorders

Multiple lines of evidence suggested that dysfunctions in D-Ser metabolism leading to an excessive or a defective production or release, might be associated with chronic neurodegeneration. D-Ser levels were shown to be greatly increased in the spinal cord of patients with familial and sporadic forms of amyotrophic lateral sclerosis (ALS), altered in Alzheimer’s disease affected individuals, and downregulated in schizophrenia (Billard, 2008; Wolosker et al., 2008). Whether the observed abnormal levels depend on the altered expression and/or activity of serine racemase or DAAO is still under investigation.

ALS is the most common adult-onset neuromuscular disorder characterized by the selective degeneration of motor neurons in the spinal cord, brain stem and motor cortex, leading to fatal paralysis. Substantial advances in understanding ALS disease mechanisms has come from the identification of pathogenic mutations in dominantly inherited familial ALS (fALS). Notably, a coding mutation in the *DAO* gene transmitted with the disorder was identified in a three generational fALS kindred

(Mitchell et al., 2010). This mutation yielded to a substitution of Arg by Trp at codon 199, and impaired the enzyme activity. The overexpression of R199W hDAAO in primary motor neuron cultures or motor neuron cell lines was reported to promote the formation of ubiquitinated protein aggregates, to activate autophagy and to increase apoptosis, whereas the wild-type protein was without effect on cell survival (Paul and de Belleruche, 2012; Paul et al., 2014). Although these pathogenic effects could be mediated primarily by the accumulation of the mutant protein, other factors might be relevant, such as the impaired activity of DAAO and the consequential dysfunctional effects on D-Ser metabolism. Accordingly, co-culturing motor neurons with glial cells expressing R199W hDAAO variant was sufficient to induce apoptosis in motor neurons, an effect reversed by the treatment with an NMDAR antagonist selective for the D-serine/glycine site. These observations indicated that the way by which the observed neurotoxic effect was transmitted crucially depended on D-Ser (Paul et al., 2014).

Interestingly, studies performed in *ddY/DAAO^{-/-}* mice showed that these animals developed an abnormal limb reflex and a significant loss of motor neurons in lumbar spinal cord at 8 months (Sasabe et al., 2012). Both in this transgenic line and in the *SOD^{G93A}* mouse model of ALS, D-Ser was shown to accumulate in the spinal cord during the progression of ALS-related abnormal processes. This was accompanied by a marked suppression of DAAO activity in the reticulospinal tract, a pathway known to play an important role in regulating motor neuron excitability (Sasabe et al., 2012). Consistently to these studies, a recently generated transgenic mouse line expressing R199W DAAO (*DAO^{R199W}*) exhibited the characteristic features of several ALS models including *SOD1^{G93A}* mice (decreased body weight, marked kyphosis and loss of motor neurons in spinal cord), albeit the overall survival of these animals appeared to be unaffected by the transgene expression (Kondori et al., 2017). Despite no overt ALS phenotype was observed in *DAO^{R199W}* mice, marked abnormal structural, and motor features associated with a significant loss of lumbar motor neurons, were evident. It was proposed that, as seen in other cases, while a mutation can cause a lethal disease in humans, it may not be possible to generate the same phenotype in a transgenic mouse model carrying the same mutation (Kondori et al., 2017). In fact, hDAAO showed fairly different biochemical properties compared to the rodent’s enzyme (Frattini et al., 2011). Notably, enhanced ubiquitination was detected in the cell bodies of large motor neurons of *DAO^{R199W}* mice, confirming that a prominent feature of the cells expressing the mutant DAAO R199W allele was the presence of ubiquitinated protein aggregates.

Two recent studies have further supported the relevance of DAAO dysfunction to ALS pathogenesis. A comprehensive exome sequencing study revealed that, among the known ALS predisposition gene, *DAO* is the only one where the presence of DNA variants is significantly associated with clinical outcome, decreasing rates of survival (Cirulli et al., 2015). In a work investigating the function of an RNA binding protein encoded by the *HnRNPA2B1* gene, and the effect of the ALS-associated mutation D290V (promoting the protein aggregation in the

nucleus and abnormal splicing events), it was found that the most significant and robust splicing change after depletion of hnRNP A2/B1 in the mouse spinal cord was the skipping of exon 9 within *DAO* gene, yielding to a shorter transcript isoform (Martinez et al., 2016). This alteration resulted in a reading frameshift and early termination of the protein. The resulting DAAO isoform was predicted to lack 2 α -helices and 3 β -sheets: it was highly unstable and its enzymatic activity was largely impaired.

Beside motor disorders, Alzheimer's disease (AD) is characterized by cognitive impairments such as dementia and neurodegeneration. Although different mechanisms, such as neuronal apoptosis and inflammatory responses, are thought to be involved in the pathogenesis, increasing evidence has suggested that alterations in various receptors might account for the progression of cognitive decline. Excitotoxicity (i.e., the cell death mediated by calcium overload) induced by the overstimulation of NMDAR has been indicated as a potent mechanism in AD pathophysiology (Tannenberg et al., 2004). In this regard, elevated D-Ser levels were reported in patients (Madeira et al., 2008) and could be considered as a pro-death signal in AD that promotes, in conjunction with glutamate, the neurotoxicity exhibited by inflammatory processes. However, the role of NMDAR activity in AD appeared to be more complex. Different studies showed impaired NMDAR signaling pathway in the cerebral cortex and hippocampus of aging brains (Billard, 2008): a defective activation of NMDAR due to reduced D-serine level was shown to occur in aged tissues (Junjaud et al., 2006; Mothet et al., 2006). Being synaptic NMDAR-mediated transmission crucial to neuronal survival, the impaired activation of the receptor (inducing apoptosis and neuronal cell death) might result in loss of neuronal plasticity and cognitive deficits in the aging brain (Ikonomidou et al., 1999; Lei et al., 2008). This NMDAR hypoactivity-induced neurodegeneration was postulated to contribute to AD pathogenesis (Olney et al., 1997; Wozniak et al., 1998) and it could be involved in the progression of aging brain from mild cognitive impairment to AD. In this regard, it has been proposed that NMDAR-enhancing agents might be beneficial for the early declining process of AD. Supporting this idea, D-Ser was shown to exert a neuroprotective effect against apoptosis, promoting neuronal survival (Esposito et al., 2012) and the DAAO competitive inhibitor sodium benzoate was found to ameliorate cognitive and overall function in patients with early phase AD (Lin et al., 2014). Furthermore, recently increased levels of DAAO have been reported in the serum of mild cognitive impairment patients, as well as mild and severe AD patients, compared to healthy individual (Lin et al., 2017). Worthy of note, the flavoenzyme levels increased with the severity of cognitive deficit and were significantly associated with D-Ser serum content.

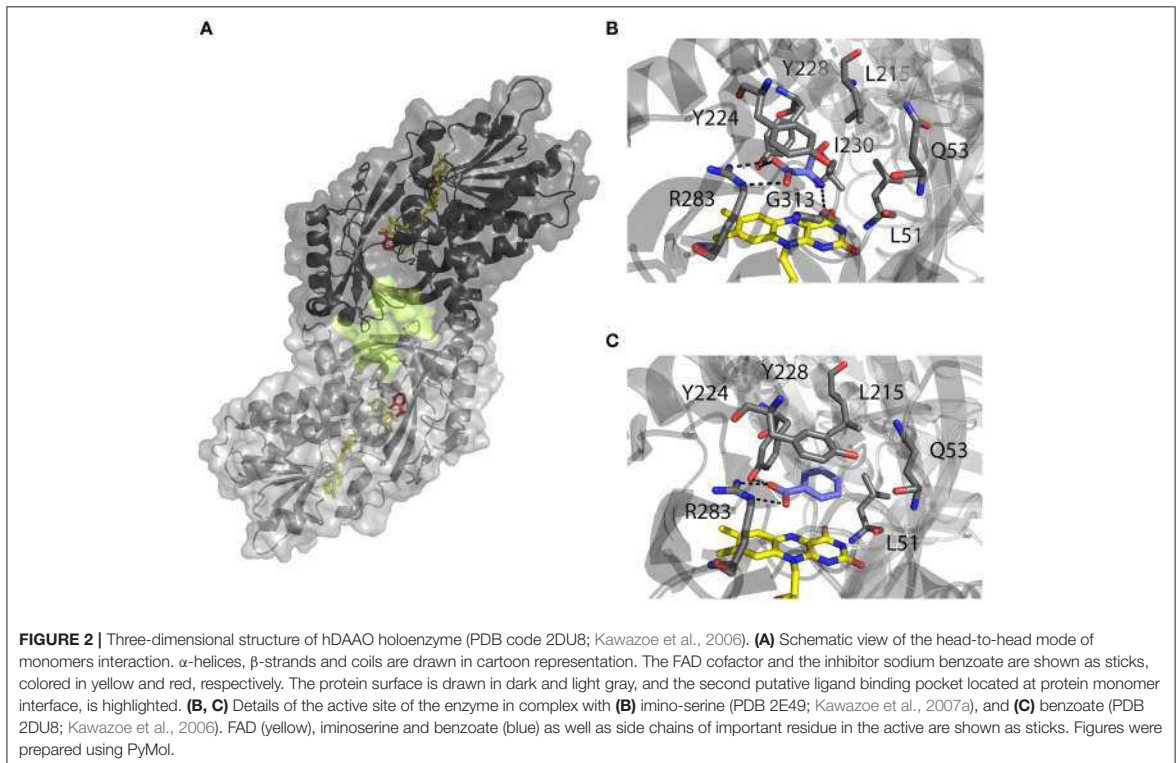
Recent studies highlighted the role of synaptic transmitters and their receptors in the etiology of psychiatric disorders. Converging pharmacological, genetic, and neuropathological studies have led to the widely accepted NMDAR hypofunction model of schizophrenia (Coyle et al., 2003; Coyle, 2006; Stone and Pilowsky, 2007). In particular, a deficiency of D-Ser signaling was proposed to be responsible for the altered activation state of the receptor. Several lines of evidence supported this hypothesis: (i)

decreased D-Ser levels were reported in serum and cerebrospinal fluid of schizophrenia affected individuals (Hashimoto et al., 2003, 2005); (ii) clinical trials demonstrated the beneficial effects of D-Ser as an add-on therapy to antipsychotic treatment (Heresco-Levy et al., 2005); (iii) D-Ser produced behavioral and neurochemical alterations consistent with clinical effects when administered to animal models (Verrall et al., 2010 and references therein). These findings suggested that DAAO, through its role in D-Ser metabolism might contribute to the proposed NMDAR dysfunction in schizophrenia. This hypothesis was strengthened by the discovery of its interaction with the product of the primate specific gene *G72*, linked to schizophrenia and encoding the small protein pLG72. Indeed, it was shown to modulate DAAO activity, even though along the years the effect of the DAAO-pLG72 protein complex formation has been contrasting: at first, pLG72 was proposed to act by increasing the enzyme activity (and accordingly it was defined DAAO activator, DAOA; Chumakov et al., 2002); while subsequent *in vitro* and cellular studies repeatedly and consistently indicated that pLG72 negatively affected DAAO functional properties, and acted by reducing its activity and destabilizing the protein structure (Sacchi et al., 2008, 2016; Pollegioni et al., 2018). Although some aspects of DAAO-pLG72 interaction need further investigations, several meta-analyses have provided a moderate degree of support for a genetic association between *G72*, *DAO*, and schizophrenia, thus sketching them in the category of schizophrenia susceptibility genes.

DAAO involvement in the pathophysiology of the neuropsychiatric disease was proposed also based on altered levels of enzyme expression and activity detected in post-mortem brain tissues from affected individuals, rather than merely on genetic analysis, which can be inconclusive in the case of a complex multifactorial disorder. Increased enzymatic activity and gene or protein expression were reported in cerebral cortex (Madeira et al., 2008), cerebellum (Kapoor et al., 2006; Verrall et al., 2007; Burnet et al., 2008), medulla oblongata and choroid plexus (Ono et al., 2009) of schizophrenic patients, suggesting that the onset of the disease is associated with abnormal DAAO levels in different brain areas.

hDAAO Biochemical Properties

hDAAO structural and biochemical properties have been extensively investigated using the recombinant enzyme produced in *E. coli* (Molla et al., 2006; Sacchi et al., 2008; Caldinelli et al., 2010). Meanwhile, the crystallographic structure was resolved (Kawazoe et al., 2006). The human enzyme was reported to be a stable homodimer, characterized by a head-to-head mode of monomer interaction (Figure 2A). Each monomer (347 amino acids, 40.3 kDa) was shown to contain a non-covalently bound FAD molecule and to be composed by 11 α -helices and 14 β -strands, that fold into two interconnected regions: a substrate binding domain, with a large twisted antiparallel β -sheet forming the active-site roof and part of the oligomerization interface; and a FAD binding domain containing the dinucleotide binding motif (Rossmann fold). The cofactor was found to be buried in the protein core in an elongated conformation, with the isoalloxazine ring located at the interface of the two domains and the *re*-face



in the inner part of the active site (Kawazoe et al., 2006; Molla, 2017).

Based on the enzyme three-dimensional structure, several considerations can be made. The substrate binds to the active site where it is positioned above the *re*-side of the cofactor, in the correct orientation with respect to the reactive N(5) of the isoalloxazine moiety: the dehydrogenation of the substrate occurs by the direct hydride transfer of the α -hydrogen from the α -carbon of the D-amino acid to the flavin N(5) (Figure 1). Several H-bond interactions concur in fixing and stabilizing the substrate in the active site (Figure 2B). Namely, α -COOH group of the substrate interacts with the active site residues Arg283 and Tyr228, whereas the α -NH₂ group is connected with Gly313 and the C(4)=O of the cofactor. The substrate side chain is located in an active site pocket made up by bulky and hydrophobic residues (i.e., Leu51, Gln53, Leu215, and Ile230; Kawazoe et al., 2006). Further, the “roof” of the active site is formed by the side chain of Tyr224 that is part of a mobile loop (216-228), which switches from a close to an open conformation to allow the product/substrate exchange during the catalysis.

hDAAO showed peculiar biochemical properties. Differently to others DAAOs (Mattevi et al., 1996; Pollegioni et al., 2007; Frattini et al., 2011), the enzyme appeared to be a homodimer, in both the holo- and the apoprotein form (Molla et al., 2006). This was proposed to depend on a distinctive charge distribution at the dimer interface, where a significantly higher

amino acidic substitution frequency compared to the overall protein was observed (33% vs. 15%, respectively; Kawazoe et al., 2006). The binding of the FAD cofactor to the human enzyme was determined as the weakest among known DAAOs ($K_d = 8.0 \mu\text{M}$ for hDAAO vs. 0.2 and $0.02 \mu\text{M}$ for pig kidney and yeast DAAOs, respectively), although the presence of a ligand in the active site stabilized the flavin interaction ($K_d = 0.3 \mu\text{M}$) (Molla et al., 2006; Caldinelli et al., 2010). Due to the low affinity of FAD interaction, hDAAO was reported to be present in solution as an equilibrium of holo- and apoprotein forms (Caldinelli et al., 2010). Benzoate binding has been recently shown to promote a conformational switch yielding a form with a higher avidity for FAD (Murtas et al., 2017a). DAAO-catalyzed oxidative deamination was demonstrated to follow a ternary-complex mechanism (Pollegioni et al., 1993; Umhau et al., 2000). For hDAAO the reductive half-reaction was very fast ($117 \pm 6 \text{ s}^{-1}$ on D-Ser) but the turnover was much slower ($6.3 \pm 1.4 \text{ s}^{-1}$), the product release representing the rate-limiting step (Molla et al., 2006; Molla, 2017). Because of the plasticity of the active site lid, hDAAO showed a wide substrate specificity. Best substrates were shown to be hydrophobic D-AAs (D-DOPA > D-Tyr > D-Phe > D-Trp); among them D-DOPA yielded to the highest k_{cat} value, although different kinetic parameters were reported (Kawazoe et al., 2007a; Murtas et al., 2017a). The human enzyme was also reported to catabolize small uncharged D-AAs (D-Cys > D-Ala > D-Pro > D-Ser) (Molla et al., 2006; Kawazoe et al.,

2007a; Frattini et al., 2011; Murtas et al., 2017a). Notably, some of them play a relevant role in neurotransmission. In particular, hDAAO showed the highest catalytic efficiency for D-cysteine, an intermediate of H₂S metabolic pathway (see above; Murtas et al., 2017a). Glycine and acidic D-AAAs were only poorly degraded by the human enzyme (Molla et al., 2006; Murtas et al., 2017a).

It has been demonstrated that hDAAO functionality is modulated by the interaction with other proteins. In particular, the enzyme was shown to specifically bind to the small and primate-specific protein pLG72: two hDAAO homodimers interacted with two pLG72 molecules in a 200 kDa protein complex (for a recent review on pLG72-hDAAO interaction see Pollegioni et al., 2018). *In vitro*, the complex formation modified hDAAO tertiary structure, causing a time-dependent loss of activity (Sacchi et al., 2008). Accordingly, at the cellular level hDAAO-pLG72 interaction positively affected D-Ser cellular levels and decreased hDAAO half-life (Sacchi et al., 2008, 2011; Cappelletti et al., 2014). The structural details of the interaction remain to be fully elucidated: a prominent role of the C-terminal region in the modulation of hDAAO activity was initially proposed (Chang et al., 2013); but further analyses performed by using different recombinant pLG72 deletion variants, while confirming that C-terminal terminal region is likely required to induce the alterations in hDAAO conformation associated with the loss of catalytic functions, indicated that the N-terminal region of the protein was crucial for the strength of the protein complex formation (Birolo et al., 2016). The enzyme activity was reported to be also negatively modulated by bassoon, a protein of the cytoskeletal matrix, enriched in the presynaptic active zone. hDAAO-bassoon interaction was proposed to play a homeostatic role in preventing D-Ser depletion by an active and extraperoxisomal hDAAO form detected in at presynaptic terminals (Popielek et al., 2011). Worthy of note, bassoon inhibitory effect might in part explain why hDAAO enzymatic activity was barely detectable in the forebrain (Verrall et al., 2007), where hDAAO was thought to be mainly expressed in neurons, albeit at fairly low levels.

Since abnormal changes in hDAAO activity leading to locally decreased D-Ser levels have been correlated with severe neurological disorders (such as schizophrenia), the design, and selection of hDAAO inhibitors to be used as drugs has gained a growing interest (Ferraris et al., 2008). The mode of binding of the substrate-competitive inhibitor benzoate to the hDAAO active site is shown in **Figure 2C**. An exhaustive dissertation about the structural details relevant for hDAAO inhibitors binding has been recently published (Molla, 2017).

Despite the tremendous work that has been done so far, there are still some aspects concerning hDAAO structural/functional relationships that must be clarified: recent computational and labeling analyses has suggested the presence of an unexpected, additional ligand binding site located at the interface between the two monomers of the holoenzyme (**Figure 2A**; Kohiki et al., 2017). This hypothesis was supported by experimental evidences showing two different phases in benzoate binding to the holoenzyme, and indicating the existence of two different conformations with different ligand affinities or two different ligand binding sites (Murtas et al., 2017a).

Noteworthy, altogether these investigations suggest that evolution has adopted sophisticated strategies to finely modulate the activity of hDAAO in order to use this enzyme in different tissues responding to several needs.

INACTIVE hDAAO VARIANTS POTENTIALLY RELATED TO NEURODEGENERATIVE DISORDERS

Based on cellular and biochemical studies, the R199W, R199Q, G183R, and G331V hDAAO variants could be related to the onset of neurodegenerative diseases. For all these protein variants, the substitution significantly reduced (when not fully abolished) the enzyme activity. This in turn, might result in increased D-Ser levels at the synapses and a consequent hyperactivation of NMDAR, a condition known to induce cytotoxicity and neuronal cell death (Mitchell et al., 2010). The G183R hDAAO variant corresponds to the coding SNP that naturally occurs in the ddY/DAAO^{-/-} mice strain expressing the homologous G181R DAAO characterized by the complete loss of the enzymatic activity (Konno and Yasumura, 1983). On the other hand, the R199W hDAAO variant has been associated with the onset of fALS (Mitchell et al., 2010) and, to date, it is the unique hDAAO variant linked to a human disease. The R199W substitution was shown, not only to strongly affect the enzyme activity (Cappelletti et al., 2015), but also to promote protein aggregation and to be responsible of primary motor neuron degeneration (Mitchell et al., 2010; Paul and de Bellerocche, 2012). The R199Q hDAAO variant corresponds to a confirmed substitution reported in the SNPs database (rs200850756). As expected, this protein variant showed biochemical features resembling those reported for the R199W one (Cappelletti et al., 2015). Finally, the G331V substitution is encoded by the reported hDAAO SNP rs4262766. Its overexpression in U87 human glioblastoma cell line resulted in low viability of the transfected cells, since it was shown to promote the formation of toxic protein aggregates and to induce apoptosis (Caldinelli et al., 2013). Among the aforementioned substituted residues, G183 and R199 are highly conserved in DAAOs from different sources (**Figure 3**).

As we can deduce from hDAAO three-dimensional structure, G183 belongs to the $\alpha 9$ α -helix, which is close to pyrophosphate and ribityl groups of the cofactor (**Figures 4A,B**). Here, the substitution of the wild-type residue with an arginine likely leads to additional electrostatic and H-bond interactions with the surrounding residues side chain, as well as with the -CO and -NH backbone groups that are in close contact with the adenine nucleotide moiety of FAD (**Figure 4B**). It has been proposed that this results in local alterations of the protein variant conformation that negatively affect the cofactor binding and its correct orientation required for hydride transfer during catalysis (Murtas et al., 2017b).

R199 is on the β -strand $\beta 8$, which lies close to the FAD and substrate binding site. Intriguingly, this residue is placed at the protein surface (~ 11 Å from the isoalloxazine ring, thus pretty close to the active site), at the center of a tight H-bond network with residues of α -helix $\alpha 10$ and β -strands $\beta 8$ and

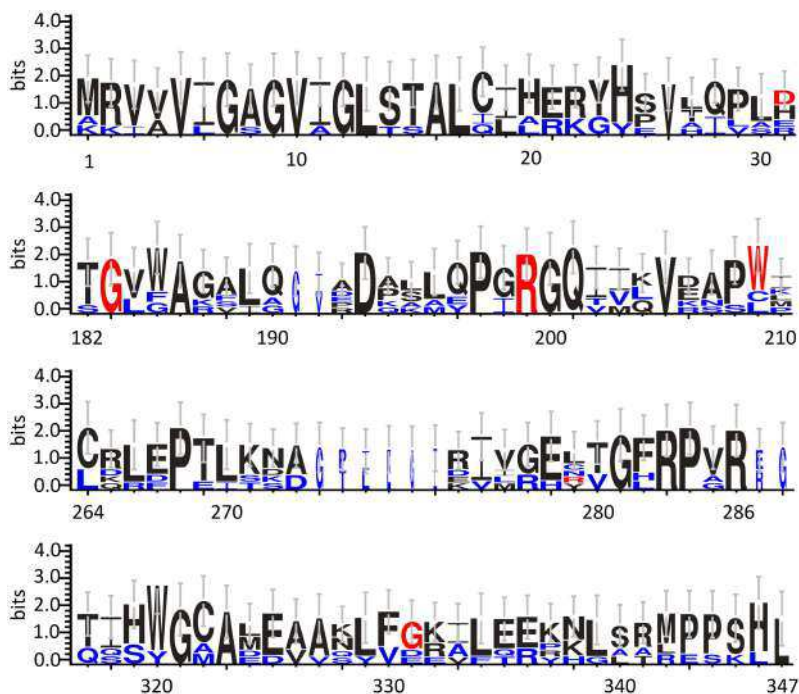


FIGURE 3 | Frequency of sequence conservation among DAAOs from different sources. WebLogo representation of conserved residues identified by the alignment of DAAOs from mammals (*Homo sapiens*, *Mus musculus*, *Rattus norvegicus*, *Sus scrofa*) and yeast (*Rhodotorula gracilis* and *Trigonopsis variabilis*). The x-axis represents amino acid position (the annotated numbering refers to the human enzyme). The y-axis indicates the sequence conservation at that position (measured in bits), whereas the height of symbols is proportional to degree of conservations of single residues. Panels represent sequence stretches of 31 amino acids containing the residues that are substituted in the hDAAO variants discussed in this review (shown in red). Residues belonging only to the yeast sequences are shown in blue. Figure prepared using WebLogo 3.0 (Crooks et al., 2004).

β 12, secondary structure elements belonging to the interface domain (Figures 4A,C). Moreover, since R199 interacts with R283, its substitution might affect the conformation of this key active site residue, possibly impairing the ability of hDAAO variants to stabilize the binding of substrate/inhibitors. Indeed, not only the carbonyl group on the main chain of R199 directly interacts with R283 side chain, but the side chain is H-bonded to T280 belonging to the same β -strand of R283 (β 12) (Figure 4C; Cappelletti et al., 2015). In this context, the substitution of R199 with a Trp has been proposed to be responsible of a significant alteration in the conformation of the loop between β 11 and α 10 due to the different steric hindrance. On the other hand, the substitution with a Gln likely causes the loss of a positive charge and consequently of the existing electrostatic interaction. Altogether, the R199W and R199Q have been suggested to promote the disruption of relevant interactions, thus affecting the overall protein conformation and the enzymatic activity (Cappelletti et al., 2015).

On the other hand, G331 appears to be highly conserved in higher organisms only (Figure 3). It is located on the C-terminal α -helix, near the protein surface, apparently exposed to the solvent (Figures 4A,D). G331 is far from both the active

site and the interface between monomers, in a region probably involved in the protein folding process and exposed in the folding intermediate(s) (Caldinelli et al., 2004). In this case, the substitution of the wild-type Gly with a Val has been proposed to affect the helix structure and produce a hydrophobic surface, which makes the hDAAO variant prone to aggregation (Caldinelli et al., 2013).

Expression in *E. coli* and Biochemical Properties

The different hDAAO variants have been overexpressed in *E. coli* as recombinant proteins fused with an N-terminal 6XHis-Tag, and subjected to further characterization. Growth conditions were modified and adapted for each hDAAO variant (Caldinelli et al., 2013; Cappelletti et al., 2015; Murtas et al., 2017b), since using the expression conditions set up for the wild-type enzyme all the protein variants were largely produced as inclusion bodies, in the insoluble fraction of the cell extract. Despite the optimized fermentation protocols led to increased levels of soluble protein expression, the purification yield was always lower than for the wild-type protein (see Table 2). The G183R hDAAO was purified as fully inactive apoprotein (Murtas et al., 2017b). Analogously,

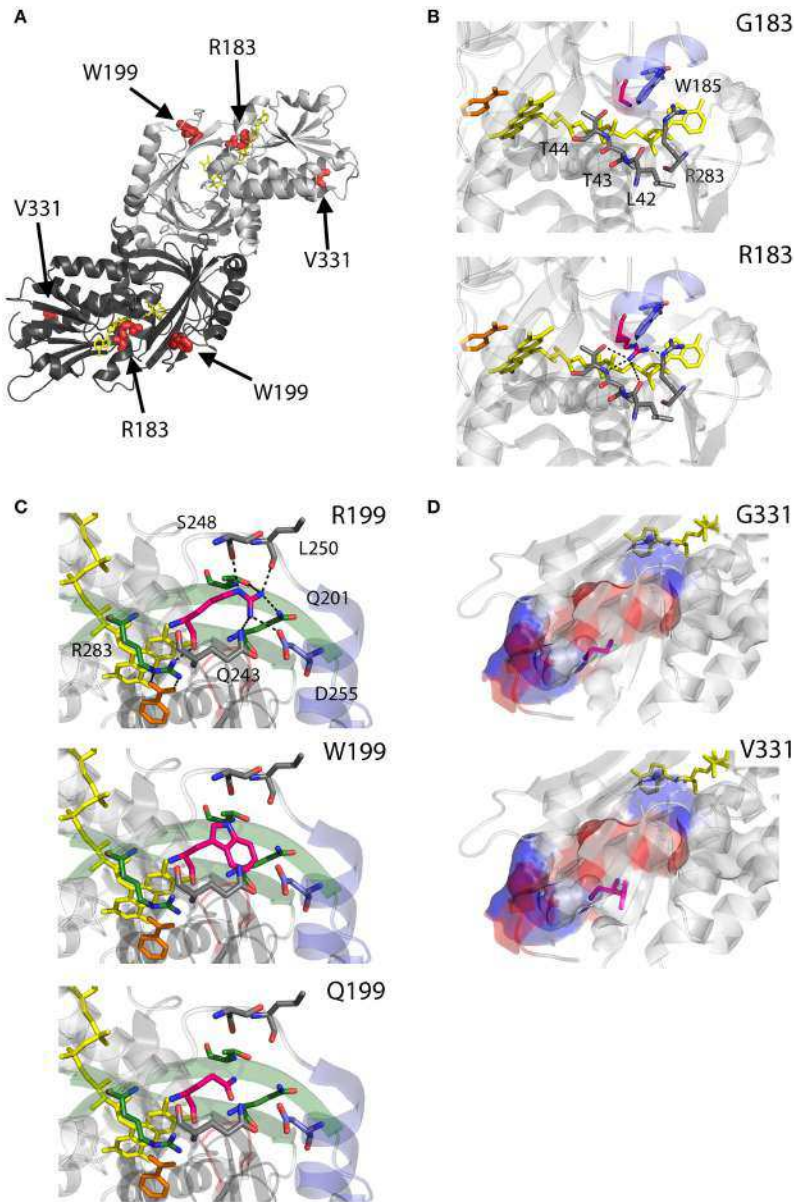


FIGURE 4 | Structural models of hDAAO inactive variants. **(A)** The position of the point mutations on the protein dimeric structure (PDB code: 2DU8; Kawazoe et al., 2006) is shown. Substituted residues encoded by SNPs are depicted as thick sticks in red, while FAD cofactor is reported in yellow. **(B–D)** Details of the protein microenvironment surrounding at the mutated residues in the different hDAAO variants. The substituted residues are shown as sticks in magenta. The surrounding residues within a distance of 4 Å are shown as sticks in gray. Loops, α -helices and β -sheets indicated in the text are shown as cartoon in red, blue and green, respectively. The substrate-competitive inhibitor benzoate and the FAD cofactor are shown as sticks in orange and yellow, respectively. H-bond interactions are reported as black dashed line. Negatively charged (blue), positively charged (red) and neutral (gray) surfaces of the C-terminal α -helix are shown in **(D)**. Figure were prepared with PyMol. Adapted from Caldinelli et al. (2013); Cappelletti et al. (2015); Murtas et al. (2017b).

the purified R199W and R199Q variants were largely purified in apoprotein form, and showed a significantly reduced specific activity compared to the wild-type hDAAO (Table 2; Cappelletti et al., 2015). On the other hand, the expression and purification yields for the G331V hDAAO were consistently too low to allow a detailed biochemical characterization. However, its estimated specific activity closely resembled the value determined for the recombinant wild-type hDAAO (Table 2; Caldinelli et al., 2013).

Several attempts were performed to reconstitute G183R hDAAO variant (Murtas et al., 2017b); however, the resulting preparation, despite showing the absorbance spectrum of the oxidized holoenzyme, was still inactive. R199W and R199Q hDAAO variants showed a dramatically reduced catalytic efficiency with respect to the wild-type enzyme, mostly due to a consistent increase in the K_m values (Table 3). Notably, when measurements were performed using 1 mM D-Ser (a concentration similar to that detected in normal brain; Hashimoto et al., 1995) the activity of R199W and R199Q hDAAO variants was undetectable (Cappelletti et al., 2015).

Furthermore, a significantly decreased cofactor binding affinity was observed for the two hDAAO variants, both in the free and benzoate complexed forms (Table 4; Cappelletti et al., 2015). On the other hand, the G183R hDAAO variant retained the FAD binding affinity, albeit the strength of the interaction drastically decreased in presence of an excess of benzoate (Table 4; Murtas et al., 2017b). The binding properties of all the variants in general appeared altered: an overall decrease in binding affinity for known competitive inhibitors compared to the wild-type enzyme has been observed (Table 4). Notably, the most pronounced changes were detected for the R199W and R199Q variants; in particular, the estimated K_d values for benzoate were 300-fold and 600-fold higher compared to the wild-type one, respectively. The ability of R199Q and G183R hDAAO to interact with the regulatory protein pLG72 was unaffected by the substitution (Cappelletti et al., 2015; Murtas et al., 2017b; Table 4). In the case of the R199W hDAAO instead, its oligomeric state (see below) made unfeasible the identification of the hDAAO-pLG72 protein complex formation.

Alterations in Protein Conformation

As determined by circular dichroism (CD) analyses, the G183R, R199W, and R199Q hDAAO holoenzymes conformation appeared to be modified with respect to the wild-type holoenzyme (Figure 5): while minor changes in secondary structure elements content were observed for G183R and R199W protein variants (Figure 5A), their tertiary structure appeared to be specially affected (Figure 5B). In particular, the near-UV CD spectrum of the G183R hDAAO holoenzyme strictly resembled the apoprotein one. Only minor alterations compared to the wild-type enzyme were instead detected in the near-UV CD spectra of the apoprotein forms of the different hDAAO variants (Figures 5C,D; Cappelletti et al., 2015; Murtas et al., 2017b). Furthermore, protein stability studies performed by analyzing the temperature sensitivity of parameters that allowed to monitor changes in secondary and tertiary structures (the CD signal at 220 nm and tryptophan fluorescence, respectively), revealed that the melting temperature estimated for the R199W and R199Q

variants was up to 13°C higher compared to the wild type one (Cappelletti et al., 2015), pointing to a decrease in the protein flexibility.

Size exclusion chromatography studies indicated that hDAAO oligomeric state was unaffected by the G183R substitution (Murtas et al., 2017b). On the other hand, the holoenzyme form of R199W hDAAO was found to be tetrameric, at concentration ≥ 1 mg/mL. Moreover, at lower concentrations, both the holo- and the apoprotein forms of the R199W and R199Q variants showed a chromatographic profile in-between a dimeric and a tetrameric state, suggesting that they assumed a less tightly packed conformation compared to the wild-type hDAAO (Figure 6, Cappelletti et al., 2015).

Cellular Studies

In Cos-7 cells expressing R199W hDAAO (following transient transfection), the inactive variant, similarly to the wild-type enzyme, was shown to be correctly targeted to peroxisomes, where it forms heterodimers with the endogenously expressed wild-type protein. This results in a significant reduction of the enzyme activity, suggesting a potential dominant negative effect of the fALS associated mutation (Mitchell et al., 2010). Accordingly, U87 human glioblastoma cells clones stably expressing G183R, R199W and R199Q hDAAO variants as chimeric protein with the N-terminal region fused with the enhanced yellow fluorescent protein (EYFP), showed significantly increased D-Ser cellular concentrations. In particular, a 7-fold increase in D-Ser levels was observed in cells expressing the G183R variant compared to cells expressing the wild-type protein (Table 5), suggesting that the availability of the neuromodulator at the synapses may be also affected (Cappelletti et al., 2015; Murtas et al., 2017b). Worthy of note, the expression of R199W and R199Q hDAAO (as well as the wild-type enzyme) did not alter U87 cells viability (Cappelletti et al., 2015), as was instead apparent in motor neurons (Mitchell et al., 2010). Similar results were obtained in cell clones expressing the G183R variant (Murtas et al., 2017b). On the other hand, U87 cells transiently expressing G331V hDAAO showed significantly reduced cells viability. Accordingly, isolating stable cell clones overexpressing this hDAAO variant was not feasible (the transfected cells did not survive to the selection procedure) and cellular studies were performed in transiently transfected cells (Caldinelli et al., 2013). The observed effect was accompanied by the formation of consistent amount of the overexpressed protein aggregates and a significant increase in apoptosis, as assessed by caspase activity detection (Caldinelli et al., 2013). Intriguingly, both the G183R and G331V hDAAO variants appeared to be partially mistargeted within the U87 transfected cells: the two variants formed extraperoxisomal protein aggregates, which largely colocalized with ubiquitin (Caldinelli et al., 2013; Murtas et al., 2017b). Both the low solubility and the cytosolic localization of G331V hDAAO, which was supposed to be active (thus to oxidize cytosolic D-Ser producing cytotoxic H_2O_2), might explain the observed low cell viability (Caldinelli et al., 2013). Notably, the overexpression of the inactive G183R hDAAO did not enhance apoptosis (Murtas et al., 2017b).

TABLE 2 | Expression conditions of recombinant hDAAO variants in *E. coli*.

hDAAO variant	Wild-type ^a	G183R ^b	R199Q ^c	R199W ^c	G331V ^d	D31H ^d	W209R ^c	R279A ^d
<i>E. coli</i> strain	BL21 (DE3) STAR	BL21 (DE3) STAR	BL21 (DE3) STAR	BL21 (DE3) STAR	Origami (DE3)	BL21 (DE3) STAR	BL21 (DE3) STAR	BL21 (DE3) STAR
FERMENTATION CONDITIONS								
Cultivation broth	TB	TB	TB	TB	TB	TB	TB	TB
Riboflavin addition (μM)	/	/	/	10	/	/	/	/
IPTG (mM)	0.1	0.6	0.6	0.6	0.1	0.1	0.6	0.1
Temperature after induction ($^{\circ}\text{C}$)	37	37	30	23	37	37	37	37
Time of collection after induction (h)	4	20	20	2	4	4	20	4
Purified protein (mg/L)	7.0	5.4	2.0	3.0	0.1	20.0	10.0	10.0
Specific activity (U/mg)	12.0	/	1.2	4.1	2.9 (11.6)*	14.0	12.0	10.5
Purity (%)	≥ 90	≥ 90	≥ 90	≥ 90	25	≥ 90	≥ 90	≥ 90

The specific activity was determined using the oxygen consumption assay (0.25 mM oxygen, 25°C) at 28 mM D-alanine in presence of an excess of FAD (200 μM).

*Value estimated based on the ~25% purity (see text for details).

^aMolla et al., 2006; ^bMurtas et al., 2017b; ^cCappelletti et al., 2015; ^dCaldinelli et al., 2013.

TABLE 3 | Apparent kinetic parameters of hDAAO variants.

hDAAO variant	D-Serine			D-Alanine		
	k_{cat} (s^{-1})	K_{m} (mM)	$k_{\text{cat}}/K_{\text{m}}$ ($\text{s}^{-1}\text{mM}^{-1}$)	k_{cat} (s^{-1})	K_{m} (mM)	$k_{\text{cat}}/K_{\text{m}}$ ($\text{s}^{-1}\text{mM}^{-1}$)
Wild-type ^a	3.0 ± 0.1	7.5 ± 3.1	0.4	5.2 ± 0.2	1.1 ± 0.2	4.7
R199Q ^b	≥ 8	≥ 2000	0.004	≥ 10	≥ 2000	0.005
R199W ^b	≥ 15	≥ 2000	0.0075	~ 15	~ 400	0.04
D31H ^c	3.0 ± 0.2	3.9 ± 0.9	0.77	6.0 ± 0.2	0.95 ± 0.1	6.3
W209R ^b	7.2 ± 0.2	17.3 ± 3.5	0.42	11.8 ± 0.2	1.2 ± 0.2	8.6
R279A ^c	2.5 ± 0.1	3.4 ± 0.5	0.74	8.6 ± 0.1	1.0 ± 0.1	8.6

The activity was assayed at air saturation (0.25 mM oxygen), 25°C, and pH 8.5.

^aMolla et al., 2006; ^bCappelletti et al., 2015; ^cCaldinelli et al., 2013.

TABLE 4 | Binding properties of hDAAO variants.

hDAAO variant	FAD (K_{d} , μM) ^a		Benzoate (K_{d} , μM)	CBIO (K_{d} , μM)	CPZ ^a (K_{d} , μM)	pLG72 ^c interaction
	Free form	Benzoate complex				
Wild-type ^d	7.9 ± 0.2	0.3 ± 0.1	$7.0 \pm 2.0^{\text{b}}$	$101 \pm 24.0^{\text{b}}$	5.0 ± 0.1	Yes
G183R ^e	8.4 ± 1.9	235 ± 26.0	$6500 \pm 400^{\text{a}}$	$628 \pm 25.0^{\text{a}}$	9.3 ± 0.2	Yes
R199Q ^f	33.5 ± 1.6	28.4 ± 3.9	$4160 \pm 230^{\text{b}}$	$342 \pm 11.0^{\text{b}}$	16.2 ± 5.3	Yes
R199W ^f	40.3 ± 2.6	14.6 ± 1.4	$2140 \pm 130^{\text{b}}$	$157 \pm 30.0^{\text{b}}$	11.1 ± 1.6	n.d.
D31H ^g	1.8 ± 0.1	0.13 ± 0.02	$4.6 \pm 0.4^{\text{b}}$	n.d.	4.8 ± 0.3	Yes
W209R ^f	1.9 ± 0.1	0.15 ± 0.001	$3.9 \pm 1.2^{\text{b}}$	$96.0 \pm 36.0^{\text{b}}$	2.0 ± 0.8	Yes
R279A ^g	0.9 ± 0.1	0.03 ± 0.002	$8.0 \pm 0.5^{\text{b}}$	n.d.	6.4 ± 0.3	Yes

^a K_{d} values determined by monitoring the quenching of protein fluorescence.

^b K_{d} values determined by monitoring the perturbation of flavin absorbance spectra.

^cAnalysis of pLG72 binding performed by gel-permeation chromatography. The hDAAO R199W elution volume is close to that of the hDAAO-pLG72 complex, making unfeasible the identification of the complex.

n.d. = not determined.

^dMolla et al., 2006; ^eMurtas et al., 2017b; ^fCappelletti et al., 2015; ^gCaldinelli et al., 2013.

Hyperactive hDAAO Variants Potentially Involved in Psychiatric Disorders

Beside the reported inactivating mutations, other amino acid substitutions were identified in hDAAO. The analysis of the

hDAAO protein sequences deposited in the databank revealed a discrepancy at positions 31 and 279, which were indicated as “sequence conflicts.” Namely, Asp31 was substituted with an His residue in a sequence reported in the Uniprot database

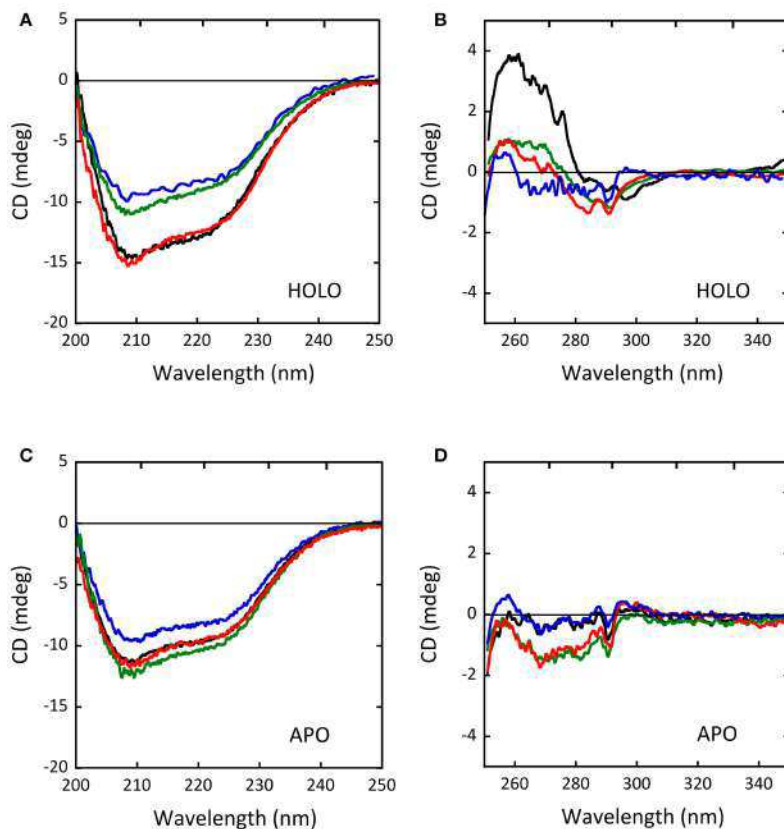


FIGURE 5 | Comparison of the CD spectra of wild-type (black), G183R (blue), R199W (green) and R199Q (red) hDAAO variants. **(A,C)** Far-UV CD spectra of **(A)** the holoenzyme and **(C)** the apoprotein forms of the hDAAO variants (0.1 mg/mL protein concentration). **(B,D)** Near-UV CD spectra of **(B)** the holoenzyme and **(D)** the apoprotein forms of the hDAAO variants (0.4 mg/mL protein concentration). From (Caldinelli et al., 2013; Cappelletti et al., 2015; Murtas et al., 2017b).

(<http://www.uniprot.org/uniprot/P14920>), and Ala279, present in the original sequence of the human *DAO* gene cloned from kidney lysates (Momoi et al., 1988), was substituted by an Arg in the subsequently deposited sequences. To date, it is still unclear whether these differences are due to polymorphisms or sequencing/cloning artifacts. On the other hand, the W209R is a substitution encoded by a confirmed SNP (rs111347906) reported in the database, but currently not associated with a human disease (Cappelletti et al., 2015).

Worthy of note, all the resulting hDAAO substitutions (D31H, R279A, and W209R) were found to exert an opposite effect on the enzyme functionality compared to the ones discussed above: they yielded to hyperactive protein variants (Caldinelli et al., 2013; Cappelletti et al., 2015). The characterization of these protein variants prompted our group to propose their potential involvement in the onset of psychiatric disorders such as schizophrenia: an excessive degradation of D-Ser caused by an abnormal increase of hDAAO enzymatic activity might result into a significant reduced availability of the neuromodulator

at the synapses and the consequent hypofunction of NMDAR. This represents a molecular mechanism that could explain many symptomatic features of schizophrenia (Coyle et al., 2003; Coyle, 2006; Stone and Pilowsky, 2007; Pollegioni and Sacchi, 2010).

D31 is a non-conserved residue (**Figure 3**) located at the β -strand $\beta 2$ on the protein surface, far from both the substrate and the flavin binding sites, as well as from the dimerization interface (**Figure 7A**). For this reason, the effect of the D31H substitution was explained in terms of a long-range interaction affecting the overall protein conformation and propagating from the site of the substitutions to other regions in the structure (Caldinelli et al., 2013). Nonetheless, it is possible to speculate that conformational alterations in this position might involve the loop between the $\beta 6$ and the $\alpha 8$, which central region is close to the nucleotide moiety of the FAD cofactor (**Figure 7B**).

Conversely, W209 is a well-conserved residue in higher organisms (**Figure 3**). It is positioned in the loop between β -strands $\beta 8$ - $\beta 9$ (close to α -helix $\alpha 4$), at the monomers interface (**Figure 7A**). However, this residue is not involved in relevant

hydrophobic interactions with other residues on the surface of the facing subunit: the loss of the indole portion of the tryptophan side chain likely induces minimal modifications of the interaction energy of the hDAAO monomers. Moreover, the positive charge provided by the W209R substitution might result in an additional electrostatic interaction with the negatively charged side chain of E85 of the facing subunit (Figure 7C), de facto stabilizing the dimeric structure (Cappelletti et al., 2015).

R279 is a further non-conserved residue (Figure 3), located on the β -strand β 12, which is involved in a double interaction: (i) it contacts the FAD binding site (it is H-bonded with the carbonyl oxygen of P41, close to the α -helix α 2 in the region containing the VAAGL motif, which has been proposed to play an important role in determining the affinity of hDAAO for the cofactor; Kawazoe et al., 2006), (ii) contributes to the definition of the interface between the two dimers (Figure 7D). The R279A mutation could affect the flavoenzyme binding affinity for the cofactor by altering the conformation of the VAAGL peptide, directly through the loss of the interaction with P41, or indirectly by a general rearrangement of the β 12- α 2 interface region (Caldinelli et al., 2013).

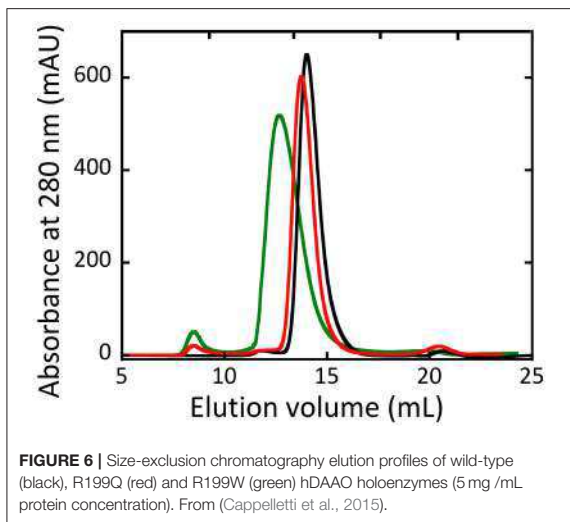


FIGURE 6 | Size-exclusion chromatography elution profiles of wild-type (black), R199Q (red) and R199W (green) hDAAO holoenzymes (5 mg /mL protein concentration). From (Cappelletti et al., 2015).

Expression *E. coli* and Biochemical Properties

Differently to the inactivating hDAAO substitutions, D31H and R279A variants were successfully overexpressed in *E. coli* and purified to homogeneity by using the same conditions set up for the wild-type protein (Table 2; Caldinelli et al., 2013). On the other hand, the fermentation conditions of the W209R variant required further optimization to obtain a final amount of protein similar to the wild-type one (Table 2; Cappelletti et al., 2015).

All these hDAAO variants retained the specific activity of the wild-type flavoenzyme (Table 2; Caldinelli et al., 2013; Cappelletti et al., 2015). They showed a significantly higher affinity for the flavin cofactor (up to 9-fold for R279A hDAAO; see Table 4), thus inducing an increase of the amount of the active holoenzyme species in solution (Caldinelli et al., 2013; Cappelletti et al., 2015). For the D31H and R279A hDAAO variants an improved catalytic efficiency was apparent, due to a decrease in the K_m value for D-Ser and a significant increase in the k_{cat} values for D-Ala (Table 3). The W209R hDAAO variant showed an increase in the apparent k_{cat} on both the substrates (Table 3). Notably, this latter variant was more active than the wild-type hDAAO when 0.3 mM D-Ser and 5 μ M FAD were present in the reaction mixture, i.e., under conditions reproducing physiological ones (Cappelletti et al., 2015).

For all hyperactive variants, no substantial alteration in inhibitors binding affinity was observed (Table 4; Caldinelli et al., 2013; Cappelletti et al., 2015). Furthermore, all variants retained the ability to interact with the hDAAO binding partner pLG72 (Caldinelli et al., 2013; Cappelletti et al., 2015).

Alterations in Protein Conformation

The CD spectra of the holoenzyme and apoprotein forms of the D31H and R279A variants appeared unaltered compared to wild-type-DAAO (Figures 8A–D), indicating that the introduced substitutions did not significantly affect the protein conformation (Caldinelli et al., 2013). On the other hand, differences in far-UV and near-UV CD spectra for the W209R variant were reported (Cappelletti et al., 2015), pointing a decreased α -helix content in the holoenzyme form (~31% of vs. 37% of wild-type protein; Figures 8A,C; Cappelletti et al., 2015). No alterations of the oligomerization state were instead observed (Caldinelli et al., 2013; Cappelletti et al., 2015).

TABLE 5 | Effect of the expression of EYFP-hDAAO on the cellular concentrations of serine enantiomers.

hDAAO variants	Stably transfected cells							Transiently transfected cells Time upon transfection			
	Wild-type ^a	G183R ^b	R199Q ^a	R199W ^a	D31H ^c	R279A ^c	24 h		48 h		
							Wild-type ^a	W209R ^a	Wild-type ^a	W209R ^a	
D-Serine (pmol)	1.5 ± 0.3	13.3 ± 1.4	5.9 ± 0.7	2.9 ± 0.9	0.59 ± 0.2	0.38 ± 0.3	12.4 ± 0.6	9.0 ± 1.0	7.1 ± 0.5	5.7 ± 0.01	
L-Serine (pmol)	72.8 ± 27.2	45.0 ± 1.6	153 ± 18.4	84.1 ± 18.3	53.7 ± 10.1	28.8 ± 10.8	203 ± 7.0	207 ± 0.8	111 ± 1.7	119 ± 10.3	
D/(D+L)-Serine (%)	2.2 ± 0.5	28.2 ± 8.3	3.7 ± 0.01	3.3 ± 0.3	1.2 ± 0.6	1.2 ± 0.6	5.8 ± 0.4	4.2 ± 0.06	6.0 ± 0.3	4.6 ± 0.04	

HPLC analyses were performed on U87 human glioblastoma cells stably or transiently expressing the different hDAAO variants.

^aCappelletti et al., 2015; ^bMurtas et al., 2017b; ^cCaldinelli et al., 2013.

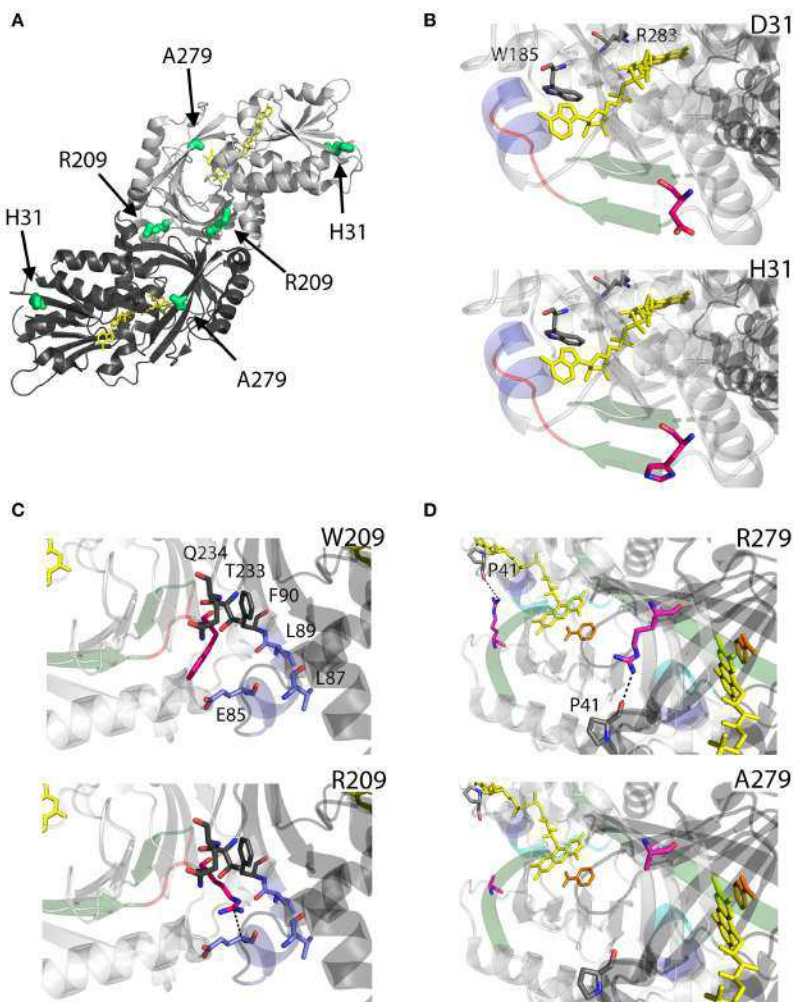


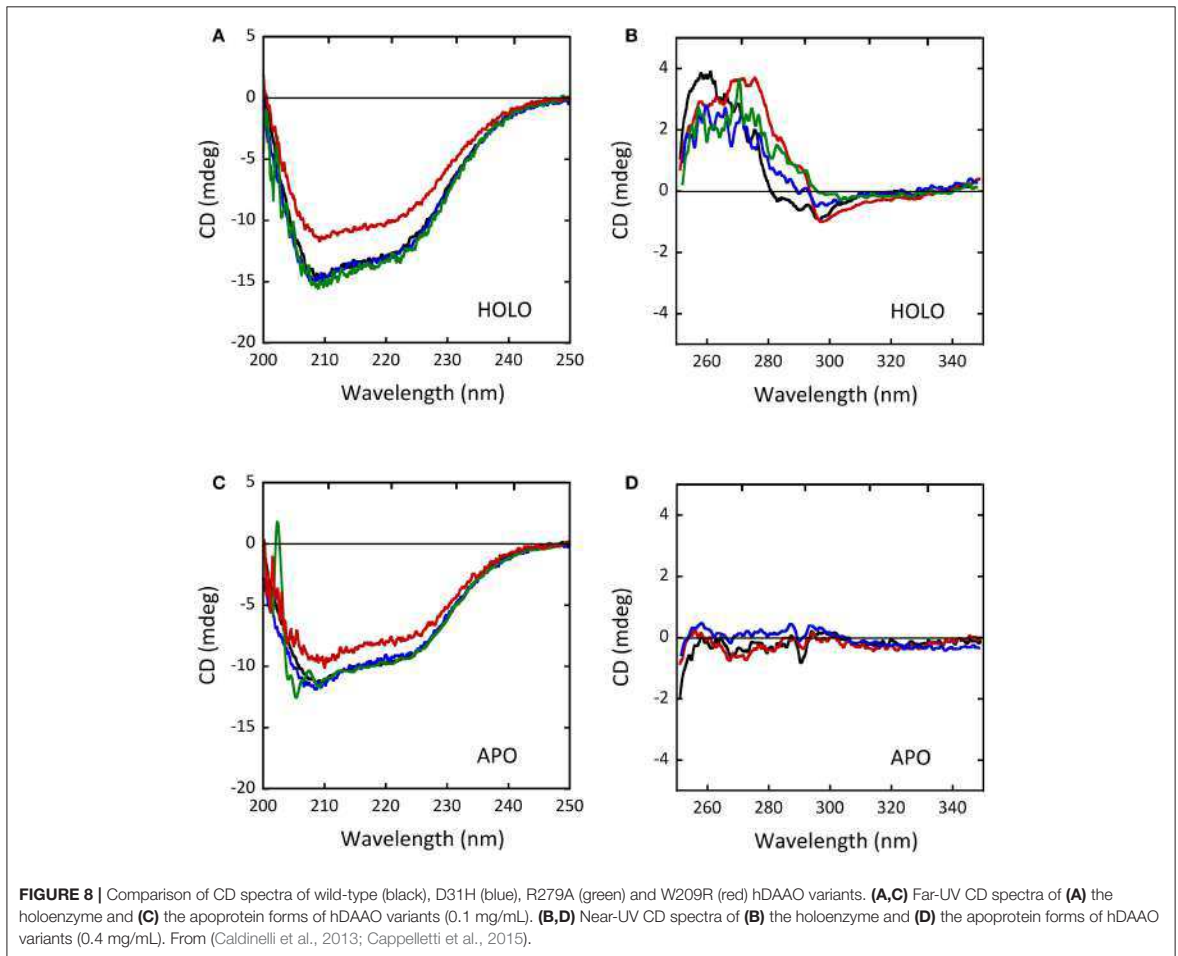
FIGURE 7 | Structural models of hDAAO hyperactive variants. **(A)** Location of the point mutations on the protein dimeric structure (PDB code: 2DU8; Kawazoe et al., 2006). Substituted residues encoded by SNPs are depicted as thick sticks in green, while FAD cofactor is reported in yellow. **(B–D)** Details of the protein microenvironment surrounding at the mutated residues in the different hDAAO variants. The substituted residues are shown as sticks in magenta. The surrounding residues within a distance of 4 Å are shown as sticks in gray. Loops, α -helices, and β -sheets indicated in the text are shown as cartoon in red, blue, and green, respectively. The substrate-competitive inhibitor benzoate and the FAD cofactor are shown as sticks in orange and yellow, respectively. The VAAGL sequence is shown as a cartoon in light blue in **(D)**. H-bond interactions are reported as black dashed line. Figure were prepared with PyMol. Adapted from Caldinelli et al. (2013); Cappelletti et al. (2015).

Cellular Studies

In transiently transfected U87 cells the D31H and R279A hDAAO variants fused with EYFP were correctly targeted: the time course of subcellular compartmentalization closely resembled that observed for the wild-type enzyme, and 72 h after transfection they were largely localized to peroxisomes. According to the biochemical characterization, HPLC analysis performed on U87 cell clones stably expressing similar levels of

D31H, R279A, or wild-type hDAAO showed that the decrease in D-Ser cellular level was significantly higher in cells expressing the hyperactive variants compared to hDAAO wild-type expressing one (Table 5). This evidence was used to further substantiate the proposed role of hDAAO on D-serine levels related to schizophrenia onset (Caldinelli et al., 2013).

On the other hand, isolating U87 cell clones stably expressing the highly active W209R hDAAO proved to be unfeasible, since



its expression was shown to significantly affect cells viability: a massive cell death was reported during the clone selection procedure (Cappelletti et al., 2015). Analyses of D-Ser cellular content were therefore performed on transiently transfected cells. As observed for the other hyperactive variants, W209R hDAAO expression resulted in strongly reduced D-Ser cellular levels compared to control cells expressing the wild-type enzyme (Table 5; Cappelletti et al., 2015). In this case however, an excessive accumulation of H_2O_2 produced by the hDAAO catalyzed reaction was suggested to represent the factor affecting cell viability after transfection (see above).

CONCLUSIONS

Structural and functional studies have highlighted the peculiar biochemical properties of hDAAO (Molla et al., 2006; Sacchi et al., 2008, 2012; Caldinelli et al., 2010; Pollegioni and Sacchi, 2010; Cappelletti et al., 2014; Murtas et al., 2017a). It only weakly binds the FAD cofactor, shows a stable homodimeric state, and

a relatively low activity on its physiological substrates (D-Ser, D-Ala, D-Cys, and D-DOPA). Moreover, hDAAO activity and half-life appears to be specifically modulated by the interaction with the regulatory protein pLG72 (Sacchi et al., 2008, 2011; Cappelletti et al., 2014; Pollegioni et al., 2018) and bassoon (Popiolek et al., 2011). The flavoenzyme activity must be finely tuned to fulfill what is thought to be its main relevant function: controlling D-Ser concentration in the brain. Altered levels of the neuromodulator may affect NMDAR functions and receptor-related processes involved in cognitive ability such learning and memory (Collingridge et al., 2013; Morris, 2013).

Dysregulation in D-Ser signaling, potentially due to altered DAAO activity, has been implicated in the NMDAR dysfunctions observed in various diseases, such as familial and sporadic ALS (Mitchell et al., 2010; Paul and de Bellerocche, 2012), AD (Tannenberg et al., 2004; Billard, 2008; Madeira et al., 2015) schizophrenia (Verrall et al., 2007; Madeira et al., 2008; Hahl et al., 2009) and chronic pain (Zhao et al., 2010; Gong et al., 2011). Accordingly, it is of great relevance to biochemically

characterize the hDAAO variants reported in protein or SNP databases, especially in the case that the introduced amino acidic substitutions significantly affect the enzyme functional properties. In this regard, hDAAO variants can be basically grouped into two classes: inactive and hyperactive.

G183R, R199W, and R199Q variants are characterized by significantly reduced or fully abolished (in the case of G183R hDAAO) enzymatic activity. They show impaired ligand binding properties due to local or general perturbation in the protein conformation (Cappelletti et al., 2015). In G183R hDAAO variant changes in secondary structure elements likely induce variations in the conformation of the FAD binding domain negatively affecting the correct binding of the cofactor (Murtas et al., 2017b). On the other hand, large modifications affecting the tertiary structure of R199W and R199Q hDAAO variants deeply impact on their catalytic efficiency (Cappelletti et al., 2015). Differently, G331V substitution affects the enzyme activity and stability because the induced changes in the C-terminal α -helix promote protein aggregation, strongly reducing the variant solubility (Caldinelli et al., 2013). On the other hand, in D31H, W209R and R279A hDAAO variants the substitutions (and eventually the induced conformational perturbations) have an opposite effect. These protein variants show slightly to significantly improved ligand binding affinities and catalytic efficiency. In particular, W209R hDAAO shows a 2-fold higher turnover number since the substitution appears to facilitate the product release from the reoxidized enzyme after the catalysis (Cappelletti et al., 2015).

Most importantly, all the reviewed hDAAO variants have been shown to directly and significantly impact on D-Ser cellular levels when they are overexpressed in a U87 cell line (Caldinelli et al., 2013; Cappelletti et al., 2015; Murtas et al., 2017b): this finding confirms their potential significance in pathological conditions where the accumulation or the excessive degradation of their physiological substrates is an important feature. It has been also highlighted that hDAAO variants aggregation and mislocation, and/or the induced overproduction of H₂O₂ (in or outside the peroxisomes), might represent important factors significantly affecting cell viability and making the effect of the expression of the different variants even more complex.

Thus, the expression of hDAAO inactive variants in cohorts of individual, as proved for R199W one, might confer susceptibility to neurodegenerative disorders such as ALS and AD, due to an abnormal accumulation of D-Ser which, when associated to elevated glutamate levels, could lead to excitotoxicity related to the hyper-activation of NMDAR. Differently, hyperactive variants might induce a deficit in NMDAR-mediated transmission due to a decreased availability

of D-Ser at the synapses and the hypofunction of the receptor, a condition that in turn has been postulated to be involved in schizophrenia (and eventually AD) onset. Their expression would also be significant in individuals affected by, or sensitive to, chronic pain. The overproduction of H₂O₂ by hDAAO hyperactive variants (together with the exaggerated depletion of D-Ser) may contribute to the elucidation of the molecular mechanism of the central sensitization typical of this neurological condition.

We are aware that, despite the key role played by hDAAO in some important physiological processes, much remains to be unraveled concerning the modulation of its functional properties. The ongoing characterization of variants corresponding to confirmed SNPs in the database will deepen our understanding of the structure/function relationships of this enzyme, and of the effect of their alteration in pathological conditions, providing effective tools to propose and design novel and more effective therapeutic treatments.

Moreover, the potential of the novel genome editing tool based on the clustered regularly interspaced short palindromic repeats (CRISPR)/CRISPR-associated protein-9 nuclease (CRISPR/Cas9) has been recently explored for modeling neurodegenerative diseases which pathomechanisms that have not yet been fully uncovered, including ALS (Kruminis-Kaszkiel et al., 2018). Indeed, both a zebrafish (Armstrong et al., 2016) and a mouse (Liu et al., 2017) ALS models have been developed by using this genome engineering technology to introduce patients-specific mutations in genes associated to the disease. Therefore, the possibility to develop animal models carrying DAAO selected activating or inactivating mutations might represent an invaluable system to investigate further the molecular mechanisms involved in pathological conditions, ranging from neuropsychiatric to neurodegenerative disorders, in which dysregulation of D-Ser metabolism likely play a key role.

AUTHOR CONTRIBUTIONS

SS designed the review. All authors analyzed the literature and wrote the manuscript.

ACKNOWLEDGMENTS

We thank the support of Fondo di Ateneo per la Ricerca and Dr. Gianluca Tomasello for help in preparing structural figures and prof. Loredano Pollegioni for helpful discussion.

GM is a Ph.D. student of the Biotechnology, Biosciences, and Surgical Technology course at Università degli Studi dell'Insubria.

REFERENCES

- Adage, T., Trillat, A. C., Quattropani, A., Perrin, D., Cavarec, L., Shaw, J., et al. (2008). *In vitro* and *in vivo* pharmacological profile of AS057278, a selective d-amino acid oxidase inhibitor with potential anti-psychotic properties. *Eur. Neuropsychopharmacol.* 18, 200–214. doi: 10.1016/j.euroneuro.2007.06.006
- Armstrong, G. A., Liao, M., You, Z., Lissouba, A., Chen, B. E., and Drapeau, P. (2016). Homology directed knockin of point mutations in the zebrafish *tardbp* and *fus* genes in ALS using the CRISPR/Cas9 System. *PLoS ONE* 11:e0150188. doi: 10.1371/journal.pone.0150188
- Banks, W. A., and Kastin, A. J. (1991). Leucine modulates peptide transport system-1 across the blood-brain barrier at a stereospecific site

- within the central nervous system. *J. Pharm. Pharmacol.* 43, 252–254. doi: 10.1111/j.2042-7158.1991.tb06678.x
- Basbaum, A. I., Bautista, D. M., Scherrer, G., and Julius, D. (2009). Cellular and molecular mechanisms of pain. *Cell* 139, 267–284. doi: 10.1016/j.cell.2009.09.028
- Billard, J. M. (2008). D-serine signalling as a prominent determinant of neuronal-glial dialogue in the healthy and diseased brain. *J. Cell. Mol. Med.* 12, 872–884. doi: 10.1111/j.1582-4934.2008.00315.x
- Birolo, L., Sacchi, S., Smaldone, G., Molla, G., Leo, G., Caldinelli, L., et al. (2016). Regulating levels of the neuromodulator d-serine in human brain: structural insight into pLG72 and D-amino acid oxidase interaction. *FEBS J.* 283, 3353–3370. doi: 10.1111/febs.13809
- Burnet, P. W., Eastwood, S. L., Bristow, G. C., Godlewska, B. R., Sikka, P., Walker, M., et al. (2008). D-amino acid oxidase activity and expression are increased in schizophrenia. *Mol. Psychiatry* 13, 658–660. doi: 10.1038/mp.2008.47
- Caldinelli, L., Iametti, S., Barbiroli, A., Bonomi, F., Piubelli, L., Ferranti, P., et al. (2004). Unfolding intermediate in the peroxisomal flavoprotein D-amino acid oxidase. *J. Biol. Chem.* 279, 28426–28434. doi: 10.1074/jbc.M403489200
- Caldinelli, L., Molla, G., Bracci, L., Lelli, B., Pileri, S., Cappelletti, P., et al. (2010). Effect of ligand binding on human D-amino acid oxidase: implications for the development of new drugs for schizophrenia treatment. *Protein Sci.* 19, 1500–1512. doi: 10.1002/pro.429
- Caldinelli, L., Sacchi, S., Molla, G., Nardini, M., and Pollegioni, L. (2013). Characterization of human DAAO variants potentially related to an increased risk of schizophrenia. *Biochim. Biophys. Acta* 1832, 400–410. doi: 10.1016/j.bbadis.2012.11.019
- Cao, X., and Bian, J. S. (2016). The role of hydrogen sulfide in renal system. *Front. Pharmacol.* 7:385. doi: 10.3389/fphar.2016.00385
- Cappelletti, P., Campomenosi, P., Pollegioni, L., and Sacchi, S. (2014). The degradation (by distinct pathways) of human D-amino acid oxidase and its interacting partner pLG72—two key proteins in D-serine catabolism in the brain. *FEBS J.* 281, 708–723. doi: 10.1111/febs.12616
- Cappelletti, P., Piubelli, L., Murtas, G., Caldinelli, L., Valentino, M., Molla, G., et al. (2015). Structure-function relationships in human d-amino acid oxidase variants corresponding to known SNPs. *Biochim. Biophys. Acta* 1854, 1150–1159. doi: 10.1016/j.bbapap.2015.02.005
- Chang, S. L., Hsieh, C. H., Chen, Y. J., Wang, C. M., Shih, C. S., Huang, P. W., et al. (2013). The C-terminal region of G72 increases D-amino acid oxidase activity. *Int. J. Mol. Sci.* 15, 29–43. doi: 10.3390/ijms15010029
- Chatterton, J. E., Awobuluyi, M., Premkumar, L. S., Takahashi, H., Talantova, M., Shin, Y., et al. (2002). Excitatory glycine receptors containing the NR3 family of NMDA receptor subunits. *Nature* 415:793. doi: 10.1038/nature715
- Chumakov, I., Blumenfeld, M., Guerasimenco, O., Cavarec, L., Palicio, M., Abderrahim, H., et al. (2002). Genetic and physiological data implicating the new human gene G72 and the gene for D-amino acid oxidase in schizophrenia. *Proc. Nat. Acad. Sci. U.S.A.* 99, 13675–13680. doi: 10.1073/pnas.182412499
- Cirulli, E. T., Lasseigne, B. N., Petrovski, S., Sapp, P. C., Dion, P. A., Leblond, C. S., et al. (2015). Exome sequencing in amyotrophic lateral sclerosis identifies risk genes and pathways. *Science* 347, 1436–1441. doi: 10.1126/science.aaa3650
- Cline, M. J., and Lehrer, R. I. (1969). D-amino acid oxidase in leukocytes: a possible D-amino-acid-linked antimicrobial system. *Proc. Natl. Acad. Sci. U.S.A.* 62, 756–763. doi: 10.1073/pnas.62.3.756
- Collingridge, G. L., Volianskis, A., Bannister, N., France, G., Hanna, L., Mercier, M., et al. (2013). The NMDA receptor as a target for cognitive enhancement. *Neuropharmacology* 64 13–26. doi: 10.1016/j.neuropharm.2012.06.051
- Coyle, J. T. (2006). Glutamate and schizophrenia: beyond the dopamine hypothesis. *Cell. Mol. Neurobiol.* 26, 363–382. doi: 10.1007/s10571-006-9062-8
- Coyle, J. T., Tsai, G., and Goff, D. (2003). Converging evidence of NMDA receptor hypofunction in the pathophysiology of schizophrenia. *Ann. N. Y. Acad. Sci.* 1003, 318–327. doi: 10.1196/annals.1300.020
- Crooks, G. E., Hon, G., Chandonia, J. M., and Brenner, S. E. (2004). WebLogo: a sequence logo generator. *Genome Res.* 14, 1188–1190. doi: 10.1101/gr.849004
- Curti, B., Ronchi, S., Branzoli, U., Ferri, G., and Williams C. H. Jr. (1973). Improved purification, amino acid analysis and molecular weight of homogeneous d-amino acid oxidase from pig kidney. *Biochim. Biophys. Acta* 327, 266–273. doi: 10.1016/0005-2744(73)90409-9
- Dabholkar, A. S. (1986). Ultrastructural localization of catalase and D-amino acid oxidase in 'normal' fetal mouse liver. *Experientia* 42, 144–147. doi: 10.1007/BF01952437
- Duplantier, A. J., Becker, S. L., Bohanon, M. J., Borzilleri, K. A., Chrnyk, B. A., Downs, J. T., et al. (2009). Discovery, S. A. R., and pharmacokinetics of a novel 3-hydroxyquinolin-2 (1H)-one series of potent d-amino acid oxidase (DAAO) inhibitors. *J. Med. Chem.* 52, 3576–3585. doi: 10.1021/jm900128w
- Eltzschig, H. K., and Eckle, T. (2011). Ischemia and reperfusion—from mechanism to translation. *Nat. Med.* 17:1391. doi: 10.1038/nm.2507
- Esposito, S., Pristerà, A., Maresca, G., Cavallaro, S., Felsani, A., Florenzano, F., et al. (2012). Contribution of serine racemase/d-serine pathway to neuronal apoptosis. *Aging Cell.* 11, 588–598. doi: 10.1111/j.1474-9726.2012.00822.x
- Ferraris, D., Duvall, B., Ko, Y. S., Thomas, A. G., Rojas, G., Majer, P., et al. (2008). Synthesis and biological evaluation of D-amino acid oxidase inhibitors. *J. Med. Chem.* 51, 3357–3359. doi: 10.1021/jm800200u
- Fitzpatrick, P. F., and Massey, V. (1982). Proton release during the reductive half-reaction of D-amino acid oxidase. *J. Biol. Chem.* 257, 9958–9962.
- Fratini, L. F., Piubelli, L., Sacchi, S., Molla, G., and Pollegioni, L. (2011). Is rat an appropriate animal model to study the involvement of d-serine catabolism in schizophrenia? insights from characterization of D-amino acid oxidase. *FEBS J.* 278, 4362–4373. doi: 10.1111/j.1742-4658.2011.08354.x
- Fuchs, S. A., Berger, R., Klomp, L. W., and de Koning, T. J. (2005). D-amino acids in the central nervous system in health and disease. *Mol. Genet. Metab.* 85, 168–180. doi: 10.1016/j.ymgme.2005.03.003
- Garcia, M. A., Meca, R., and Leite, D. (2007). The role of renal sympathetic nervous system in the pathogenesis of ischemic acute renal failure. *Eur. J. Pharmacol.* 481, 241–248. doi: 10.1016/j.ejphar.2003.09.036
- Gong, N., Gao, Z. Y., Wang, Y. C., Li, X. Y., Huang, J. L., Hashimoto, K., et al. (2011). A series of D-amino acid oxidase inhibitors specifically prevents and reverses formalin-induced tonic pain in rats. *J. Pharmacol. Exp. Ther.* 336, 282–293. doi: 10.1124/jpet.110.172353
- Gong, N., Li, X. Y., Xiao, Q., and Wang, Y. X. (2014). Identification of a novel spinal dorsal horn astroglial D-amino acid oxidase-hydrogen peroxide pathway involved in morphine antinociceptive tolerance. *Anesthesiology* 120, 962–975. doi: 10.1097/ALN.0b013e3182a66d2a
- Guidotti, T. L. (2010). Hydrogen sulfide: advances in understanding human toxicity. *Int. J. Toxicol.* 29, 569–581. doi: 10.1177/1091581810384882
- Habl, G., Zink, M., Petroianu, G., Bauer, M., Schneider-Axmann, T., von Wilmsdorff, M., et al. (2009). Increased D-amino acid oxidase expression in the bilateral hippocampal CA4 of schizophrenic patients: a post-mortem study. *J. Neural Transm.* 116, 1657–1665. doi: 10.1007/s00702-009-0312-z
- Hamase, K., Homma, H., Takigawa, Y., Fukushima, T., Santa, T., and Imai, K. (1997). Regional distribution and postnatal changes of D-amino acids in rat brain. *Biochim. Biophys. Acta* 1334, 214–222. doi: 10.1016/S0304-4165(96)00095-5
- Hamasu, K., Shigemi, K., Tsuneyoshi, Y., Yamane, H., Sato, H., Denbow, D. M., et al. (2010). Intracerebroventricular injection of L-proline and D-proline induces sedative and hypnotic effects by different mechanisms under an acute stressful condition in chicks. *Amino Acids* 38, 57–64. doi: 10.1007/s00726-008-0204-9
- Hashimoto, A., Nishikawa, T., Konno, R., Niwa, A., Yasumura, Y., Oka, T., et al. (1993). Free D-serine, D-aspartate and D-alanine in central nervous system and serum in mutant mice lacking D-amino acid oxidase. *Neurosci. Lett.* 152, 33–36. doi: 10.1016/0304-3940(93)90476-2
- Hashimoto, A., Oka, T., and Nishikawa, T. (1995). Extracellular concentration of endogenous free D-serine in the rat brain as revealed by *in vivo* microdialysis. *Neuroscience* 66, 635–643. doi: 10.1016/0306-4522(94)00597-X
- Hashimoto, K., Engberg, G., Shimizu, E., Nordin, C., Lindström, L. H., and Iyo, M. (2005). Reduced D-serine to total serine ratio in the cerebrospinal fluid of drug naïve schizophrenic patients. *Prog. Neuropsychopharmacol. Biol. Psychiatry* 29, 767–769. doi: 10.1016/j.pnpbp.2005.04.023
- Hashimoto, K., Fukushima, T., Shimizu, E., Komatsu, N., Watanabe, H., Shinoda, N., et al. (2003). Decreased serum levels of D-serine in patients with schizophrenia: evidence in support of the N-methyl-D-aspartate receptor hypofunction hypothesis of schizophrenia. *Arch. Gen. Psychiatry* 60, 572–576. doi: 10.1001/archpsyc.60.6.572
- Heresco-Levy, U., Javitt, D. C., Ebstein, R., Vass, A., Lichtenberg, P., Bar, G., et al. (2005). D-serine efficacy as add-on pharmacotherapy to risperidone

- and olanzapine for treatment-refractory schizophrenia. *Biol. Psychiatry* 57, 577–585. doi: 10.1016/j.biopsych.2004.12.037
- Hopkins, S. C., Zhao, F. Y., Bowen, C. A., Fang, X., Wei, H., Heffernan, M. L., et al. (2013). Pharmacodynamic effects of a D-amino acid oxidase inhibitor indicate a spinal site of action in rat models of neuropathic pain. *J. Pharmacol. Exp. Ther.* 345, 502–511. doi: 10.1124/jpet.113.204016
- Horiike, K., Tojo, H., Arai, R., Nozaki, M., and Maeda, T. (1994). D-amino acid oxidase is confined to the lower brain stem and cerebellum in rat brain: regional differentiation of astrocytes. *Brain Res.* 652, 297–303. doi: 10.1016/0006-8993(94)90240-2
- Ikonomidou, C., Bosch, F., Miksa, M., Bittigau, P., Vöckler, J., Dikranian, K., et al. (1999). Blockade of NMDA receptors and apoptotic neurodegeneration in the developing brain. *Science* 283, 70–74. doi: 10.1126/science.283.5398.70
- Junjaud, G., Rouaud, E., Turpin, F., Mothet, J. P., and Billard, J. M. (2006). Age-related effects of the neuromodulator D-serine on neurotransmission and synaptic potentiation in the CA1 hippocampal area of the rat. *J. Neurochem.* 98, 1159–1166. doi: 10.1111/j.1471-4159.2006.03944.x
- Kapoor, R., and Kapoor, V. (1997). Distribution of D-amino acid oxidase (DAO) activity in the medulla and thoracic spinal cord of the rat: implications for a role for D-serine in autonomic function. *Brain Res.* 771, 351–355. doi: 10.1016/S0006-8993(97)00886-X
- Kapoor, R., Lim, K. S., Cheng, A., Garrick, T., and Kapoor, V. (2006). Preliminary evidence for a link between schizophrenia and NMDA-glycine site receptor ligand metabolic enzymes, d-amino acid oxidase (DAAO) and kynurenine aminotransferase-1 (KAT-1). *Brain Res.* 1106, 205–210. doi: 10.1016/j.brainres.2006.05.082
- Kawazoe, T., Park, H. K., Iwana, S., Tsuge, H., and Fukui, K. (2007b). Human D-amino acid oxidase: an update and review. *Chem. Rec.* 7, 305–315. doi: 10.1002/ctr.20129
- Kawazoe, T., Tsuge, H., Imagawa, T., Aki, K., Kuramitsu, S., and Fukui, K. (2007a). Structural basis of D-DOPA oxidation by D-amino acid oxidase: alternative pathway for dopamine biosynthesis. *Biochem. Biophys. Res. Commun.* 355, 385–391. doi: 10.1016/j.bbrc.2007.01.181
- Kawazoe, T., Tsuge, H., Pilone, M. S., and Fukui, K. (2006). Crystal structure of human D-amino acid oxidase: context-dependent variability of the backbone conformation of the VAAGL hydrophobic stretch located at the si-face of the flavin ring. *Protein Sci.* 15, 2708–2717. doi: 10.1110/ps.062421606
- Khoronenkova, S. V., and Tishkov, V. I. (2008). D-amino acid oxidase: physiological role and applications. *Biochemistry* 73, 1511–1518. doi: 10.1134/S0006297908130105
- Kohiki, T., Sato, Y., Nishikawa, Y., Yorita, K., Sagawa, I., Denda, M., et al. (2017). Elucidation of inhibitor-binding pocket of D-amino acid oxidase using docking simulation and N-sulfanylethylamide-based labeling technology. *Org. Biomol. Chem.* 15, 5289–5297. doi: 10.1039/C7OB00633K
- Koibuchi, N., Konno, R., Matsuzaki, S., Ohtake, H., Niwa, A., and Yamaoka, S. (1995). Localization of D-amino acid oxidase mRNA in the mouse kidney and the effect of testosterone treatment. *Histochem. Cell Biol.* 104, 349–355. doi: 10.1007/BF01458128
- Kondori, N. R., Paul, P., Robbins, J. P., Liu, K., Hildyard, J. C. W., Wells, D. J., et al. (2017). Characterisation of the pathogenic effects of the *in vivo* expression of an ALS-linked mutation in D-amino acid oxidase: phenotype and loss of spinal cord motor neurons. *PLoS ONE* 12:e0188912. doi: 10.1371/journal.pone.0188912
- Konno, R., and Yasumura, Y. (1983). Mouse mutant deficient in D-amino acid oxidase activity. *Genetics* 103, 277–285.
- Konno, R., Ikeda, M., Yamaguchi, K., Ueda, Y., and Niwa, A. (2000). Nephrotoxicity of D-propargylglycine in mice. *Arch. Toxicol.* 74, 473–479. doi: 10.1007/s002040000156
- Konno, R., Sasaki, M., Asakura, S., Fukui, K., Enami, J., and Niwa, A. (1997). D-amino acid oxidase is not present in the mouse liver. *Biochim. Biophys. Acta* 1335, 173–181. doi: 10.1016/S0304-4165(96)00136-5
- Krebs, H. A. (1935). Metabolism of amino-acids: deamination of amino-acids. *Biochem. J.* 29, 1620–1644. doi: 10.1042/bj0291620
- Krug, A. W., Volker, K., Dantzer, W. H., and Silbernagl, S. (2007). Why is d-serine nephrotoxic and α -aminoisobutyric acid protective?. *Am. J. Physiol. Renal Physiol.* 293, F382–F390. doi: 10.1152/ajprenal.00441.2006
- Krumins-Kaszkiel, E., Juranek, J., Maksymowicz, W., and Wojtkiewicz, J. (2018). CRISPR/Cas9 technology as an emerging tool for targeting Amyotrophic Lateral Sclerosis (ALS). *Int. J. Mol. Sci.* 19:E906. doi: 10.3390/ijms19030906
- Latremoliere, A., and Woolf, C. J. (2009). Central sensitization: a generator of pain hypersensitivity by central neural plasticity. *J. Pain.* 10, 895–926. doi: 10.1016/j.jpain.2009.06.012
- Lei, G., Xia, Y., and Johnson, K. M. (2008). The role of Akt-GSK-3 β signaling and synaptic strength in phencyclidine-induced neurodegeneration. *Neuropsychopharmacology* 33, 1343–1353. doi: 10.1038/sj.npp.1301511
- Lin, C. H., Huang, Y. J., Lin, C. J., Lane, H. Y., and Tsai, G. E. (2014). NMDA neurotransmission dysfunction in mild cognitive impairment and Alzheimer's disease. *Curr. Pharm. Des.* 20, 5169–5179. doi: 10.2174/1381612819666140110115603
- Lin, T. S., Tsai, H. J., Lee, C. H., Song, Y. Q., Huang, R. S., Hsieh-Li, H. M., et al. (2017). An improved drugs screening system reveals that baicalein ameliorates the AP5/AMPA/NMDA-induced depolarization of neurons. *J. Alzheimer's Dis.* 56, 959–976. doi: 10.3233/JAD-160898
- Liu, E. T., Bolcun-Filas, E., Grass, D. S., Lutz, C., Murray, S., Shultz, L., et al. (2017). Of mice and CRISPR: the post-CRISPR future of the mouse as a model system for the human condition. *EMBO Rep.* 18, 187–193. doi: 10.15252/embr.201643717
- Lu, J. M., Gong, N., Wang, Y. C., and Wang, Y. X. (2012). D-Amino acid oxidase-mediated increase in spinal hydrogen peroxide is mainly responsible for formalin-induced tonic pain. *Br. J. Pharmacol.* 165, 1941–1955. doi: 10.1111/j.1476-5381.2011.01680
- Madeira, C., Freitas, M. E., Vargas-Lopes, C., Wolosker, H., and Panizzutti, R. (2008). Increased brain D-amino acid oxidase (DAAO) activity in schizophrenia. *Schizophr. Res.* 101, 76–83. doi: 10.1016/j.schres.2008.02.002
- Madeira, C., Lourenco, M. V., Vargas-Lopes, C., Suemoto, C. K., Brandão, C. O., Reis, T., et al. (2015). D-Serine levels in Alzheimer's disease: implications for novel biomarker development. *Transl. Psychiatry* 5:561. doi: 10.1038/tp.2015.52
- Maekawa, M., Okamura, T., Kasai, N., Hori, Y., Summer, K. H., and Konno, R. (2005). D-amino acid oxidase is involved in D-serine-induced nephrotoxicity. *Chem. Res. Toxicol.* 18, 1678–1682. doi: 10.1021/tx0500326
- Martinez, F. J., Pratt, G. A., Van Nostrand, E. L., Batra, R., Huelga, S. C., Kapeli, K., et al. (2016). Protein-RNA networks regulated by normal and ALS-associated mutant HNRNP281 in the nervous system. *Neuron* 92, 780–795. doi: 10.1016/j.neuron.2016.09.050
- Mattevi, A., Vanoni, M. A., Todone, F., Rizzi, M., Teplyakov, A., Coda, A., et al. (1996). Crystal structure of D-amino acid oxidase: a case of active site mirror-image convergent evolution with flavocytochrome b2. *Proc. Natl. Acad. Sci. U.S.A.* 93, 7496–7501. doi: 10.1073/pnas.93.15.7496
- Mitchell, J., Paul, P., Chen, H. J., Morris, A., Payling, M., Falchi, M., et al. (2010). Familial amyotrophic lateral sclerosis is associated with a mutation in D-amino acid oxidase. *Proc. Natl. Acad. Sci. U.S.A.* 107, 7556–7561. doi: 10.1073/pnas.0914128107
- Molla, G. (2017). Competitive inhibitors unveil structure/function relationships in human D-amino acid oxidase. *Front. Mol. Biosci.* 4:80. doi: 10.3389/fmolb.2017.00080
- Molla, G., Sacchi, S., Bernasconi, M., Pilone, M. S., Fukui, K., and Polegioni, L. (2006). Characterization of human D-amino acid oxidase. *FEBS Lett.* 580, 2358–2364. doi: 10.1016/j.febslet.2006.03.045
- Momoi, K., Fukui, K., Watanabe, F., and Miyake, Y. (1988). Molecular cloning and sequence analysis of cDNA encoding human kidney D-amino acid oxidase. *FEBS Lett.* 238, 180–184. doi: 10.1016/0014-5793(88)80252-7
- Moreno, S., Nardacci, R., Cimini, A., and Cerù, M. P. (1999). Immunocytochemical localization of D-amino acid oxidase in rat brain. *J. Neurocytol.* 28, 169–185. doi: 10.1023/A:1007064504007
- Morris, G. (2013). NMDA receptors and memory encoding. *Neuropharmacology* 74, 32–40. doi: 10.1016/j.neuropharm.2013.04.014
- Mothet, J. P., Rouaud, E., Sinet, P. M., Potier, B., Jouveanceau, A., Dutar, P., et al. (2006). A critical role for the glial-derived neuromodulator D-serine in the age-related deficits of cellular mechanisms of learning and memory. *Aging Cell* 5, 267–274. doi: 10.1111/j.1474-9726.2006.00216.x
- Murtas, G., Caldinelli, L., Cappelletti, P., Sacchi, S., and Polegioni, L. (2017b). Human d-amino acid oxidase: the inactive G183R variant. *Biochim. Biophys. Acta* 1866, 822–830. doi: 10.1016/j.bbapap.2017.12.007

- Murtas, G., Sacchi, S., Valentino, M., and Pollegioni, L. (2017a). Biochemical properties of human D-amino acid oxidase. *Front. Mol. Biosci.* 4:88. doi: 10.3389/fmolb.2017.00088
- Nagata, Y. (1992). Involvement of D-amino acid oxidase in elimination of D-serine in mouse brain. *Experientia* 48, 753–755.
- Nagata, Y., Konno, R., Yasumura, Y., and Akino, T. (1989). Involvement of D-amino acid oxidase in elimination of free D-amino acids in mice. *Biochem. J.* 257, 291–292. doi: 10.1042/bj2570291
- Nagata, Y., Masui, R., and Akino, T. (1992). The presence of free D-serine, D-alanine and D-proline in human plasma. *Experientia* 48, 986–988. doi: 10.1007/BF01919147
- Olney, J. W., Wozniak, D. F., and Farber, N. B. (1997). Excitotoxic neurodegeneration in Alzheimer disease: new hypothesis and new therapeutic strategies. *Arch. Neurol.* 54, 1234–1240. doi: 10.1001/archneur.1997.00550220042012
- Ono, K., Shishido, Y., Park, H. K., Kawazoe, T., Iwana, S., Chung, S. P., et al. (2009). Potential pathophysiological role of D-amino acid oxidase in schizophrenia: immunohistochemical and in situ hybridization study of the expression in human and rat brain. *J. Neural. Transm.* 116, 1335–1347. doi: 10.1007/s00702-009-0289-7
- Paul, P., and de Belleruche, J. (2012). The role of D-amino acids in amyotrophic lateral sclerosis pathogenesis: a review. *Amino Acids* 43, 1823–1831. doi: 10.1007/s00726-012-1385-9
- Paul, P., Murphy, T., Oseni, Z., Sivalokanathan, S., and de Belleruche, J. S. (2014). Pathogenic effects of amyotrophic lateral sclerosis-linked mutation in D-amino acid oxidase are mediated by D-serine. *Neurobiol. Aging* 35, 876–885. doi: 10.1016/j.neurobiolaging.2013.09.005
- Pollegioni, L., and Sacchi, S. (2010). Metabolism of the neuromodulator D-serine. *Cell. Mol. Life Sci.* 67, 2387–2404. doi: 10.1007/s00018-010-0307-9
- Pollegioni, L., Butò, S., Tischer, W., Ghisla, S., and Pilone, M. S. (1993). Characterization of D-amino acid oxidase from *Trigonopsis variabilis*. *Biochem. Mol. Biol. Int.* 31, 709–717.
- Pollegioni, L., Piubelli, L., Molla, G., and Rosini, E. (2018). D-Amino acid oxidase-pLG72 interaction and D-serine modulation. *Front. Mol. Biosci.* 5:3. doi: 10.3389/fmolb.2018.00003
- Pollegioni, L., Piubelli, L., Sacchi, S., Pilone, M. S., and Molla, G. (2007). Physiological functions of D-amino acid oxidases: from yeast to humans. *Cell. Mol. Life Sci.* 64, 1373–1394. doi: 10.1007/s00018-007-6558-4
- Popiolek, M., Ross, J. F., Charych, E., Chanda, P., Gundelfinger, E. D., Moss, S. J., et al. (2011). D-amino acid oxidase activity is inhibited by an interaction with bassoon protein at the presynaptic active zone. *J. Biol. Chem.* 286, 28867–28875. doi: 10.1074/jbc.M111.262063
- Prathapasinghe, G. A., Siow, Y. L., Xu, Z., and Karmin, O. (2008). Inhibition of cystathionine- β -synthase activity during renal ischemia-reperfusion: role of pH and nitric oxide. *Am. J. Physiol. Renal Physiol.* 295, F912–F922. doi: 10.1152/ajprenal.00040.2008
- Sacchi, S., Bernasconi, M., Martineau, M., Mothet, J. P., Ruzzene, M., Pilone, M. S., et al. (2008). pLG72 modulates intracellular D-serine levels through its interaction with D-amino acid oxidase: effect on schizophrenia susceptibility. *J. Biol. Chem.* 283, 22244–22256. doi: 10.1074/jbc.M70915.3200
- Sacchi, S., Binelli, G., and Pollegioni, L. (2016). G72 primate-specific gene: a still enigmatic element in psychiatric disorders. *Cell. Mol. Life Sci.* 73, 2029–2039. doi: 10.1007/s00018-016-2165-6
- Sacchi, S., Caldinelli, L., Cappelletti, P., Pollegioni, L., and Molla, G. (2012). Structure-function relationships in human D-amino acid oxidase. *Amino Acids* 43, 1833–1850. doi: 10.1007/s00726-012-1345-4
- Sacchi, S., Cappelletti, P., Giovannardi, S., and Pollegioni, L. (2011). Evidence for the interaction of D-amino acid oxidase with pLG72 in a glial cell line. *Mol. Cell. Neurosci.* 48, 20–28. doi: 10.1016/j.mcn.2011.06.001
- Sasabe, J., Miyoshi, Y., Rakoff-Nahoum, S., Zhang, T., Mita, M., Davis, B. M., et al. (2016). Interplay between microbial D-amino acids and host d-amino acid oxidase modifies murine mucosal defence and gut microbiota. *Nat. Microbiol.* 1:16125. doi: 10.1038/nmicrobiol.2016.125
- Sasabe, J., Miyoshi, Y., Suzuki, M., Mita, M., Konno, R., Matsuoka, M., et al. (2012). D-amino acid oxidase controls motoneuron degeneration through D-serine. *Proc. Natl. Acad. Sci.* 109, 627–632. doi: 10.1073/pnas.1114439109
- Sasabe, J., Suzuki, M., Imanishi, N., and Aiso, S. (2014). Activity of D-amino acid oxidase is widespread in the human central nervous system. *Front. Synaptic Neurosci.* 6:14. doi: 10.3389/fnsyn.2014.00014
- Shibuya, N., Koike, S., Tanaka, M., Ishigami-Yuasa, M., Kimura, Y., Ogasawara, Y., et al. (2013). A novel pathway for the production of hydrogen sulfide from D-cysteine in mammalian cells. *Nat. Commun.* 4:1366. doi: 10.1038/ncomms2371
- Stone, J. M., and Pilowsky, L. S. (2007). Novel targets for drugs in schizophrenia. *CNS Neurol. Disord. Drug Targets* 6, 265–272. doi: 10.2174/187152707781387323
- Takarada, T., Takahata, Y., Iemata, M., Hinoi, E., Uno, K., Hirai, T., et al. (2009). Interference with cellular differentiation by D-serine through antagonism at N-methyl-D-aspartate receptors composed of NR1 and NR3A subunits in chondrocytes. *J. Cell. Physiol.* 220, 756–764. doi: 10.1002/jcp.21821
- Tannenber, R. K., Scott, H. L., Westphalen, R. I., and Dodd, P. R. (2004). The identification and characterization of excitotoxic nerve-endings in Alzheimer disease. *Curr. Alzheimer Res.* 1, 11–25. doi: 10.2174/156720504380591
- Umhau, S., Pollegioni, L., Molla, G., Diederichs, K., Welte, W., Pilone, M. S., et al. (2000). The x-ray structure of D-amino acid oxidase at very high resolution identifies the chemical mechanism of flavin-dependent substrate dehydrogenation. *Proc. Natl. Acad. Sci. U.S.A.* 97, 12463–12468. doi: 10.1073/pnas.97.23.12463
- Verrall, L., Burnet, P. W., Betts, J. F., and Harrison, P. J. (2010). The neurobiology of D-amino acid oxidase and its involvement in schizophrenia. *Mol. Psychiatry* 15:122. doi: 10.1038/mp.2009.99
- Verrall, L., Walker, M., Rawlings, N., Benzel, I., Kew, J. N., Harrison, P. J., et al. (2007). D-Amino acid oxidase and serine racemase in human brain: normal distribution and altered expression in schizophrenia. *Eur. J. Neurosci.* 26, 1657–1669. doi: 10.1111/j.1460-9568.2007.05769.x
- Wake, K., Yamazaki, H., Hanzawa, S., Konno, R., Sakio, H., Niwa, A., et al. (2001). Exaggerated responses to chronic nociceptive stimuli and enhancement of N-methyl-D-aspartate receptor-mediated synaptic transmission in mutant mice lacking D-amino acid oxidase. *Neurosci. Lett.* 297, 25–28. doi: 10.1016/S0304-3940(00)01658-X
- Wang, H., Wolosker, H., Pevsner, J., Snyder, S. H., and Selkoe, D. J. (2000). Regulation of rat magnocellular neurosecretory system by D-aspartate: evidence for biological role(s) of a naturally occurring free D-amino acid in mammals. *Endocrinol. J.* 167, 247–252. doi: 10.1677/joe.0.1670247
- Wang, L. Z., and Zhu, X. Z. (2003). Spatiotemporal relationships among D-serine, serine racemase, and D-amino acid oxidase during mouse postnatal development. *Acta Pharmacol. Sin.* 24, 965–974.
- Wei, H., Gong, N., Huang, J. L., Fan, H., Ma, A. N., Li, X. Y., et al. (2013). Spinal D-amino acid oxidase contributes to mechanical pain hypersensitivity induced by sleep deprivation in the rat. *Pharmacol. Biochem. Behav.* 111, 30–36. doi: 10.1016/j.pbb.2013.08.003
- Wolosker, H. (2011). Serine racemase and the serine shuttle between neurons and astrocytes. *Biochim. Biophys. Acta* 1814, 1558–1566. doi: 10.1016/j.bbapap.2011.01.001
- Wolosker, H., and Radziszewsky, I. (2013). The serine shuttle between glia and neurons: implications for neurotransmission and neurodegeneration. *Biochem. Soc. Trans.* 41, 1546–1550. doi: 10.1042/BST20130220
- Wolosker, H., Dumin, E., Balan, L., and Foltyn, V. N. (2008). D-amino acids in the brain: D-serine in neurotransmission and neurodegeneration. *FEBS J.* 275, 3514–3526. doi: 10.1111/j.1742-4658.2008.06515.x
- Wolosker, H., Panizzutti, R., and De Miranda, J. (2002). Neurobiology through the looking-glass: D-serine as a new glial-derived transmitter. *Neurochem. Int.* 41, 327–332. doi: 10.1016/S0197-0186(02)00055-4
- Wozniak, D. F., Dikranian, K., Ishimaru, M. J., Nardi, A., Corso, T. D., Tenkova, T., et al. (1998). Disseminated corticolimbic neuronal degeneration induced in rat brain by MK-801: potential relevance to Alzheimer's disease. *Neurobiol. Dis.* 5, 305–322. doi: 10.1006/nbdi.1998.0206

- Yagi, K., Naoi, M., Harada, M., Okamura, K., Hidaka, H., Ozawa, T., et al. (1967). Structure and function of D-amino acid oxidase. *Biochem. J.* 61, 580–597. doi: 10.1093/oxfordjournals.jbchem.a128588
- Zhang, H., Qi, L., Lin, Y., Mao, L., and Chen, Y. (2012). Study on the decrease of renal D-amino acid oxidase activity in the rat after renal ischemia by chiral ligand exchange capillary electrophoresis. *Amino Acids* 42, 337–345. doi: 10.1007/s00726-010-0811-0
- Zhao, W. J., Gao, Z. Y., Wei, H., Nie, H. Z., Zhao, Q., Zhou, X. J., et al. (2010). Spinal D-amino acid oxidase contributes to neuropathic pain in rats. *J. Pharmacol. Exp. Ther.* 332, 248–254. doi: 10.1124/jpet.109.158816

Conflict of Interest Statement: The authors declare that the research was conducted in the absence of any commercial or financial relationships that could be construed as a potential conflict of interest.

Copyright © 2018 Sacchi, Cappelletti and Murtas. This is an open-access article distributed under the terms of the Creative Commons Attribution License (CC BY). The use, distribution or reproduction in other forums is permitted, provided the original author(s) and the copyright owner are credited and that the original publication in this journal is cited, in accordance with accepted academic practice. No use, distribution or reproduction is permitted which does not comply with these terms.



Human D-Amino Acid Oxidase: Structure, Function, and Regulation

Loredano Pollegioni*, Silvia Sacchi and Giulia Murtas

Dipartimento di Biotecnologie e Scienze della Vita, Università degli Studi dell'Insubria, Varese, Italy

OPEN ACCESS

Edited by:

Andrea Mozzarelli,
Università degli Studi di Parma, Italy

Reviewed by:

Vladimir I. Tishkov,
Lomonosov Moscow State University,
Russia

Robert Stephen Phillips,
University of Georgia, United States

Piero Andrea Temussi,
Università degli Studi di Napoli
Federico II, Italy

*Correspondence:

Loredano Pollegioni
loredano.pollegioni@uninsubria.it

Specialty section:

This article was submitted to
Structural Biology,
a section of the journal
Frontiers in Molecular Biosciences

Received: 03 September 2018

Accepted: 12 November 2018

Published: 28 November 2018

Citation:

Pollegioni L, Sacchi S and Murtas G
(2018) Human D-Amino Acid Oxidase:
Structure, Function, and Regulation.
Front. Mol. Biosci. 5:107.
doi: 10.3389/fmolb.2018.00107

D-Amino acid oxidase (DAAO) is an FAD-containing flavoenzyme that catalyzes with absolute stereoselectivity the oxidative deamination of all natural D-amino acids, the only exception being the acidic ones. This flavoenzyme plays different roles during evolution and in different tissues in humans. Its three-dimensional structure is well conserved during evolution: minute changes are responsible for the functional differences between enzymes from microorganism sources and those from humans. In recent years several investigations focused on human DAAO, mainly because of its role in degrading the neuromodulator D-serine in the central nervous system. D-Serine is the main coagonist of N-methyl D-aspartate receptors, i.e., excitatory amino acid receptors critically involved in main brain functions and pathologic conditions. Human DAAO possesses a weak interaction with the FAD cofactor; thus, *in vivo* it should be largely present in the inactive, apoprotein form. Binding of active-site ligands and the substrate stabilizes flavin binding, thus pushing the acquisition of catalytic competence. Interestingly, the kinetic efficiency of the enzyme on D-serine is very low. Human DAAO interacts with various proteins, in this way modulating its activity, targeting, and cell stability. The known properties of human DAAO suggest that its activity must be finely tuned to fulfill a main physiological function such as the control of D-serine levels in the brain. At present, studies are focusing on the epigenetic modulation of human DAAO expression and the role of post-translational modifications on its main biochemical properties at the cellular level.

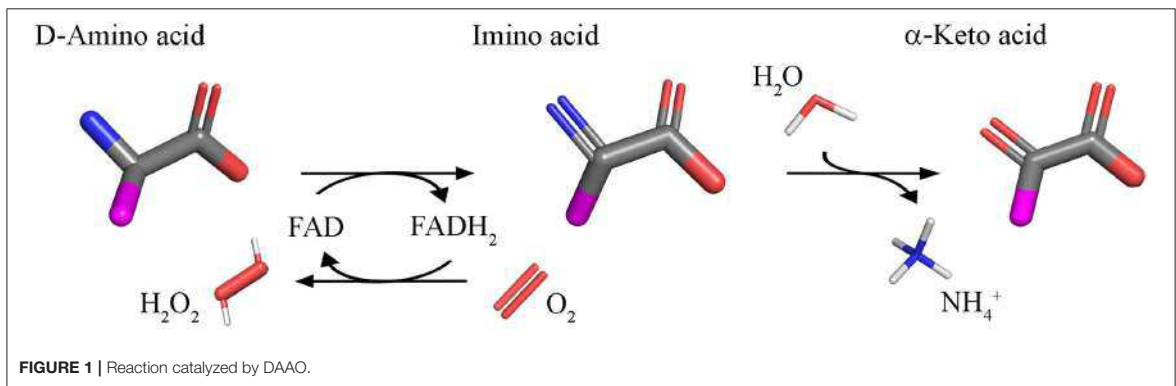
Keywords: D-amino acid oxidase, D-serine, substrate specificity, structure-function relationships, NMDA receptor

INTRODUCTION

Using FAD as cofactor, D-amino acid oxidase (DAAO, EC 1.4.3.3) catalyzes with strict stereoselectivity the oxidative deamination of neutral D-amino acids. DAAO has been discovered in pig kidney in 1935 (Krebs, 1935) and during the years it has been investigated as a prototype of FAD-dependent oxidases and has been the object of a plethora of studies: 96,325 publications concerning DAAO have appeared over the years (Scopus, 1 October 2018) with a significant increase from 2000 onward. D-Amino acids are dehydrogenated by DAAO into imino acids that spontaneously hydrolyzed to the corresponding α -keto acids and ammonia; the reoxidation of FADH₂ on molecular oxygen generated hydrogen peroxide (Figure 1).

The reaction catalyzed by DAAO is of biotechnological relevance since it can be used in biocatalysis (to produce α -keto acids from D-amino acids or 7-aminocephalosporanic acid from

Abbreviations: ALS, amyotrophic lateral sclerosis; CBIO, 5-chloro-benzo[d]isoxazol-3-ol; fALS, familial amyotrophic lateral sclerosis; DAAO, D-amino acid oxidase; hDAAO, human DAAO; NMDAR, N-methyl-D-aspartate type glutamate receptor; SR, serine racemase.



cephalosporin C, to resolve racemic mixtures of natural and synthetic amino acids, etc.), in biosensors, and in cancer therapy, to mention only the main applications (Pilone and Pollegioni, 2002; Caligiuri et al., 2006a,b; Pollegioni and Molla, 2011). For such a use, DAAO was isolated from microorganisms: those from *Trigonopsis variabilis* and *Rhodotorula gracilis* have been investigated in depth (Pollegioni et al., 2002, 2008; Arroyo et al., 2007).

The investigations on DAAO from higher organisms started in the 1980s. The enzyme's physiological role was long debated largely because the levels of D-amino acids were barely detectable and their presence in many tissues was questioned. Later on, appreciable levels of various D-amino acids were determined in brain and other tissues based on improved analytical methods (mainly high-performance liquid chromatography) (Nagata, 1992; Nagata et al., 1992; Hashimoto et al., 1993; Hamase et al., 1997). This cleared the path to identifying specific physiological roles for D-amino acids (Wang et al., 2000; Wolosker et al., 2002; Fuchs et al., 2005) and to propose for DAAO a key role in their metabolic control. Here, the ability of D-serine to act in the central nervous system as a coagonist of N-methyl D-aspartate receptors (NMDAR), excitatory amino acid receptors critically involved in learning and memory, stimulated the field.

D-Serine is mainly synthesized in neurons by racemization of the L-enantiomer catalyzed by the pyridoxal phosphate-dependent enzyme serine racemase (SR, EC 5.1.1.18) (Wolosker et al., 1999). L-Serine is provided by astrocytes possessing a specific metabolic pathway, referred to as the “phosphorylated pathway,” the primary route for the net synthesis of L-serine in the brain, considering the low permeability of the amino acid at the blood-brain barrier (Furuya et al., 2000). SR can also catabolize D- and L-serine through an α,β-elimination reaction to give pyruvate (Foltyn et al., 2005). From a cellular point of view, SR is a “complex” enzyme since its activity is modulated by energy level (ATP), metal ions, post-translational modifications, and protein interactors; for details, see (Pollegioni and Sacchi, 2010; Conti et al., 2011; Dellafora et al., 2015; Beato et al., 2016). Once released by neurons, D-serine is rapidly taken up and stored in astrocytes (Wolosker, 2011; Wolosker and Radziszhevsky, 2013). SR is poorly expressed in astrocytes, which

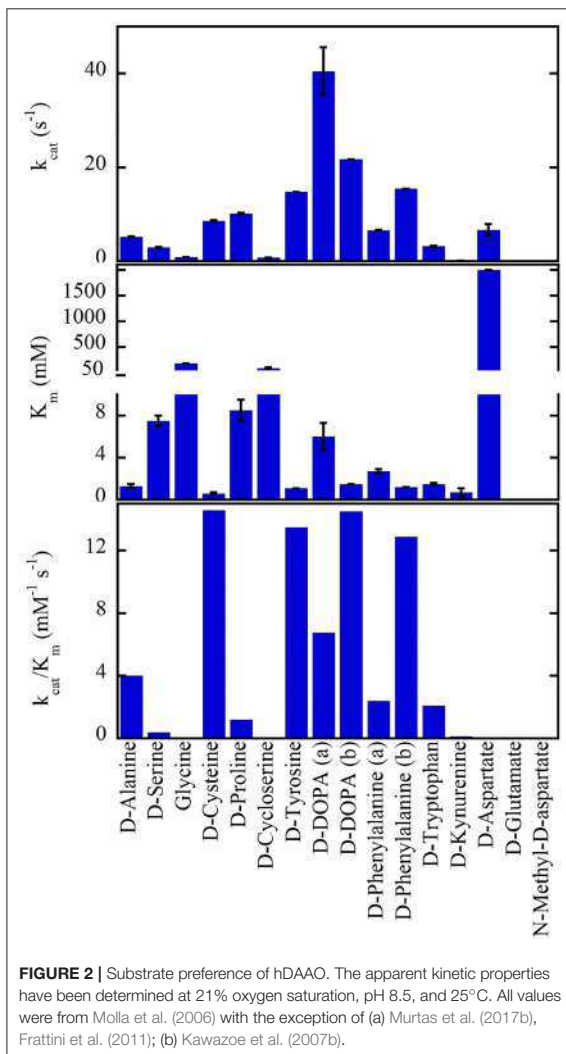
instead produce DAAO; in these cells the flavoenzyme indirectly controls its availability at the synapse by regulating D-serine cellular concentrations and affects the activation level of NMDAR by modulating the occupancy of the co-agonist site.

ROLE OF DAAO IN PHYSIOLOGICAL AND PATHOLOGICAL CONDITIONS

DAO gene is present in a single copy in human chromosome 12 (12q23-24 region) (Konno, 2001, AA): its structure has been detailed in Figure 3 of Pollegioni et al. (2007). A definite report of the DAO gene and protein expression in human tissues, with a particular focus on the brain regions, was recently reported, see Table 1 in Sacchi et al. (2018) and Figure 2 of Molla (2017). The highest amount of DAAO protein is observed in liver and kidney: in the latter organ, the enzyme is expressed in proximal tubule cells (Koibuchi et al., 1995; Sasabe et al., 2014a). DAAO was associated with chronic, pathologic renal damage, e.g., D-serine and D-propargylglycine induced nephrotoxicity due to DAAO-mediated generation of H₂O₂ (Konno et al., 2000; Maekawa et al., 2005; Krug et al., 2007).

The elucidation of the physiological functions of DAAO was accelerated by investigating the mutant ddY/DAAO^{-/-} mice strain expressing the inactive G181R enzyme variant (Konno and Yasumura, 1983): large amounts of D-amino acids were excreted in the urine of these animals. Accordingly, in liver and kidney (as well as in the urinary tract and in colon) DAAO eliminates D-amino acids originating in the cell walls of intestinal bacteria, from endogenous racemization, or from the diet. Indeed, increased D-serine levels were apparent in brain regions normally characterized by high DAAO expression in wild-type animals (Morikawa et al., 2001; Miyoshi et al., 2009).

In kidney and brain, the flavoenzyme is a component of the DAAO/3-MST pathway related to hydrogen sulfide (H₂S) generation (Shibuya et al., 2013). Within peroxisomes, DAAO metabolizes D-cysteine (mostly provided by food) to 3-mercaptopyruvate, which is then imported into mitochondria where it is converted to H₂S by 3-mercaptopyruvate sulfurtransferase (3MST). H₂S regulates kidney excretory



function and modulates blood pressure by affecting the release of renin.

The expression of DAAO was also reported in the granule fraction of mature human granulocytes (specifically on the cell surface), where it was proposed to participate in recognizing and counteracting foreign, phagocytosed microorganisms (Cline and Lehrer, 1969; Robinson et al., 1978). Within the phagosome, DAAO metabolizes D-alanine (derived from the peptidoglycan of the bacterial cell wall) producing H_2O_2 , which in turn is the oxidant substrate for myeloperoxidase that converts chloride to hypochlorous acid, a strongly microbicidal compound. Compared to the wild-type strain, the aforementioned *ddY/DAAO*^{-/-} mice show a higher susceptibility to *S. aureus* infection (Nakamura et al., 2012).

It was recently reported that DAAO plays a role in controlling the homeostasis of gut microbiota (Sasabe et al., 2016): DAAO (protein and activity) was identified in the proximal and middle small intestine of mice and humans, associated to the villus epithelium. A proteolyzed form of mouse DAAO was reported to be secreted in the lumen by goblet cells: this extracellular form is likely secreted by an N-terminal signal peptide and cleaved at the level of a putative cleavage site also located at the N-terminus (Sasabe et al., 2016). The H_2O_2 generated by DAAO during the catabolism of free D-amino acids of microbial origin represents an important factor in host defense (it protects the mucosal surface from the cholera pathogen) and in modifying microbiota composition (Sasabe et al., 2016).

In the central nervous system, DAAO is the enzyme mainly responsible for catabolism of D-serine: notably, in rodents and humans DAAO expression mirrors D-serine distribution. DAAO (activity and immunoreactivity) was mainly detected in cerebellum and, at lower levels, in the forebrain (Verrall et al., 2007; Madeira et al., 2008). A quite recent investigation confirmed DAAO expression in human forebrain regions and, at the same time, also highlighted that its activity is present in the white matter, throughout the corticospinal tract, and in the spinal gray matter, where it is localized in astrocytes mainly situated in the motor pathway (Sasabe et al., 2014b). The significant hDAAO activity assayed in spinal cord and brain stem is coherent with the proposed function in preventing excitotoxic cell death.

Morover, hDAAO activity was identified in dopaminergic neurons of the nigrostriatal system (Sasabe et al., 2014b): hDAAO is known to efficiently metabolize D-DOPA (see below); thus, the enzyme could affect the metabolism of dopamine, norepinephrine, and epinephrine.

In spinal cord neurons, NMDARs are expressed and are involved in the development of ongoing pain states via central sensitization (Latremoliere and Woolf, 2009). The tonic, pain-related behavior was amplified in the *ddY/DAAO*^{-/-} mice strain (Wake et al., 2001): the boost in the second phase of the formalin response is due to the potentiated NMDAR activation by the ensuing increased D-serine concentration. Later on, the role of DAAO as a pronociceptive factor in the spinal cord was confirmed (Zhao et al., 2010; Gong et al., 2011). Notably, the administration of DAAO inhibitors in rat models of tonic and chronic pain reversed pain-related behaviors and decreased the electrophysiological activity in spinal cord dorsal horn neurons and peripheral afferent inputs (Hopkins et al., 2013a). Among the putative ways in which DAAO is involved in chronic pain, a change in local levels of reactive oxygen species has been reported for formalin-induced pain (Lu et al., 2012). In this case, by inhibiting DAAO activity, a decrease in the production of spinal H_2O_2 levels is apparent (Lu et al., 2012; Gong et al., 2014). Interestingly, spinal DAAO has been also involved in pain hypersensitivity induced by perturbing sleep-regulating circuitries in the central nervous system through the deprivation of sleep, a process that generates pain hypersensitivity with no nerve or tissue injury (Wei et al., 2013). The H_2O_2 generated by DAAO could target the pronociceptive TRPA1 channel expressed by central terminals of primary afferent nerve fibers in the spinal dorsal horn.

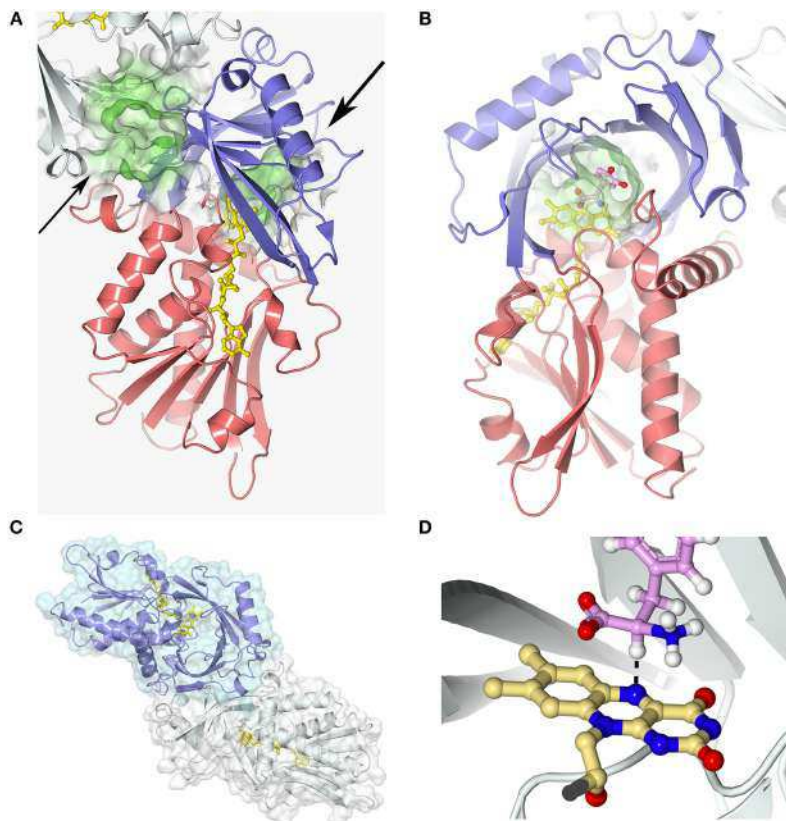


FIGURE 3 | hDAAO three-dimensional structure (pdb codes 2e49). **(A)** The hDAAO protomer is constituted by two domains: the substrate and the FAD-binding domain (in blue and red, respectively). The entrance to the active site is indicated by a large arrow. The thin arrow indicates the putative additional ligand-binding site (Kohiki et al., 2017). **(B)** The substrate is located above the *re*-side of the isoalloxazine ring of FAD, in a cavity of $\sim 220 \text{ \AA}^3$. **(C)** hDAAO is a stable homodimer, characterized by a head-to-head mode of monomer interaction (Kawazoe et al., 2006). **(D)** The substrate dehydrogenation ensues by the direct hydride transfer of the α -H from the α -C of the D-amino acid to the flavin N(5), see dotted line (Umhau et al., 2000). Following hydride transfer, a negative charge is generated on the reduced flavin, which is stabilized by the positive charge generated on the imino group of the product. This figure has been generated by modeling a D-Tyr molecule instead of the original ligand imino serine. Figure prepared with 3dproteinimaging.com.

Amotrophic lateral sclerosis (ALS) is a rapidly progressing, adult-onset, neuromuscular disease distinguished by the selective loss of motor neurons. A recent, comprehensive, exome-sequencing study revealed that the only DNA variants associated with clinical outcome of ALS and with lower rates of survival are located on the *DAO* gene (Cirulli et al., 2015). Actually, the R199W DAAO substitution was identified in a three-generational familial ALS (fALS) kindred (Mitchell et al., 2010). This substitution impaired DAAO activity, boosted the formation of ubiquitinated protein aggregates, promoted autophagy activation, and increased apoptosis when the protein was overexpressed in motor neuron cell lines or primary motor neuron cultures (Paul and de Bellerche, 2012; Paul et al., 2014). The transgenic mouse lines expressing R199W DAAO ($\text{DAO}^{\text{R199W}}$) were unaffected in survival although they exhibited the features common to several ALS mice models, i.e., decreased

body weight, marked kyphosis, and loss of motor neurons in spinal cord (Kondori et al., 2017). Recently, it was reported that the most significant and robust splicing change after depletion of hnRNP A2/B1 in the mouse spinal cord was the skipping of exon nine within *DAO* gene, yielding a reading frameshift and early termination of the protein, predicted to lack 2 α -helices and 3 β -sheets and to generate a highly unstable and inactive variant (Martinez et al., 2016).

Impaired NMDAR signaling pathways are known to occur in the hippocampus and cerebral cortex of aging brains (Billard, 2008); in aged tissues a hypoactivation of NMDAR is related to decreased D-serine levels (Junjaud et al., 2006; Mothet et al., 2006). Neurodegeneration induced by NMDAR hypoactivity was also proposed to contribute to AD and to be related to the progression of aging brain from mild cognitive impairment to AD (Olney et al., 1997; Wozniak et al., 1998). Compared to

healthy individuals, the serum levels of DAAO are increased in patients affected by mild cognitive impairment and mild and severe AD (Lin et al., 2017), and DAAO levels correlate with the severity of cognitive deficit and with the D-serine level.

Alterations in D-serine levels have been observed in Alzheimer's disease (AD) and have been suggested to represent a pro-death signal (Billard, 2008; Madeira et al., 2015).

An NMDAR hypofunction was also related to schizophrenia (Coyle et al., 2003; Coyle, 2006; Stone and Pilowsky, 2007): the altered activation state of the receptor was proposed to depend on a deficiency in D-serine signaling (Hashimoto et al., 2003, 2005; Verrall et al., 2010). The protein and activity levels of hDAAO were altered in post-mortem brain tissues from schizophrenic patients in cerebral cortex (Madeira et al., 2008), cerebellum (Kapoor et al., 2006; Verrall et al., 2007; Burnet et al., 2008), medulla oblongata, and choroid plexus (Ono et al., 2009). Further support comes from the discovery that the *G72* gene, encoding the small protein pLG72, the main hDAAO-specific binding protein (see below), has been linked to schizophrenia (Chumakov et al., 2002; Sacchi et al., 2008, 2016; Pollegioni et al., 2018). Additional meta-analyses supported a genetic association between *DAO*, *G72*, and schizophrenia: they have been classified as schizophrenia susceptibility genes (Sacchi et al., 2016).

CELLULAR PROPERTIES OF hDAAO

DAAO is considered a marker of peroxisomes since it contains a classical PTS1 signal at the C-terminus (Horiike et al., 1994; Moreno et al., 1999). Notably, an active DAAO form has been reported in the cytosol, both in glial cells and neurons (Sacchi et al., 2008, 2011; Popiolek et al., 2011). In astrocytes overexpressing hDAAO, the cytosolic form seems to transiently accumulate in this compartment before targeting peroxisomes (Sacchi et al., 2011). Recent reports on rats demonstrated that DAAO is present both in the cytosol and nuclei of proximal tubule epithelial cells following treatment with the drug propiverine (Luks et al., 2017a,b) and that intestinal epithelial cells in mice secrete the flavoenzyme into the lumen (Sasabe et al., 2016).

The degradation pathway of hDAAO was investigated in U87 glioblastoma cells stably expressing the flavoenzyme fused to the C-terminus of the enhanced yellow fluorescent protein (EYFP, thus generating a peroxisomal chimeric protein) or at the N-terminus (thus producing a cytosolic chimeric protein since the PTS1 signal is masked). hDAAO is a long-lived protein showing a half-life > 60 h. The peroxisomal EYFP-hDAAO is degraded via the lysosomal/endosomal pathway, whereas the cytosolic hDAAO-EYFP protein is ubiquitinated and targets the proteasome. Overexpression of the interacting protein pLG72 (showing a rapid turnover, half-life in the 25–40 min range) increases the turnover of DAAO (half-life ~6 h) (Sacchi et al., 2011): hDAAO-pLG72 complex formation seems to represent a means to play a protective role against excessive D-serine depletion by the active, cytosolic enzyme (see below).

BIOCHEMICAL PROPERTIES

General Properties

A comparison of the main biochemical properties of mammalian DAAOs is reported in Sacchi et al. (2012). Recombinant hDAAO is produced in fairly large amounts in *E. coli* cells (Kawazoe et al., 2006; Molla et al., 2006; Romano et al., 2009). It is purified as active holoenzyme by adding exogenous FAD to the purification buffers: hDAAO shows the classical properties of flavoprotein oxidases, such as a quick reaction with O₂ in the reduced form and stabilization of the anionic red flavin semiquinone.

In the 6–10 pH range, hDAAO shows a good activity and stability (Murtas et al., 2017b). From the fitting of the activity values determined at different pH values, two dissociations were apparent: a pK_a of 2.5 and 11.1, respectively. Notably, the enzyme is fully stable after 60 min of incubation at 4°C at pH values ≥3.0 and ≤10.0. The flavoenzyme is stable up to 45°C, a temperature corresponding to the optimum for the enzymatic activity. The melting temperature determined following the loss of activity was ~55°C (Murtas et al., 2017b), higher than the values determined using the changes in protein fluorescence intensity (Caldinelli et al., 2010): this result suggests that the alteration in protein conformation brings forward the loss of enzymatic activity.

hDAAO activity is not affected by the presence of divalent ions (Ca²⁺ and Mg²⁺) and/or nucleotides. Similarly, the reducing agent N-acetyl-cysteine, a derivative of L-cysteine, acting as antioxidant and anti-inflammatory agent and that is able to modulate NMDAR activity (Kumar, 2015), does not affect the activity of hDAAO (Murtas et al., 2017b).

Substrate Specificity

hDAAO shows a wide substrate acceptance: the best substrates are hydrophobic and bulky D-amino acids (D-DOPA > D-Tyr > D-Phe > D-Trp, **Figure 2**). The highest *k_{cat}* value was determined for D-3,4-dihydroxy-phenylalanine (D-DOPA) (Kawazoe et al., 2007a,b; Murtas et al., 2017a,b), also showing a high affinity due to two additional H-bonds between the OH-groups of the substrate and His217 and Gln53 (Kawazoe et al., 2007a). However, the oxidation of D-DOPA is hindered by the substrate inhibition effect, K_i of 0.5 (Murtas et al., 2017b) or 41 mM (Kawazoe et al., 2007b).

hDAAO is also active on small, uncharged D-amino acids (D-Cys > D-Ala > D-Pro > D-Ser) (Molla et al., 2006; Kawazoe et al., 2007b; Frattini et al., 2011; Murtas et al., 2017b). Purified recombinant hDAAO shows a low catalytic efficiency on what is known as the main physiological substrate, D-serine. Whether *in vivo* (and especially in glial cells) an increase in kinetic efficiency is achieved by the binding with a cellular compound (i.e., a protein or a small size ligand) or by a post-translational modification is still unknown: this issue deserves further investigations. The highest catalytic efficiency was determined for D-cysteine, a compound involved in H₂S generation (see above) (Shibuya et al., 2013).

hDAAO is not active on glycine and acidic D-amino acids (NMDA and D-Glu) while the activity on D-Asp is hampered by the high apparent K_m (in the molar range) (Molla et al., 2006; Murtas et al., 2017b). hDAAO also oxidizes D-kyurenine

with an apparent K_m value (0.7 mM) resembling that determined for D-cysteine. Kynurenic acid, the product of D-kynurenine oxidation, binds to the modulatory glycine site of the NMDAR resulting in an inhibitory effect. Furthermore, hDAAO is also active on D-cycloserine, an NMDAR modulator (Kumar, 2015).

The substrate promiscuity of hDAAO supports the hypothesis that this flavoenzyme might play a role in different tissues and cells.

The activity of hDAAO on D-serine is partially inhibited by the L-enantiomer (Murtas et al., 2017b). L-Serine acts as competitive inhibitor (K_i of 26.2 mM). Under anaerobic conditions L-serine, as well as L-alanine or L-valine, are able to reduce FAD. However, a physiological concentration of L-serine (corresponding to ≤ 2 mM in brain tissues and in blood) (Weatherly et al., 2017) should not modify the oxidation of D-serine by hDAAO.

Kinetic Mechanism

For all known DAAOs, the oxidative deamination of D-amino acids follows a ternary-complex mechanism (Pollegioni et al., 1993; Umhau et al., 2000; Molla et al., 2006). The substrate dehydrogenation ensues by the direct hydride transfer of the α -H from the α -C of the D-amino acid to the flavin N(5); please see below and **Figure 3D**. The distance between these atoms is 3.6 Å in the hDAAO-imino serine complex: owing to the tetrahedral geometry of the substrate α -C, the mentioned atoms should be closer in the Michaelis complex (~ 3.2 Å). Following hydride transfer, the reduced flavin is negatively charged: the positive charge of the product imino group electrostatically stabilizes the reduced cofactor.

For mammalian DAAOs, and especially for hDAAO, the first half of the reaction (the reductive half-reaction), namely, the conversion of the tetrahedral D-amino acid into the planar imino acid coupled to the flavin reduction is fast (117 ± 6 s⁻¹ on D-serine), significantly faster than turnover (6.3 ± 1.4 s⁻¹). The rate-limiting step in hDAAO catalysis is the product release (Molla et al., 2006; Molla, 2017). The rate of imino acid release from the reduced enzyme is < 1 s⁻¹, too slow to allow the reoxidation step to start from the free, reduced enzyme. Accordingly, reoxidation must start from the corresponding reduced enzyme-imino acid complex: the second-order reaction corresponds to 1.25×10^5 M⁻¹s⁻¹.

hDAAO STRUCTURAL-FUNCTIONAL PROPERTIES

Overall Structure

Each hDAAO protomer contains 347 amino acids (40.3 kDa), harbors one molecule of FAD, and is composed of 11 α -helices and 14 β -strands. hDAAO is constituted by two interconnected regions: an FAD-binding domain containing the dinucleotide binding motif (Rossmann fold) and a substrate-binding domain in which a large, twisted, antiparallel β -sheet forms the active-site roof and part of the oligomerization interface (**Figures 3A,B**). hDAAO is a stable homodimer: the two monomers interact via a head-to-head geometry (**Figure 3C**; Kawazoe et al., 2006).

In the active site, the substrate is located above the *re*-side of the isoalloxazine ring of FAD, in a cavity of ~ 220 Å³ (**Figure 3B**). The substrate is bound via several hydrogen bonds in the correct orientation with respect to the flavin N(5) position for catalysis to proceed: the α -carboxylic group of the substrate electrostatically interacts with Arg283 and Tyr228, whereas the α -amino group interacts with Gly313 and the C(4)=O of FAD. The side chain of the substrate is placed in a pocket made up of hydrophobic residues (Leu51, Gln53, Leu215, and Ile230), named the substrate-specificity pocket (Kawazoe et al., 2006). The active-site “roof” is shaped by the side chain of Tyr224, a residue belonging to a mobile loop (216–228): the product/substrate exchange during catalysis is facilitated by the switch of this residue from a closed to an open conformation. This conformational change significantly influences the enzyme properties: limiting the turnover, increasing the hydrophobicity of the active site, and allowing hDAAO to bind large substrates (Molla et al., 2006; Kawazoe et al., 2007b).

The strict stereoselectivity of DAAO for the D-enantiomer of the amino acids is rationalized by the four-location model for enantioselectivity (Mesecar et al., 2000; Umhau et al., 2000; Mörtl et al., 2004). According to this model, the substrate establishes three interactions—using the α -carboxylic group, the α -amino group and the side chain—with the active site residues indicated above: the exact binding produces a “functional direction” exemplified by the alignment of the α -H of the substrate and the N(5) of FAD, which allows hydride transfer (**Figure 3D**).

Oligomeric Structure

Different from other DAAOs (Mattevi et al., 1996; Pollegioni et al., 2007; Frattini et al., 2011), an 80 kDa homodimer is generated by both the holo- and the apoprotein form of hDAAO (Molla et al., 2006). This results from a distinguishing charge distribution at the dimer interface (a region corresponding to $\sim 1,500$ Å², i.e., the 9.8% of the overall solvent accessible surface, **Figure 3C**), where a significantly higher amino acidic substitution frequency was observed than for the overall protein (33 vs. 15%, respectively) (Kawazoe et al., 2006). Notably, the urea-induced dissociation of dimeric hDAAO generates protein conformers prone to aggregation (Caldinelli et al., 2009).

FAD Binding

In hDAAO the FAD cofactor shows an elongated conformation and it is buried in the protein core: the isoalloxazine ring is located at the interface between the two subdomains with the *re*-side facing the interior of the active site (Kawazoe et al., 2006; Molla, 2017). At this side of the flavin ring, the conformation of the surrounding residues is highly conserved among mammalian DAAOs. Conversely, at the *si*-face, the conformation of the hydrophobic stretch (47-VAAGL-51, a structurally ambivalent peptide) differs between the human and porcine enzymes, causing loss of the H-bond between Ala49 and N(5) of the cofactor and likely decreasing the strength of the interaction of the flavin cofactor and the rate of flavin reduction (Kawazoe et al., 2006).

hDAAO possesses the weakest binding of the FAD cofactor ($K_d = 8.0 \mu\text{M}$) among known DAAOs ($K_d = 0.2$ and $0.02 \mu\text{M}$ for pig and yeast DAAOs, respectively). Accordingly, hDAAO exists in solution as an equilibrium of holo- and apoprotein forms (Caldinelli et al., 2010). The presence of an active-site ligand increases the affinity of the flavin to the protein moiety, $K_d = 0.3 \mu\text{M}$ (Molla et al., 2006; Caldinelli et al., 2010). Quenching of protein fluorescence intensity during titration of the apoprotein with the cofactor, in the presence or absence of sodium benzoate, is a biphasic process (Murtas et al., 2017b), suggesting that the apoprotein form exists in two conformations with differing cofactor binding affinity: the higher intensity amplitude associated with the first phase observed in the presence of benzoate indicates that binding of an active-site ligand favors the protein conformation with the higher avidity for FAD (Murtas et al., 2017b). A second possibility is the presence of two binding sites. Here, a recent investigation based on computational and labeling analyses suggests that an additional ligand-binding site is located at the monomer-monomer interface (Figure 3A; Kohiki et al., 2017).

The holoenzyme reconstitution is a sequential process: in the first step, FAD binds the apoprotein moiety and recovers the catalytic activity; in the second step, a slow, secondary conformational change generates the final holoenzyme conformation (Caldinelli et al., 2009). Notably, the first step is 20-fold faster when benzoate is present (Caldinelli et al., 2010).

The melting temperature for the unfolding of the holoenzyme is 6–9°C higher than for the corresponding apoprotein (Caldinelli et al., 2009).

The observed increase in cofactor binding affinity in the presence of benzoate suggested that, in addition to the different conformation of the hydrophobic VAAGL sequence observed in the hDAAO-benzoate complex (Kawazoe et al., 2006), an alternative conformation of the substrate-free enzyme should exist that binds the cofactor less efficiently (Murtas et al., 2017b). In any case, the structure of the free enzyme form (PDB 2e48) overlaps that of the hDAAO-benzoate complex (PDB 2du8).

Based on the *in vivo* concentration of FAD ($\sim 5 \mu\text{M}$), it is conceivable that in the cell an equilibrium between the hDAAO holoenzyme (active) and the apoprotein (inactive) form exists, with the latter one being predominant in the absence of an active-site ligand.

Ligand Binding

hDAAO inhibitors can essentially be grouped into substrate-competitive and cofactor-competitive inhibitors (Molla et al., 2006; Sacchi et al., 2012; Terry-Lorenzo et al., 2014; Molla, 2017). Among the active-site ligands, small aromatic (aryl) carboxylic acids or acid isosteres are powerful hDAAO inhibitors used as scaffolds for developing novel drugs (see below). These compounds, such as benzoate, *o*-aminobenzoate, substituted quinilones, or 4H-furo[3,2-*b*]pyrrole-5-carboxylic acid (Figure 4), bind the flavoenzyme similarly to the substrate: the inhibitor COOH group (or the corresponding C=O or OH substituents) interacts with Arg283 and Tyr228, an H-bond donor binds Gly313, and the remaining part interacts with the hydrophobic region of the active site (that can accommodate

molecules containing 12–13 atoms) (Duplantier et al., 2009). In the hDAAO-inhibitor complex, the side chain of Tyr224 is shifted toward the inner part of the active site and forms a strong π - π stacking interaction, “sandwich,” between its aryl chain and the *re*-side of the isoalloxazine ring of the cofactor. The strongest interaction is observed when the aromatic rings are slightly displaced [i.e., with 3-hydroxyquinolin-2(1H)-one] (Figure 4) and not perfectly stacked (i.e., with benzoate). When saturated analogs of these compounds are used, a drop in the binding affinity is apparent, indicating the relevance of the π - π stacking interaction.

The binding of aromatic carboxylic acids to the hDAAO holoenzyme inhibits the flavoenzyme and perturbs its absorbance spectrum in the visible region. For example, benzoate yields a shoulder at ~ 497 nm ($K_d = 7 \mu\text{M}$ and $K_i = 9.7 \mu\text{M}$) (Kawazoe et al., 2006; Molla et al., 2006); anthranilate binding generates a spread classical charge transfer band at ~ 580 nm ($K_d = 40 \mu\text{M}$) (Molla et al., 2006). The ligand-binding site is present in the apoprotein form, too, as made apparent by the alteration in protein fluorescence and in thermostability of the latter hDAAO form when the substrate D-serine or the substrate analog trifluoro-D-alanine is added (Caldinelli et al., 2009, 2010).

Conversely to benzoate, for the binding of the inhibitor 6-chloro-benzo[d]isoxazol-3-ol (CBIO) (Figure 4) to hDAAO a single-step binding process is evident and the K_d value estimated following the quenching of protein fluorescence intensity corresponds well to the K_d , IC_{50} , and K_i values determined using different methods.

ADP and CPZ (Figure 4) (IC_{50} of 580 and $5 \mu\text{M}$, respectively) behave as FAD-competitive inhibitors for binding to hDAAO (Iwana et al., 2008; Sacchi et al., 2008; Terry-Lorenzo et al., 2014). In particular, CPZ binding generates a protein conformation more sensitive to proteolysis and thermal unfolding than the native holoenzyme (Caldinelli et al., 2010). The near-UV CD spectra show that the tertiary structure of hDAAO-CPZ complex differs from that of the hDAAO-FAD: the former more closely resembles that of the apoprotein (Caldinelli et al., 2010).

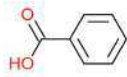
Notably, the ligands D-serine, FAD, benzoate, and CPZ did not affect the formation of the hDAAO-pLG72 complex (see below).

MODULATION OF hDAAO ACTIVITY

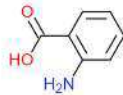
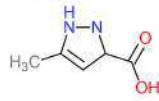
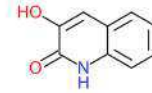
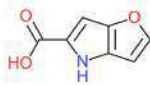
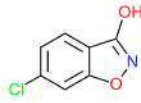
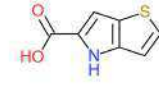
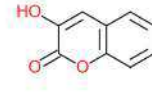
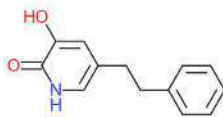
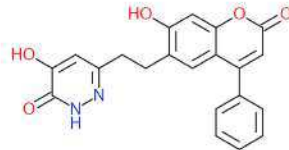
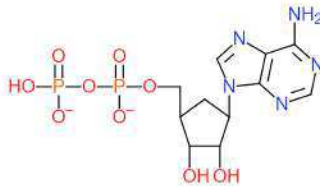
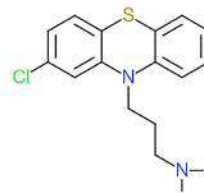
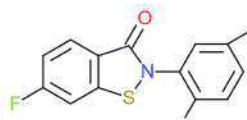
By Protein Interaction

Human flavoenzyme function is modulated by interacting with various proteins. hDAAO, through the PTS1-type peroxisomal-targeting signal, interacts with the Pex5p receptor, a protein involved in protein import and in the assembly of peroxisomes (Ghosh and Berg, 2010).

Genome-wide association studies and meta-studies in different populations have linked polymorphisms in the gene encoding pLG72 protein with schizophrenia and other psychiatric diseases (Drews et al., 2013; Sacchi et al., 2016; Pollegioni et al., 2018). In particular, hDAAO specifically binds to the primate-specific protein pLG72: two hDAAO homodimers interact with two pLG72 molecules, yielding a 200-kDa protein complex ($K_d = 0.08$ – $0.53 \mu\text{M}$); for a recent

Substrate-competitive hDAAO inhibitors:

Benzoate

o-Aminobenzoate
(anthranilic acid)5-Methyl-pyrazole-
3-carboxylate3-Hydroxyquinolin-
2(1H)-one4H-Furo[3,2-b]pyrrole-
5-carboxylic acid6-Chloro-benzo[d]
isoxazole-3-ol
(CBIO)4H-Thieno[3,2-b]pyrrole-
5-carboxylic acid3-Hydroxy-2H-
chromen-2-one3-Hydroxy-5-(2-phenylethyl)
pyridin-2(1H)-one4-Hydroxy-6-[2-(7-hydroxy-2-oxo-
4-phenyl-2H-chromen-6-yl)
ethyl]pyridazin-3(2H)-one**FAD-competitive hDAAO inhibitors:**Adenosine diphosphate
(ADP)Chlorpromazine
(CPZ)**Substrate- and FAD-competitive inhibitor:**2-(2,5-dimethylphenyl)-6-fluorobenzo[d]
isothiazol-3(2H)-on**FIGURE 4 |** Structural formula of selected hDAAO inhibitors classified based on their mechanism of enzyme inhibition.

review (see Pollegioni et al., 2018). *In vitro*, the formation of the 200-kDa complex does not alter the kinetic parameters or the binding with the FAD cofactor of hDAAO, but rather induces a change in its overall tertiary structure, causing a time-dependent inactivation (Sacchi et al., 2008). By using low-resolution techniques (i.e., limited proteolysis coupled to mass spectroscopy and cross-linking experiments) structural elements involved in forming the interface surface in the hDAAO-pLG72 complex have been identified, highlighting the role of the N-terminal region of pLG72 in forming the oligomerization interface (Birolo et al., 2016; Sacchi et al., 2017). hDAAO in transiently transfected glial cells (i.e., the U87 human glioblastoma cell line) is largely localized in peroxisomes but also present in cytosol (Sacchi et al., 2011) while pLG72 shows a mitochondrial localization. We proposed that, in this model cell system, newly synthesized hDAAO interacts with pLG72 on the cytosolic side of the outer mitochondrial membrane (Sacchi et al., 2011). Such an interaction increases the D-serine/total serine ratio and decreases hDAAO activity and half-life, see above (Sacchi et al., 2008, 2011; Cappelletti et al., 2014). We recently proposed that pLG72 (itself or recruiting further proteins) might target the cytosolic form of hDAAO to the ubiquitin-proteasome system, thus starting its degradation (Cappelletti et al., 2014). This mechanism could represent a further process to regulate the D-serine levels in the hindbrain where the flavoenzyme is expressed in glial cells.

Analogously, the activity of hDAAO is negatively regulated by bassoon, a component of the cytoskeletal matrix, mainly located at the presynaptic active zone. The hDAAO-bassoon complex formation has been proposed to prevent D-serine depletion acting on the active, extraperoxisomal enzyme form located at presynaptic terminals (Popielek et al., 2011). The inhibitory effect of bassoon may account for the difficulties in detecting hDAAO activity in the forebrain (Verrall et al., 2007), a region where the enzyme is mostly expressed in neurons.

By hDAAO Inhibitors

Abnormal changes in hDAAO activity yielding locally decreased D-serine levels have been correlated with neurological disorders (e.g., schizophrenia); therefore, the identification of hDAAO inhibitors (to slowing down the neuromodulator degradation process) to be used as drugs has garnered growing interest. This treatment has beneficial effects on cognition and learning functions (Hopkins et al., 2013b).

More than 500 substrate-competitive inhibitors have been identified so far (Gilson et al., 2016). Analogously to the substrate, their chemical structure contains a planar moiety which interacts with the active-site residues close to the FAD cofactor isoalloxazine ring and a second portion which is positioned in the substrate side-chain binding pocket. The “core” of the planar moiety is usually formed by one or two fused rings (one of which might be aromatic) and contains at least a carboxylic group to establish the H-bond interaction with Arg283. The second part of the inhibitor molecule corresponds to the side chain of the substrate: this portion, depending on the size and chemical features, forms further interactions with residues belonging to the substrate specificity pocket and/or to the active site entrance.

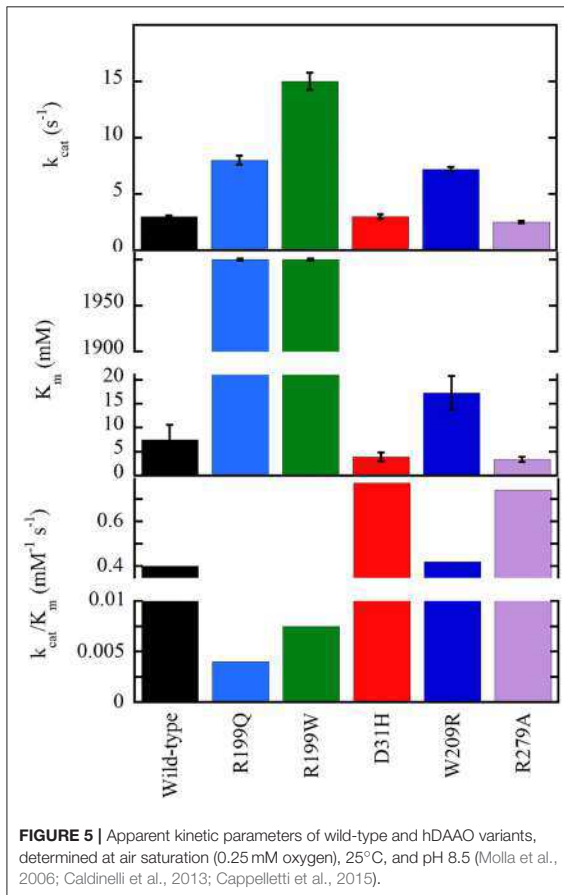
A comprehensive review about the details of inhibitor binding to hDAAO has been published recently (Molla, 2017). It ranks classical and novel compounds in four classes:

- (i) classical inhibitors: typically single-ring ligands, i.e., benzoate, anthranilate, and improved variations (Sacchi et al., 2012; Katane et al., 2013). The compound 5-methylpyrazole-3-carboxylic (**Figure 4**) acid is a prototype of this class of compounds in which two C atoms of the ring are substituted by N: the optimized H-bonds network allows a high affinity for hDAAO ($K_i = 0.39 \mu\text{M}$). This compound crosses the blood-brain barrier in rats, thus raising the D-serine level in certain brain regions (Adage et al., 2008);
- (ii) second-generation inhibitors: larger compounds than classical inhibitors since they are characterized by two substituted, heterocyclically fused rings, which form additional H-bonds and van der Waals interactions with residues forming the active site, i.e., compounds derived from 3-hydroxyquinolin-2(1H)-one and CBIO (Ferraris et al., 2008; Katane et al., 2013). The main drawback of the last compound is the low passage through the blood-brain barrier: such a compound does not increase D-serine levels in the brain (Ferraris et al., 2008);
- (iii) third-generation inhibitors: bulky and flexible compounds whose side chain binds to an additional “subpocket” at the entrance of the active site generated by a conformational change in Tyr224 induced by ligand binding (Raje et al., 2013; Terry-Lorenzo et al., 2014);
- (iv) novel-generation inhibitors: molecules that can interact with the hDAAO-pLG72 complex since they contain the “ebsulfur” (2-phenyl-2,3-dihydro-1,2-benzothiazol-3-one) substructure that forms S-S thiol bonds with the cysteines of hDAAO, when the protein is partially unfolded due to pLG72 binding (Terry-Lorenzo et al., 2015). Compound [2-(2,5-dimethylphenyl)-6-fluorobenzo[d]isothiazol-3(2H)-on (**Figure 4**) inhibits hDAAO, acting as both FAD- and D-serine-competitive inhibitor. The so-called “compound 22,” classified as a class C compound by Terry-Lorenzo et al. (2015), only acts as hDAAO inhibitor under oxidizing conditions. This compound does not dissociate from the flavoenzyme in jump-dilution experiments and stably inactivate the enzyme: recovery of the DAAO activity is obtained only by adding a reducing agent.

By Single Point Substitutions

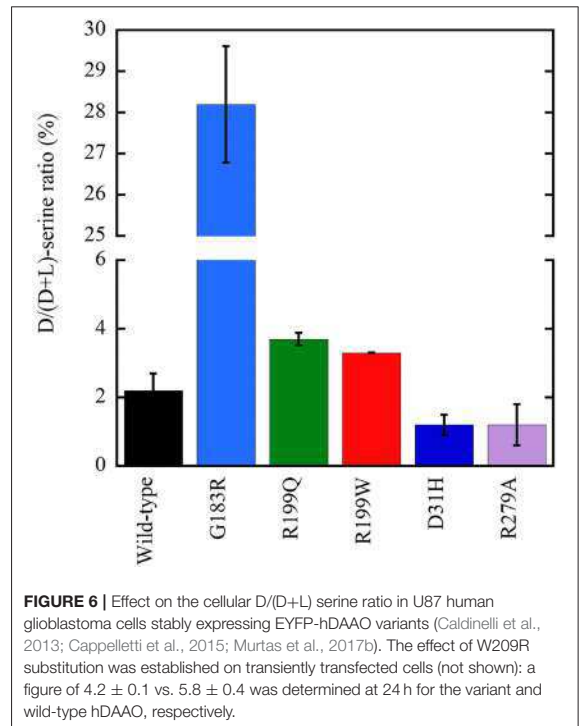
Based on biochemical properties, hDAAO variants corresponding to known single nucleotide polymorphisms or sequence conflicts have been grouped into two classes: hypoactive and hyperactive; for a recent review (see Sacchi et al., 2018). The conditions and levels of recombinant expression of seven variants of hDAAO are reported in Table 2 of Sacchi et al. (2018).

The G183R, R199W, and R199Q hDAAOs show significantly decreased enzymatic activity (or fully abolished for the latter variant, see **Figure 5**), and a perturbation of the conformation: (a) in G183R hDAAO, corresponding to the coding mutation occurring in the ddY/DAAO^{-/-} mice strain expressing the inactive G181R DAAO (Konno and Yasumura, 1983), alterations



in secondary structure elements likely alter the conformation of the flavin binding domain and thus negatively affect the cofactor binding (Murtas et al., 2017a); (b) the tertiary structure of R199W (the variant associated with the onset of FALS) and R199Q variants is significantly altered: this favors aggregation propensity but does not modify the interaction with pLG72 (Cappelletti et al., 2015; Murtas et al., 2017a); (c) in G331V hDAAO the change in the C-terminal α -helix promotes protein aggregation, strongly affecting the variant solubility (Caldinelli et al., 2013). At the cellular level, both G183R and G331V variants were partly mistargeted: they formed cytosolic protein aggregates, which largely colocalized with ubiquitin, and resulted in increased apoptosis (Caldinelli et al., 2013; Murtas et al., 2017a).

On the other hand, the D31H, W209R, and R279A substitutions have the opposite effect on hDAAO activity, resulting in slightly or significantly improved catalytic efficiency (Figure 5) and FAD affinity. For example, a 2-fold increased turnover number was apparent for the W209R hDAAO, which was more active than the wild-type hDAAO using 0.3 mM D-serine and 5 μ M FAD, i.e., concentrations resembling physiological conditions (Cappelletti et al., 2015).



Following overexpression in U87 cells, all the investigated hDAAO variants significantly altered the cellular levels of D-serine (Figure 6; Caldinelli et al., 2013; Cappelletti et al., 2015; Murtas et al., 2017a). The expression of inactive variants of hDAAO could produce susceptibility to neurodegenerative disorders due to augmented D-serine levels which, when paralleled by elevated glutamate levels, could lead to hyperactivation of NMDAR and thus to excitotoxicity. In contrast, a deficit in NMDAR-mediated transmission might be related to the expression of hyperactive variants due to an abnormal decrease in D-serine at the synapses, as proposed in schizophrenia onset. Furthermore, hDAAO hyperactive variants produce nonphysiological levels of H_2O_2 : this process could contribute to the molecular mechanism of the central sensitization typical of chronic pain.

To delve into the structure-function relationships in mammalian DAAOs, alanine-scanning analysis of first and second shell residues of the enzyme from pig prompted the focus on active-site lid residues (region 221–225) and on the positions 55 and 56 in hDAAO (Subramanian et al., 2018). Molecular dynamics simulations identified a narrow tunnel that could provide access to the active site of hDAAO, named tunnel T1. The Y55 residue was suggested to be involved in anchoring the lid loop in the closed conformation (its dynamics are hampered by Y314), modulating the solvent access and substrate/product exchange at the active site and separating T1 from an additional, putative tunnel. The Y55A substitution facilitated accessibility of

the active site: a 2-fold increase in specific activity on D-Trp was observed.

BY POST-TRANSLATION MODIFICATIONS

The molecular mechanisms by which hDAAO expression and acquisition of catalytic activity are achieved inside the cell are still largely unknown: a fine and careful regulation through post-translational modification(s) is expected. Actually, hDAAO was proposed to be regulated by nitrosylation (Shoji et al., 2006). In detail, the activity of DAAO, in a membrane fraction of U87 glioblastoma cells, was enhanced by NO in a dose-dependent manner. The authors proposed that, in astrocytes, NO may inhibit SR and enhance hDAAO activities thus accelerating D-serine degradation. Following D-serine supply from astrocytes to neurons, synthesis of nitric oxide in neurons may temporarily be increased, yielding a feedback regulation of the neuromodulator.

CONCLUSIONS

With the final aim to use hDAAO in different tissues responding to several needs, evolution adopted complicated regulatory strategies to modulate the activity of the flavoenzyme. In human brain tissues, hDAAO should be mainly present in the apoprotein, inactive form considering the physiological concentration of FAD and its weak interaction with the apoprotein moiety. Conversion of the inactive hDAAO apoprotein into the active holoenzyme is facilitated by the presence of an active-site ligand, such as the substrate: this represents an efficient way to maintain the level of selected D-amino acids in the physiological range.

REFERENCES

- Adage, T., Trillat, A. C., Quattropiani, A., Perrin, D., Cavarec, L., Shaw, J., et al. (2008). *In vitro* and *in vivo* pharmacological profile of AS057278, a selective D-amino acid oxidase inhibitor with potential anti-psychotic properties. *Eur. Neuropsychopharmacol.* 18, 200–214. doi: 10.1016/j.euroneuro.2007.06.006
- Arroyo, M., Menéndez, M., García, J. L., Campillo, N., Hormigo, D., de la Mata, I., et al. (2007). The role of cofactor binding in tryptophan accessibility and conformational stability of His-tagged D-amino acid oxidase from *Trigonopsis variabilis*. *Biochim. Biophys. Acta* 1774, 556–565. doi: 10.1016/j.bbapap.2007.03.009
- Beato, C., Pecchini, C., Cocconcelli, C., Campanini, B., Marchetti, M., Pieroni, M., et al. (2016). Cyclopropane derivatives as potential human serine racemase inhibitors: unveiling novel insights into a difficult target. *J. Enzyme. Inhib. Med. Chem.* 31, 645–652. doi: 10.3109/14756366.2015.1057720
- Billard, J. M. (2008). D-serine signalling as a prominent determinant of neuronal-glia dialogue in the healthy and diseased brain. *J. Cell. Mol. Med.* 12, 872–884. doi: 10.1111/j.1582-4934.2008.00315.x
- Birolo, L., Sacchi, S., Smaldone, G., Molla, G., Leo, G., Caldinelli, L., et al. (2016). Regulating levels of the neuromodulator D-serine in human brain: structural insight into pLG72 and D-amino acid oxidase interaction. *FEBS J.* 283, 3353–3370. doi: 10.1111/febs.13809
- Burnet, P. W., Eastwood, S. L., Bristow, G. C., Godlewska, B. R., Sikka, P., Walker, M., et al. (2008). D-amino acid oxidase activity and expression are increased in schizophrenia. *Mol. Psychiatry.* 13, 658–660. doi: 10.1038/mp.2008.47

We are conscious that, despite the important role played by hDAAO in main physiological processes, the modulation of its functional properties is still largely unknown. A main issue is the modulation of the activity by post-translational modifications (as known for serine racemase) and by further interacting proteins. A second matter is the role of hDAAO activity in important human diseases. Here, a way to elucidate links with cell functions is represented by the investigation of the role of epigenetic modifications on DAO gene expression in different cells and tissues during development and pathological conditions. In this regard, a CpG methylation analysis of the DAO promoter was performed recently and brain region-specific epiallelic profiles were detected in schizophrenic patients and healthy controls (Keller et al., 2018). These different methylation signatures have been proposed to be indicative of cell populations containing the DAO gene in different functional states.

The known properties of hDAAO strengthen our belief that the flavoenzyme activity must be finely tuned to fulfill a main physiological function such as the control of D-serine levels in the brain.

AUTHOR CONTRIBUTIONS

LP designed the review. All authors analyzed the literature and wrote the manuscript.

ACKNOWLEDGMENTS

We thank the support of Fondo di Ateneo per la Ricerca and Dr. Gianluca Tomasello for help in preparing structural figures. GM is a Ph.D. student of the Biotechnology, Biosciences and Surgical Technology course at Università degli Studi dell'Insubria.

- Caldinelli, L., Molla, G., Bracci, L., Lelli, B., Pileri, S., Cappelletti, P., et al. (2010). Effect of ligand binding on human D-amino acid oxidase: implications for the development of new drugs for schizophrenia treatment. *Protein Sci.* 19, 1500–1512. doi: 10.1002/pro.429
- Caldinelli, L., Molla, G., Sacchi, S., Pilone, M. S., and Pollegioni, L. (2009). Relevance of weak flavin binding in human D-amino acid oxidase. *Protein Sci.* 18, 801–810. doi: 10.1002/pro.86
- Caldinelli, L., Sacchi, S., Molla, G., Nardini, M., and Pollegioni, L. (2013). Characterization of human DAAO variants potentially related to an increased risk of schizophrenia. *Biochim. Biophys. Acta* 1832, 400–410. doi: 10.1016/j.bbadis.2012.11.019
- Caligiuri, A., D'Arrigo, P., Gefflaut, T., Molla, G., Pollegioni, L., Rosini, E., et al. (2006b). Multistep enzyme catalysed deracemisation of 2-naphthyl alanine. *Biocatal. Biotrans.* 24, 409–413. doi: 10.1080/10242420601033878
- Caligiuri, A., D'Arrigo, P., Rosini, E., Tessaro, D., Molla, G., Servi, S., et al. (2006a). Enzymatic conversion of unnatural amino acids by yeast D-amino acid oxidase. *Adv. Synth. Catal.* 348, 2183–2190. doi: 10.1002/adsc.200606188
- Cappelletti, P., Campomenosi, P., Pollegioni, L., and Sacchi, S. (2014). The degradation (by distinct pathways) of human D-amino acid oxidase and its interacting partner pLG72—two key proteins in D-serine catabolism in the brain. *FEBS J.* 281, 708–723. doi: 10.1111/febs.12616
- Cappelletti, P., Piubelli, L., Murtas, G., Caldinelli, L., Valentino, M., Molla, G., et al. (2015). Structure-function relationships in human d-amino acid oxidase variants corresponding to known SNPs. *Biochim. Biophys. Acta* 1854, 1150–1159. doi: 10.1016/j.bbapap.2015.02.005

- Chumakov, I., Blumenfeld, M., Guerassimenko, O., Cavarec, L., Palicio, M., Abderrahim, H., et al. (2002). Genetic and physiological data implicating the new human gene G72 and the gene for D-amino acid oxidase in schizophrenia. *Proc. Natl. Acad. Sci. U.S.A.* 99, 13675–13680. doi: 10.1073/pnas.182412499
- Cirulli, E. T., Lasseigne, B. N., Petrovski, S., Sapp, P. C., Dion, P. A., Leblond, C. S., et al. (2015). Exome sequencing in amyotrophic lateral sclerosis identifies risk genes and pathways. *Science* 347, 1436–1441. doi: 10.1126/science.aaa3650
- Cline, M. J., and Lehrer, R. I. (1969). D-amino acid oxidase in leukocytes: a possible D-amino-acid-linked antimicrobial system. *Proc. Natl. Acad. Sci. U.S.A.* 62, 756–763. doi: 10.1073/pnas.62.3.756
- Conti, P., Tamborini, L., Pinto, A., Blondel, A., Minoprio, P., Mozzarelli, A., et al. (2011). Drug discovery targeting amino acid racemases. *Chem. Rev.* 111, 6919–6946. doi: 10.1021/cr2000702
- Coyle, J. T. (2006). Glutamate and schizophrenia: beyond the dopamine hypothesis. *Cell. Mol. Neurobiol.* 26, 363–382. doi: 10.1007/s10571-006-9062-8
- Coyle, J. T., Tsai, G., and Goff, D. (2003). Converging evidence of NMDA receptor hypofunction in the pathophysiology of schizophrenia. *Ann. N. Y. Acad. Sci.* 1003, 318–327. doi: 10.1196/annals.1300.020
- Dellaflora, L., Marchetti, M., Spyrikis, F., Orlandi, V., Campanini, B., Cruciani, G., et al. (2015). Expanding the chemical space of human serine racemase inhibitors. *Bioorg. Med. Chem. Lett.* 25, 4297–4303. doi: 10.1016/j.bmcl.2015.07.081
- Drews, E., Otte, D. M., and Zimmer, A. (2013). Involvement of the primate specific gene G72 in schizophrenia: From genetic studies to pathomechanisms. *Neurosci. Biobehav. Rev.* 37, 2410–2417. doi: 10.1016/j.neubiorev.2012.10.009
- Duplantier, A. J., Becker, S. L., Bohanon, M. J., Borzilleri, K. A., Chrnyk, B. A., Downs, J. T., et al. (2009). Discovery, SAR, and pharmacokinetics of a novel 3-hydroxyquinolin-2 (1H)-one series of potent d-amino acid oxidase (DAAO) inhibitors. *J. Med. Chem.* 52, 3576–3585. doi: 10.1021/jm90128w
- Ferraris, D., Duvall, B., Ko, Y. S., Thomas, A. G., Rojas, G., Majer, P., et al. (2008). Synthesis and biological evaluation of D-amino acid oxidase inhibitors. *J. Med. Chem.* 51, 3357–3359. doi: 10.1021/jm800200u
- Foltyn, V. N., Bendikov, I., De Miranda, J., Panizzutti, R., Dumin, E., Shleper, M., et al. (2005). Serine racemase modulates intracellular D-serine levels through an α - β -elimination activity. *J. Biol. Chem.* 280, 1754–1763. doi: 10.1074/jbc.M405726200
- Fratini, L. F., Piubelli, L., Sacchi, S., Molla, G., and Pollegioni, L. (2011). Is rat an appropriate animal model to study the involvement of D-serine catabolism in schizophrenia? Insights from characterization of D-amino acid oxidase. *FEBS J.* 278, 4362–4373. doi: 10.1111/j.1742-4658.2011.08354.x
- Fuchs, S. A., Berger, R., Klomp, L. W., and de Koning, T. J. (2005). D-amino acids in the central nervous system in health and disease. *Mol. Genet. Metab.* 85, 168–180. doi: 10.1016/j.ymgme.2005.03.003
- Furuya, S., Tabata, T., Mitoma, J., Yamada, K., Yamasaki, M., Makino, A., et al. (2000). L-serine and glycine serve as major astroglia-derived trophic factors for cerebellar Purkinje neurons. *Proc. Natl. Acad. Sci. U.S.A.* 97, 11528–11533. doi: 10.1073/pnas.200364497
- Ghosh, D., and Berg, J. M. (2010). A proteome-wide perspective on peroxisome targeting signal 1(PTS1)-Pex5p affinities. *J. Am. Chem. Soc.* 132, 3973–3979. doi: 10.1021/ja9109049
- Gilson, M. K., Liu, T., Baitaluk, M., Nicola, G., Hwang, L., and Chong, J. (2016). BindingDB in 2015: a public database for medicinal chemistry, computational chemistry and systems pharmacology. *Nucleic Acids Res.* 44, D1045–D1053. doi: 10.1093/nar/gkv1072
- Gong, N., Gao, Z. Y., Wang, Y. C., Li, X. Y., Huang, J. L., Hashimoto, K., et al. (2011). A series of D-amino acid oxidase inhibitors specifically prevents and reverses formalin-induced tonic pain in rats. *J. Pharmacol. Exp. Ther.* 336, 282–293. doi: 10.1124/jpet.110.172353
- Gong, N., Li, X. Y., Xiao, Q., and Wang, Y. X. (2014). Identification of a novel spinal dorsal horn astroglial D-amino acid oxidase-hydrogen peroxide pathway involved in morphine antinociceptive tolerance. *Anesthesiology* 120, 962–975. doi: 10.1097/ALN.0b013e3182a66d2a
- Hamas, K., Homma, H., Takigawa, Y., Fukushima, T., Santa, T., and Imai, K. (1997). Regional distribution and postnatal changes of D-amino acids in rat brain. *Biochim. Biophys. Acta* 1334, 214–222. doi: 10.1016/S0304-4165(96)00095-5
- Hashimoto, A., Nishikawa, T., Konno, R., Niwa, A., Yasumura, Y., Oka, T., et al. (1993). Free D-serine, D-aspartate and D-alanine in central nervous system and serum in mutant mice lacking D-amino acid oxidase. *Neurosci. Lett.* 152, 33–36. doi: 10.1016/0304-3940(93)90476-2
- Hashimoto, K., Engberg, G., Shimizu, E., Nordin, C., Lindström, L. H., and Iyo, M. (2005). Reduced D-serine to total serine ratio in the cerebrospinal fluid of drug naïve schizophrenic patients. *Prog. Neuropsychopharmacol. Biol. Psychiatry.* 29, 767–769. doi: 10.1016/j.pnpbp.2005.04.023
- Hashimoto, K., Fukushima, T., Shimizu, E., Komatsu, N., Watanabe, H., Shinoda, N., et al. (2003). Decreased serum levels of D-serine in patients with schizophrenia: evidence in support of the N-methyl-D-aspartate receptor hypofunction hypothesis of schizophrenia. *Arch. Gen. Psychiatry* 60, 572–576. doi: 10.1001/archpsyc.60.6.572
- Hopkins, S. C., Campbell, U. C., Heffernan, M. L., Spear, K. L., Jeggo, R. D., Spanswick, D. C., et al. (2013b). Effects of D-amino acid oxidase inhibition on memory performance and long-term potentiation *in vivo*. *Pharmacol. Res. Perspect.* 1:e00007. doi: 10.1002/prp2.7
- Hopkins, S. C., Zhao, F. Y., Bowen, C. A., Fang, X., Wei, H., Heffernan, M. L., et al. (2013a). Pharmacodynamic effects of a D-amino acid oxidase inhibitor indicate a spinal site of action in rat models of neuropathic pain. *J. Pharmacol. Exp. Ther.* 345, 502–511. doi: 10.1124/jpet.113.204016
- Horiike, K., Tojo, H., Arai, R., Nozaki, M., and Maeda, T. (1994). D-amino acid oxidase is confined to the lower brain stem and cerebellum in rat brain: regional differentiation of astrocytes. *Brain Res.* 652, 297–303. doi: 10.1016/0006-8993(94)90240-2
- Iwana, S., Kawazoe, T., Park, H. K., Tsuchiya, K., Ono, K., Yorita, K., et al. (2008). Chlorpromazine oligomer is a potentially active substance that inhibits human D-amino acid oxidase, product of a susceptibility gene for schizophrenia. *J. Enzyme. Inhib. Med. Chem.* 23, 901–911. doi: 10.1080/14756360701745478
- Junjaud, G., Rouaud, E., Turpin, F., Mothet, J. P., and Billard, J. M. (2006). Age-related effects of the neuromodulator D-serine on neurotransmission and synaptic potentiation in the CA1 hippocampal area of the rat. *J. Neurochem.* 98, 1159–1166. doi: 10.1111/j.1471-4159.2006.03944.x
- Kapoor, R., Lim, K. S., Cheng, A., Garrick, T., and Kapoor, V. (2006). Preliminary evidence for a link between schizophrenia and NMDA-glycine site receptor ligand metabolic enzymes, D-amino acid oxidase (DAAO) and kynurenine aminotransferase-1 (KAT-1). *Brain Res.* 1106, 205–210. doi: 10.1016/j.brainres.2006.05.082
- Katane, M., Osaka, N., Matsuda, S., Maeda, K., Kawata, T., Saitoh, Y., et al. (2013). Identification of novel D-amino acid oxidase inhibitors by *in silico* screening and their functional characterization *in vitro*. *J. Med. Chem.* 56, 1894–1907. doi: 10.1021/jm3017865
- Kawazoe, T., Park, H. K., Iwana, S., Tsuge, H., and Fukui, K. (2007b). Human D-amino acid oxidase: an update and review. *Chem. Rec.* 7, 305–315. doi: 10.1002/tcr.20129
- Kawazoe, T., Tsuge, H., Imagawa, T., Aki, K., Kuramitsu, S., and Fukui, K. (2007a). Structural basis of D-DOPA oxidation by D-amino acid oxidase: alternative pathway for dopamine biosynthesis. *Biochem. Biophys. Res. Commun.* 355, 385–391. doi: 10.1016/j.bbrc.2007.01.181
- Kawazoe, T., Tsuge, H., Pilone, M. S., and Fukui, K. (2006). Crystal structure of human D-amino acid oxidase: context-dependent variability of the backbone conformation of the VAAGL hydrophobic stretch located at the *si*-face of the flavin ring. *Protein Sci.* 15, 2708–2717. doi: 10.1110/ps.062421606
- Keller, S., Punzo, D., Cuomo, M., Affinito, O., Coretti, L., Sacchi S., et al. (2018). DNA methylation landscape of the genes regulating D-serine and D-aspartate metabolism in post-mortem brain from controls and subjects with schizophrenia. *Sci. Rep.* 8:10163. doi: 10.1038/s41598-018-28332-x
- Kohiki, T., Sato, Y., Nishikawa, Y., Yorita, K., Sagawa, I., Denda, M., et al. (2017). Elucidation of inhibitor-binding pocket of D-amino acid oxidase using docking simulation and N-sulfanylanilide-based labeling technology. *Org. Biomol. Chem.* 15, 5289–5297. doi: 10.1039/C7OB00633K
- Koibuchi, N., Konno, R., Matsuzaki, S., Ohtake, H., Niwa, A., and Yamaoka, K. (1995). Localization of D-amino acid oxidase mRNA in the mouse kidney and the effect of testosterone treatment. *Histochem. Cell Biol.* 104, 349–355. doi: 10.1007/BF01458128
- Kondori, N. R., Paul, P., Robbins, J. P., Liu, K., Hildyard, J. C., Wells, D. J., et al. (2017). Characterisation of the pathogenic effects of the *in vivo* expression of an ALS-linked mutation in D-amino acid oxidase:

- phenotype and loss of spinal cord motor neurons. *PLoS ONE* 12:e0188912. doi: 10.1371/journal.pone.0188912
- Konno, R. (2001). Assignment of D-amino-acid oxidase gene to a human and a mouse chromosome. *Amino Acids*, 20, 401–408. doi: 10.1007/s007260170036
- Konno, R., Ikeda, M., Yamaguchi, K., Ueda, Y., and Niwa, A. (2000). Nephrotoxicity of D-propargylglycine in mice. *Arch. Toxicol.* 74, 473–479. doi: 10.1007/s002040000156
- Konno, R., and Yasumura, Y. (1983). Mouse mutant deficient in D-amino acid oxidase activity. *Genetics*, 103, 277–285.
- Krebs, H. A. (1935). Metabolism of amino-acids: deamination of amino-acids. *Biochem. J.* 29, 1620–1644. doi: 10.1042/bj0291620
- Krug, A. W., Volker, K., Dantzer, W. H., and Silbernagl, S. (2007). Why is D-serine nephrotoxic and α -aminoisobutyric acid protective? *Am. J. Physiol. Renal Physiol.* 293, F382–F390. doi: 10.1152/ajprenal.00441.2006
- Kumar, A. (2015). NMDA Receptor function during senescence: implication on cognitive performance. *Front. Neurosci.* 9:473. doi: 10.3389/fnins.2015.00473
- Lattremoliere, A., and Woolf, C. J. (2009). Central sensitization: a generator of pain hypersensitivity by central neural plasticity. *J. Pain*, 10, 895–926. doi: 10.1016/j.jpain.2009.06.012
- Lin, T. S., Tsai, H. J., Lee, C. H., Song, Y. Q., Huang, R. S., Hsieh-Li, H. M., et al. (2017). An improved drugs screening system reveals that baicalein ameliorates the $\text{A}\beta$ /AMPA/NMDA-induced depolarization of neurons. *J. Alzheimers Dis.* 56, 959–976. doi: 10.3233/JAD-160898
- Lu, J. M., Gong, N., Wang, Y. C., and Wang, Y. X. (2012). D-Amino acid oxidase-mediated increase in spinal hydrogen peroxide is mainly responsible for formalin-induced tonic pain. *Br. J. Pharmacol.* 165, 1941–1955. doi: 10.1111/j.1476-5381.2011.01680.x
- Luks, L., Maier, M. Y., Sacchi, S., Pollegioni, L., and Dietrich, D. R. (2017a). Understanding renal nuclear protein accumulation: an in vitro approach to explain an in vivo phenomenon. *Arch. Toxicol.* 91, 3599–3611. doi: 10.1007/s00204-017-1970-5
- Luks, L., Sacchi, S., Pollegioni, L., and Dietrich, D. R. (2017b). Novel insights into renal D-amino acid oxidase accumulation: propiverine changes DAAO localization and peroxisomal size in vivo. *Arch. Toxicol.* 91, 427–437. doi: 10.1007/s00204-016-1685-z
- Madeira, C., Freitas, M. E., Vargas-Lopes, C., Wolosker, H., and Panizzutti, R. (2008). Increased brain D-amino acid oxidase (DAAO) activity in schizophrenia. *Schizophr. Res.* 101, 76–83. doi: 10.1016/j.schres.2008.02.002
- Madeira, C., Lourenco, M. V., Vargas-Lopes, C., Suemoto, C. K., Brandão, C. O., Reis, T., et al. (2015). D-Serine levels in Alzheimer's disease: implications for novel biomarker development. *Transl. Psychiatry* 5:561. doi: 10.1038/tp.2015.52
- Maekawa, M., Okamura, T., Kasai, N., Hori, Y., Sumner, K. H., and Konno, R. (2005). D-amino-acid oxidase is involved in D-serine-induced nephrotoxicity. *Chem. Res. Toxicol.* 18, 1678–1682. doi: 10.1021/tx0500326
- Martinez, F. J., Pratt, G. A., Van Nostrand, E. L., Batra, R., Huelga, S. C., Kapeli, K., et al. (2016). Protein-RNA networks regulated by normal and ALS-associated mutant HNRNPA2B1 in the nervous system. *Neuron* 92, 780–795. doi: 10.1016/j.neuron.2016.09.050
- Mattevi, A., Vanoni, M. A., Todone, F., Rizzi, M., Teplyakov, A., Coda, A., et al. (1996). Crystal structure of D-amino acid oxidase: a case of active site mirror-image convergent evolution with flavocytochrome b2. *Proc. Nat. Acad. Sci. U.S.A.* 93, 7496–7501. doi: 10.1073/pnas.93.15.7496
- Mesecar, A. D., Koshland, D. E., and Jr. (2000). Sites of binding and orientation in a four-location model for protein stereospecificity. *IUBMB Life* 49, 457–466. doi: 10.1080/152165400410326
- Mitchell, J., Paul, P., Chen, H. J., Morris, A., Payling, M., Falchi, M., et al. (2010). Familial amyotrophic lateral sclerosis is associated with a mutation in D-amino acid oxidase. *Proc. Natl. Acad. Sci. U.S.A.* 107, 7556–7561. doi: 10.1073/pnas.0914128107
- Miyoshi, Y., Hamase, K., Tojo, Y., Mita, M., Konno, R., and Zaitzu, K. (2009). Determination of D-serine and D-alanine in the tissues and physiological fluids of mice with various D-amino-acid oxidase activities using two-dimensional high-performance liquid chromatography with fluorescence detection. *J. Chromatogr. B* 877, 2506–2512. doi: 10.1016/j.jchromb.2009.06.028
- Molla, G. (2017). Competitive inhibitors unveil structure/function relationships in human D-amino acid oxidase. *Front. Mol. Biosci.* 4:80. doi: 10.3389/fmolb.2017.00080
- Molla, G., Sacchi, S., Bernasconi, M., Pilone, M. S., Fukui, K., and Polegioni, L. (2006). Characterization of human D-amino acid oxidase. *FEBS Lett.* 580, 2358–2364. doi: 10.1016/j.febslet.2006.03.045
- Moreno, S., Nardacci, R., Cimini, A., and Cerù, M. P. (1999). Immunocytochemical localization of D-amino acid oxidase in rat brain. *J. Neurocytol.* 28, 169–185. doi: 10.1023/A:1007064504007
- Morikawa, A., Hamase, K., Inoue, T., Konno, R., Niwa, A., and Zaitzu, K. (2001). Determination of free D-aspartic acid, D-serine and D-alanine in the brain of mutant mice lacking D-amino-acid oxidase activity. *J. Chromatogr. B Biomed. Sci. Appl.* 757, 119–125. doi: 10.1016/S0378-4347(01)00131-1
- Mörtl, M., Diederichs, K., Welte, W., Molla, G., Motteran, L., Andriolo, G., et al. (2004). Structure-function correlation in glycine oxidase from *Bacillus subtilis*. *J. Biol. Chem.* 279, 29718–29727. doi: 10.1074/jbc.M401224200
- Mothet, J. P., Rouaud, E., Sinet, P. M., Potier, M., Jouveanceau, A., Dutar, P., et al. (2006). A critical role for the glial-derived neuromodulator D-serine in the age-related deficits of cellular mechanisms of learning and memory. *Aging Cell* 5, 267–274. doi: 10.1111/j.1474-9726.2006.00216.x
- Murtas, G., Caldinelli, L., Cappelletti, P., Sacchi, S., and Pollegioni, L. (2017a). Human D-amino acid oxidase: the inactive G183R variant. *Biochim. Biophys. Acta* 7, 822–830. doi: 10.1016/j.bbapap.2017.12.007
- Murtas, G., Sacchi, S., Valentino, M., and Pollegioni, L. (2017b). Biochemical properties of human D-amino acid oxidase. *Front. Mol. Biosci.* 4:88. doi: 10.3389/fmolb.2017.00088
- Nagata, Y. (1992). Involvement of D-amino acid oxidase in elimination of D-serine in mouse brain. *Experientia* 48, 753–755. doi: 10.1007/BF02124295
- Nagata, Y., Masui, R., and Akino, T. (1992). The presence of free D-serine, D-alanine and D-proline in human plasma. *Experientia* 48, 986–988. doi: 10.1007/BF01919147
- Nakamura, H., Fang, J., and Maeda, H. (2012). Protective role of D-amino acid oxidase against *Staphylococcus aureus* infection. *Infect. Immun.* 80, 1546–1553. doi: 10.1128/IAI.06214-11
- Olney, J. W., Wozniak, D. F., and Farber, N. B. (1997). Excitotoxic neurodegeneration in Alzheimer disease: new hypothesis and new therapeutic strategies. *Arch. Neurol.* 54, 1234–1240. doi: 10.1001/archneur.1997.00550220042012
- Ono, K., Shishido, Y., Park, H. K., Kawazoe, T., Iwano, S., Chung, S. P., et al. (2009). Potential pathophysiological role of D-amino acid oxidase in schizophrenia: immunohistochemical and in situ hybridization study of the expression in human and rat brain. *J. Neural. Transm.* 116, 1335–1347. doi: 10.1007/s00702-009-0289-7
- Paul, P., and de Belleruche, J. (2012). The role of D-amino acids in amyotrophic lateral sclerosis pathogenesis: a review. *Amino Acids*, 43, 1823–1831. doi: 10.1007/s00726-012-1385-9
- Paul, P., Murphy, T., Oseni, Z., Sivalokanathan, S., and de Belleruche, J. S. (2014). Pathogenic effects of amyotrophic lateral sclerosis-linked mutation in D-amino acid oxidase are mediated by D-serine. *Neurobiol. Aging* 35, 876–885. doi: 10.1016/j.neurobiolaging.2013.09.005
- Pilone, M. S., and Pollegioni, L. (2002). D-Aminoacid oxidase as an industrial biocatalyst. *Biocatal. Biotransform.* 20, 145–159. doi: 10.1080/10242420290020679
- Pollegioni, L., Buto, S., Tischer, W., Ghisla, S., and Pilone, M. S. (1993). Characterization of D-amino acid oxidase from *Trigonopsis variabilis*. *Biochem. Mol. Biol. Int.* 31, 709–717.
- Pollegioni, L., Diederichs, K., Molla, G., Umhau, S., Welte, W., Ghisla, S., et al. (2002). Yeast D-amino acid oxidase: structural basis of its catalytic properties. *J. Mol. Biol.* 324, 535–546. doi: 10.1016/S0022-2836(02)01062-8
- Pollegioni, L., and Molla, G. (2011). New biotech applications from evolved D-amino acid oxidases. *Trends Biotechnol.* 29, 276–283. doi: 10.1016/j.tibtech.2011.01.010
- Pollegioni, L., Molla, G., Sacchi, S., Rosini, E., Verga, R., and Pilone, M. S. (2008). Properties and applications of microbial D-amino acid oxidases: current state and perspectives. *Appl. Microbiol. Biotechnol.* 78, 1–16. doi: 10.1007/s00253-007-1282-4

- Pollegioni, L., Piubelli, L., Molla, G., and Rosini, E. (2018). D-Amino acid oxidase-pLG72 interaction and D-serine modulation. *Front. Mol. Biosci.* 5:3. doi: 10.3389/fmolb.2018.00003
- Pollegioni, L., Piubelli, L., Sacchi, S., Pilone, M. S., and Molla, G. (2007). Physiological functions of D-amino acid oxidases: from yeast to humans. *Cell. Mol. Life Sci.* 64, 1373–1394. doi: 10.1007/s00018-007-6558-4
- Pollegioni, L., and Sacchi, S. (2010). Metabolism of the neuromodulator D-serine. *Cell. Mol. Life Sci.* 67, 2387–2404. doi: 10.1007/s00018-010-0307-9
- Popielek, M., Ross, J. F., Charych, E., Chanda, P., Gundelfinger, E. D., Moss, S. J., et al. (2011). D-amino acid oxidase activity is inhibited by an interaction with bassoon protein at the presynaptic active zone. *J. Biol. Chem.* 286, 28867–28875. doi: 10.1074/jbc.M111.262063
- Raje, M., Hin, N., Duvall, B., Ferraris, D. V., Berry, J. F., Thomas, A. G., et al. (2013). Synthesis of kojic acid derivatives as secondary binding site probes of D-amino acid oxidase. *Bioorganic Med. Chem. Lett.* 23, 3910–3913. doi: 10.1016/j.bmcl.2013.04.062
- Robinson, J. M., Briggs, R. T., and Karnovsky, M. J. (1978). Localization of D-amino acid oxidase on the cell surface of human polymorphonuclear leukocytes. *J. Cell Biol.* 77, 59–71. doi: 10.1083/jcb.77.1.59
- Romano, D., Molla, G., Pollegioni, L., and Marinelli, F. (2009). Optimization of human D-amino acid oxidase expression in *Escherichia coli*. *Protein Expr. Purif.* 68, 72–78. doi: 10.1016/j.pep.2009.05.013
- Sacchi, S., Bernasconi, M., Martineau, M., Mothet, J. P., Ruzzene, M., Pilone, M. S., et al. (2008). pLG72 modulates intracellular D-serine levels through its interaction with D-amino acid oxidase: effect on schizophrenia susceptibility. *J. Biol. Chem.* 283, 22244–22256. doi: 10.1074/jbc.M709153200
- Sacchi, S., Binelli, G., and Pollegioni, L. (2016). G72 primate-specific gene: a still enigmatic element in psychiatric disorders. *Cell. Mol. Life Sci.* 73, 2029–2039. doi: 10.1007/s00018-016-2165-6
- Sacchi, S., Caldinelli, L., Cappelletti, P., Pollegioni, L., and Molla, G. (2012). Structure-function relationships in human D-amino acid oxidase. *Amino Acids.* 43, 1833–1850. doi: 10.1007/s00726-012-1345-4
- Sacchi, S., Cappelletti, P., Giovannardi, S., and Pollegioni, L. (2011). Evidence for the interaction of D-amino acid oxidase with pLG72 in a glial cell line. *Mol. Cell Neurosci.* 48, 20–28. doi: 10.1016/j.mcn.2011.06.001
- Sacchi, S., Cappelletti, P., and Murtas, G. (2018). Biochemical properties of human D-amino acid oxidase variants and their potential significance in pathologies. *Front. Mol. Biosci.* 5:55. doi: 10.3389/fmolb.2018.00055
- Sacchi, S., Cappelletti, P., Pirone, L., Smaldone, G., Pedone, E., and Pollegioni, L. (2017). Elucidating the role of the pLG72 R30K substitution in schizophrenia susceptibility. *FEBS Lett.* 591, 646–655. doi: 10.1002/1873-3468.12585
- Sasabe, J., Miyoshi, Y., Rakoff-Nahoum, S., Zhang, T., Mita, M., Davis, B. M., et al. (2016). Interplay between microbial D-amino acids and host D-amino acid oxidase modifies murine mucosal defence and gut microbiota. *Nat. Microbiol.* 1:16125. doi: 10.1038/nmicrobiol.2016.125
- Sasabe, J., Suzuki, M., Imanishi, N., and Aiso, S. (2014b). Activity of D-amino acid oxidase is widespread in the human central nervous system. *Front. Synaptic Neurosci.* 6:14. doi: 10.3389/fnsyn.2014.00014
- Sasabe, J., Suzuki, M., Miyoshi, Y., Tojo, Y., Okamura, C., Ito, S., et al. (2014a). Ischemic acute kidney injury perturbs homeostasis of serine enantiomers in the body fluid in mice: early detection of renal dysfunction using the ratio of serine enantiomers. *PLoS ONE* 9:e86504. doi: 10.1371/journal.pone.0086504
- Shibuya, N., Koike, S., Tanaka, M., Ishigami-Yuasa, M., Kimura, Y., Ogasawara, Y., et al. (2013). A novel pathway for the production of hydrogen sulfide from D-cysteine in mammalian cells. *Nat. Commun.* 4:1366. doi: 10.1038/ncomms2371
- Shoji, K., Mariotto, S., Ciampa, A. R., and Suzuki, H. (2006). Mutual regulation between serine and nitric oxide metabolism in human glioblastoma cells. *Neurosci Lett.* 394, 163–167. doi: 10.1016/j.neulet.2005.10.064
- Stone, J. M., and Pilowsky, L. S. (2007). Novel targets for drugs in schizophrenia. *C.N.S. Neurol. Disord. Drug Targets.* 6, 265–272. doi: 10.2174/187152707781387323
- Subramanian, K., Góra, A., Spruijt, R., Mitusinska, K., Suarez-Diez, M., Martins Dos Santos, V., et al. (2018). Modulating D-amino acid oxidase (DAAO) substrate specificity through facilitated solvent access. *PLoS ONE* 13:e0198990. doi: 10.1371/journal.pone.0198990
- Terry-Lorenzo, R. T., Chun, L. E., Brown, S. P., Heffernan, M. L., Fang, Q. K., Orsini, M. A., et al. (2014). Novel human D-amino acid oxidase inhibitors stabilize an active-site lid-open conformation. *Biosci. Rep.* 34, U487–U205. doi: 10.1042/BSR20140071
- Terry-Lorenzo, R. T., Masuda, K., Sugao, K., Fang, Q. K., Orsini, M. A., Sacchi, S., et al. (2015). High-throughput screening strategy identifies allosteric, covalent human D-amino acid oxidase inhibitor. *J. Biomol. Screen.* 20, 1218–1231. doi: 10.1177/1087057115600413
- Umhau, S., Pollegioni, L., Molla, G., Diederichs, K., Welte, W., Pilone, M. S., et al. (2000). The X-ray structure of D-amino acid oxidase at very high resolution identifies the chemical mechanism of flavin-dependent substrate dehydrogenation. *Proc. Natl. Acad. Sci. U.S.A.* 97, 12463–12468. doi: 10.1073/pnas.97.23.12463
- Verrall, L., Burnet, P. W. J., Betts, J. F., and Harrison, P. J. (2010). The neurobiology of D-amino acid oxidase and its involvement in schizophrenia. *Mol. Psychiatry.* 15:122. doi: 10.1038/mp.2009.99
- Verrall, L., Walker, M., Rawlings, N., Benzel, I., Kew, J. N., Harrison, P. J., et al. (2007). D-Amino acid oxidase and serine racemase in human brain: normal distribution and altered expression in schizophrenia. *Eur. J. Neurosci.* 26, 1657–1669. doi: 10.1111/j.1460-9568.2007.05769.x
- Wake, K., Yamazaki, H., Hanzawa, S., Konno, R., Sakio, H., Niwa, A., et al. (2001). Exaggerated responses to chronic nociceptive stimuli and enhancement of N-methyl-D-aspartate receptor-mediated synaptic transmission in mutant mice lacking D-amino acid oxidase. *Neurosci. Lett.* 297, 25–28. doi: 10.1016/S0304-3940(00)01658-X
- Wang, H., Wolosker, H., Pevsner, J., Snyder, S. H., and Selkoe, D. J. (2000). Regulation of rat magnocellular neurosecretory system by D-aspartate: evidence for biological role(s) of a naturally occurring free D-amino acid in mammals. *Endocrinol.* 167, 247–252. doi: 10.1677/joe.0.1670247
- Weatherly, C. A., Du, S., Parpia, C., Santos, P. T., Hartman, A. L., and Armstrong, D. W. (2017). D-Amino acid levels in perfused mouse brain tissue and blood: a comparative study. *A. C. S. Chem. Neurosci.* 8, 1251–1261. doi: 10.1021/acscchemneuro.6b00398
- Wei, H., Gong, N., Huang, J. L., Fan, H., Ma, A. N., Li, X. Y., et al. (2013). Spinal D-amino acid oxidase contributes to mechanical pain hypersensitivity induced by sleep deprivation in the rat. *Pharmacol Biochem Behav.* 111, 30–36. doi: 10.1016/j.pbb.2013.08.003
- Wolosker, H. (2011). Serine racemase and the serine shuttle between neurons and astrocytes. *Biochim. Biophys. Acta* 1814, 1558–1566. doi: 10.1016/j.bbapap.2011.01.001
- Wolosker, H., Blackshaw, S., and Snyder, S. H. (1999). Serine racemase: a glial enzyme synthesizing D-serine to regulate glutamate-N-methyl-D-aspartate neurotransmission. *Proc. Natl. Acad. Sci. U.S.A.* 96, 13409–13414. doi: 10.1073/pnas.96.23.13409
- Wolosker, H., Panizzutti, R., and de Miranda, J. (2002). Neurobiology through the looking-glass: D-serine as a new glial-derived transmitter. *Neurochem. Int.* 41, 327–332. doi: 10.1016/S0197-0186(02)00055-4
- Wolosker, H., and Radziszewsky, I. (2013). The serine shuttle between glia and neurons: implications for neurotransmission and neurodegeneration. *Biochem. Soc. Trans.* 41, 1546–1550. doi: 10.1042/BST20130220
- Wozniak, D. F., Dikranian, K., Ishimaru, M. J., Nardi, A., Corso, T. D., Tenkova, T., et al. (1998). Disseminated corticolimbic neuronal degeneration induced in rat brain by MK-801: potential relevance to Alzheimer's disease. *Neurobiol. Dis.* 5, 305–322. doi: 10.1006/mbdi.1998.0206
- Zhao, W. J., Gao, Z. Y., Wei, H., Nie, H. Z., Zhao, Q., Zhou, X. J., et al. (2010). Spinal D-amino acid oxidase contributes to neuropathic pain in rats. *J. Pharmacol. Exp. Ther.* 332, 248–254. doi: 10.1124/jpet.109.158816

Conflict of Interest Statement: The authors declare that the research was conducted in the absence of any commercial or financial relationships that could be construed as a potential conflict of interest.

Copyright © 2018 Pollegioni, Sacchi and Murtas. This is an open-access article distributed under the terms of the Creative Commons Attribution License (CC BY). The use, distribution or reproduction in other forums is permitted, provided the original author(s) and the copyright owner(s) are credited and that the original publication in this journal is cited, in accordance with accepted academic practice. No use, distribution or reproduction is permitted which does not comply with these terms.